University of Alberta

THE EFFECTS OF HYPELIPIDEMIA ON THE DISPOSITION AND METABOLISM OF AMIODARONE IN RATS

By: ©

Anooshirvan Shayeganpour

A THESIS SUBMITTED TO THE:
Faculty of Graduate Studies and Research in partial fulfillment of the requirement for the
degree of **DOCTOR OF PHILISOPHY**
IN
PHARMACEUTICAL SCIENCES
Faculty of Pharmacy and Pharmaceutical Sciences, University of Alberta,
Edmonton, Alberta, Canada

Spring 2008

Library and
Archives Canada

Published Heritage
Branch

395 Wellington Street
Ottawa ON K1A 0N4
Canada

Bibliothèque et
Archives Canada

Direction du
Patrimoine de l'édition

395, rue Wellington
Ottawa ON K1A 0N4
Canada

Your file Votre référence
ISBN: 978-0-494-45598-2
Our file Notre référence
ISBN: 978-0-494-45598-2

NOTICE:
The author has granted a non-exclusive license allowing Library and Archives Canada to reproduce, publish, archive, preserve, conserve, communicate to the public by telecommunication or on the Internet, loan, distribute and sell theses worldwide, for commercial or non-commercial purposes, in microform, paper, electronic and/or any other formats.

The author retains copyright ownership and moral rights in this thesis. Neither the thesis nor substantial extracts from it may be printed or otherwise reproduced without the author's permission.

AVIS:
L'auteur a accordé une licence non exclusive permettant à la Bibliothèque et Archives Canada de reproduire, publier, archiver, sauvegarder, conserver, transmettre au public par télécommunication ou par l'Internet, prêter, distribuer et vendre des thèses partout dans le monde, à des fins commerciales ou autres, sur support microforme, papier, électronique et/ou autres formats.

L'auteur conserve la propriété du droit d'auteur et des droits moraux qui protège cette thèse. Ni la thèse ni des extraits substantiels de celle-ci ne doivent être imprimés ou autrement reproduits sans son autorisation.

In compliance with the Canadian Privacy Act some supporting forms may have been removed from this thesis.

While these forms may be included in the document page count, their removal does not represent any loss of content from the thesis.

Conformément à la loi canadienne sur la protection de la vie privée, quelques formulaires secondaires ont été enlevés de cette thèse.

Bien que ces formulaires aient inclus dans la pagination, il n'y aura aucun contenu manquant.

Canada

ABSTRACT

The current work examined the effect of hyperlipidemia (HL) on the disposition and metabolism of amiodarone (AM), a first line agent in the treatment of tachyarrhythmia, in rat. The studies used systemic hyperlipidemic and simulated high fat meal rat models. For this purpose a modified preexisting HPLC assay was used, and a novel sensitive LC/MS method was developed. The latter enabled us to measure low levels of AM and desethylamiodarone (DEA), the active metabolite of AM, in biological specimens.

Hyperlipidemia caused increases in the plasma levels of AM due to significant decreases in clearance, volume of distribution and unbound fraction of drug. Oral lipid caused a significant increase in plasma AUC and a significant decrease in clearance of AM after intravenous doses. This was accompanied by an increase in the oral bioavailability of drug. In vitro distribution of AM and DEA in normolipidemic (NL) and HL human and rat plasma fractions indicated that HL caused a major shift of AM and DEA from lipoprotein deficient (LPDP) fraction to triglyceride rich lipoprotein (TRL) fraction in both species.

Tissue distribution studies suggested that the increase in plasma concentration of AM in HL did not lead to decreases in all of the tissues. Indeed, the influence of HL on AM distribution was not uniform, but rather tissue-specific. The changes in DEA tissue AUC as a result of HL were not always in line with those observed for AM.

HL also caused a decrease in the metabolism of AM to DEA in rat liver. The decrease in Clint was in line with the reduction in selective expression of some of the CYP isoforms known to be involved in the metabolism of AM in the rat. Involvement of some of these enzymes including CYP1A1 and CYP3A1/2, both of which are present in intestinal and hepatic microsomes of rats, was demonstrated using some chemical and immunoinhibition techniques.

Evaluation of the effect of oral lipid on the intestinal metabolism of AM to DEA was accomplished using an in vitro everted gut metabolism technique. Pretreatment of rats with peanut oil caused a decrease in metabolizing efficiency in the intestine.

To:

My lovely wife Heidi and my wonderful sons Kasra and Parsa

ACKNOWLEDGMENT

I would like to extend my supreme gratitude to my supervisor, friend and teacher Dr. Dion R. Brocks for teaching and helping me in achieving my greatest commitment of my professional life. His support and guidance in different stages of my graduate career are greatfully appreciated.

I would also like to extend my special appreciation to my supervisory committee members, Dr. Ayman O.El.Kadi and Dr. Fakhredin Jamali for their generous guidance and supports during the long career of my graduate studies.

I extend my special thanks to Dr. Kishor M. Wasan and Stephen Lee from the University of British Columbia, Faculty of Pharmaceutical Sciences for their kind suggestions and cooperation in some parts of this research.

I would like to acknowledge my lab partners Jigar, Dalia, Marwa and Srividya for creating a wonderful research environment in the lab.

I would like to thank the staff members of the Faculty of Pharmacy and Pharmaceutical Sciences, University of Alberta for their cooperation and kindness.

I sincerely express my deep feeling of gratitude to my parents for their support and love.

Last, and certainly not least, my profound gratitude is forwarded to the most precious gems of my life, my lovely wife Heidi and my incredible sons Kasra and Parsa. There is no doubt that this fulfillment is acheived mostly through their enthusiastic support and infinite patience.

TABLE OF CONTENTS

1 INTRODUCTION 1
  1.1 Lipid 1
  1.2 Lipid metabolism 1
    1.2.1 Lipid digestion 1
      1.2.1.1 Pre-duodenal enzymatic digestion 2
      1.2.1.2 Bile and bile salt micelles, emulsification process 4
      1.2.1.3 Intestinal enzymatic digestion of triglycerdes, the function of triglyceride lipase and colipase 5
      1.2.1.4 Enzymatic intestinal digestion of dietary phospholipids 8
      1.2.1.5 Enzymatic intestinal digestion of dietary cholesterol and cholestryl ester 9
    1.2.2 Absorption of the digested lipids 10
      1.2.2.1 Passive diffusion of micellar lipids, unstirred water layer theory 10
      1.2.2.2 Transport mediated absorption of lipids 11
    1.2.3 Intracellular metabolism of absorbed lipids 13
    1.2.4 Multiple cholesterol transport pathways 14
    1.2.5 Formation of intestinal lipoproteins 15
      1.2.5.1 Independent assembly of VLDL and CMs 15
      1.2.5.2 Sequential assembly of intestinal lipoproteins 17
        a) Assembly of primordial lipoproteins 17
        b) Synthesis of triglyceride-rich lipid droplets 18
        c) Core expansion 19
      1.2.5.3 Transport of CM and VLDL from the Golgi complex of the enterocytes to the intracellular space and lamina propria 20
      1.2.5.4 Catabolism of CMs and VLDL (Lipolysis) 21
      1.2.5.5 Hepatic uptake of CM-remnants 23
        a) Sequestration 23
        b) Processing 23
        c) Internalization 24

1.2.5.6 Exogenous cholesterol metabolism 25
1.2.5.7 Hepatic uptake of VLDL-remnants 26
1.2.5.8 Biosynthesis of hepatic VLDL 26
1.2.5.9 VLDL metabolism 27
1.2.5.10 Lipolytic conversion of IDL to LDL, role of hepatic lipase 28
1.2.5.11 LDL uptake by liver and extrahepatic tissues, role of LDL and scavenger receptors 30
1.2.5.12 Interconversion of IDL and HDL 32
1.2.5.13 Reverse cholesterol transport 32
1.2.5.14 HDL biosynthesis, the role of reverse cholesterol transport 32
a) First step, movement of free cholesterol to HDL 32
b) Second step, esterification of free cholesterol to cholestryl ester 33
c) Third step, exchange of CE with TGs from HDL to LDL and VLDL 35
d) Fourth step, transfer of CE to liver 35
1.3 Effect of lipids on pharmacokinetics of drugs 36
1.3.1 Lipids and absorption of drugs 36
1.3.1.1 Fat and gastric emptying time 36
1.3.1.2 The role of bile in drug solubilization and dissolution 38
1.3.2 Prediction of drug and high fat meal interactions 40
1.3.3 Lymphatic absorption of drugs 42
1.3.3.1 Physiochemical properties of drug molecules and their lymphatic absorption 43
1.3.3.2 Quantity and types of lipids in CM (vehicles) and lymphatic absorption of drugs 44
1.3.4 Lipids and drug distribution 45
1.3.4.1 Lipids and blood flow rate 46
1.3.4.2 Lipids and permeability 48
1.3.4.3 Lipids and drug protein binding 51
1.3.4.4 Hyperlipidemia and tissue distribution 55
1.3.4.5 Lipids and drug transporters 57
1.3.5 Lipids and elimination of drugs 59

1.3.5.1 Lipids and drug metabolizing enzymes 62
1.4 Animal models of hyperlipidemia 67
1.5 Amiodarone 71
1.5.1 Chemical Structure 71
1.5.2 Pharmacology and Pharmacodynamics 72
1.5.3 Pharmacokinetics 73
1.5.4 Metabolism 73
1.6 Rationale and hypotheses 75
1.6.1 Rationale 75
1.6.2 Hypothesis 78
1.6.2.1 Pharmacokinetics of AM in hyperlipidemia and high fat meal simulated rat model 78
1.6.2.2 Determination of the enzyme (s) involved in the metabolism of AM to DEA in rat 78
1.6.2.3 Effect of hyperlipidemia on tissue distribution of AM and DEA in rat 78
1.6.2.4 Effect of hyperlipidemia on hepatic metabolism of AM to DEA in rat 79
1.6.2.5 Effect of oral lipid on intestinal metabolism of AM to DEA in rat 79
1.7 Objectives 81
Based on the rational of thesis as indicated, the following items were listed as the objective of the study 81
Development of an LC/MS method for AM and DEA measurement in rat specimens 81
Pharmacokinetics of AM in hyperlipidemia and high fat meal simulated rat model 81
Determination of the enzyme(s) involved in the metabolism of AM to DEA in rat 81
Effect of hyperlipidemia on tissue distribution of AM and DEA in rat 81
Effect of hyperlipidemia on hepatic metabolism of AM to DEA in rat 81
Effect of oral lipid on intestinal metabolism of AM to DEA in rat 81
2 EXPERIMENTAL 82
2.1 Materials 82
2.2 Methods 83
2.2.1 Assays 83

2.2.1.1 Instrumentation 83
a) HPLC 83
b) LC/MS 83
2.2.1.2 Preparation of standard and stock solutions for drug analysis 84
2.2.2 Extraction techniques 85
2.2.2.1 HPLC 85
2.2.2.2 LC/MS 85
2.2.3 Analytical techniques 86
2.2.3.1 HPLC 86
2.2.3.2 LC/MS 86
2.2.4 Standard curves 87
2.2.4.1 Pharmacokinetics and studies of distribution of AM and DEA in lipoprotein fraction in plasma 87
2.2.4.2 Microsomal studies 87
2.2.4.3 Tissue distribution and everted gut studies 87
2.2.5 Quantification of AM and DEA 87
2.2.5.1 Validation of modified HPLC method for DEA assay 88
2.2.5.2 Validation of LC/MS method 88
2.2.6 In vivo and in vitro studies 89
2.2.6.1 Rat pharmacokinetics and tissue distribution studies 90
a) Surgical procedures 90
b) Dosing and sample collection 90
I. Preparation of dosing solutions 90
II. Sample collection in the pharmacokinetic studies 91
III. Sample collection in tissue distribution studies 91
2.2.6.2 Everted gut metabolism 92
2.2.7 Animal allocations 93
2.2.7.1 Pharmacokinetic studies 93
2.2.7.2 Tissue distribution 94
2.2.7.3 Everted gut metabolism 94
2.2.8 In vitro studies 95

2.2.8.1 Distribution of AM and DEA in human and rat plasma lipid fractions (in vitro) 95
- a) Treatment of plasma samples 95
- b) Separation of lipoprotein components 95
- c) Lipid measurement 96

2.2.8.2 Microsomal studies 96
- a) Microsomal preparation 97
- b) Lowry assay method for protein concentration in microsomal preparations 97
- c) Total CYP450 measurement 98
- d) Microsomal incubation studies 99
- e) Chemical inhibition and immunoinhibition studies in rat liver and intestinal microsomes 99
- f) Metabolism by heterogeneously expressed CYP enzymes 99
- g) Western blot analysis 100

2.2.9 Data analysis 101
2.2.9.1 Pharmacokinetic analysis 101
2.2.9.2 Tissue distribution 102
2.2.9.3 Lipoprotein fraction distribution studies 102
2.2.9.4 Microsomal studies 102
2.2.10 Statistical analysis 103
2.2.10.1 Pharmacokinetic studies 103
2.2.10.2 Tissue distribution 103
2.2.10.3 Everted gut metabolism 104
2.2.10.4 Lipoprotein fraction distribution studies 104
2.2.10.5 Microsomal studies 104
2.2.10.6 Western blot 105
2.3 Results 106
2.3.1 Assays 106
2.3.1.1 HPLC 106
a) Chromatography 106

b) Assay validation 107
2.3.1.2 LC/MS 108
c) Chromatography 108
d) Assay validation 111
2.3.2 Pharmacokinetics 113
2.3.2.1 The effect of hyperlipidemia and high fat meal on the pharmacokinetics of AM 113
2.3.2.2 Drug interaction 128
2.3.3 Tissue distribution 139
2.3.4 In vitro everted gut metabolism 148
2.3.5 In vitro distribution of AM and DEA in NL and HL lipoprotein plasma fractions of human and rat 152
2.3.5.1 Triglyceride (TG) and cholesterol (CHOL) measurement 152
2.3.5.2 Recovery 155
2.3.5.3 Comparison of normolipidemic and hyperlipidemic plasma 156
2.3.5.4 Interspecies differences 158
2.3.5.5 Comparison of the ratio of DEA to AM in different fractions 159
2.3.6 In vitro metabolism of AM to DEA in hepatic and intestine of rat (Microsomal studies) 161
2.3.6.1 Part 1- Microsomal incubation studies for the identification of enzymes involved in the metabolism of AM to DEA 161
a) Metabolism of AM in liver 161
b) Metabolism of AM in Jejunum 166
c) Chemical Inhibition in liver 170
d) Chemical inhibition in intestine 173
e) Inhibition constant 177
f) Immunoinhibition studies 178
2.3.6.2 Part 2- Effect of hyperlipidemia on the hepatic metabolism of AM to DEA 181
2.3.7 Western blot analysis 192
3 DISCUSSION AND CONCLUSION 193

3.1 Discussion 193
3.1.1 A liquid chromatography-mass spectrometry assay method for simultaneous determination of amiodarone and desethylamiodarone in rat specimens 193
3.1.2 Pharmacokinetics of Amiodarone in Hyperlipidemic and High Fat Meal Simulated Rat Models 196
3.1.3 Determination of the enzyme (s) involved in the metabolism of amiodarone in rat liver and intestine of rat: The contribution of Cytochrome P450 3A isoforms 199
3.1.4 The influence of hyperlipoproteinemia on in vitro distribution of amiodarone and desethylamiodarone in human and rat plasma lipoproteins 202
3.1.5 The impact of hyperlipidemia on the tissue distribution and hepatic metabolism of amiodarone and its active metabolite desethylamiodarone in the rat 205
3.1.6 The impact of lipids on the intestinal metabolism of amiodarone to desethylamiodarone in the rat 211
Conclusion 216
Future Directions 219

LIST OF TABLES

Table 1: Validation data for DEA measured by the HPLC method from 35 to 1000ng/ml (intraday) (n=5) 108

Table 2: Validation data for the assay of AM and DEA in rat plasma by LC/MS 112

Table 3: The individual relevant pharmacokinetic data in seven normolipidemic (NL) rats after the intravenous administration 115

Table 4: The individual relevant pharmacokinetic data in seven peanut oil+1% cholesterol treated rats after the intravenous administration of 25 mg/kg of AM 117

Table 5: The individual relevant pharmacokinetic data in seven P-407 treated rats after the intravenous administration of 25 mg/kg of AM 119

Table 6: The individual relevant pharmacokinetic data in six NL rats after the oral administration of 50 mg/kg of AM 122

Table 7: The individual relevant pharmacokinetic data in six peanut oil +1% cholesterol treated rats after the oral administration of 50 mg/kg of AM 124

Table 8: Pharmacokinetics of amiodarone after administration to rats in control (fasted normolipidemic) rats and in animals pretreated with peanut oil or poloxamer 407 127

Table 9: The individual relevant pharmacokinetic data in drug interaction study after iv administration of 25 mg/kg of AM to six control rats 129

Table 10: The individual relevant pharmacokinetic data in drug interaction study after iv administration of 25 mg/kg of AM to six KTZ treated rats 131

Table 11: The individual relevant pharmacokinetic data in five control rats after oral administration of 50mg/kg of AM 133

Table 12: The individual relevant pharmacokinetic data in drug interaction study after oral administration of 50 mg/kg 135

Table 13: Pharmacokinetic parameters (mean±SD, range in parenthesis) of amiodarone and desethylamiodarone after i.v. and oral administration in rats in the absence (controls) and presence of oral ketoconazole (17.1 mg/kg × 3 doses over 1 day) 138

Table 14: The mean± SD of the AUC0-72 (μg.h/g) of AM and DEA in different tissues of Sprague –Dawley rats after IV injection of 25 mg/kg of AM 142

Table 15: The mean ±SD cholesterol and triglyceride present in human and rat plasma samples before the separation of lipoprotein fractions 153

Table 16: The mean ±SD triglyceride and cholesterol concentrations (mg/dL) in plasma lipoprotein fractions from normolipidemic (NL) and hyperlipidemic (HL) plasma specimens of human and rat 154

Table 17: Association of AM and DEA in each fraction of normolipidemic (NL) and hyperlipidemic (HL) human and rat plasma samples 155

Table 18: Percentage of association of AM and DEA in each fraction of normolipidemic (NL) and hyperlipidemic (HL) human and rat plasma samples 157

Table 19: Ratio (mean±SD) of DEA: AM within each fraction derived from normolipidemic (NL) and hyperlipidemic (HL) plasma 160

Table 20: Rate of In vitro metabolism of AM to DEA in four individual rat livers (Real data) 162

Table 21: Rate of In vitro metabolism of AM to DEA in four individual rat livers (Fitted data) 163

Table 22: Enzyme kinetic parameters for DEA formation by individual rat liver microsomes, based on results of fitted data 165

Table 23: Rate of In vitro microsomal metabolism of AM to DEA in four individual intestines (Real data) 167

Table 24: Effect of increasing concentrations of ketoconazole on DEA formation in the presence of three concentrations of AM in liver microsomes 171

Table 25: Effect of increasing concentrations of ketoconazole on DEA formation in the presence of three concentrations of AM in rat intestinal microsomes 174

Table 26: Determination of kinetic parameters in rat liver microsomes based on fitting data on a two enzyme model 177

Table 27: Rate of In vitro metabolism of AM to DEA in four individual rat normolipidemic (NL) livers (Real data) 183

Table 28: Rate of In vitro metabolism of AM to DEA in four individual normolipidemic (NL) rat livers (Fitted data) 184

Table 29: Rate of In vitro metabolism of AM to DEA in four individual hyperlipidemic (HL) rat livers (Real data) 185

Table 30: Rate of In vitro metabolism of AM to DEA in four individual hyperlipidemic (HL) rat livers (Fitted data) 186

Table 31: Enzyme kinetic parameters for desethylamiodarone formation by rat NL and HL liver microsomes from four individual rats, based on results of fitting of data 191

Table 32: Available methods for determination of amiodarone (AM) and desethylamiodarone (DEA) in biological fluids, using mass detection 194

List OF FIGURES

Figure 1: Stereochemistry of TG structure. The R1, R2 and R3 represent the fatty acids acylated at the sn-1, sn-2 and sn-3 positions, respectively. Adapted from [10] 3

Figure 2: Gastric lipase cleaves off a fatty acid residue from the glycerol skeleton of triglycerides (TGs), leading to formation of a diglyceride and free fatty acid. 3

Figure 3: The amphiphilic structure of a representative bile salt with both lipophilic and hydrophilic groups. Hydrophilic groups are circled. 4

Figure 4: Pancreatic lipase cleaves off two fatty acid residues from the glycerol skeleton of triglycerides (TGs), leading to formation of a monoglyceride and two free fatty acids. 6

Figure 5: Schematic depiction of Lipase activation by colipase and a mixed micelle in duodenum. Coilpase facilitates the binding of lipase to triglyceride emulsion. Colipase forms a 1:1 complex with bile salt micelles at a common binding site. Colipase first attaches to the oil- water interface and lipase binds to colipase. Configuration of both inactive lipase and colipase change when they take part in the active complex form........ 7

Figure 6: Fatty acids and monoglyceride liberation from fat globules by lipase. These end products are aggregated into micelles, which are in equilibrium with the dissolved molecules, fatty acids and MGs. Simple diffusion is the most prevalent method for crossing of FAs and MGs from intestinal epithelium. 8

Figure 7: The role of the unstirred water layer in lipid absorption.................................. 11

Figure 8: Triacylglycetrol biosynthesis pathways in intestinal.mucosal cells might pass through one of the two main pathways. Monoglycerol (MG) pathway is involved in the direct acylation of absorbed MGs with activated free FAs (activated with acethyl coA). This pathway is exclusive for intestinal mucosal cells. The second pathway, which takes place in most tissues is involved in the activation of glycerol phosphate by acethyl coA, to form phosphatidic acid, dephosphorilation of phosphatidic acid to form DG and then TG by further acethylation. From [6] and [55]. 14

Figure 9: The role of rough endoplasmic reticulum and Golgi complex in CM and VLDL biosynthesis in intestinal lumen. The source of apo B48 and apo B100 are different. Apo B48 is synthesized in the rough endoplasmic reticulum of enterocytes; however liver is the source of Apo B100. These two forms of apolipoproteins are transported to smooth endoplasmic reticulum and take part in the synthesis of partially mature CM or immature VLDL. Golgi complex is the organ for further maturation of CM and VLDL. 16

Figure 10: Assembly of primordial lipoproteins.In this step apo B is associated with PLs and neutral lipids (TGs). MTP has the crutial role in release of primordial lipoproteins from the ER membrane. 18

Figure 11: The formation of a TG-rich lipid droplet. This step is independent of apo B. The size of these droplets increases by adding more TGs to their core. Pluronic L81 is able to block this step and decrease the stability of lipid droplets.................................. 19

Figure 12: Formation of VLDL and CMs in core expansion process. In this step, primordial lipoproteins and TG rich lipid droplets fuse together to form large size CMs or intestinal VLDL. 20

Figure 13: Absorption and transport of lipids in enterocytes. The absorption of MGs and FAs into enterocytes is followed by TG synthesis, which in turn package into CMs or VLDL. CMs then exocytose into intestinal fluid and enter lymph via lacteals................ 21

Figure 14: Catabolism of CMs by liver in three steps of sequestartion (interaction of CM-remnants with either HSPGs matrix or cell surface receptors in the space of Disse), processing (further processing of CM remnenrs including lipid transfer or lipolysis in the space of Disse) and internalization (taking up of enriched remnants by hepatocytes via lipoprotein receptors). From [81]... 25

Figure 15: VLDL biosynthesis in hepatic cells. This procedure starts with the association of TAG droplets with PL and apo B containing VLDL precursors in the reticuloendothelial system of hepatocytes. 27

Figure 16: VLDL catabolism in body. VLDL particles are synthesized in liver and catabolized by LPL to IDL and consequently LDL. Specific apolipoproteins are involved in the biosynthesis and uptake of these particles in hepatic tissue. Furthermore, CETP is an important enzyme in the transport of TG and CEs between HDL, IDL or LDL. 28

Figure 17: Role of scavenger receptors in the removal of LDL particles and atherosclerosis. Atherosclerosis starts with retention and subsequent oxidization of LDL particles to oxLDL within the matrix of vascular intima. To remove these potentially harmful particles (oxLDL), circulating monocytes migrate through endothelial layer into intima, where they start to differentiate into macrophages. The scavenger receptors which are located on the surface of macrophages recognize and remove oxLDL. The saturation of macrophages with oxLDL results into the formation of foam cells. Stimulation of Monocytes by interleukin-6 and migrated vascular smooth muscle cells results into the releasing of tissue factor, which by itself can activate the formation of thrombin from prothrombin. Thrombin by itself can activate fibrin formation. Over production of dimers and macrophage derived apoptotic bodies results into fibrin proteolysis in both circulatiuon and advanced atherosclerotic lesions. From [107] 31

Figure 18: Chemical structure of amiodarone. Shaded area (butyl side chain) is one of the main part of the molecule responsible for the unique pharmacokinetic properties of AM. 71

Figure 19: HPLC chromatograms of drug free rat plasma, extracted rat plasma spiked with 500 ng/ml of AM and DEA and extracted plasma from traeated rats with 25 mg/kg of AM as single iv injection, 48 postdose. Both samples were spiked with 1500 ng/ml of ET before extraction procedure 106

Figure 20: A representative standard curve of DEA in rat plasma (From 35 to 1000 ng/ml). Data weighted by a factor of 1/concentration 107

Figure 21: Mass spectra of drug (AM) (*m/z*=645.92), metabolite (DEA) (*m/z*=617.90 and 546.84) and ethopropazine (internal standard) (*m/z*=313.09) 109

Figure 22: Overlay SIR chromatograms of blank plasma, I.S. (4.32 min), DEA (9.74 min) and AM (10.0 min) after extraction from rat plasma 109

Figure 23: Linearity of the LC-MS assay in rat plasma from 2.5 to 1000 ng/ml for both AM and DEA 110

Figure 24: Linearity of the assay in rat liver from 5-1000 ng/ml for both AM and DEA 111

Figure 25: Individual plasma concentration versus time curves of AM in seven normolipidemic (NL) control rats after iv injection of 25 mg/kg of drug 116

Figure 26: Individual plasma concentration versus time curves of AM in seven rats treated with 1% cholesterol in peanut oil after iv injection of 25 mg/kg of drug 118

Figure 27: Individual plasma concentration versus time curves of AM in seven P-407 treated rats after iv injection of 25 mg/kg of drug 120

Figure 28: Mean ± SD plasma concentration versus time profile of amiodarone after 25 mg/kg intravenous doses of amiodarone HCl given to normolipidemic (n=7), hyperlipidemic (PLX treated or HL rats n=7) peanut oil fed (n=7) rats 121
Figure 29: Individual plasma concentration versus time curves of AM in six control rats after oral administration of 50 mg/kg of drug 123
Figure 30: Individual plasma concentration versus time curves of AM in six peanut oil-treated rats (PO) after oral administration of 50 mg/kg of drug 125
Figure 31: Mean ± SD plasma concentration versus time profile of amiodarone for the first 24 h after 50 mg/kg oral doses of amiodarone HCl given to normolipidemic (n=6) and peanut oil fed (n=6) rats 126
Figure 32: Individual plasma concentration versus time curves of AM in six control rats after iv administration of 25 mg/kg of AM 130
Figure 33: Individual plasma concentration versus time curves of AM in six KTZ treated rats after iv administration of 25 mg/kg of AM 132
Figure 34: Individual plasma concentration versus time curves of AM in five control rats after oral administration of 50 mg/kg of AM (drug interaction study) 134
Figure 35: Individual plasma concentration versus time curves of AM in five KTZ-treated rats after oral administration of 50 mg/kg of AM 136
Figure 36: Mean ± SD plasma concentration versus time profile of amiodarone with and without ketoconazole after single 25 mg/kg intravenous (A) or 50 mg/kg oral (B) doses of amiodarone HCl 137
Figure 37: Amiodarone concentration-time profile in plasma, lung, liver, kidney, spleen, fat, brain and heart following single intravenous administration of 25 mg/kg in of amiodarone in control (NL) and P-407-treated (HL) rats 143
Figure 38: Desethylamiodarone concentration–time profile in plasma, lung, liver, kidney, spleen, fat, brain and heart following single iv. administration of 25 mg/kg of amiodarone in control (NL) and P-407-treated (HL) rats 144
Figure 39: The examination of the effect of hyperlipidemia on distribution of amiodarone and desethylamiodarone in thyroid glands 24 h postdose 145

Figure 40: Kp of postdistributive concentrations. Asterisks indicate the significant differences (P<0.05) between the normolipidemic and hyperlipidemic rats. Kp indicates the ratio of tissue to plasma concentrations ... 146

Figure 41: The ratio of postdistributive concentrations of DEA to AM. Asterisks indicate the significant differences (P<0.05) between the normolipidemic and hyperlipidemic rats ... 147

Figure 42: Concentrations of AM and DEA in gut segments (G1-G5) after incubation of everted gut for 2 hours. Treatments ... 150

Figure 43: The ratio of DEA to AM in each segment expressed as a percent of the total amount of AM present in each segment (G1-G5). Treatments were rats given normal diet, with guts incubated with control (Krebs-Heinseleit, CON), 5% SBS in Krebs-Heinseleit (5), 25% SBS in Krebs-Heinseleit (25), and peanut oil treated rats (PO), with guts incubated with 25% SBS in Krebs-Heinseleit ... 151

Figure 44: Concentrations of AM, DEA and metabolite: drug ratio, when all segments (G1-G5) from incubations involving 25% SBS were combined. Broken lines between groups indicate significant differences. 25% SBS in Krebs-Heinseleit (25), peanut oil treated rats (PO), with guts incubated with 25% SBS in Krebs-Heinseleit, 25% SBS in Krebs-Heinseleit with 5% Intralipid (INLP) ... 152

Figure 45: Association of amiodarone (AM) and desethylamiodarone (DEA) with lipoprotein fractions isolated from hyperlipidemic (HL) or normolipidemic (NL) plasma, expressed as percent of total recovery of drug and metabolite. Continuous lines over fractions indicates lack of significance between fractions encompassed by the lines; fractions not encompassed within lines are significantly different from those fractions encompassed by the lines (Kruskal-Wallis One Way Analysis of Variance on Ranks, p<0.05) ... 158

Figure 46: Mean±SD differences between human and rat for disposition of AM and DEA within different lipoprotein fractions from NL and HL plasma. * represent significant differences. (Student's unpaired t-test, p<0.05) ... 159

Figure 47: Rate of DEA formation in liver microsomes of Sprague-Dawley rat after 30 min incubation with increasing concentration of AM (Fitted data) ... 164

Figure 48: Rate of DEA formation in intestinal microsomes of Sprague-Dawley rat after 30 min incubation with increasing concentration of AM 168

Figure 49: Rate (mean ± SD) of DEA formation in liver (A) and intestinal (B) microsomes of Sprague-Dawley rat after 30 min incubation with increasing concentration of AM (x-axis) 169

Figure 50: Effect of increasing concentrations of ketoconazole on DEA formation in individual liver microsomes of four individual rats.. 172

Figure 51: Effect of increasing concentrations of KTZ on DEA formation in individual intestinal microsomes of four individual rats.. 175

Figure 52: Effect of increasing concentrations of ketoconazole on DEA formation (y-axis) in the presence of three concentrations of AM. A. Liver microsomes, B. Intestinal microsomes. Breaks between horizontal lines above data bars denote significant differences from other data at the same concentration of AM (Duncan's multiple range post-hoc test)... 176

Figure 53: Determination of ki in rat liver microsomes by Dixon plot. Data were fitted to a two enzyme model with results of model fits being represented by the solid lines..... 178

Figure 54: Immunoinhibition studies in liver and intestinal (gut) microsomal protein (0.4 mg/ml) coincubated with amiodarone (64 and 94 μM for liver and intestine respectively) and antibodies to either A.) CYP1A2; B.) CYP2B1/2 or C.) CYP3A2. Matching control incubations without antibody are shown.. 179

Figure 55: Formation of DEA from 37.6 μM AM in the presence of CYP1A1 or CYP3A1 Supersomes, in the absence (control) and presence of 18.8 μM KTZ. Asterisks denote significant difference from corresponding control incubation.. 180

Figure 56: Comparison the levels of total P450 in normolipidemic and hyperlipidemic rat liver microsomes. Asterisks denotes the significant difference between two groups (P<0.05) 182

Figure 57: Michaelis-Menten plots (single liver microsomes) in the formation of desethylamiodarone from amiodarone (AM) in normolipidemic (NL) and hyperlipidemic (HL) liver microsomes of Sprague- Dawley rat (Fitted data)... 187

Figure 58: Eadie-Hofstee plots (single liver microsomes) in the formation of desethylamiodarone from amiodarone (AM) in normolipidemic (NL) and hyperlipidemic (HL) liver microsomes of Sprague- Dawley rat (Fitted data).. 188

Figure 59: Clearance plots (single liver microsomes) in the formation of desethylamiodarone from amiodarone (AM) in normolipidemic (NL) and hyperlipidemic (HL) liver microsomes of Sprague- Dawley rat (Fitted data).. 189

Figure 60: Representative Michaelis-Menthen (A), Eadie-Hofstee (B) and clearance (C) plots in formation of desethylamiodarone from amiodarone (AM) in normolipidemic (NL) and hyperlipidemic (HL) liver microsomes of Sprague- Dawley rat 190

Figure 61: The effect of hyperlipidemia (HL) on expression of different P450 enzymes in Sprague- Dawley rat liver microsomes shown by Western blot.................................... 192

Figure 62: Concentrations of AM, DEA and metabolite:drug ratio when all segments (G1-G5) were combined. Broken lines between groups indicate significant differences. Krebs-Henseleit (CON), 5% SBS in Krebs-Heinseleit (5), 25% SBS in Krebs-Heinseleit (25), 25% SBS in Krebs-Heinseleit in peanut oil rats (PO).. 215

ABREVIATIONS AND SYMBOLS

µL	Microliter
µM	Micromolar
µm	Micrometer
µmol	Micromol
~	Approximately
ABC	ATP-Binding cassette
AM	Amiodarone
Apo	Apolipoprotein
ATP	Adenosine triphosphate
AUC	Area under the concentration versus time curve
BBB	Blood Brain Barrier
BSA	Bovine serum albumin
CAD	Coronary artery disease
CE	Cholestryl ester
CEL	Carboxyl ester lipase
CETP	Cholestryl ester transfer protein
CHOL	Cholesterol
CL	Total body Clearance
CL/F	Body clearance after oral dose
Clint	Intrinsic clearance
CLmax	Clearance maximum
CM	Chylomicron
Cmax	Peak plasma drug concentration
CMC	Critical micellar concentration
CV	Coefficient of variation
CYA	Cyclosporine A
CYP	Cytochrome P450
CYP450	Cytochrome P450

DEA	Desethylamiodarone
DG	Diglyceride
ELISA	Enzyme linked ImmunoSorbent Assay
F	Oral bioavailability
fa/fa	Fatty/Fatty
FAs	Fatty acids
GIT	Gastrointestinal tract
GST	Glutathione S-transferase
GTG	Gold thioglucose
HCl	Hydrochloric acid
HDL	High density lipoprotein
HF	Halofantrine
HFD	High fat diet
HPL	Hepatic lipase
HL	Hyperlipidemia (Hyperlipidemic)
HPLC	High performance liquid chromatography
Hrs	Hours
HSPG	Heparin sulfate proteoglycan
i.p	Intraperitonealy
i.v	Intravenously
IDL	Intermediate density lipoprotein
IgG	Immunoglobuline G
INLP	Intralipid
IS	Internal standard
KCl	Potassium chloride
KH	Krebs-Heinseleit bicarbonate buffer
KH_2PO_4	Potassium dihydrogen phosphate
Km	Affinity constant
Kp	Tissue to plasma concentration
Kpu	Tissue AUC to unbound plasma concentration

KTZ	Ketoconazole
LC-MS	Liquid chromatography-mass spectrometery
LCAT	Lecithin-cholesterol acyl transferase
LDL	Low density lipoprotein
LLQ	Lower limit of quantification
Log p	Logaritm partition coefficient
INLP	Intralipid
LPC	Lysophosphatidylcholine
LPDP	Lipoprotein deficient fraction
LPL	Lipoprotein lipase
LPs	Lipoproteins
MDR	Multi drug resistance associated protein
MFO	Mixed function oxidase
MG	Monoglyceride
mg/dl	Miligram/deciliter
mg/kg	Milligram/kilogram
$MgSo_4$	Magnesium sulfate
Min	Minutes
mRNA	Messenger RNA
MS	Mass spectrometer
MTP	Microsomal triglyceride transfer protein
MUFA	Mono unsaturated fatty acids
NADPH	β-Nicotinamide adenine dinucleotide phosphate tetra sodium
ng	Nanogram
NL	Normolipidemic
nm	Nanometer
OATP	Organic anion transport protein
°C	Degree celsius
oxLDL	Oxidized LDL

P-407	Poloxamer 407
P-450	Cytochrome P-450
PC	Phosphatidylcholine
PCBs	Polychlorinated biphenyls
P-gp	P-glycoprotein
PL	Phospholipid
PLX	Poloxamer 407
PUFA	Poly unsaturated fatty aids
r^2	Correlation coefficient
RCT	Reverse cholesterol transport
rpm	Rotations per minute
SBS	Simulated bile solution
SD	Standard deviation
SIR	Selective ion recorder
SR-B1	Scavenger receptor B1
t1/2	Terminal elimination phase half-life
TAG	Triacylglycerol
TG	Triglyceride
T_{lag}	Lag time
Tmax	Time to reach C_{max}
TPN	Total parentral nutrition
TRL	Triglyceride-rich lipoproteins
u/ml	Unit/milliliter
UGT	UDP-glucoronyltransferase
UV	Ultraviolet
V/V	Volume/Volume
VCR	Vincristine
Vd	Volume of distribution
Vdss	Volume of distribution at steady state
VLDL	Very low density lipoprotein
Vmax	Maximum rate of formation

Vmax/km	Intrinsic clearance
Vs.	Versus
W/V	Weight/Volume
W/W	Weight/Weight
α	Level of significance
λ_z	Elimination rate constant

1 INTRODUCTION

1.1 *Lipid*

Lipids comprise the average 30-40% of the daily energy intake of a regular person's diet in North America [1]. Due to the link between the amount of fat in diet and range of chronic diseases, more attention has been attributed toward this macro constituent of the diet in recent years [2]. A downward trend had been observed in the total fat consumption during 1965-1991. Unfortunately this downward trend is not associated with a decrease in the consumption of saturated fats that play a critical role in the progression of coronary heart diseases, which in turn represents a major public health concern [3].

Regardless of the effect of lipids in coronary diseases, lipids play a pivotal role in the normal physiology of the human body. Among different kinds of lipids, CHOL and PLs are categorized as structural macronutrients. The biological role of these macronutrients in the fundamental structure of cell membranes and steroid hormones has been a topic of many research papers in the last few years. Triglycerides [4], the other important class of macronutrient is an important energy source for cells. Some other lipophilic materials such as phytosterols, flavonoids, carotenoids, polyphenols, isothiocyanates, indoles, terpenoids, and fat soluble vitamins are categorized under micronutrients [5]. The vast biological roles of these micronutrients should be considered separately.

1.2 *Lipid metabolism*

1.2.1 Lipid digestion

Lipid digestion is a complex process comprising different steps including pre-duodenal digestion, emulsification, intestinal digestion, absorption and transport of digested lipids, intracellular metabolism and formation of lipoproteins. Each single step is considered in detail as follows.

1.2.1.1 Pre-duodenal enzymatic digestion

The secretion of lingual lipase from Ebner's glands at the mouth is the starting point for lipid digestion (Hamosh, Ganot et al. 1979; Mu and Hoy 2004). The lipase activity of this enzyme is not sufficient to completely digest the dietary lipids; however the transport of lingual lipase along with food to the stomach has an additive effect on the activity of gastric lipase or acid lipase secreted by gastric mucosa. It has been observed that the lipase activity of this enzyme is dependent upon the pH of the gastric moiety. The highest activity of gastric lipase is detected in the stomach fundus [6]. The medium chain fatty acids are more susceptible than long and short chain fatty acids to hydrolysis at the optimum pH of gastric lipase activity. Hydrolysis in the stomach takes place for only 10-30% of dietary fat [7]. The substrate of such an enzymatic procedure is the triglyceride (TG) content of fat food, which comprises about 90% of the dietary fat [8] (Figure 1). The main products of such a hydrolytic procedure are diglycerides and fatty acids. Both lipases preferentially hydrolyze the sn-3 ester bond resulting to formation of sn1, 2 – diglycerides [9, 10] (Figure 2).

In spite of the lingual and gastric lipase activities in the upper part of the GI tract, most of the lipid digestion does not start until lipids reach the small intestine [11]. The reason is the incompatibility between the HCl-rich water content of stomach and the lipophilicity of dietary fats which prevents ingested fat from efficiently mixing with the rest of the stomach contents. Therefore, large fat globules are formed with the very high surface area in the stomach. Gastric lipase lacks the ability to digest the formed large fat globules in stomach because most parts of the lipid globules are not accessible by gastric lipase [11].

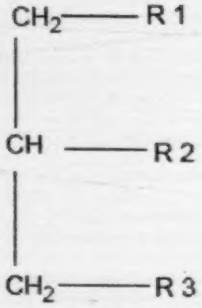
CH2
R 1
CH
R 2
CH2
R 3

Figure 1: Stereochemistry of TG structure. The R1, R2 and R3 represent the fatty acids acylated at the sn-1, sn-2 and sn-3 positions, respectively. Adapted from [10]

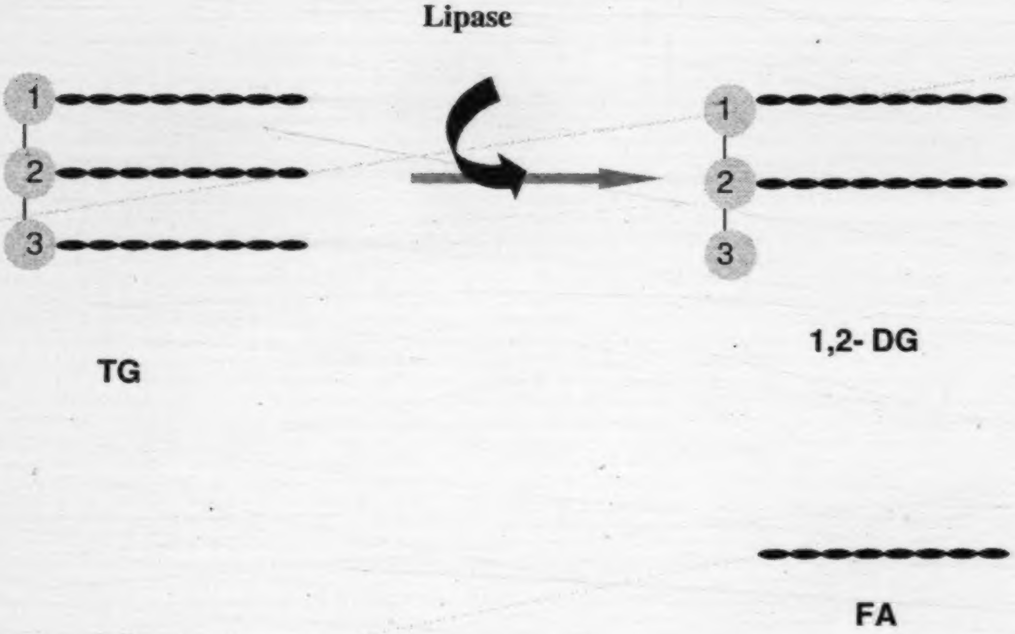
Lipase
1
2
3
TG
1
2
3
1,2- DG
FA

Figure 2: Gastric lipase cleaves off a fatty acid residue from the glycerol skeleton of triglycerides (TGs), leading to formation of a diglyceride and free fatty acid.

1.2.1.2 Bile and bile salt micelles, emulsification process

In humans, transport of the high surface area fat globules to the proximal small intestine (duodenum) stimulates the secretion of bile from the gall bladder [11]. Bile is composed of water (84%), bile salts (11.5%), cholesterol (CHOL) (0.5%), lecithin (3%) and some other components such as bile pigments (1%) [11]. The most important constituent of bile is the bile acids. Bile salts are the structurally modified derivatives of CHOL (Figures 3, 4), which interestingly possesses both polar (hydroxyl and carboxyl groups) and non polar groups [11]. The amphiphilic characteristics of CHOL or in more general terms, bile acids enables them to bind to both hydrophilic and lipophilic molecules [11]. In contact with large fat globules, the hydrophobic side of bile salts faces inward and makes a contact with fat globules, but the hydrophilic part faces outward. In this case, the polar coating of fat globules can make contact with the water content of digestive fluid in the intestine and break apart into smaller droplets called micelles. This process is called emulsification [11].

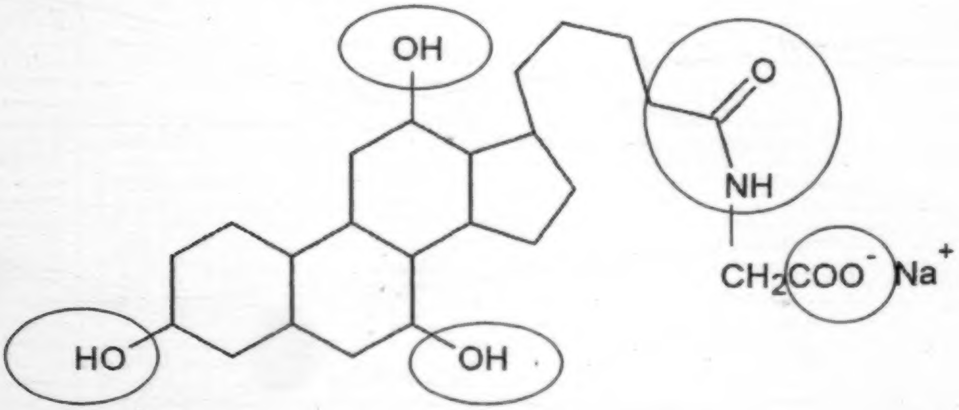

Figure 3: The amphiphilic structure of a representative bile salt with both lipophilic and hydrophilic groups. Hydrophilic groups are circled.

In fact, emulsification is the first step involved in the enzymatic hydrolysis of dietary TGs [11]. As it was noted earlier, different processes are involved in the digestion of the other constituents of dietary lipids such as PLs and CEs, which are delivered untouched to the duodenum lumen. The processes involved in digestion of PLs and CEs will be considered later.

1.2.1.3 Intestinal enzymatic digestion of triglycerdes, the function of triglyceride lipase and colipase

The formed micelles are the substrates of enzymatic digestion of the pancreatic lipase. Pancreatic lipase is abundant in pancreatic juice, representing 2-3% of the total presented protein [12]. Pancreatic lipase or pancreatic triglyceride lipase is released from pancreatic tissue into the duodenum in response to cholecystokinin [13], which is a regulatory peptide secreted by mucosal cells in the duodenum. PTL breaks down triglycerides at the 1 and 3 positions leading to the formation of 2-monoglycerides (2-MG) and fatty acids (FA) [14] (Figure 4). 2-MG is the most prominent form of the MGs, although some 1-MG may also form from the isomerization process of 2-MG to 1-MG [15].

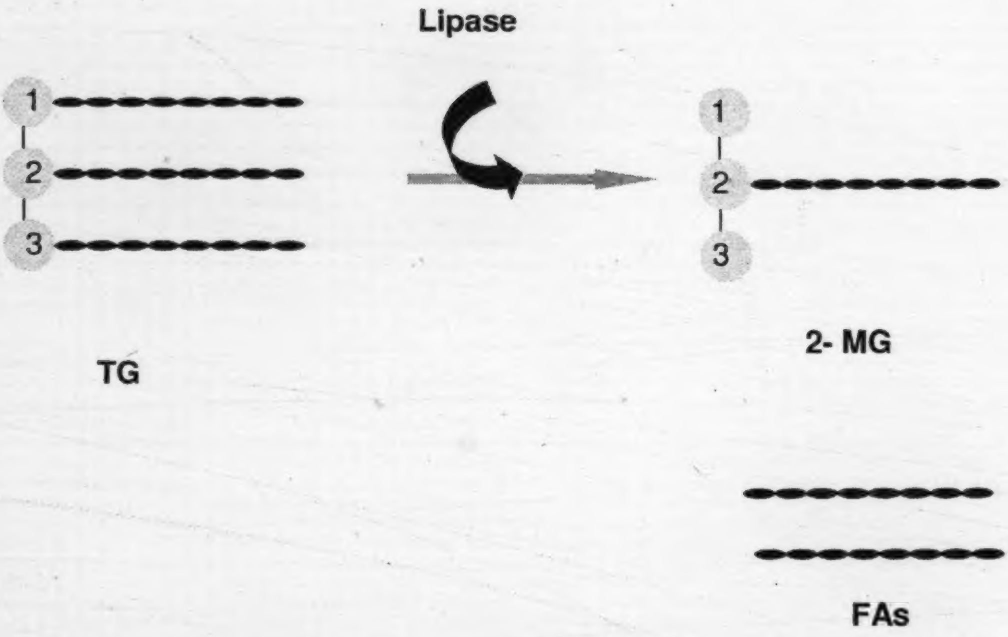

Figure 4: Pancreatic lipase cleaves off two fatty acid residues from the glycerol skeleton of triglycerides (TGs), leading to formation of a monoglyceride and two free fatty acids.

The presence of colipase is required for the normal digestive action of PTL [16]. Colipase is a cofactor that binds to oil emulsions and facilitates the binding of lipase to triglyceride emulsion. It also prevents the irreversible inactivation of lipase, which might be exerted by high concentrations of bile salts. In other words, in the presence of very low concentrations of bile salts, lipase demonstrates some lipophilic properties. When the bile salt concentration increases and reaches the critical micellar concentration (CMC), lipophilic properties of lipase are completely inhibited. The inhibition of the lipophilic activity can be reversed by the addition of colipase [17]. It has been identified that colipase first attaches to the oil- water interface and lipase binds to colipase. The lipase and colipase complex at the interface prevents the irreversible inactivation of lipase by triglyceride and at the same time allows lipase to approach the interface [17, 18]. It has been reported that colipase also forms a 1:1 complex with bile salt micelles at a common binding site [18-20]. (Figure 5, 6)

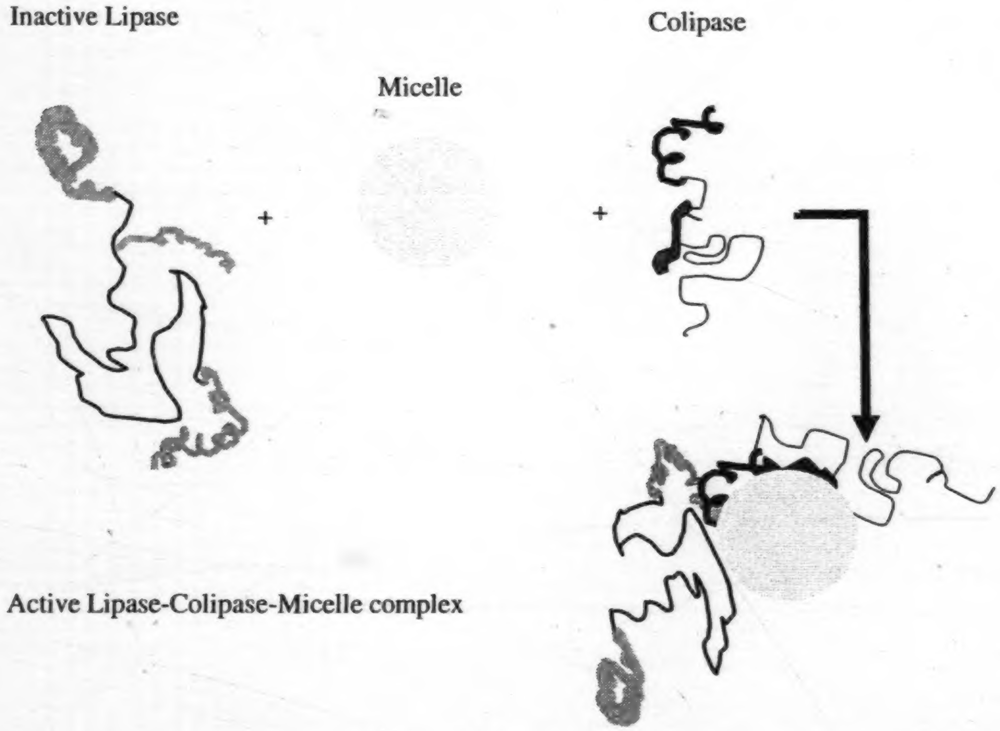
Inactive Lipase
Micelle
Colipase
+
+
Active Lipase-Colipase-Micelle complex

Figure 5: Schematic depiction of Lipase activation by colipase and a mixed micelle in duodenum. Coilpase facilitates the binding of lipase to triglyceride emulsion. Colipase forms a 1:1 complex with bile salt micelles at a common binding site. Colipase first attaches to the oil- water interface and lipase binds to colipase. Configuration of both inactive lipase and colipase change when they take part in the active complex form.

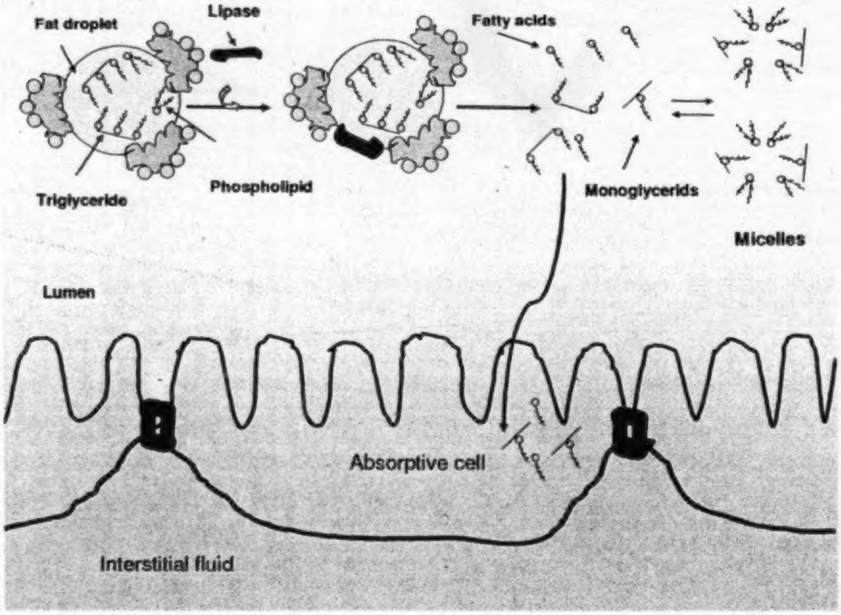
Fat droplet
Lipase
Fatty acids
Triglyceride
Phospholipid
Monoglycerids
Micelles
Lumen
Absorptive cell
Interstitial fluid

Figure 6: Fatty acids and monoglyceride liberation from fat globules by lipase. These end products are aggregated into micelles, which are in equilibrium with the dissolved molecules, fatty acids and MGs. Simple diffusion is the most prevalent method for crossing of FAs and MGs from intestinal epithelium.

1.2.1.4 Enzymatic intestinal digestion of dietary phospholipids

The digestion of PLs takes place in the small intestine; therefore gastric lipase has no role in the digestion of PL. The predominant PL in bile is phosphatidylcholine (PC), which is found along with CHOL and bile salts [12]. PC is the substrate of pancreatic phospholipase A_2 in the intestinal lumen. Phospholipase A_2 acts on the sn-2 position of PC to yield FA and lysophosphatidylcholine (LPC) [21].

1.2.1.5 Enzymatic intestinal digestion of dietary cholesterol and cholestryl ester

Only 8-15% of the dietary CHOL is found as its ester form with fatty acids (CE). The remaining 85-92% is present as its free form [22]. The dietary CHOL appearing in duodenal lumen is mixed with CHOL secreted from the liver into the bile and PL as vesicles or in bile salt micelles [23]. Additionally, TGs are also available in these lipid emulsions. The digestion of CHOL in lipid emulsions needs the primary digestion of PLs and TGs in the lipid emulsion particles by the lipase/colipase hydrolysis [24]. In addition to PTL and phospholipase A_2, some other enzymes and proteins such as carboxyl ester lipase (CEL) and pancreatic triglyceride lipase-related protein 1 and 2, which are similar in their structure to PTL, are available in pancreatic juice and are secreted prior to cholesterol digestion [22]. CEL is the enzyme that starts the hydrolyzation of CEs and facilitates the absorption of dietary CEs in the small intestine [25]. CEL is also called cholestryl ester hydrolase [26] or bile salt stimulated lipase or bile salt stimulated cholesterol esterase. Bile acids increase the activity of cholestryl esterase, which not only hydrolyzes CEs but also hydrolyzes TGs and phosphoglycerides [25, 27].

Along with digestion of TGs by PTL into free FAs and MGs in duodenum and upper jejunum, phospholipase A2 also digests PLs into free FAs and lysophopholipid as discussed earlier. The digested products, as well as ingested and biliary CHOL are incorporated into bile salt mixed micelles, which facilitate their absorption [22]. The absorption of bile salt mixed micelles is facilitated by the function of the unstirred water layer. The importance of this layer in the absorption of bile salt mixed micelle will be discussed in the following paragraphs. A delay in TG hydrolysis due to the lack of PTL in the intestinal lumen substantially reduces CHOL absorption in PTL -/- mice, but minimally affects fat absorption [28]. It has been demonstrated that in the absence of PTL, PTLRP-2, which is the major TG hydrolytic enzyme in neonates and remains present at the very low levels in adult pancreatic juice [29], may potentially serve as the compensatory enzyme [22].

Another enzyme, which may have a compensatory function in the absence of PTL, is CEL. It has been identified that CEL has a wide substrate reactivity including its hydrolysis of CEs, TGs, PLs and lysophospholipids [30].

1.2.2 Absorption of the digested lipids

Although passive diffusion is identified as the predominant pathway for absorption of micellar 2-MG and FAs through intestinal epithelial cells (enterocytes) [31, 32], some other investigators have indicated the existence of a binding protein associated with the absorption of FAs and CHOL [33, 34].

Absorption of LPC, which is the product of enzymatic reaction of phospholipase A_2 upon sn-2 position of PC, is mainly performed by reacylation of LPs to PC [35]

1.2.2.1 Passive diffusion of micellar lipids, unstirred water layer theory

The importance of micellar solubilization in the passive absorption of 2-MG and FAs was discussed by Dietschy [36]. Later, the importance of their theory in the absorption of CHOL was also identified [22]. According to their theory, which is called the unstirred water layer theory, the brush border membrane of enterocytes is separated from the bulk fluid phase in the intestinal lumen by an unstirred water layer. This layer does not mix with the bulk phase in the intestinal epithelial cells. Solute molecules in the intestinal lumen have access to the brush border membrane by diffusion across the unstirred water layer. Due to the low solubility of FA, MG and CHOL in this water layer, the number of the molecules that have access to the brush border membrane is small. When MG, FA and CHOL form the micellar form, their access to brush border membrane enhances. Consequently, the number of the MG and FA and CHOL micelles will increase although there is a decrease in the delivery speed of these molecules [33, 34, 36, 37]. (Figure 7)

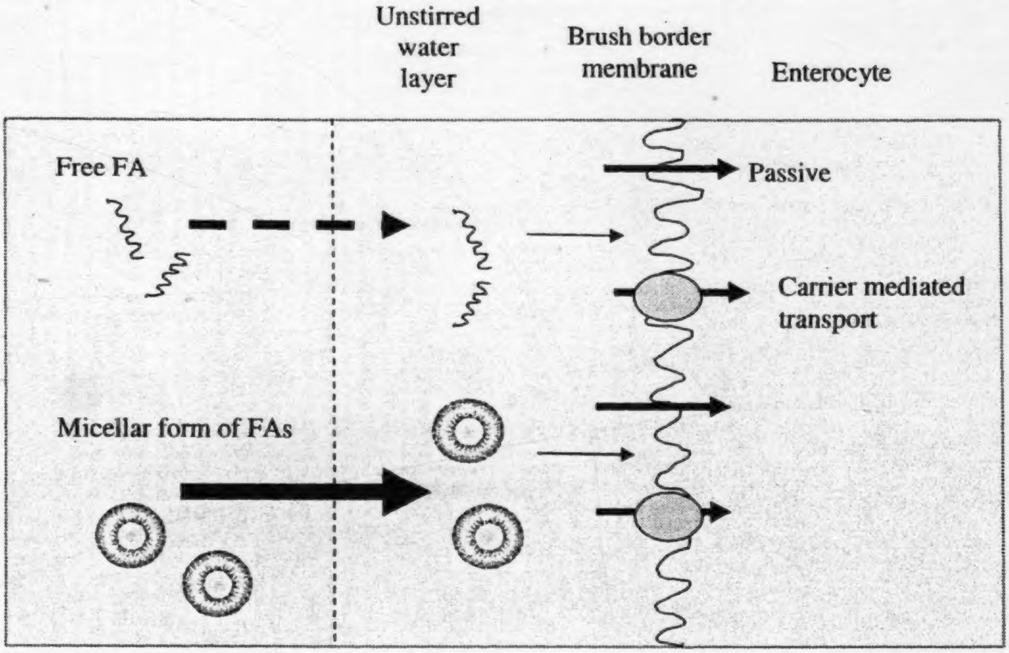

Figure 7: The role of the unstirred water layer in lipid absorption. The unstirred water layer seperates the brush border membrane (apical membrane) from the bulk fluid phase in the small intestine. The transport of free fatty acids from this membrane is carried out by passive diffusion; however in the transport of micelles, the carrier proteins are involved.

1.2.2.2 Transport mediated absorption of lipids

As was pointed out earlier, some investigators have indicated the existence of an active process in transport of FAs and MGs through intestinal epithelial cells. It means that their transport is facilitated by some transport proteins [33]. Chow and Hollander showed a dual concentration dependent and carrier mediated transport for linoleic acid uptake [37]. They demonstrated that at low concentrations of linoleate, a carrier mediated system is available for the transport of FAs through intestinal epithelial cells; however at high concentrations of FAs, their transport will be accomplished by simple diffusion. In other words, the transport protein will be saturated at the high concentrations of FAs [38].

Stremmel et al. [33] indicated that FA transport protein is not only able to transport FAs but also takes part in the transport of CHOL.

The importance of bile salt micelles in absorption of CHOL was discussed earlier. Currently, two major hypotheses are being considered in absorption of CHOL in the brush border membranes in the intestine. The first one considers the energy-independent passive diffusion process in which micellar CHOL is in equilibrium with monomolecular CHOL in solution. The absorption of CHOL is carried out by a concentration gradient in the brush border membrane [36, 39]. ABC transporters regulate the absorption of CHOL by this method [40].

A class of transport membrane protein known as ATP Binding Cassette (ABC) transporter located on the brush border membrane of the intestine regulates the amount of CHOL absorbed in the intestine. Studies with nuclear hormone receptor retinoid X Receptor) and liver X Receptor) agonists have demonstrated that the expression of ABCA1 gene is concomitant with a decrease in CHOL absorption from the intestinal lumen. These findings have been proven by both in vitro and in vivo experiments [40]. The study of Mulligan et al. [4] showed that ABCA1 transporters are located at the basolateral instead of apical membrane of enterocytes, and limit the CHOL absorption by secreting the internalized CHOL back to the intestine lumen [22]. Newer studies have indicated that apolipoprotein A1 (apo A-1) may also play a part in the back transport of CHOL by ABCA1 [41]. Recently, the function of two specific ABC half-transporters (ABCG5 and ABCG8) in pumping sterols out of enterocytes and hepatocytes was identified [42].

The second hypothesis involved in absorption of micellar CHOL is a protein mediated process [43]. The discovery of some inhibitors such as sterol glycoside (tiqueside [44] or L-166, 143) and ezetimibe [45, 46] has supported the protein mediated process in the absorption of micellar CHOL from enterocytes. This transport protein is called scavenger receptor-class B 1(SR-B1) [46]. Among the inhibitors of SR-B1, ezetimibe is found to be an effective CHOL- lowering agent in therapy [5, 47, 48]. Pancreatic cholesterol esterase

A protein, which is found in the brush border membrane of enterocytes, is identified as a second carrier of micellar CHOL [49]. Recently, a new carrier protein in the transport of CHOL in intestinal brush border has also been identified. The Niemann-Pick C1 Like 1 protein has been shown to play a pivotal role in the absorption of intestinal CHOL [50]. The Niemann-Pick C1 Like 1 protein gene is highly expressed in the brush border membrane of enterocytes and ezetimibe, a drug that inhibits CHOL absorption, had no effect in Niemann-Pick C1 Like 1 protein knockout mice [50].

1.2.3 Intracellular metabolism of absorbed lipids

Ockner and Maning in 1974 isolated and characterized the fatty acid binding protein from the rat jejunum by a gel filtration technique [38]. Fatty acid binding protein might participate in the translocation of FAs from the plasma membrane of enterocytes to the endoplasmic reticulum, where the biosynthesis of more complex lipids takes place [51, 52]. It has been observed that the level of fatty acid binding protein changes with the amount of dietary fat. The mechanism of such a change is not understood [52]. On the other hand, the translocation of CHOL from the outer mitochondrial membrane to the inner mitochondrial membrane in enterocytes is carried out by the function of non specific sterol carrier protein or sterol carrier protein 2 [51, 53]. sterol carrier protein 2 mediates other physiological functions such as microsomal conversion of lanosterol to CHOL and conversion of CHOL to CE [53].

The transported FAs and MGs in endoplasmic reticulum of enterocytes will take part in a reconstitution process and form TG. The main pathway involved in biosynthesis of TG in the intestinal mucosa is called the MG pathway in which 2-MG is reacylated into TG by the consecutive actions of monoglyceride acyl transferase and diacylglycerol acyltransferase. The enzymes involved in this pathway are present in a complex called "triglyceride synthetase" [54] (Figure 8).

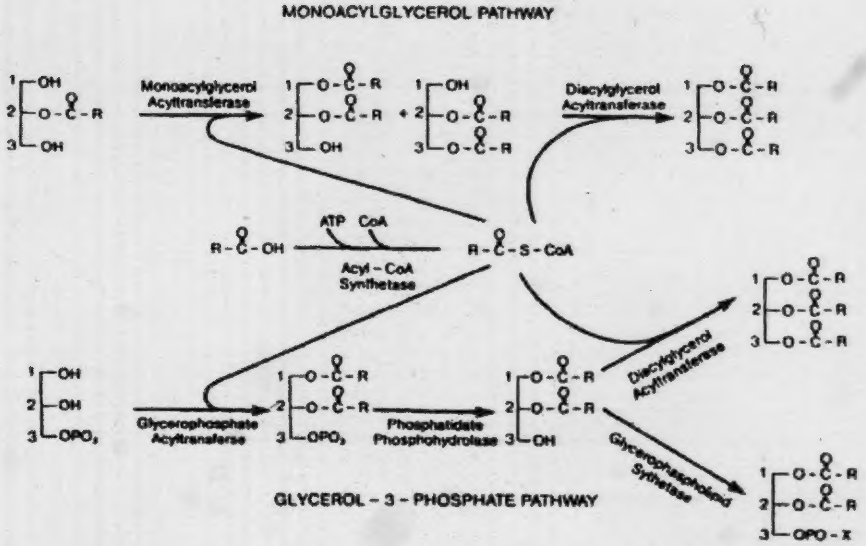
MONOACYLGLYCEROL PATHWAY
Monoacylglycerol Acyltransferase
Diacylglycerol Acyltransferase
ATP CoA
Acyl - CoA Synthetase
R-C-S-CoA
Glycerophosphate Acyltransferase
Phosphatidate Phosphohydrolase
Diacylglycerol Acyltransferase
Glycerophospholipid Synthetase
GLYCEROL - 3 - PHOSPHATE PATHWAY

Figure 8: Triacylglycetrol biosynthesis pathways in intestinal.mucosal cells might pass through one of the two main pathways. Monoglycerol (MG) pathway is involved in the direct acylation of absorbed MGs with activated free FAs (activated with acethyl coA). This pathway is exclusive for intestinal mucosal cells. The second pathway, which takes place in most tissues is involved in the activation of glycerol phosphate by acethyl coA, to form phosphatidic acid, dephosphorilation of phosphatidic acid to form DG and then TG by further acethylation. From [6] and [55].

The transported CHOL, is esterified to CE mostly by acylcoenzyme A:cholesterol acyltransferase2 [42]. LPC, which is the product of PLs digestion, is also reacylated to PC in enterocytes [9].

1.2.4 Multiple cholesterol transport pathways

It is believed that the dietary CHOL enters the body as a part of chylomicrons (CMs). Iqbal et al. showed that the transport of CHOL in rat enterocytes involves multiple mechanisms, classified into apo B-dependent and apo B-independent pathways [56]. Both of the pathways transport free CHOL, but CEs were secreted by the apo B-dependent pathway [41]. The apo B-independent pathway or apo A-1 pathway is the pathway that transport CHOL out of the cell by ABCA1 carriers and was discussed earlier.

1.2.5 Formation of intestinal lipoproteins

There are two separate theories for the synthesis of CMs or VLDL in enterocytes.

1.2.5.1 Independent assembly of VLDL and CMs

Tso et al. hypothesized the first theory, in which two independent pathways are involved in the synthesis of CMs and VLDL. The CM pathway but not the VLDL pathway is inhibited by Pluronic L18 [57]. The newly formed TGs and CEs as well as PCs are transferred to a nascent apolipoprotein B-48 or apo B-100 that have already been synthesized in rough endoplasmic reticulum. This process is facilitated by the action of the microsomal triglyceride transfer protein (MTP) in smooth endoplasmic reticulum [13, 58] and forms partially mature chylomicrons (CM) or premature VLDL in endoplasmic reticulum. It is well understood that MTP is involved in the formation of VLDL. This procedure might take place in either enterocytes or hepatocytes [50]. The difference between CM and VLDL in the intestine is the size of their apolipoprotein. The CM apolipoprotein is apo B-48 (260 KD), however VLDL has apo B-100 (550 KD). Apo B-100 of hepatic and intestinal origin, while apo B-48 is only of intestinal origin [13]. During fasting, VLDLs are the major lipoproteins secreted by the intestine [59, 60], however, CMs become the major lipoproteins following fat feeding [61] (Figure 9). Hayashi et al. showed that fat feeding increases the size but not the number of CMs produced by the small intestine [61].

In either fasted or postprandial states, the premature CMs or premature VLDLs, which are in their vesicle forms and called pre-chylomicron transport vesicles or pre-VLDL transport vesicles, transfer TGs and CEs from the endoplasmic reticulum to intestinal Golgi apparatus in a unidirectional manner [62]. Vesicles are produced by a budding mechanism involving coat proteins that capture specific cargo molecules (the complex of Apo B, CEs and TGs) to the Golgi apparatus. The vesicles are covered with COPII proteins, which have three subunits called Sar1p, Sec13/31p, and Sec23/24p [63] and can fuse directly to the intestinal Golgi apparatus in vitro [64]. PCTV formed in the absence of Sar1 are unable to fuse to Golgi and cannot deliver CMs to the Golgi apparatus [64]. It has been shown that the pre CMs and pre VLDL have different structures from mature CM and VLDL released from Golgi apparatus [65]. For instance, carbohydrate components are added to premature CMs or VLDL and they will be secreted to lymph [13]. Furthermore, the PL composition of CM and VLDL isolated from intestine is different from pre CMs and pre VLDL [65]. Therefore, the Golgi complex has the ability to change the structure of pre CM and VLDL and modify them to mature forms.

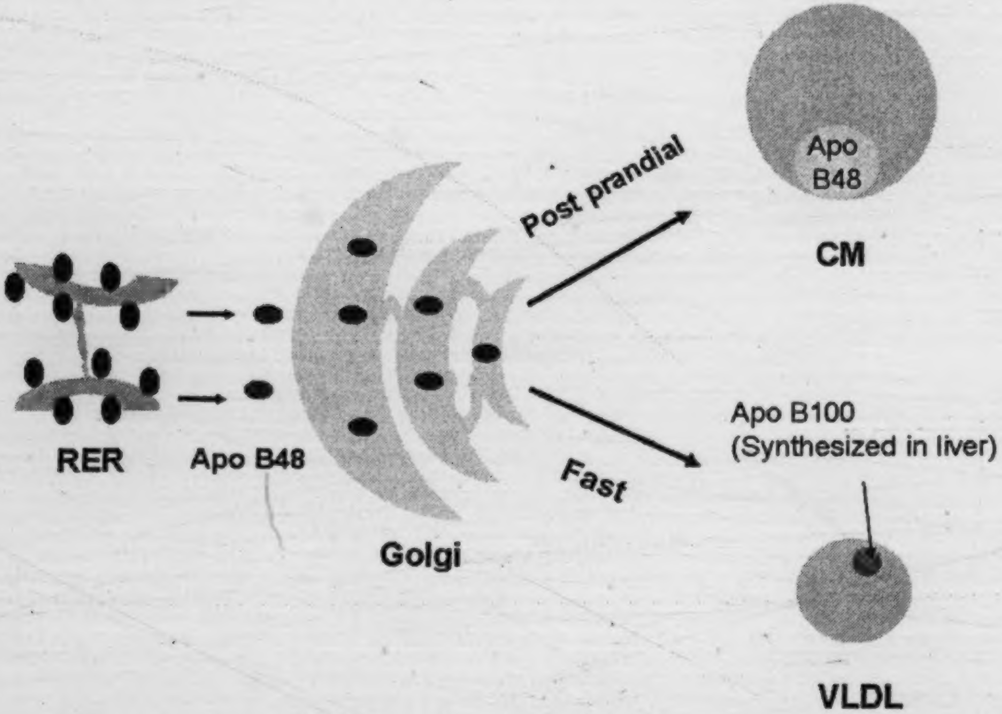

Figure 9: The role of rough endoplasmic reticulum and Golgi complex in CM and VLDL biosynthesis in intestinal lumen. The source of apo B48 and apo B100 are different. Apo B48 is synthesized in the rough endoplasmic reticulum of enterocytes; however liver is the source of Apo B100. These two forms of apolipoproteins are transported to smooth endoplasmic reticulum and take part in the synthesis of partially mature CM or immature VLDL. Golgi complex is the organ for further maturation of CM and VLDL.

1.2.5.2 Sequential assembly of intestinal lipoproteins

Hussain hypothesized the second theory in the formation of CM or VLDL particles in enterocytes [66]. Based on his theory, there are sequential steps involved in the assembly of intestinal lipoproteins. The CM assembly is suggested to be involved in three independent events: (1) formation of primordial lipoproteins; (2) synthesis of triglyceride-rich 'lipid droplets' of various sizes; and (3) biosynthesis of various lipoproteins (VLDL, small CM and large CM) in a process called core expansion. Core expansion most likely involves fusion of 'primordial lipoproteins' with 'luminal triglyceride-rich lipid droplets.' Pluronic L81 is proposed to inhibit the formation of larger lipid droplets due to de-stabilization of their surface and thus interferes with the formation of larger lipid droplets required for CM assembly.

In his theory, Hussain answered some questions about the role of MTP (microsomal triglyceride transfer protein) in the formation of primordial lipoprotein particles, the relationship between the length of apolipoprotein and the size of formed lipoprotein, the rate limiting step in the formation of TGs and the place that core expansion occurs [66].

a) Assembly of primordial lipoproteins

This is the first step in the assembly and secretion of intestinal lipoproteins. In this step, apo B, which is released from rough endoplasmic reticulum is associated with PLs and neutral lipids [66, 67]. The assembly of PL rich primordial lipoprotein occurs mainly in the SER lumen. It is thought that PL stabilizes the CMs and covers about 80% of their surface [68]. The size of the primordial lipoproteins is determined by the length of apo B polypeptide [66] Normally, the synthesis of primordial lipoprotein starts with apo B-48. It is expected that apo B-48 would form a primordial lipoprotein of HDL size [66]. Consequently, the assembled primordial lipoprotein is called HDL size chylomicron [66]. MTP plays a critical role in the assembly of HDL size chylomicron. It has been demonstrated that MTP may transfer neutral lipids to the site of association with apo B-48 in the ER membrane [67]. This may initiate the formation of primordial lipoproteins by saturation of the PL monolayer or bilayer with neutral lipids [69]. MTP can also help in the release of primordial lipoproteins from the ER membrane and act as a chaperon in this step [70] (Figure 10).

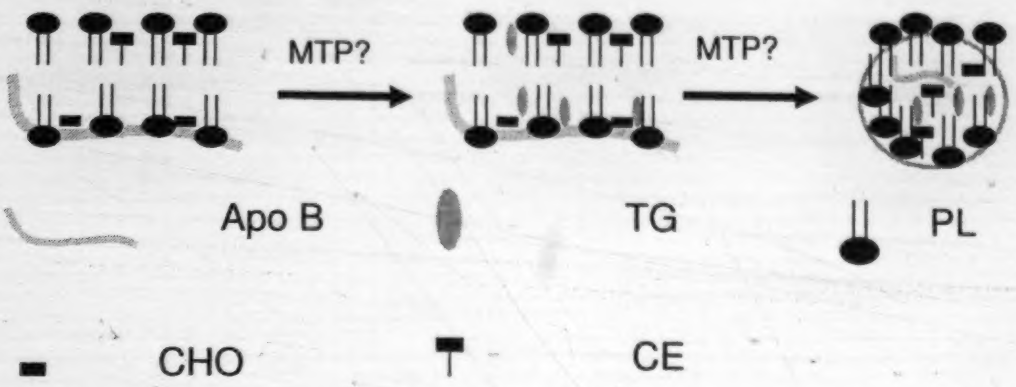

Figure 10: Assembly of primordial lipoproteins.In this step apo B is associated with PLs and neutral lipids (TGs). MTP has the crutial role in release of primordial lipoproteins from the ER membrane.

b) Synthesis of triglyceride-rich lipid droplets

It is proposed that progressively larger TG-rich lipid droplets are synthesized in the SER lumen during the postprandial state, and their synthesis is independent of apo B synthesis [71]. The formation of TG-rich lipid droplets starts with the action of diacylglycerol acyltransferase, which proceeds as an ongoing resource for the neutral lipid droplets. Again, the role of MTP in this step is critical. MTP can stabilize and facilitate the formation of assembled neutral lipid droplets. Pluronic L81 has been shown to decrease the stability of these lipid droplets [66] (Figure 11).

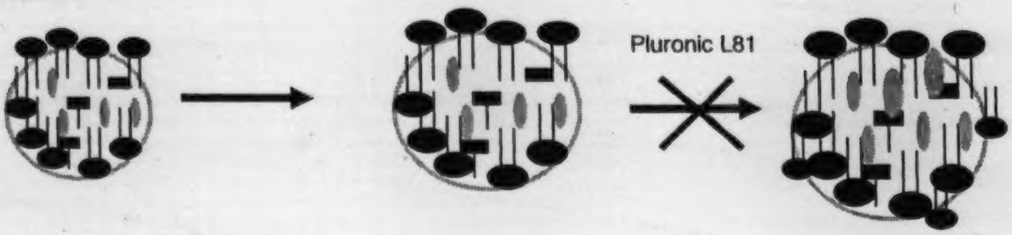

Figure 11: The formation of a TG-rich lipid droplet. This step is independent of apo B. The size of these droplets increases by adding more TGs to their core. Pluronic L81 is able to block this step and decrease the stability of lipid droplets.

c) Core expansion

Fusion of TG-rich lipid droplets and primordial lipoproteins result in the expansion of the core of the HDL size chylomicron. The size of the TG droplet may determine the size of the synthesized lipoprotein. The core expansion is crucial for the secretion of lipid droplets; it renders lipid droplets secretion competent [66]. The synthesized CMs are large in size and called Large size chylomicron [67] (Figure 12).

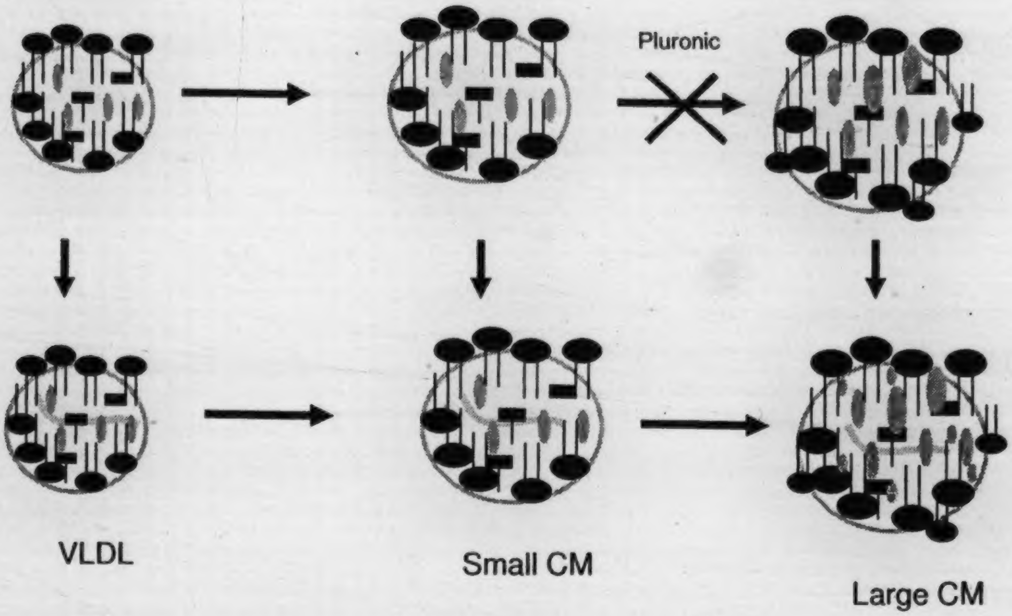

Figure 12: Formation of VLDL and CMs in core expansion process. In this step, primordial lipoproteins and TG rich lipid droplets fuse together to form large size CMs or intestinal VLDL.

1.2.5.3 Transport of CM and VLDL from the Golgi complex of the enterocytes to the intracellular space and lamina propria

The intercellular space is normally compressed when there is no active fluid and electrolyte absorption. The basolateral membranes of the neighboring enterocytes are close together, separated by 15-30 nm. After fluid absorption, the intracellular space expands up to 2-3 μm and creates a vast space between the basolateral membranes [72]. Basal membranes of enterocytes are in close contact with a barrier called the basement membrane. The basement membrane separates the enterocytes from lamina proportia. Lamina proportia has a connective tissue moiety and contains lymphocytes, plasma cells and mast cells. It is also well supplied with lymph and blood vessels [65]. The lacteals are the enteric section of the lymphatic system and have openings in their walls that are large enough to allow CMs and VLDLs to pass through [8]. CMs have diameters of 1000 Å to 1 μm [73] and due to their size cannot enter the blood stream directly. In other words, they are too large to cross capillary walls [8]. The flow of the lymphatic fluid carries the CMs and VLDL to the blood stream and releases them to the general circulation by the thoracic duct [8, 74].(Figure 13)

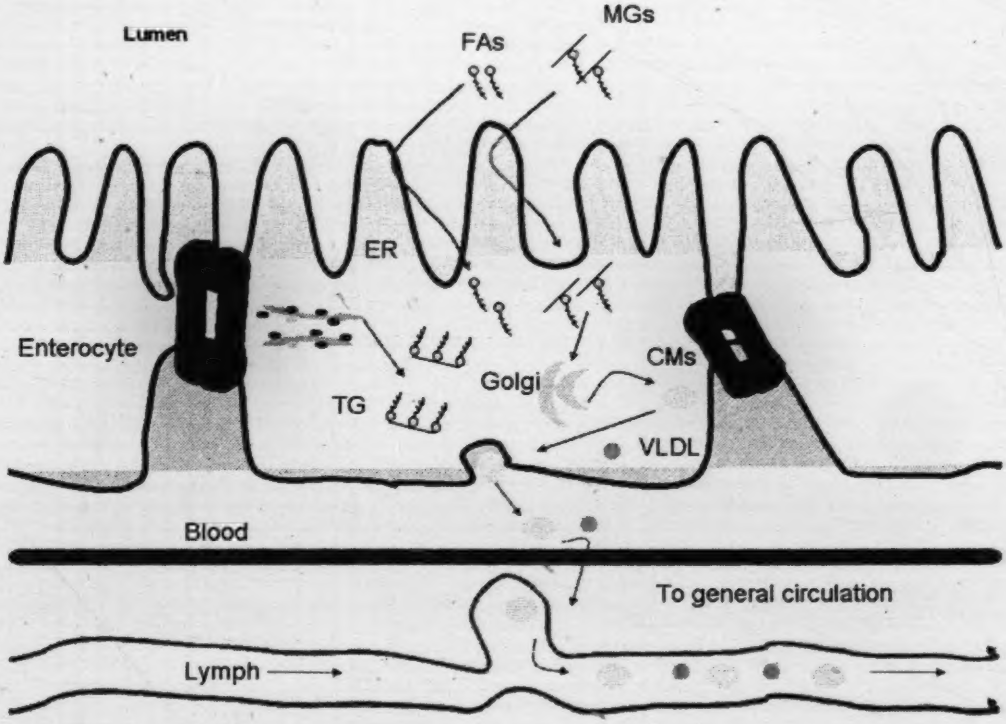

Figure 13: Absorption and transport of lipids in enterocytes. The absorption of MGs and FAs into enterocytes is followed by TG synthesis, which in turn package into CMs or VLDL. CMs then exocytose into intestinal fluid and enter lymph via lacteals.

1.2.5.4 Catabolism of CMs and VLDL (Lipolysis)

✓

The half life for the CL of CMs from blood stream is faster than VLDL and does not take more than 5 minutes [75, 76]. LPL is an enzyme that has a significant role in hydrolysis of CM and VLDL [77] and is present in the capillary endothelium [78]. There is a competition between CMs and VLDL for available LPL on the capillary endothelium [76]. It has been observed that VLDL accumulates in human plasma after oral fat ingestion. This is due to delayed lipolysis of the VLDL particles because of a failure to compete efficiently with CMs for the sites of LPL [79]. Although the number of VLDL particles (apoB-100 containing particles) postprandially are more than CMs (apoB-48 containing particles), the clearance of CM triglyceride particles is faster than VLDL TG particles [76]. One of the reasons can be the presence of apo CII and apo E in CMs. Apo CII is a cofactor of LPL and facilitates the hydrolysis of TGs in CM particles and delivery of TGs to muscles and adipose tissues [80]. On the other hand, apo E is important in the clearance and uptake of CM-remnants into hepatic tissue [80, 81].

After escaping from catabolism on the capillary endothelium, the lung and heart are the first organs that CMs and VLDL encounter [74]. Zechner reported the important role of the lung and heart in catabolism of CM particles. He described the tissue specific expression of LPL in lung and heart [82]. Cardiac LPL is probably required to generate fatty acids for optimal heart function [74]. The generated free fatty acids are taken up into myocardium by simple diffusion and by fatty acid transporters [83]. LPL also modulates the binding of TG-rich lipoprotein particles to the VLDL receptors. Apo E plays a very important role in binding of lipoprotein rich particles to VLDL receptors which are not only present in heart but also are present in other tissues such as muscles and adipose tissue [83]. In addition to lung, heart, adipose tissue and capillary endothelium, there are some other tissues, which have high concentrations of LPL. Liver is specifically very important in this aspect and has a specific kind of LPL. Phospholipolysis, which has been demonstrated to be an essential step in remnant formation and hepatic lipase (HPL), has considerable phospholipase activity [80].

It is presumed that the local concentration of LPL in muscle and adipose tissue allows the targeting of nutrients in the form of free fatty acids to those tissues [74]. The free fatty acids in these tissues will be used for energy production [81].

Regardless of where LPL is located, heparin sulfate proteoglycan (HSPG)-bound LPL hydrolyzes some surface and core lipids of CM [74]. The CM- remnants formed in the LPL reaction are rapidly taken up by the liver [25]. Removal of CM-remnant is very important, because the accumulation of remnants leads to hypercholesterolemia [81]. Felts et al. [84]suggested that during degradation of CM by LPL, the lipase becomes associated with the partially degraded CMs and is released from the endothelium. Subsequently, it can work as a docking protein and anchor the CM-remnants to the liver. Lipolysis is not only important in diminishing the size of CM but also is important to change the conformation of resident apolipoprotein in the molecule. This procedure is helpful in acquisition of other apo E molecules from plasma.

1.2.5.5 Hepatic uptake of CM-remnants

The generated molecules are small enough and are able to enter the space of Disse in the liver [81]. Three consecutive steps will take place in liver after CM-remnants are introduced to the space of Disse [81]

1- Sequestration
2- Processing
3- Internalization

a) Sequestration

In the space of Disse, there are both proteoglycan matrix and cell surface receptors. CM-remnants can interact with either HSPGs matrix or cell surface receptors [80, 85]. The particles that bind to receptors are internalized and degraded [86]. Apo E plays a significant role in binding of CM-remnant to HSPGs and sequestration [81] (Figure 14).

b) Processing

After sequestration, remnant particles spend more time in the space of Disse and are not liberated in plasma. During this time, which may take 30 minutes, remnants may undergo further processing. This processing contains lipid transfer, lipolysis of the sequestered particles and enrichment of these particles with apo E [81]. It is possible that lipid components are liberated from the particles and selectively transferred by receptor-independent pathways. For example, CEs can be selectively transferred from HDL to the cell plasma membrane independent of protein uptake [87]. Apo E is important in activation of hepatic lipase and is helpful in the lipolysis of remnant lipids [88]. It also may be involved in the selective transfer of CEs to hepatocytes [87]. Furthermore, it can interact with sequestered lipoproteins and help in the process of receptor-mediated endocytosis of particles [89]. HPL can also facilitate the targeting of these particles to low density receptor related protein. In addition of HPL, LPL .transported to liver can process these particles for internalization [81]. The remnants that are not enriched with apo E can not be recognized by low density receptor related protein and can not be internalized [81] (Figure 14).

c) Internalization

The enriched remnants are subsequently taken up by hepatocytes via receptor mediated endocytosis and degraded in lysosomes [75]. The involved proteins in this procedure are LDL receptors and low density receptor related protein [90, 91]. In familial hyperlipidemia due to variety of mutations in the LDL receptors, CM remnants are cleared by CM remnant-receptor protein, which is expressed exclusively in liver [92] (Figure 14).

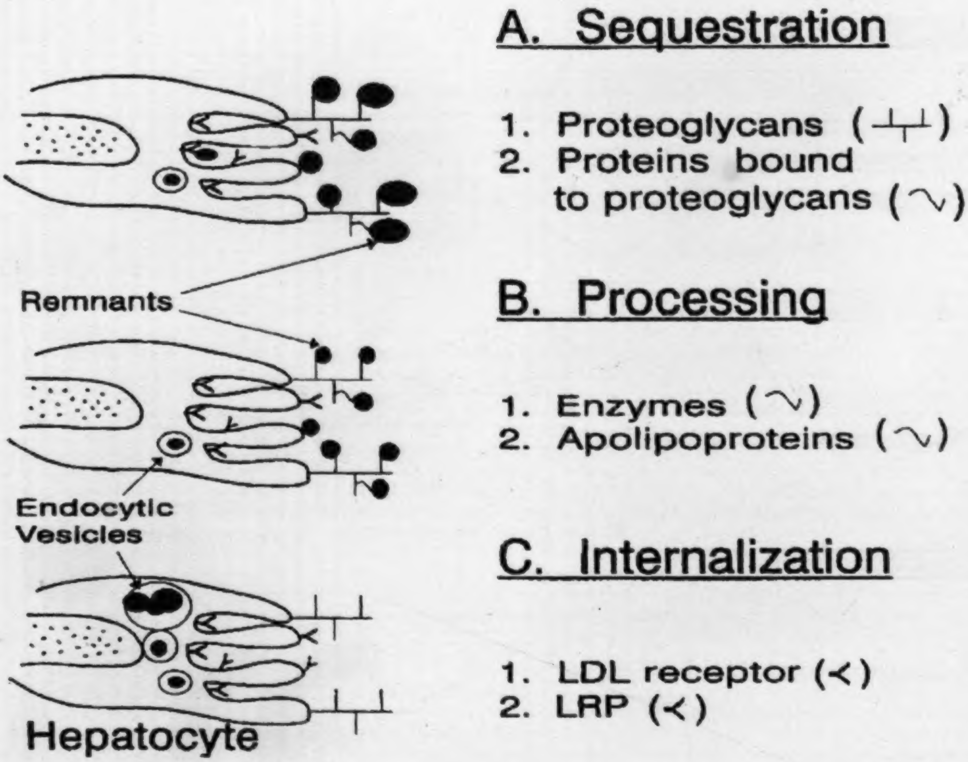
A. Sequestration
1. Proteoglycans (┴┬┴)
2. Proteins bound to proteoglycans (⌒∨)
Remnants
B. Processing
1. Enzymes (⌒∨)
2. Apolipoproteins (⌒∨)
Endocytic Vesicles
C. Internalization
1. LDL receptor (<)
2. LRP (<)
Hepatocyte

Figure 14: Catabolism of CMs by liver in three steps of sequestartion (interaction of CM-remnants with either HSPGs matrix or cell surface receptors in the space of Disse), processing (further processing of CM remnenrs including lipid transfer or lipolysis in the space of Disse) and internalization (taking up of enriched remnants by hepatocytes via lipoprotein receptors). From [81]

1.2.5.6 Exogenous cholesterol metabolism

Cholesterol esters (CEs), which have been taken by CM- remnants to hepatic tissue, are eliminated in the bile either as unsterified cholesterol or bile salts. Much of the CHOL and bile salts secreted by the liver are reabsorbed in the intestine and again delivered to the liver for excretion. During each cycle, some part of the CHOL or bile salts escapes reabsorption and is lost in the feces [75].

1.2.5.7 Hepatic uptake of VLDL-remnants

It is believed that the catabolism of VLDL-remnants is very similar to CM-remnants [80]. VLDL-remnants after this stage will take part in the same metabolic process as endogenous VLDL which is the primary source of VLDL source in the body.

1.2.5.8 Biosynthesis of hepatic VLDL

The endogenously synthesized TGs are carried by the VLDL, which are secreted by hepatocytes. Alexander and colleagues in 1976 proposed the mechanism of VLDL assembly in hepatocytes [93]. Based on their hypothesis, there are two separate stages in the assembly process of VLDL in hepatocytes. The location of every stage is different within the hepatocelullar secretory apparatus. At the first stage a small quantity of TAG becomes associated with apo B during its co-translational translocation. A PL shell encapsulates the TAG and results in the formation of a small, dense, apo B-containing VLDL precursor in the endoplasmic reticulum. MTP has a significant role in the formation of VLDL precursors. During the second stage, a larger droplet of TAG will associate with the small VLDL precursor to form a mature VLDL particle. This process is dependent on the activity of ARF-1 (ADP-Ribosylation Factor -1), which provides phosphatidic acid by the activation of phospholipase D [93, 94] (Figure 15). Incorporation of CHOL in hepatic VLDL is carried out by the function of few enzymes. Acyl Co A-cholesterol acyl transferase 1, 2 (ACAT 1, 2) has the function of inversion of free CHOL to CEs. The association of CEs and TG rich droplets is carried out by MTP [95]. The packaging of TGs, PLs and CHOL into lipoproteins (VLDL) in liver is dependent on the availability of CHOL. When dietary CHOL is available, liver uses that source for the biosynthesis of lipoproteins. When the dietary CHOL is not sufficient, CHOL will be synthesized by liver. In this procedure, the activation of the rate controlling enzyme 3-hydroxy 3- methylglutaryl Co enzyme A reductase A occurs [75].

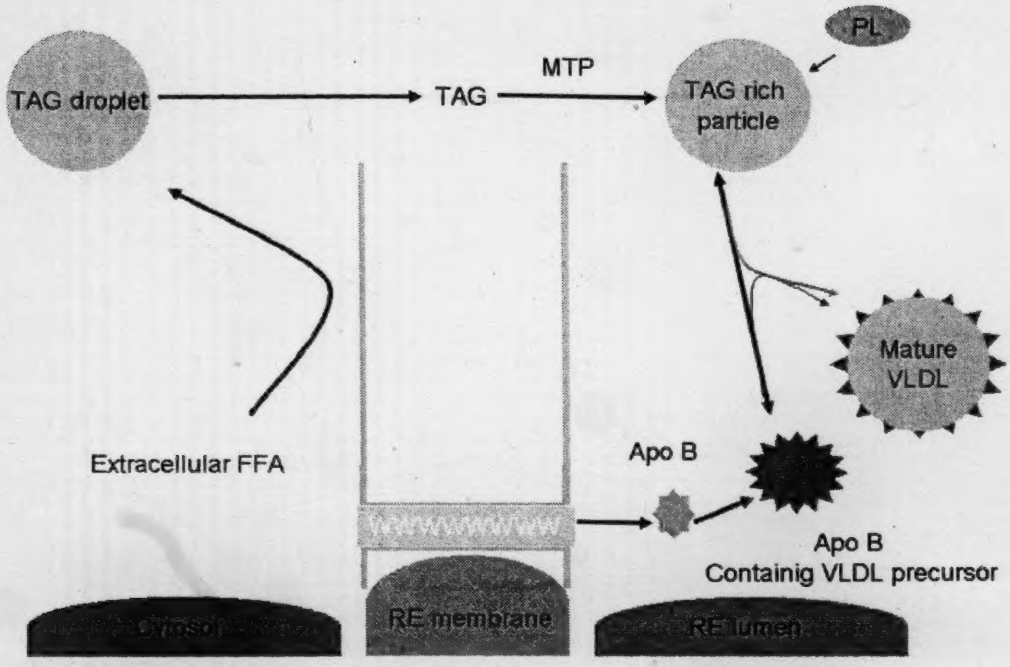
PL
TAG droplet
TAG
MTP
TAG rich particle
Mature VLDL
Extracellular FFA
Apo B
Apo B
Containig VLDL precursor
Cytosol
RE membrane
RE lumen

Figure 15: VLDL biosynthesis in hepatic cells. This procedure starts with the association of TAG droplets with PL and apo B containing VLDL precursors in the reticuloendothelial system of hepatocytes.

1.2.5.9 VLDL metabolism

VLDL derived postprandially or from hepatic tissue has apo B-100 instead of apo B-48 in CMs [80]. This may show its susceptibility to be metabolized by a different pathway. No matter what source VLDL has (synthesized in liver or intestine), the formed VLDL are enriched with CEs and are the substrates of cholestryl ester transfer protein (CETP). CETP mediates equimolar exchange of HDL-CEs with VLDL-TGs in plasma. It also stimulates the hetero-exchange of VLDL-TGs with LDL-CEs [96] and will be discussed in more details later. The percentage of apo E in these particles is high and probably has more affinity to LDL-receptors [80, 97]. The uptake of VLDL particles by LDL receptors in hepatocytes is similar to LDL particles and might not be affected by HSPG, because they have apo B-100 instead of apo B-48 [74]. As they progress along their delipidation process, they will fall into the intermediate density lipoprotein (IDL) category and because they contain apo E and decreasing amounts of apo Cs, they take part in the remnant removal pathway [80]. IDL has a smaller particle size and more density than its mother lipoprotein VLDL [75]. (Figure 16)

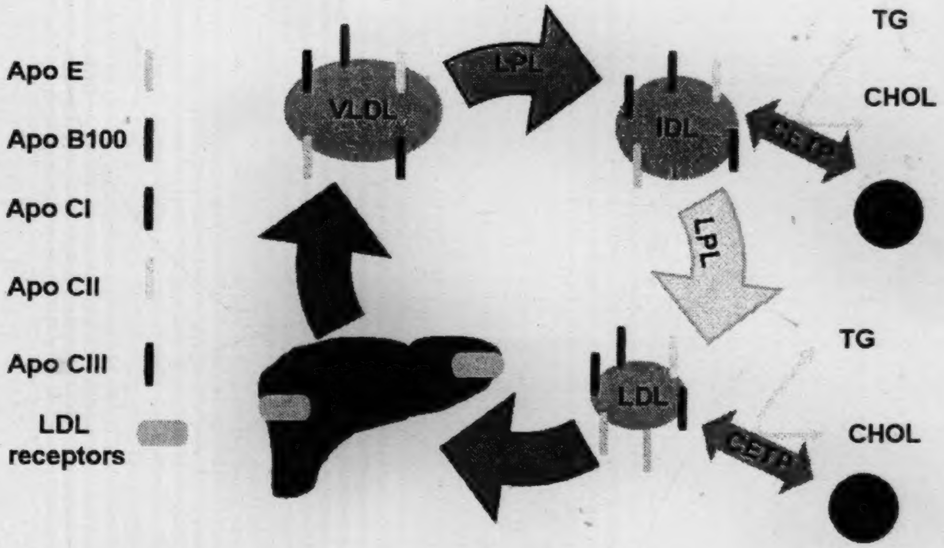

Figure 16: VLDL catabolism in body. VLDL particles are synthesized in liver and catabolized by LPL to IDL and consequently LDL. Specific apolipoproteins are involved in the biosynthesis and uptake of these particles in hepatic tissue. Furthermore, CETP is an important enzyme in the transport of TG and CEs between HDL, IDL or LDL.

1.2.5.10 Lipolytic conversion of IDL to LDL, role of hepatic lipase

The IDL released into the circulation then undergoes a further conversion, in which most of the remaining TGs in their core are cleaved and all of the apolipoprotein except apo B on their surface is lost. The resultant particles are mostly but not always, LDL, which have more CEs in their core and more apo B in their surface [75].

The further lipolytic conversion of IDL to LDL is catalyzed by the function of some other enzymes such as hepatic lipase (HPL) and CETP. Between these enzymes, it seems that HL plays a pivotal role in the normal metabolic procedure of LDL [98]. Furthermore, HPL has a key activity in remodeling of VLDL remnant and HDL [99]. Therefore, the site of conversion of IDL to LDL is speculated to be liver sinusoids [75]. HPL, is synthesized and secreted by liver and is bound to heparin sulphate proteoglycans (HSPGs) in the parenchymal cell surfaces in the space of Disse [99, 100]. In addition to liver, HPL is found in adrenal glands, ovaries and macrophages [100]. HPL hydrolyses both PLs and TGs of lipoproteins and is a member of the lipase superfamily [101]. It acts as phospholipase A1 and hydrolyzes FAs at their sn-1, 3 positions of TGs. Therefore it has phospholipase A1 and triglyceridase activity [100]. In addition to its lipolytic activity, it makes a ligand with proteoglycan and LRP to promote the hepatic uptake of lipoproteins including remnants, LDL and HDL (apo B-100-, and apo B-48- containing lipoproteins) [101, 102]. In this way, HPL connects plasma lipid transport to intracellular lipid metabolism in the liver [100].

It seems that the absence of HL results in the accumulation of TG-rich lipoproteins and buoyant, large LDL particles [98, 100, 101]. These large apo B-100 containing LDL will obtain their normal density in incubation with HPL [100]. IDL-like lipoproteins also accumulate in conditions characterized by decreased HPL activity, such as hypothyroidism. [103]. IDL is critical in progression of coronary artery disease (CAD) and accumulation of IDL results in the high risk of CAD. On the other hand, it seems that the overexpression of HPL leads to the formation of small, dense LDL particles that are atherogenic themselves [100]. Therefore, the role of HL in CAD in human is controversial and is a matter of debate. In spite of such a controversial role in CAD, HPL is likely to modulate the genetic regulation of other enzymes involved in the metabolism of lipoproteins.

1.2.5.11 LDL uptake by liver and extrahepatic tissues, role of LDL and scavenger receptors

LDL particles contain about two-thirds of the total plasma CHOL in normal subjects. Delivery of this amount of CHOL to peripheral tissues and liver is accomplished by the interaction of LDL particles and high affinity LDL receptors, located in plasma membrane regions called coated pits. These pits pinch off the LDL particles and form LDL lysosomes. The formed lysosomes expose the LDL particles to the action of hydrolytic enzymes that degrade apo B to amino acids. On the other hand, CEs are hydrolyzed by an acid lipase and the liberated CHOL leaves the lysosomes for use in cellular function [75]. By this procedure, the LDL receptors allow the targeting and forward delivery of CHOL from the liver to individual peripheral tissues. Delivery of CHOL by LDL receptors suppresses the synthesis of CHOL in every tissue because CHOL can be synthesized in every individual cell in mammalians in unusual conditions [92].

LDL receptors are not the only removal mechanism of LDL particles. During the last ten years the most interesting studies in atherogenesis were focused on scavenger receptors, the second mechanism involved in removal of LDL particles [104]. Different classes of scavenger receptors family (A, B, D, E, F, G, and H) have been recognized in recent years, based on their ability to recognize modified lipoproteins. The scavenger receptors are located in macrophages or the reticuloendothelial system and remove potential harmful materials from the arterial wall [104]. When the plasma level of LDL increases, scavenger cells degrade the increasing amounts of LDL; however when overloaded with CEs, they are converted into foam cells which are the components of atherosclerotic plaques [75]. The mechanism underlying the formation of foam cells is dependent on the formation of the oxidized form of LDL, which forms by the penetration of LDL particles into the artery wall and their adherence to proteoglycan. This interaction is thought to trap LDL particles and increase their susceptibility to oxidation [105]. It has been estimated that 33-66% of plasma LDL in human is degraded by LDL receptors and the remainder is degraded by scavenger receptors [75]. Between different classes of scavenger receptors, SR-B1 is found to be important due to its function as an HDL receptor. It is able to mediate the selective uptake of CEs from HDL [104]. In addition to liver, SR-B1 is also expressed in adrenal, testes and ovaries [106]. These tissues are in need of continuous amounts of CHOL [104].

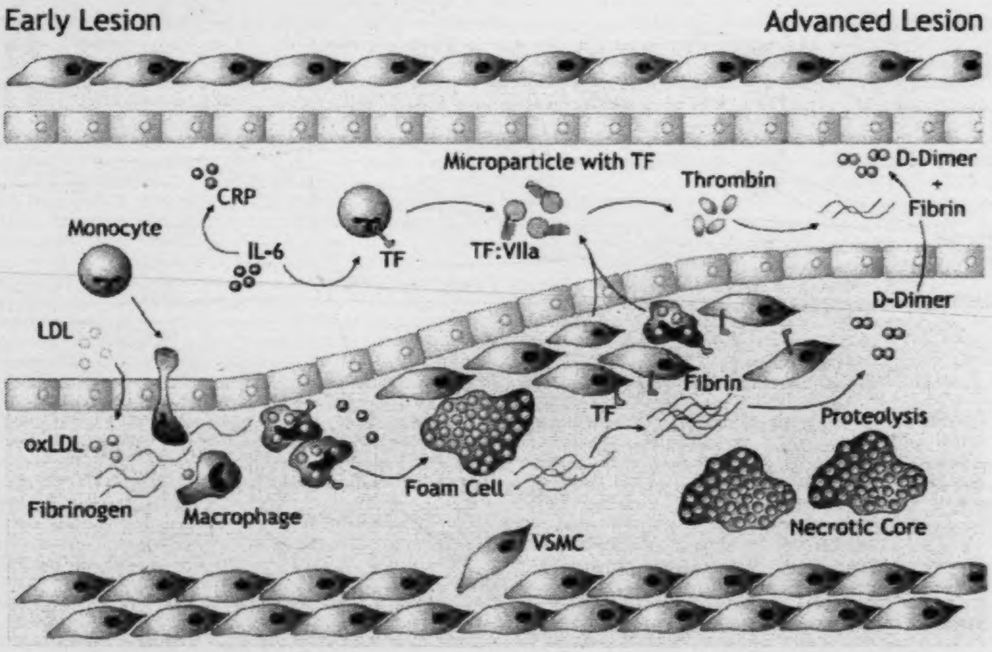
Early Lesion
Advanced Lesion
Microparticle with TF
Thrombin
D-Dimer
+
Fibrin
CRP
Monocyte
IL-6
TF
TF:VIIa
D-Dimer
LDL
Fibrin
TF
Proteolysis
oxLDL
Foam Cell
Fibrinogen
Macrophage
Necrotic Core
VSMC

Figure 17: Role of scavenger receptors in the removal of LDL particles and atherosclerosis. Atherosclerosis starts with retention and subsequent oxidization of LDL particles to oxLDL within the matrix of vascular intima. To remove these potentially harmful particles (oxLDL), circulating monocytes migrate through endothelial layer into intima, where they start to differentiate into macrophages. The scavenger receptors which are located on the surface of macrophages recognize and remove oxLDL. The saturation of macrophages with oxLDL results into the formation of foam cells. Stimulation of Monocytes by interleukin-6 and migrated vascular smooth muscle cells results into the releasing of tissue factor, which by itself can activate the formation of thrombin from prothrombin. Thrombin by itself can activate fibrin formation. Over production of dimers and macrophage derived apoptotic bodies results into fibrin proteolysis in both circulatiuon and advanced atherosclerotic lesions. From [107]

1.2.5.12 Interconversion of IDL and HDL

PLs and CEs are the excess surface materials in conversion of VLDL to IDL. These components can be transferred to HDL. On the other hand, HDL particles can interact with an enzyme in plasma called lecithin-cholesterol acyl transferase (LCAT). This enzyme esterifies the CHOL from fatty acids derived from the 2- position of lecithin, the major PL of plasma. The newly synthesized CE is transferred back to IDL from HDL particles. The net result of such an exchange reaction is the replacement of the most of the TG in the core of the VLDL with CEs [75].

1.2.5.13 Reverse cholesterol transport

Reverse cholesterol transport (RCT) is the reverse movement of CHOL from peripheral tissues to the liver throughout plasma. It is carried out by low and high density lipoproteins. LDL transports CHOL from liver to peripheral tissues, whereas HDL transports CHOL from peripheral tissues back to liver for extraction of bile acids and biosynthesis of steroid hormones [108]. CHOL in bile also might be reabsorbed in intestine and secreted along with dietary CHOL into the intestinal lymph as described before [109]. RCT and the involved enzymes are very important in the biosynthesis of HDL and are discussed in further details.

1.2.5.14 HDL biosynthesis, the role of reverse cholesterol transport

RCT is composed of four different steps. The first step in RCT is the movement of free CHOL from cells in the peripheral tissues to HDL. In the second step, CHOL in HDL which is its free form will be esterified and CE generated. LCAT is the enzyme responsible for such a conversion. LCAT helps the HDL to mature and the concentration of CE continues to rise. The third step is involved in the exchange of CE with TGs from HDL to LDL and VLDL. This step is mediated by CETP. The fourth step (last step) is involved in the transfer of CEs to the liver through LDL receptors.

a) First step, movement of free cholesterol to HDL

Movement of free CHOL (unsterified form) from peripheral tissues to HDL as the acceptor particle is the first step in RCT. This fraction of free CHOL is one quarter of total plasma free CHOL [109]. The acceptor molecule is available in two forms of free apo A-1 or prebeta-1 HDL. Prebeta-1 HDL is a small lipid– poor HDL particle. These two forms of apoA-1 take part in separate but parallel transport mechanisms [110]. Lipid-free apo A-1 is the first source for HDL biosynthesis in body. Due to the low levels of apo A-1 in plasma, investigators initially did not consider it as an important factor; however, recently a significant role of apo A-1 in the biosynthesis of HDL has been reported [111]. The synthesis of apoA-1 occurs in human liver and small intestine as pro-protein [112]. After the secretion into the plasma, it is rapidly cleaved to apo A-1 [109]. Barter et al. also reported the existence of apo A-1 in in-vitro human incubations of HDL, demonstrating the dissociation of apo A-1 from HDL [113].

Transfer of free CHOL from peripheral cells to HDL is accomplished by either diffusion based or receptor-dependent mechanisms [109]. In the diffusion–based mechanism, free CHOL and PLs diffuse from the cell membrane into the fluid phase. Albumin may play a role as a shuttle protein between the plasma membrane and HDL particles [110]. In the receptor mediated mechanism cell surface HDL-binding protein is involved in the transport of CHOL from a pool of newly synthesized CHOL in the reticulum endoplasmic [109]. A protein kinase mechanism is involved in the transfer of free CHOL to receptor bound HDL particles. This pathway is independent of LCAT activity [110].

Lipid free apo A-1 is quite unstable and avidly binds to PL and CHOL molecules to form prebeta-1 HDL particles [109]. Prebeta-1 HDL is a loosely folded high α-helix asymmetric molecule [111] and binds to the cell surfaces by specific apo A-1 receptors.

b) Second step, esterification of free cholesterol to cholestryl ester

The combination of more CHOL and PLs (lecithin) with prebeta-1 HDL results in the formation of discoid HDL [114] or prebeta-2 HDL [109]. X-ray crystallographic studies have confirmed the belt like conformation of discoid HDL. This structure is in contrast to the picket fence conformation that has been favored for over 20 years [114]. The number of apo A-1 per particle of discoid HDL is three [109]. The enzymes involved in the formation of discoid HDL are unclear; however, once apo A-1 is assembled into discs, they become the most potent physiological activator of plasma LCAT [114]. On the other hand, discoid HDL is the most important substrate of LCAT [109]. This enzyme has a role in the growth and maturation of HDL particles [110]. LCAT catalyzes the conversion of free CHOL (derived from tissues) and PC (lecithine) to CEs and LPC respectively on the surface of discoid HDL and thereby transforms discoid HDL to the spherical form (α-activity) [108, 110, 114]. The function of LCAT is not limited to HDL. Esterification of free CHOL is also accomplished in TG-rich lipoproteins (ß-activity) [110]. It can transfer 2-acyl groups of lecithin and phosphatidylethanolamine to the free hydroxyl group of fatty alcohols (especially CHOL) to generate CEs and lysolecithin. It also catalyzes the exchange of acyl groups between lecithin and lysolecithin [109]. The esterification of CHOL in HDL prevents its re-entry to peripheral cells and allows further accumulation of CHOL in peripheral cells [110]. Prebeta-2 HDL or discoid HDL is rich in lecithin and contains a smaller proportion of sphingomyelin and CHOL [109]. The difference between prebeta-1 HDL and prebeta-2 HDL is mainly due to their PL or lecithin content. Prebeta-2 HDL is rich in lecithin and contains lower amounts of CHOL [109]. Both prebeta-1 HDL and prebeta-2 HDL are present in large concentrations in large vessel lymph [109]. Large numbers of prebeta1-HDL particles in lymph inhibits the activity of LCAT. Eventually, uptake of CHOL and PLs by prebeta-1 HDL changes the conformation of small lipid-poor particle to discoid prebeta-2 and spheroid lipid loaded-HDL3 [110]. Spheroid lipid-loaded HDL3 has other lipoproteins such as apo AII, which in turn increases the size and lipid content of discoid prebeta-2 HDL. The large forme of HDL is called α-HDL [109]. Enlargement of discs by CHOL and lecithin is the function of LCAT on parenchymal cells [109].

α-HDL is a migrating fraction and initial acceptor for the major part of the CHOL transferred from LDL in response to plasma LCAT activity. The esterification of free CHOL transferred from LDL takes place almost completely within the α–HDL fraction. Apo AII, which is secreted by the liver, plays an important role in the metabolism of celsl and LDL derived CHOL [109].

c) Third step, exchange of CE with TGs from HDL to LDL and VLDL

CETP mediates the transfer of CE from HDL to LDL and VLDL and exchanges it with TGs. As a matter of fact the transfer of CE is accomplished from apo A-1 particles (HDL) to particles containing apo B (VLDL and LDL) [110]. Binding of CETP to HDL is due to the high molar concentration and high affinity of HDL to CETP relative to other lipoproteins [115]. The interaction of CETP and lipoproteins is mediated by hydrophilic and ionic interactions [115]. CETP has higher affinity for negative charged particles and therefore the incorporation of lipolysis-derived fatty acids into lipoproteins increases the binding of CETP and increases the ability of these particles to serve as substrates for CE transfer [115].

This function of CETP is related to the function of another lipid transport protein, which is called PL transfer protein [110]. It also plays an important role in the transport of apo A-1 between cholesterol ester -rich HDL2 and HDL3 particles, and cholesterol-poor pre beta HDL particles. The newly generated pre beta HDL particles act as the acceptors of cellular CHOL following efflux into the plasma [110]. It seems that the synthesis of CETP in liver is induced by a high fat, high CHOL diet [116]. Exercise increase HDL and decrease CETP levels. In fact an increase in CETP levels might be atherogenic because it can transfer the CE from HDL to VLDL and LDL, thus promoting CE deposition.

d) Fourth step, transfer of CE to liver

The remaining CEs in the HDL particles will be transferred to liver by the catalytic action of HPL.HPL mediates the conversion of TG-rich HDL_2 to TG-poor HDL_3 particles. By this conversion, CEs, PLs, FAs and glycerol are released and taken up by the liver. Lipid-poor HDL and free apo A-1 will also return to the periphery to enter the cycle again [110].

1.3 *Effect of lipids on pharmacokinetics of drugs*

1.3.1 Lipids and absorption of drugs

Lipids can have significant effects on the oral absorption of drugs. These effects can increase or decrease the efficacy of drugs by enhancing or diminishing their bioavailability [117]. The clinical importance of such interactions might be manifested on the rate and extent of absorption of drugs, which is normally assessed by characterization of C_{max} (peak plasma drug concentration), T_{max} (time to reach C_{max}) and AUC (area under concentration versus time curve). There are some different rate limiting steps that define the effects of lipids on the absorption of drugs. Among them gastric emptying time, dissolution rate and solubilization of drugs are defined as the most important ones.

1.3.1.1 Fat and gastric emptying time

Food intake sparks the release of the number of peptides from endocrine cells in the lining of the GI tract, thus mediating the digestion and absorption of nutrients. The various functions of these peptides alter the gastric secretion, motility, gall bladder contraction and hepatic blood flow from their fasted state [118]. The absorption of orally administered drugs might be affected by these GI changes, which in turn can exert variability in drug plasma levels and clinical responses. Chemical reactions between drug molecules and food components and also physiochemical properties of a drug may determine the influence of food on drug absorption [118].

For liposoluble drugs, the rate of absorption of drug is determined by the dissolution of drug in GI tract. In the fasted state, a migrating motor complex controls the emptying time of stomach contents including dissolved and undissolved drugs into the small intestine. This time is randomly around 2 hours following oral drug administration. In a fed state, food contents interrupt the migrating motor complex; therefore the emptying time is longer. For liposoluble drugs, this time is longer [118].Therefore, oral administration of poorly-soluble drugs in the fed-state provides a longer gastric residence time for drug dissolution and a controlled emptying time of drug in the small intestine (duodenum) [5, 118]. Furthermore, the fed state stimulates the secretion of pancreatic and other GIT fluids that increases the total GI fluid volume for drug dissolution [118]. Increase in both drug absorption rate and extent due to a decrease in gastric emptying time is manifested as a higher C_{max} and a correspondingly longer T_{max} or lag time (T_{lag}) [119]. Among food contents the lipid components have the largest capacity to delay gastric emptying time [120].

Sunesen et al. [121] demonstrated that the absolute bioavailability of danazol, a very lipophilic drug increased from 11% to 44% in normal subjects, when ingested with fat food. C_{max}, T_{max} and T_{lag} increased 2.4, 1.3 and 3.14 fold respectively. A prolonged gastric emptying period, which is exerted by fat food, might be the reason for such effects. Similarly, Fleisher et al. [117] observed increase in drug plasma levels of phenytoin after oral Intralipid (INLP) administration in dogs. They observed two- fold increases in both AUC and C_{max} of phenytoin following the administration of oral INLP.

Conversely, lipid or fat food might decrease the absorption of acid-labile and ionizable drugs by delaying their presentation to the duodenum. Lower C_{max} and longer T_{max} are the pharmacokinetic manifestation of these effects [5, 119]. The longer T_{max} due to delayed absorption may be expressed as larger mean residence time [119]. For example it has been shown that fatty food decreases the bioavailability of avitriptan, partly due to changing gastric emptying time and gastric motility [122]. Similarly, high fat food reduces the C_{max} and AUC of oral tacrolimus by the factor of 77.1% and 33.4% respectively. However T_{max} increased 373%. These data suggests that high fat meals possibly prolong gastric emptying time [123].

Although fat in food prolongs the gastric emptying period, which by itself affects the absorption of some drugs, the absorption of other drugs is not affected by fat content in food. For instance, Teo et al. observed no significant differences in C_{max} and AUC of thalidomide in the presence and absence of a high fat meal in healthy subjects; however T_{max} and T_{lag} were significantly delayed [124]. Similarly Brocks et al. demonstrated no effect on C_{max}, T_{max}, AUC and oral bioavailability of cyclosporine A after a high fat meal administration to laboratory rat [125]. Furthermore, no effect on C_{max}, T_{max}, AUC and oral bioavailability of methylphenidate was observed in healthy subjects after the ingestion of a high fat breakfast [126]. In this study two different dosages of 18 and 36 mg/kg of methylphenidate were administered to healthy subjects and plasma concentrations of both parent drug and metabolite α-phenyl 2-piperidine acetic acid of methylphenidate were measured. Although C_{max} and AUC of both methylphenidate and α-phenyl 2-piperidine acetic acid were slightly higher than in the fasted state, the differences were not significant [126].

1.3.1.2 The role of bile in drug solubilization and dissolution

It has been demonstrated that the increased intestinal uptake of liposoluble drugs is not only due to the delay in gastric emptying time, but also due to the secretion of bile salts which by itself might increase the dissolution rate and solubilization of these drugs [127]. Bile salts along with other components of biliary secretion such as PLs, CHOL, TGs, ions and pigments modify drug bioavailability [128]. Bile salt solubilization is known to be responsible for the increased bioavailability of many drugs including griseofulvin [129-131], halofantrine [132, 133], ketoconazole [131] and gemfibrozil [134].

Bile salt secretion is a result of gall bladder contraction due to ingestion of a high fat meal. In response to lipid and fat food, cholecysokinin contracts the gall bladder and relaxes the sphincter of Oddi, which leads to the liberation of bile . Concentrations of bile salts, especially cholic acid and deoxycholic acid in the fasted state between 1 and 4 mmol/L, increasing to 10-20 mmol/l in the fed state [135]. In order to have an effect on drug absorption, the concentrations of bile salts should be higher than CMC [136]. Bile salts and the products of lipid digestion (monoglycerides) and lecithin decrease the CMC and increase the size and number of micelles. Micellization of drug can also increase the apparent diffusion coefficient of drug and increase the solubilization capacity [137].

An increase in the rate of dissolution might be due to either a decrease in the interfacial energy barrier between solid drug and dissolution medium or an increase in the solubility via micellar solubilization [137]. Improvement in the solubilization of indometacin [138], danazol [139] and mefenamic acid [140] is mediated by micellar solubilization. Bile salts can also increase the rate of dissolution by increasing the wetting of drugs [137]. Increases in the dissolution of phenylbutazone [138], triamcinolone, hydrocortisone, dexametasone and betametazone [139] is the result of such a mechanism.

It seems that log octanol/water partition coefficient *(log p)* of these drugs is the key factor in determining the involved mechanism of dissolution [137]. The l*og p* values of the aforementioned steroids range between 1.01-1.94 (moderately liposoluble); however danazol has *log p* value of 4.5 (highly liposoluble) [139]. Based on this mechanism, we can conclude that the increase in the absorption of most lipophilic drugs after high fat food is due to the increase in solubility via micellar solubilization. Examples of these drugs are tepoxalin [141], amiodarone [142, 143], halofantrine [144], mefloquine [145], mebendazole [146, 147], quazepam [148], cilostazole [149].

Simple bile salt micelle formation appears to be the predominant mechanism in the increase of the rate of dissolution of the drugs that are dissolved by the wetting procedure however a mixed micellar system appeares to be the major mechanism for drugs that use solubilization for improving dissolution [128]. Simple bile salt micelles are only composed of drug and bile salts; however in a mixed micellar system lecithin or a fatty acid is also added to bile salt micelles [137].

There is a controversial situation in the effect of bile on the absorption of drugs. Although bile salts have an enhancing effect on the absorption of most lipophilic drugs, the absorption of some hydrophilic drugs such as paracetamol and theophylline are not affected by bile salts [146]. Tukker et al. demonstrated minor and negligible effects of sodium taurocholate on the absorption of paracetamol and theophylline [131]. In addition, formation of a simple or mixed bile salt micelle system affects the permeability and stability of different peptides including insulin. It has been demonstrated that stability and permeability of insulin are increased in simple bile salt micelles (composed of sodium taurocholate or sodium glycolate and insulin) in comparison with control insulin or a bile salt fatty acid mixed micellar system (composed of sodium taurocholate, linoleic acid and insulin) [150]. Similarly, Dongowski et al. observed decreases in AUC and C_{max} of quinine in rabbit in the presence of a simple bile salt micelle system consisting of sodium deoxycholic acid and a mixed bile salt micellar system consisting of sodium deoxycholic acid, palmitic acid and /or lecithin [151].

Pafenolol, tubocurarine, neomycin and kanamycin are other examples of drugs that form insoluble complexes with bile salts, and their absorption is inhibited in the presence of bile salts [137].

1.3.2 Prediction of drug and high fat meal interactions

Amidon and co-workers devised a biopharmaceutical classification system that categorizes drugs into four different classes according to their solubility and permeability. Specifically, class I includes highly soluble, highly permeable drugs. This class includes small hydrophilic drugs that are not ionized in the GI tract. Some weak acids and bases such as valproic acid, ketoprofen, disopyramide, verapamil and metoprolol are categorized in this class. Some other inert drugs such as paracetamol are also categorized in this class. Class II includes low soluble, highly permeable drugs. Some water-insoluble drugs such as amiodarone, atrovastatin, danazol, dapsone, indinavir, ketoconazole (KTZ), lovastatin and tacrolimus are categorized under class II drugs. Class III includes highly soluble-low permeable drugs. Some weak acids and bases such as furasemide and bidisomide are also classified in this group. For class IV which includes low soluble- low permeable drugs, acetazolamide, amphotericin, ciprofloxacin and digoxin are good examples [152] .

Fleisher et al. used biopharmaceutical classification system to predict food effects on drug bioavailability [117]. Benet et al. [153] added the time to peak exposure (T_{max}) to their predictions and used this categorization for exclusive a high fat meal-drug interactions. According to these predictions, high fat meal has no significant effect on the bioavailability of class I drugs, however, T_{max} might be increased with high fat meal consumption due to a delay in stomach emptying time.

It is predicted that high fat meals will increase the extent of bioavailability of class II drugs. This increase might have an effect on peak time (T_{max}). High fat meals may inhibit both influx and efflux drug transporter proteins; therefore a decrease in peak time could be due to the inhibition of efflux proteins. On other hand, an increase in peak time might be due to the slowing of stomach emptying time, which is additionally due to the solubilization of drug in the intestinal lumen (e.g. micelle formation). A combination of these two factors may also increase the bioavailability of class II drugs. In this case, a combination of these two factors will usually be dominated by the delayed emptying. This will be true in cases where membrane permeation is passive, such as for the immunosuppressants cyclosporine, tacrolimus and sirolimus [153].

It has been observed that formulation markedly affects the high fat meal effect on class II compounds. This is true especially when solubility of class II compounds is increased by modification of formulation. For example, the new microemulsion formulation of cyclosporine (Neoral) eliminates the food effects associated with the olive oil formulation of cyclosporine (Sandimmune) [153].

The extent of bioavailability of class III compounds will decrease after high fat meal consumption. The probable reason is the inhibition of uptake transporters such as organic anion transporting polypeptide by the fat content of the food in the intestine. This inhibition procedure is followed by a decrease in intestinal drug uptake of compounds with high soluble- low permeable properties. As noted, some drugs of this category might be substrate of efflux proteins in the intestinal lumen. Depending upon whether the drug is the substrate of efflux or influx proteins, an increase or no effect in the extent of bioavailability of drug may be observed. One would expect to see an increase in peak time (T_{max}), due to a combination of delayed stomach emptying time and slower absorption [153].

For class IV compounds, prediction of the effect of food on bioavailability of these compounds is difficult. This complexity is due to the occurrance of all the interacting effects mentioned for class II and class III drugs. Due to Benet opinion, increase in the bioavailability of this group has been resulted from both increase in the solubilization of drug and inhibition of efflux proteins in the intestine lumen [153].

1.3.3 Lymphatic absorption of drugs

The intestinal lymphatic pathway is known as a specific and important transport pathway of lipids and lipid derivatives. Incorporation of liposoluble drugs with fat content of food and then their association with intestinal lipoproteins (CMs and VLDL) increases the accessibility of this group of drugs to the intestinal lymphatic system, which bypasses hepatic first pass metabolism and consequently increases the bioavailability of liposoluble drugs [154]. The mechanism underlying the association of drugs with CMs is not completely understood. Also, little is known about the intracellular sites, the role of transport proteins and the mechanism involved in the transport of associated drug molecule in lipid particles inside the enterocytes. One possibility is that the drug might be incorporated in the core part of CM during its formation. Another possibility might be related to the association of drug molecule in CM in their final stage of formation. Also these two processes might take place at the same time [155].

In vitro cultures of Caco-2 cells [156] and complimentary in vivo conscious intestinal lymph duct cannulated animal models [157] provide excellent experimental models to investigate the role of different factors involved in the lymphatic absorption of drugs. Based on these studies physiochemical properties of the drug molecules as well as the quantity and types of the lipids in the CM define the association properties of drug and CM particles [158].

1.3.3.1 Physiochemical properties of drug molecules and their lymphatic absorption

The chemical structure of a drug molecule is one of the important factors in determination of lymphatic absorption of drugs. Porter and Charman [159] demonstrated the relationship between *log p* (log octanol/water partition coefficient) and lymphatic absorption of drugs. Based on his research, *log p* values more than 5 and Tg solubility more than 50 mg/ml are the minimum requirements for appreciable lymphatic transport. They also demonstrated a relationship between molecular weight and the lymphatic transport of drugs. Based on their research, small lipophilic molecules can be absorbed in either lymph or blood flow, however for either large (MW>10,000 Da) or extremely lipophilic molecules the absorption through leaky lymphatic endothelium is favored [159].

Hoffman and Gershkovich [160] incubated eleven different lipophilic compounds (vitamin E, vitamin D3, halofantrine, probucol, diazepam, bifonazole, paclitaxel, testosterone, cyclosporine A, benzo α-pyrene and p-p' DDT) with CM emulsions separated from rat blood for 1 hour. For diazepam, testosterone, paclitaxel and cyclosporine A, less than 5% of drugs were found associated with CM. p-p' DDT, halofantrine, vitamin D3, vitamin E, benzo α-pyrene were found to have the most efficient uptake by CMs. Probucol and bifonazole showed moderate efficiency of association with CMs. They found a linear correlation (r^2=0.94, p<0.0001) between intestinal lymphatic bioavailability of lipophilic molecules and the percentage of drug associated with CMs derived from rat plasma. In an attempt to establish a correlation between intestinal lymphatic bioavailability of molecules and physiochemical properties of tested molecules, including molecular weight, *log p* and solubility in long chain TGs, they found a moderate correlation between intestinal lymphatic bioavailability and *log p* (r^2= 0.5, P=0.0326). A moderate correlation was also found between intestinal lymphatic bioavailability and the solubility in long chain TGs (r^2= 0.55, P=0.0341), whereas the correlation between intestinal lymphatic bioavailability and molecular weight was poor (r^2= 0.12, P=0.3828) [160]. The linear correlation between the degree of uptake of compounds by isolated CMs and intestinal lymphatic transport suggests that there are similar factors governing these two processes [160]. Therefore, the degree of association of lipophilic molecules with isolated chylomicrons can be used as a simple screening model for estimation of intestinal lymphatic transport potential of drug molecules [160].

1.3.3.2 Quantity and types of lipids in CM (vehicles) and lymphatic absorption of drugs

Caliph et al. demonstrated the effect of the chain length of fatty acid vehicles on absolute oral bioavailability and intestinal lymphatic transport of halofantrine (HF) in lymph cannulated and non cannulated rats [161]. They demonstrated that the extent of mesantric-lymphatic transport of HF increases from 2.2 to 5.5 and to 15.8% respectively following the co-administration of short (C4), medium (C8-10) and long (C18) chain triglyceride vehicles.

The degree of unsaturation of the fatty acid vehicle (oleic acid=C18:1, linoleic acid=C18:2 and linolenic acid= C18:3) on intestinal transport of HF free base was also a matter of investigation by Holm et al. [158]. The results showed that linoleic acid was superior to linolenic acid but not significantly different from oleic acid [158]. The reason might be related to an increase in the ability to form CM production [154].

The digestibility of the lipid vehicle also plays an important role in the transport of the lipid vehicle to the lymphatic system. Palin et al. used arachis oil, Miglyol 812 (fractionated coconut oil) and liquid paraffin as lipid vehicles to transport of DDT to lymphatic system. The results of their study demonstrated that non-digestible vehicle (Liquid paraffin) is less efficient in transport DDT to the lymphatic system [162].

In addition to the importance of fatty acids on the lymphatic transport of drugs, the structure of some surfactants that might be added to some specific formulations (lipid-based formulations) to aid vehicle dispersion and drug solubilization in the gastrointestinal tract [163] is also imperative in lymphatic transport of some drugs. Some of these surfactants such as Tween 80 (polysorbate 80) and Cremophor EL have been shown to inhibit P-glycoprotein (P-gp) activity and increase the permeability of drug substrates [57, 164]. In addition, some other investigators reported the inhibitory role of Pluronic L81 on the secretion of triglyceride-rich lipoproteins, most specially CMs in rats (Tso and Gollamudi 1984) and Caco-2 cells [165]. Seeballuck et al. investigated the role of polysorbate 60 and 80 on the secretion of CMs in both in vivo (rat) and in vitro (Caco-2 cells) models [156]. Unlike Pluronic L81, they found a stimulation effect of polysorbate 80 on the secretory function of CMs. They successfully interpreted a relationship between the saturation of the long chain fatty acid moiety of polysorbates and stimulatory effect on the secretion of CMs. Polysorbate 60 is a sorbitan ester of a long chain saturated fatty acid, stearic acid (C18:0), however, polysorbate 80 is the sorbitan ester of the unsaturated fatty acid, oleic acid (C18:1). The stimulant effect of polysorbate 80 on CM secretion in both in vitro and in vivo models (concentration 4 and 10%) was suggested in this study, although the mechanism was not identified clearly [156].

Unlike polysorbate 80, polysorbate 60 had the ability to increase the secretion of LDL in Caco-2 cells in the fasted state, but the reason was not clear [156]. Unfortunately, the authors did not mention the effect of polysorbate 60 on LDL secretion in the rat model.

1.3.4 Lipids and drug distribution

Distribution of drugs is dependent on two major components, rate and extent of distribution. Drug distribution rate is mostly dependent on the rate of perfusion and the permeability of tissues. Tissue perfusion is determined by blood flow of each tissue; however permeability of tissues is a function of physiochemical properties of drugs including oil/water partition coefficient, pk_a and molecular size of drug molecules. On the other hand, distribution extent is dictated by protein binding of drugs in plasma and tissues [166].

1.3.4.1 Lipids and blood flow rate

The impact of food on the rate of distribution of drugs is a very complicated process. Perfusion of tissues as an important factor in determination of drug distribution rate is shown to be affected by the presence of food. In basal conditions, the gastrointestinal tract (GI) receives about 20-25% of normal cardiac output, although the distribution of blood flow is not uniform at the GI wall. At rest, 70-80% of GI blood flow is received by the mucosal layer; however serosal and muscular layers receive 15-25% of GI blood flow. The submocusa layer is the less perfused layer and receives just 5% of GI blood flow. The submucosal layer is the intestinal layer in which the majority of absorptive, metabolic and P-gp activities reside. This partial flow leads to slow dispersion of drugs into the circulation and a longer transit time within the intestinal tissue [167].

In the presence of food, GI blood flow increases to 200% of the basal condition. This increase in blood flow is temporary and lasts for 2-3 hours. This condition is called postprandial hyperemia. Most of this increase in blood flow is received by the mucosal microcirculation which is closed in the unfed state and is open to receive this extra blood after ingestion of food [168]. The surplus in blood flow is compensated for by an increase in cardiac output and decrease in the blood flow of other tissues. The hyperemia starts at the stomach and then forward down to the ileum [168]. In the absence of bile salts, glucose is the most effective agent for the initiation of hyperemia, but when bile salts are present, long chain fatty acids overcome glucose for the initiation of hyperemia [168]. In general, all nutrients, especially lipid micelles require oxygen delivery. During hyperemia, partial pressure of oxygen in the intestinal vili decreases. A decrease in oxygen partial pressure stimulates the generation of NO, a potent endothelium derived vasodilator generated by a family of a P-450 like enzymes called nitric oxide synthetase, which directly induces the relaxation of vascular smooth muscle cells [168]. NO has more physiological functions that are protective for intestinal endothelium, and its lack leads to endothelial dysfunction, increased platelet adhesion and enhance a risk of thrombosis [169].

There are other studies that verify the effect of different lipids in decreasing oxygen pressure in intestinal endothelium and impairing vasodilation. For instance, it has been reported that high fat meals and meals with ordinary fat content impair endothelium dependent vasodilation in humans [170]. Steer et al. demonstrated that a regiment containing over 30% of fat might result to impaired function of the vascular endothelium [171]. Also, impaired flow mediated vasodilation of the brachial artery for at least 4 hours was identified in healthy subjects after high fat meal ingestion [172]. Cross-sectional studies also demonstrated that a high saturated fatty acid diet resulted in impaired endothelial function compared with polyunsaturated fatty acids and monounsaturated fatty acids [169]. It has also been shown that treatment of high cholesterolemic patients with niacin increased their HDL level and resulted in an improvement in endothelial function [173].

The change in intestinal blood flow following high fat food, which results in relaxation of endothelial vascular smooth muscle in mucosa layer, may be altered when the drug is administered postprandially, due to the decreased the residence time of the drug in the intestinal tissue [167]. The issue regarding the coadministration of fat food and drug is very complex and is determined by the physiochemical properties of the drug molecule [137].

The effect of dietary lipids on blood perfusion is not limited to the GI tract. Dayanikli et al. demonstrated reduced coronary flow reserve in hypercholesterolemic patients [3]. Also the aortic and coronary flow rates were shown to reduced in isolated perfused heart of the rat [174].

It has been observed that hepatic blood flow is also affected by a fatty liver. Seifalian et al. showed a significantly reduced portal blood flow and hepatic microcirculation in the hepatic steatosis rat model [175]. An inverse correlation was observed between the degree of fat infiltration and both total hepatic blood flow and flow in the microcirculation in human.[176]. On the other hand, the protective effect of dietary omega-3 poly unsaturated fatty acids on the accumulation of lipids in hepatic tissue and tissue injury was observed in an ischemic mouse model. A decrease in the extent of Kupffer cell activity and increase in microcirculation were the net result of such a protection [177].

1.3.4.2 Lipids and permeability

Permeability is an important factor for passage of drug molecules through the biological barriers. Permeability of drugs not only affects absorption but also affects distribution and elimination of drugs. Due to the importance of fat as an essential constituent of biological membranes, considerable amount of research has been accomplished on the effects of different lipids on the composition and function of cell membranes, including the activity of membrane bound enzymes and transporters. For instance, Keelan et al. demonstrated that different kinds of dietary lipids alter the structure, fluidity and transport function of cell membranes [178-180]. The mechanism of these effects might be related to alteration of PL fatty acid composition in brush border membrane [181]. It also has been observed that fatty acids actively contribute in the regulation of tight junctions in epithelial cells [182]. Such alterations might have significant effects on the permeability of jejunum to some nutrients such as glucose and dietary lipids [178, 183]. The net effect of these alterations might be beneficial [19, 183] or detrimental for patients with diabetes or hyperlipidemia [184]. The kind of dietary lipids is the most important factor in determination of PL fatty acid composition of the brush border cell membrane in the jejunum. Rrabbits fed with different fatty acid compositions showed different absorptivity strength on their intestinal brush border membrane for glucose and dietary lipids [185].

In addition to the effect of dietary lipids on composition and function of jejunum, the impact of dietary lipid on the intestinal transport and permeability of some marker drugs were also determined by some other investigators. Charman et al. clarified the significant effects of dietary fatty acids on the active, passive and efflux transport of some drugs in excised rat jejunum [186]. Based on their research, the in vitro passive paracellular permeability of mannitol, transcellular diffusion of diazepam, active transport of glucose and efflux transport of digoxin in brush border membrane of excised rat jejunum were determined in different groups of rats fed with 18.4% w/w of butter [containing saturated fatty acids], olive oil [containing mono unsaturated fatty acids (MUFA)], safflower oil [containing ω-6 poly unsaturated fatty acids (ω-6 PUFA)] and fish oil [containing ω-3 poly unsaturated fatty acids(ω-3 PUFA)]. The permeability of these drugs then was compared with a group of rats fed with standard chow diet (containing 5.2% fat) [186]. The paracellular transport of mannitol via the tight junctions did not show any significant difference between the different diet groups, however the transcellular diffusion of diazepam was more pronounced and showed a significant decrease in ω-3 PUFA and ω-6 PUFA animals compared to the control group [186]. On the other hand, the effect of dietary lipid on active transport of glucose by Na^+/K^+ ATPase pump demonstrated a moderate but not significant enhancement in the m-s (mucosal to serosal) flux of D-glucose in rats fed with SFA, MUFA and ω-3 PUFA diets relative to the chow-fed rats. In contrast, enriching the diet with ω-6 PUFA was associated with a significant inhibition of D-glucose transport in the m-s direction [186]. ATP-dependent efflux transport of digoxin (P-glycoprotein mediated efflux) was found to be reduced in high-fat chow animals compared with control chow-fed rats, although no lipid specific trend was observed. A decrease in efflux transport of digoxin was correspondingly observed in s-m (serosal to mucosal) flux of drug. The existence of unspecificity in high-fat chow compared to chow-fed rats suggests a specific change in brush boarder membrane lipid structure [186].

The mechanism underlying the effect of fat on the permeability of drugs from the intestine is not completely known; however it is believed that, lipids such as monoglycerides and fatty acids and PLs are surface-active compounds and show permeability enhancing effects in pharmaceutical studies [137]. It is hypothesized that surface-active lipids, formed after normal lipid digestion increase the permeability of the intestinal epithelium to poorly absorbed compounds, allergens and toxins by either affecting tight junctions (increase paracellular route) or causing cell damages that disrupts the integrity of the intestinal epithelium. Destabilization of the membrane might also increase the absorptivity of compounds by the transcellular route [187]. In vitro experiments in Caco -2 cells indicated that the absorption enhancement potency decreases in the order FAs>MGs>DGs [187]. It was found that among fatty acids, the high chain fatty acids (eicosapentaenoic acid C=20 and docosahexaenoic acid C=22) are more efficient than medium chain fatty acids (oleic acid C=18) at increasing the permeability of insulin in the intestinal epithelium [188].

In addition to natural fat and lipid nutrients, some artificial lipids have been synthesized to increase the permeability of water-insoluble drugs from intestinal epithelium. For instance, a lipid based formulation made of 1,2-dimyristoyl-sn-glycero-3-phosphatidylcholine phospholipid was successfully used for increasing the permeability of piroxicam in an in vitro Caco-2 cell model [189].

The effect of lipids on permeability of drugs is not limited to the intestine. For instance, an inhibitory effect of medium chain fatty acids on the liver permeability to alcohol and endotoxin was observed. In these cases medium chain fatty acids were able to protect the liver from injury by inhibition of the production of free radicals and tumor necrosis factor-α from Kupffer cells [190, 191].

In brain, Yamagata et al. demonstrated the regulatory role of gamma-linolenic acid and eicosapentaenoic acid on the tight junctions in blood brain barrier (BBB) [192]. They showed that eicosapentaenoic acid and gamma-linolenic acid can induce the sealing of tight junctions in brain capillary endothelial cells [192]. On the other hand, Kim et al. demonstrated that unsaturated fatty acids (oleic and linolenic acids) increase vascular permeability and reversiblly disruption on BBB, which might be beneficial for delivery of chemotherapeutic agents to brain tumors; however the toxic effects of such disruption should not be ignored. The mechanism of such reversibility is not known [193].

In addition to tight junctions, other transport systems available in the BBB for delivery of different substances, passive transport and active transport systems as well as receptor-mediated transport, P-glycoprotein, OATP (Organic anion transport protein), multiple organic anion transporters and LDL receptors) [194-196] might be affected by fat products.

There are growing evidences that cholesterol and lipid nutrients are transported to the brain by LDL receptors. Some critical enzymes in lipid metabolism, such as LCAT have also been identified in brain [195]. Furthermore, it has been observed that MDR1 (Multi drug resistance associated protein 1) can mediate the transport of cholesterol from the plasma membrane to the endoplasmic reticulum. Chylomicron remnants down-regulate the ABCA1 [197]. Therefore, there is an interaction between cholesterol and chylomicrons on LDL-receptors and P-glycoprotein. The importance of this interaction for the transport of drugs to the brain via BBB is not well understood.

1.3.4.3 Lipids and drug protein binding

Perhaps the most important effect of lipids on extent of distribution of drugs is attributed to lipid fractions of plasma and the binding of drugs to lipoproteins. It has been demonstrated that lipophilic drugs as well as amphiphilic lipids (PLs and CHOL) and some lipid-soluble vitamins can be transported in plasma as complexes of lipoproteins [198]. It has been demonstrated that the unbound fraction of drugs can be distributed into different tissues and exert the pharmacological action of the drugs, although the blood or plasma concentration of unbound drugs might not always show the concentrations of drug in the target tissue [199]. However some plasma protein bound drugs seem to cross the BBB [200].

The distribution of lipophilic drugs in lipoprotein subclasses in plasma determines the efficacy and safety of drug compounds [201]. The distribution of different lipophilic compounds in lipoprotein fractions is dependent upon many factors, including species differences, health state conditions, drug formulation and fed or fasted state conditions. These specific properties affect the pharmacokinetic and pharmacodynamics of the compound associated with lipoprotein subclasses. For instance, in vitro distribution of amphotericin B in lipoprotein subclasses in rabbit plasma depends upon fasted or fed states as well as formulation [202]. Wasan et al. demonstrated that amphotericin B associates mostly with lipoprotein deficient serum (LPDP) in fasted rabbits, which is composed of albumin and α1-acid glycoprotein; however in cholesterol fed rabbits, amphotericin B accumulates mostly in LDL/ VLDL fractions [202]. It was observed that a change in the formulation of amphotericin B to a lipid complex completely modified the association of drug to HDL subclass. Fasted or fed state did not determine the association of the lipid complex formulation of amphotericin B in rabbit plasma [202].

Brocks et al. have shown interspecies similarities in the distribution of halofantrine enantiomers between rat, dog and human [203]. They also noted that the uptake of the (+) halofantrine enantiomer was related to percent of apolar core lipid in the lipoprotein fractions however, the uptake of the (-) halofantrine enantiomer was independent of apolar core lipid in the lipoprotein fractions [203]. Humberstone et al. suggested that binding of halofantrine to plasma lipoprotein modifies its pharmacological effect. They demonstrated that the in vitro IC_{50} of halofantrine against *Plasmodium falciparum* was significantly decreased in the presence of 10% postprandial serum [204].

Distribution of nystatin and a liposomal formulation of nystatin were studied in three different species, human, dog and rat by Ramaswamy et al. [205]. They found that in all three species, the majority of nystatin was recovered in the LPDP fraction. After 5 and 60 minutes of incubation with normolipidemic serum of each species, the percentage of recovered nystatin in the HDL fraction was higher for the liposomal formulation than nystatin itself [205].

The distribution of cyclosporine in lipoprotein subclasses in normolipidemic and hyperlipidemic plasma is a matter of debate between different investigators. It has been shown that cyclosporine undergoes nonspecific dissolution in the lipophilic core of the different lipoprotein subclasses instead of binding to a specific binding site [206]. The distribution of cyclosporine in different subclasses of lipoproteins is independent of concentration [207, 208] and time of incubation [208]. Incubation of cyclosporine A with normolipidemic human serum indicates that this drug associates more with VLDL and

IDL (triglyceride rich lipoproteins) [207]. In vitro incubation of lipoproteins containing cyclosporine A showed that cyclosporine can transfer between lipoproteins. Free lipoproteins can accept the cyclosporine in their different fractions (VLDL to LDL, LDL to VLDL, VLDL to medium density HDL and LDL to HDL-M) [209]. It is believed that the transfer of drug between different lipoprotein subclasses is partially influenced by lipid transfer protein I or cholestryl ester transfer protein [201, 208]. It is believed that this enzyme facilitates the transfer of core lipoprotein lipids, CE and TG, one third of the coat lipoprotein lipid and PC between different plasma lipoproteins. Due to the association of cyclosporine in core lipoprotein lipid and the inability of CETP to distinguishing between exogenous drug associated with the lipoprotein core and endogenous lipid-like-particles, transfer of drug in different lipoprotein subclasses will be accomplished by such a simple mechanism [201]. The influence of dyslipidaemia on the distribution of cyclosporine in different lipoprotein subclasses was examined by Wasan et al. [210]. They found that the percentage of cyclosporine in LDL and VLDL was 32%, however this number increased to 46, 54 and 6% in hypercholesterolemic and hypertriglyceridemic patients and patients with both elevated triglyceride and cholesterol levels, respectively. On the other hand, the association of cyclosporine with HDL decreased from 40% to 20% in all dyslipidemic patients under study. Also the percentage of cyclosporine in the LPDP fraction decreased from 20% to 13 % in patients with both elevated triglyceride and cholesterol levels [210].

Procyshyn et al. examined the effect of HL on in the vitro distribution of haloperidol in human plasma [211]. They showed that increases in cholesterol concentration resulted in a of haloperidol from LPDP to LDL; however, an increase in triglyceride in plasma redistribute resulted in redistribution of this drug from LPDP to LDL and VLDL [211]. Similar results were observed with clozapine. The clozapine consumers show a degree of increase at triglyceride level in their plasma, which might contribute to the clinical efficacy of clozapine [211, 212]. An increased association of clozapine with the VLDL fraction during chronic administration of clozapine might increase its permeability to the brain through the BBB [211].

The in vitro distribution of five hydrophobic macrocyclic lactones (moxidectin, doramectin, ivermectin, abamectin and eprinomectin) in plasma proteins of several animal species including human was examined by Lespine et al. They found that almost 90% of the drugs under investigation were associated with lipoprotein fractions of plasma in goats. There was a closely similar distribution profile for all of the five tested drugs in lipoprotein fractions of goat plasma. Preferentially 80-92% of the drugs were associated with HDL. Only 6-11% of drugs were associated with LDL and a minor proportion of the drugs was found in VLDL [168]. Different species including cow, sheep, pig, rabbit and human showed similar profiles for the association of moxidectin. This means that in all species, most of the drug was associated with HDL, although association of the moxidectin in HDL showed a significant difference in different species. The existence of significant differences between species can be attributed to the different concentration of cholesterol in plasma lipoprotein fractions of the species under investigation. In goat 73% of systemic cholesterol is transported by HDL. In humans in contrast, only 34% of systemic cholesterol is associated in HDL. This number is 84% in the cow and more than 54% in other three species. In humans more than 58% is associated with LDL. These differences express the significant difference of distribution of these drugs in HDL of different species [168].

In addition to the in vitro distribution of different drugs with lipoprotein subclasses, some in vivo studies also have been conducted on the effect of lipoprotein binding on distribution of drugs in different tissues, which was expressed as volume of distribution. For instance, Brocks et al. found that Vd_{ss} of cyclosporine was significantly lower in hyperlipidemic rats compared with normal rats [125]. In a similar study, Nakamura et al. demonstrated a lower ratio of blood to tissue (liver, kidneys, heart, muscles) concentrations of cyclosporine A, 5 and 120 minutes after injection of 10 mg/kg of a single iv dose to pseudohypertriglyceridemic rat model, although the values of 5 minutes for all of the tissues showed statistically significant differences [213]. Wojcicki et al. also showed a 48% decrease in volume of distribution of propranalol in hypertriglyceridemic patients compared to normal patients [214]. Brocks and Wasan [132] showed a stereoselective decrease in the Vd_{ss} of halofantrine in hyperlipidemic rats.

They demonstrated 26- and 36-fold decreases at volume of distribution of (+) and (-) halofantrine enantiomers respectively. Charman et al. observed a 21% decrease in volume of distribution of halofantrine in beagle dogs after iv administration of 1.6 mg/kg of drug in fasted and fed states [204]. In all of these studies, the decrease in volume of distribution was attributed somehow to a decrease in the unbound fraction of drugs due to lipoprotein binding.

Bassissi et al. examined the influence of dyslipidaemia on pharmacokinetics of moxidectine, a potent anti parasitic drug, in rabbit [215]. The comparison of pharmacokinetic parameters of a single subcutaneous dose of moxidectine at the dose of 300 μg/kg over a 32 day period after drug administration in control and high fat meal ingested rabbits (2.5% w/v coconut oil enriched with 1% cholesterol for 21 days prior to experimentation and 15 days thereafter) demonstrated a significant decrease in volume of distribution after oral dose (72%) of the drug. The authors also showed that dyslipidaemia affected the distribution of moxidectine in lipoprotein fractions. The recovery of moxidectine in HDL, LDL and VLDL fractions of regular fed animals were 84.6, 10 and 2% respectively. Following administration of moxidectine to high fat meal fed rabbits, the association of moxidectine shifted to LDL (60.9%) and VLDL fractions (15%) with a significant decrease in the HDL fraction (22.2%). Based on this observation, they concluded that change in the pharmacokinetic parameters of the highly lipophilic drug, moxidectine was the result of change in the level of triglyceride and cholesterol in dyslipidaemia, which in turn causes the increase in the numbers of circulating VLDL and LDL particles and increase the level of association of moxidectine with these particles [215].

1.3.4.4 Hyperlipidemia and tissue distribution

In general, the distribution of drug to tissues in the HL state has been poorly studied. The relationship of HL and tissue distribution has been studied by several investigators in recent years. Riou et al. observed the increase in intrinsic myocardial washout kinetics of ^{99m}TC-NOET (bis (N-ethoxy, N-ethyldithiocarbamato) nitrido technetium (V) after intravenous administration of a high dose of INLP to anesthetized dog model [216]. Also, the cardiac kinetics of ^{99m}TC- NOET was accelerated after intravenous injection of tracer in obese, hyperlipidemic Zucker rats with circulating lipid levels similar to those encountered clinically in hyperlipidemic patients [217]. The biodistribution of ^{99m}TC-NOET, 60 minutes after the injection of the tracers showed that the cardiac, spleen and lung activities of drug decreased in Zucker rats as compared with animals from the lean group, whereas blood, liver, kidney and fat activities were not significantly different between the 2 groups of animals [217].

In a study on tissue distribution of a single intravenous dose of 10 mg/kg of cyclosporine A in pseudo-hypertriglyceridemic Wistar rats (induced by intravenous injection of lipid emulsion containing soybean oil 20 g/dL, egg yolk phosphatides 2.4 g/dL, 2.0 g/kg body weight at 30 min before cyclosporine A administration), the blood to tissue ratio of cyclosporine A decreased significantly 5 min after the drug administration in liver, kidney, heart and muscles [218] The lipid emulsion in this study did not contain apolipoprotein. On the other hand, the AUC of cyclosporine A increased significantly in kidney and liver and decreased substantially in spleen and heart of the hyperlipidemic rat model (hyperlipidemia was induced by ip injection of 1g/kg of poloxamer 407) compared to normolipidemic rats who received a single 5 mg/kg dose of CyA as intravenous bolus [219]. Aliabadi et al. observed significant increase in distribution of cyclosporine A in plasma, blood, kidney and liver of HL rats receiving a single 5 mg/kg of CYA compared to normolipidemic (NL) rats. Conversely, they observed decrease in the concentration of drug in the heart and spleen of HL rats. The increase in the concentration of drug in kidney and liver of HL rats was attributed to the affinity of cyclosporine toward LDL or VLDL receptors; however, the decrease in the concentration of drug in some other tissues was attributed to decreased unbound fraction [219].

In another study the kidney levels of amphotericin B were observed to be substantially higher in the obese Zucker rat model in comparison with control lean rats [220].

1.3.4.5 Lipids and drug transporters

Most of the studies regarding the effect of lipids on drug transporters were conducted on P-gp and MDR proteins, although recently different investigators such as Benet at the University of California have focused on the effect of fat on other drug transport proteins such as OATPs, organic cationic transporters and organic cationic transport proteins [153].

The effect of lipids on P-gp activity is controversial and somewhat confusing and completely dependent on the kinds and concentrations of lipids. The influence of CHOL on P-glycoprotein drug binding properties was studied by Saeki et al. [221]. They used purified P-glycoprotein reconstituted into liposomes with different cholesterol contents. When the PC was at its highest amount (PC:CHOL=10:0) the binding of azidopine was at its lowest activity. They observed a maximal P-glycoprotein [^{3}H] azidopine (photoaffinity vinblastine analogue) binding at 20% of cholesterol weight ratio (PC: CHOL=8:2). Interestingly, when the CHOL content was increased higher, the binding activity diminished. Therefore, high CHOL levels could inhibit P-glycoprotein transporter activity.

There are other supportive references regarding the inhibitory effect of cholesterol on P-glycoprotein and MDR cells. A direct correlation between the increase in the CHOL/PL ratio and vincristine (VCR) resistance degree was observed in two MDR sub cell lines (VDR/P60 and VCR/P200) derived from L5178Y cells. The CHOL/PL ratio was inversely related to the rates of VCR influx. CHOL depletion in both L5178Y-sensitive and MDR-resistant cells resulted in an increase in the rate of vincristine uptake. Although both VCR/P cell sublines, but not the sensitive parental cells, expressed the P-glycoprotein in their plasma membranes, there were no differences in drug efflux and retention between resistant and parental cells. These results indicated the modulatory role of CHOL on permeation of VCR through the plasma membrane. Therefore increased levels of CHOL/PL are responsible for the lower drug accumulation and greater resistance in these multi drug-resistant cells [222]. Berleur et al. suggested that the interaction of vinblastine with phosphatidyPC) liposomes was dependent on dipolar interaction (positive charge of vinblastine and the negative charge of PC). This interaction could in turn deform the lipid bilayer and permit drug penetration [223]. Thus, an increase in the CHOL/PL ratio could reduce the MDR drug-lipid interaction and increase in drug influx in MDR cells.

Sinicrope et al. at the University of Chicago, demonstrated that the increase of lipid membrane fluidity by benzyl alcohol in rat liver canalicular vesicles, where P-glycoprotein is normally expressed, inhibited ATP-dependent [^{3}H] daunomycin or [^{3}H] vinblastine accumulation [224]. Since cholesterol is the main lipid involved in plasma membrane fluidity and the percentage of cholesterol is important for the binding activity of the cell membrane, decreased efflux activity of P-glycoprotein could be expected to result from any change in the optimal plasma membrane fluidity [223].

Several studies carried out by Metherall et al. [225] have suggested that P-gp transporter activity is involved in the increase of cellular cholesterol. They observed a direct correlation between the ability of steroid hormones to inhibit MDR and their ability to inhibit cholesterol biosynthesis. Non-steroidal MDR inhibitors were also shown to inhibit both cholesterol biosynthesis and cholesterol esterification. Both types of reactions occur in the endoplasmic reticulum. Therefore the MDR transporter activity could play a role in their movement from the plasma membrane to the endoplasmic reticulum. Taking this into account, it could be speculated that in certain cell types or cell conditions, an increased P-gp transporter activity could lead to an increased cholesterol biosynthesis. An overly high cholesterol content could thus contribute to the inhibition of P-gp transporter activity [223].

The role of lipids other than cholesterol on P-glycoprotein was also studied by other investigators. Modok et al. assessed the function of reconstituted form of P-glycoprotein into liposome form comprising sphingomyeline, egg PC or saturated dipalmitoyl phosphatidylcholine in the presence and absence of high amounts of cholesterol (45% mol/mol) using an ATPase activity reaction [226]. Nicardipine and XR9576 were used to modulate ATPase activity of P-glycoprotein. They demonstrated that the nature of ATP hydrolysis was not significantly altered by the nature of the lipid species; however the potencies of nicardipine and XR9576 to modulate the ATPase activity of P-glycoprotein were increased in the sphingolipid-based proteoliposomes [226]. It has been observed that cholesterol and sphingomyeline interact with high affinity and this interaction is responsible for localization of cholesterol to the plasma membrane [227]. Reducing the sphingomyelin level by adding exogenous sphingomyelinase releases the cholesterol from the plasma membrane, allowing it to enter intracellular pools, which leads to increased CHOL esterification and HMG-CoA reductase degradation [227].

The role of oil on the transporters other than P-gp has also been investigated. The role of fat free or fat containing TPN (total parentral nutrition) in the change of hepatic xenobiotic transporters of infant rats was studied by a group of scientists at the University of Tokushima, Japan. They used three-week-old male Sprague-Dawley rats and divided them into three groups: group 1 received a control oral diet, group 2 received TPN without fat, and group 3 received TPN with 20% of its calories from fat (soybean oil emulsion). Surprisingly they observed lower mRNA levels of Mdr2, Bile salt export pump (BSEP), Mrp2, Mrp6, Oct1 and Oat2 transporters in infant rats nourished with fat-free TPN (group 2) compared to normal oral diet nourished rats (group 1). The levels of Mdr1b, Mrp1 and Mrp5 mRNA in this group were 16-fold higher than the control group (group 1). On the other hand, the changes in these mRNA expression levels in the rats fed with TPN containing 20% soy bean oil emulsion (group 3), was smaller than the fat free nourished group, but the expression levels of Mdr1b, Mrp1, Mrp5, Mrp6 and Oat2 mRNA were not significantly different from the fat free nourished group [228].

1.3.5 Lipids and elimination of drugs

The effect of lipids on the elimination of drugs is a very broad topic. It has been observed that lipid and lipid fractions can affect not only hepatic clearance and metabolism of drugs but also renal clearance. This effect on renal clearance of drugs might be due to the significant role of the kidneys in lipoprotein metabolism [229]. Unfortunately, our knowledge is just limited to the physiological role of kidney in clearance of lipoproteins and our understanding about the net clinical effect of such an effect on the excretion of drugs is unclear.

There are many factors that might affect the CL of drugs including physiological, pharmacological, pathological and genetic factors. Among them, the effect of protein binding has been studied in details. The capacity and the extent of binding of drugs to proteins are dependent on the physiochemical properties of the drug molecules. There are a number of plasma proteins known to be involved in drug binding. Albumin, α1-acid glycoprotein [230], lipoproteins [231] and cortisol binding proteins [232] are recognized as the most important proteins involved in the process of protein binding. Among the plasma proteins, lipoproteins are important in binding of lipophilic drugs. These proteins are known to carry lipids and fat in plasma and deliver them to different tissues for metabolic necessities [233]. After the ingestion of a high fat meal or following lipid metabolic disorders, the concentration of triglyceride-rich lipoprotein fractions increases in plasma. Lipophilic drugs, which normally bind to lipoproteins, are carried by different lipoprotein fractions in plasma. A decrease in the unbound fraction of lipophilic drugs following binding to lipoproteins is the normal consequence of such a procedure. Since only free drug molecules can be cleared from plasma, a decrease in the unbound fraction of lipophilic drugs after their binding to lipoproteins is expected to decrease their plasma clearance; however, it might not always be true.

There are some examples regarding the decreased effect of fat food or hyperlipidemia on plasma clearance of lipophilic drugs. Brocks and Wasan observed a decrease in the clearance of halofantrine enantiomers in high fat-meal fed rats [132]. In hyperlipidemic rats the decrease in clearance of drug was not stereoselective compared to control rats (~11-fold). Peanut oil caused a significant 28% reduction in clearance of the (-), but not the (+) enantiomer (mean clearance reduced 11%) of halofantrine. The unbound fraction in hyperlipidemia decreased around 90% for both of the enantiomers [132].

Bassissi et al. examined the influence of dyslipidaemia on the pharmacokinetics of moxidectine, a potent antiparasitic drug, in rabbits [215]. The comparison of pharmacokinetic parameters of a single subcutaneous dose of moxidectine at a dose of 300 μg/kg over a 32 day period after drug administration in control and high fat meal ingested rabbits (2.5 w/v coconut oil enriched with 1% cholesterol for 21 days prior experimentation and 15 days thereafter) demonstrated a significant increase in AUC and Cmax (2.8 and 2.5-fold, respectively) and significant decreases in CL/F (64%) of the drug.

Eliot et al. [234] showed the significant effects of hyperlipidemia on area under the concentration vs. time curve, total body clearance and CL/F of nifedipine following the administration of nifedipine to rats. The ip injection of polaxamer-407(P-407) was used to induce hyperlipidemia in rat. 48 h after the administration of P-407 nifedipine (6mg/kg) was administered either orally, intraperitonealy or intravenously. Hyperlipidemia significantly decreased total body clearance of nifedipine by 38% and CL/F by 45 and 42% following po and ip doses, respectively, thereby increasing AUC, Cmax and half life. Concomitantly, hyperlipidemia significantly lowered the unbound fraction in plasma by 31%. The authors concluded that the change in total body clearance and CL/F of nifedipine in hyperlipidemic rats was mostly related to the altered binding of drug to plasma proteins.

In another study study was accomplished at the Merck Research Laboratories on the pharmacokinetics of two novel peroxisome proliferator-activated receptor agonists, MRL-I[(2R)-7-[3-[2-chloro-4-(4-fluorophenoxy)phenoxy]propoxy]-2-ethyl-3,4- dihydro-2H-benzopyran-2-carboxylic acid] and MRL-II [(2R)-7-[3-[2-chloro-4-(2,2,2-trifluoroethoxy)phenoxy]propoxy]-3,4-dihydro-2-methyl-2H-benzopyran-2-carboxylic acid], in obese Zucker and lean Sprague-Dawley rats following a single intravenous administration. The plasma clearance of both MRL-I and MRL-II was significantly lower in obese Zucker rats (4- and 2-fold, respectively) compared with Sprague-Dawley rat, [218].

As it was noted earlier, administration of a high fat meal or hyperlipidemia and the consequent increase in lipoprotein levels in plasma is not always associated with an increase in AUC and a decrease in CL of drugs. A good example of this phenomenon was observed in the study of cyclosporine pharmacokinetics in high-fat meal and hyperlipidemic rat models [125]. It has been observed that hyperlipidemia and oral lipids did not have any significant effect on clearance of cyclosporine, although the unbound fraction decreased 61% in hyperlipidemia [125]. Gupta and Benet demonstrated contrary results in humans and observed an increase in the clearance of cyclosporine in healthy volunteers [235].

Taken together, it seems that a decrease in the unbound fraction of drugs in plasma in hyperlipidemia or following high fat meal ingestion does not completely explain the change in clearance of drugs. Conversely, the lipophilic structure of drug molecules and their affinity for different lipoprotein fractions in plasma might be more important in this regard.

1.3.5.1 Lipids and drug metabolizing enzymes

Drug metabolism reactions might normally be carried out through one or more of the following three steps. The first step involves conversion of drug molecule to a more polar substance by introducing or unmasking polar functional groups via oxidation, reduction or hydrolytic reactions. In the second step, unmasked groups are conjugated with conjugating enzymes [236]. At the third step, the conjugated molecules are excreted by transporters through liver and/or kidney. CYP, monoamine oxidase (MAO) and epoxide hydrolase are some of the enzymes that are involved in the first step of metabolic reactions. Some of the important enzymes in the second step are uridine diphosphate glucoronyl transferase and glutathione S-transferase [236]. The third step is mostly carried on by drug transporters such as OATs (organic anionic transporters), organic cationic transport proteins and P-gp [237].

The role of P450 enzymes in the metabolic procedures of some endogenous compounds such as arachidonic acid in the body was recognized about two decades ago; however its importance was largely ignored at that time [238]. Nowadays, the importance of arachidonic acid metabolism by P450 in the regulation of the vascular tonicity and kidney function is recognized [238]. Realizing the possible importance of the interaction between arachidonic acid and P450 in the control of physiological function shown by some investigators, the probable role of lipids in the regulation of P450 for the metabolism of exogenous compounds was also studied by other investigators.

The CYP and UGT enzymes are buried in the lipid bilayer of smooth endoplasmic reticulum membranes as insoluble enzymes. The complex of lipid, P450 and CYP450-reductase to form mixed function oxidase (MFO), are necessary for the first step of drug metabolism. It has been observed that the amount of fat in food might influence the drug metabolizing enzymes as well as MFOs [239]. Yoo et al. [240] examined the effect of low fat diet on the activity and amount of CYP2E1, CYP1A2 and CYP2B2 in rats and found that the levels of these enzymes are very low in these rats. Dannenberg and Zakim demonstrated that the activity of UDP-glucotransferase in rat is regulated by fat content of food [241]. The level of some drug metabolizing enzymes such as P450 and UGT and also microsomal fluidity, were reported to be higher in rats nourished with fish oil in comparison with rats fed with olive or corn oil, however, adding cholesterol to rats diet decreased microsomal fluidity [242]. It was also reported that the composition of polyunsaturated fatty acids in PL was a key role in determining the activity of MFO [243]. Kato et al. examined the influence of high n-6 fatty acids (safflower oil containing linolenic acid and γ -linolenic acid and arachidonic acid [20:4(n-6)]) and n-3 fatty acids (fish and perilla oil containing α-linoleic acid, eicosapentaenoic acid [20:5(n-3)] and docosahexaenoic acid[22:6(n-3)]) in food on the fatty acid composition and drug metabolizing enzymes in rat liver microsomes [244]. The results showed that after three weeks of feeding the rats with safflower oil, the content of γ -linolenic acid in the microsomes was increased. It was also observed that the content of arachidonic acid in the rat microsomes was 5 fold higher than the rats fed with perilla oil.

Conversely, the fatty acids in rats fed with perilla oil had more α-linoleic acid, eicosapentaenoic acid and docosahexaenoic acid. The level of P450 was also affected by the fatty acid composition of food. There was no significant difference observed in the expression of CYP1A1, CYP1A2 and CYP2E1 in rats fed with safflower or perilla oil, however, the level of CYP4A1 was lower in rat fed with safflower oil. CYP4A1 is responsible for the metabolism of prostaglandins and leukotrienes. The results of the experiments also showed that the protein level of UGT in rats fed with perilla oil was significantly higher than in the rats fed with safflower oil (1.7 fold) [244].

Yang et al. examined the inducing effect of fish oil on hepatic levels of epoxide hydrolase, glutathione S-transferase (GST) and UDP-glucotransferase [245]. The results of this group of investigators demonstrated that fish oil induced the level of epoxide hydrolase in the liver of male Wistar rats fed for three weeks with either fat free diet, 5% corn oil or 5% w/w Menhaden fish oil (1.8 fold), however the effect of corn oil on the level of this enzyme was not significant [245]. Fish oil also showed an inducing effect on the level of UDP-glucotransferase (near 3 fold). Similar results were also observed on the level of glutathione S-transferase with fish oil (2.4 fold) [245]. Ko et al. [246] also verified the inducing effect of fish oil on the level of glutathione S-transferase in the liver of weaning rat.

The studies of Chen et al. showed that the rats fed with high fish oil diet had 85 and 51% higher PROD (cytochrome 7-pentoxyresorufin O-dealkylase) activity in their liver ($P<0.05$) compared with those fed with low or high corn oil diet. The GST activity in the high fish oil and high corn oil groups was 33 and 18% higher than that in the low corn oil group, respectively ($P<0.05$). Increasing garlic oil with different doses (0, 30, 80, 200 mg/kg) increased GST activity. Northern and Western blot analysis revealed that dietary fish oil increased both hepatic CYP2B1 and placental GST mRNA and protein levels. Hepatic CYP2B1 and placental GST mRNA and protein levels were also dose-dependently increased by garlic oil treatment [247].

The effect of dietary lipid on the level of phase 2 enzymes in the rat intestine was a matter of investigation by Dannenberg et al. They examined the effects of 3 weeks of fat free and isocaloric control diet containing 5% corn or fish oil on the activity of UDP-glucotransferase and GST of rat small intestine [248]. The rats fed with fish oil showed 2-fold higher activity of UDP-glucotransferase in comparison with rats fed with fat-free diet. Although the activity of this enzyme was higher in corn oil fed rats than fat free diet rats, the increase was not significant. Also the level of GST activity was highest in cytosol prepared from rats fed with the fish oil diet and lowest in rats fed with fat free diet (1194±50 vs. 432±24 nmol/mg/min). Treatment of rats with corn oil diet led to intermediate level of enzyme activity (685±15 nmol/mg/min). Similar results were observed on enzyme levels by immunoblotting assays, which confirm the induction effect of fish oil on these enzymes [248]. The induction effect of fish oil on these enzymes in the intestine of rats explains the decreased level of azoxymethane-induced colon cancer in F334 rats fed with fish oil in comparison with corn oil-fed rats. Fish oil has more omega-3 fatty acids and corn oil contains more omega-6 fatty acids [249].

In a recent study, mice were exposed to two different regimens of high fat diet (HFD-1 or HFD-2) for 40 days and the expression of different phase I and phase II enzymes and drug transporters were measured in the liver and intestine of these animals. In order to show the importance of nutrition on the level of different drug metabolizing enzymes, a positive obese group and a control regular fat nourished group were also included in this study. The obesity in the positive obese group was induced without a high fat diet and with the administration of 300 mg/kg of gold thioglucose (GTG) intraperitonealy.

The regimen of the HFD-1 contained a high fat diet from oriental yeast comprised of 36% fat, 22% protein, and 35% carbohydrate. HFD-2 contained 32% fat, 26% protein, and 29% carbohydrate. HFD-2 contained safflower oil and less lard than HFD-1. The chow of the regular nourished groups contained oriental yeast, 5% fat, 24% protein and 54% carbohydrate for the same period. These animals were kept on regular chow for 4 weeks. All of the animals were sacrificed after their nutritional periods and their liver and small intestines were excised. Hepatic and intestinal microsomal protein was prepared. Western blot analysis was performed and the expression of the CYP protein was compared in all of the groups. Furthermore, reverse transcription polymerase chain reaction was performed on extracted total RNA. In all of the groups, plasma TG, CHOL and glucose levels as well as liver CHOL and TG were measured. The results comparing plasma TG, CHOL and glucose levels in control nourished, HFD-1 and HFD-2 demonstrated the significant increase in the levels of plasma glucose, plasma CHOL and liver TG in both HFD groups. On the other hand no significant increases were observed in the level of plasma glucose, TG and CHOL of GTG obese mice, but the hepatic TG level was significantly higher than the control group in this group.

In terms of CYP enzymes, the results comparing the control and HFD-1and HFD-2 groups demonstrated that the expression of CYP3A11 decreased significantly in the livers of both HFD groups. The reduction was observed to be in both protein and mRNA levels. The reduction of CYP2C9 was significant in the liver of the HFD-2, but not the HFD-1 group. In contrast, the level of CYP2E1 protein was increased in both HFD-1 and HFD-2; however the difference was not significant in either the mRNA or expression level. In intestine, the expression of other P450s including CYP2Bs, CYP2Cs and CYP2E1 slightly decreased in both groups but the difference was not significant in any of the HFD groups. In terms of phase II drug metabolizing enzymes and transporters, RT-PCR analyses with RNAs prepared from mice fed HFD-1 demonstrated that hepatic mRNA levels of UDP-glucuronosyltransferases (Ugt1a1 and Ugt2b5), sulfotransferases (St1a4 and St2a9), and drug transporters (Mdr1a, Mrp2, Mrp3 and Oatp4/Slco1b2) were not affected significantly, although there was a tendency toward a decrease for Ugt1a1 and Oatp4 mRNAs.

Comparing the western blot and mRNA levels of different hepatic CYP450 enzymes in control and GTG obese rats indicated no effect on the levels of CYP3A11 and CYP2C9; however in obese mice CYP1A2 and CYP2E1 mRNA levels were decreased whereas CYP2B10 and CYP4A10 mRNA levels were increased [250].

1.4 *Animal models of hyperlipidemia*

The assessment of the pathophysiological effects hyperlipidemia (HL) on on vital systems has been the focus of research interest among many biochemical and physiological investigators. The inital steps toward understanding the role of HL on cardiovascular diseases was mostly obtained by working on animal models and in vitro systems. Choosing proper animal models is important and the biochemistry of lipids in the species compared to humans [113]. Rodents, including rats and mice, share a close resemblance in lipid biochemical pathways with humans. This resemblance is facilitated by the involvement of the same set of genes in controlling the lipoprotein metabolism of both species [251]. In spite of this resemblance, rodents, and especially mice are identified as animals resistant to the development of atherosclerosis [252], due to the accumulation of plasma CHOL mostly in HDL fraction [251].

Historically, different approaches have been taken to produce a desirable hyperlipidemic animal model. The apparently simplest method involves the chronic administration of high fat meal [253, 254]. However, this simplicity is marred by the long and tedious process (weeks) required to obtain a hyperlipidemic state. Furthermore, it is not natural for an herbivorous animal to have a diet enriched in lipids; a Western type of diet and specially hypercholesterolemia has been used in the majority of murine models to induce HL [252].

Alternatively, HL can be induced by administering exogenous chemicals. Among them, polychlorinated biphenyls [255], triton-W1339 [256], isotretinoin [257], estrogen [258] and P-407 [259] have been used in this regard. The mechanism responsible for the resultant increases in the TG and CHOL and consequently lipoprotein levels are unique for each of these exogenous materials. For example, the increase in the level of CHOL by triton-W1339 administration is a result of the depletion of hepatic CHOL, which in turn induces an increase in hepatic HMG-CoA reductase activity and cholesterogenesis [260]. Similarly, the mechanism involved in the cholesterogenic effects of polychlorinated biphenyls is related to an increase in the hepatic HMG-CoA reductase activity; however, increases at the levels of HDL, VLDL and LDL in rats orally administered polychlorinated biphenyls are related to the compensational mechanisms involved in the increase of CHOL levels in liver. In other words, the high concentration of CHOL in liver is compensated for by the increase at the level of HDL to carry the liver CHOL to the blood circulation. Also it is possible that the liver tries to maintain a normal lipid level by increasing the synthesis of LDL and VLDL more than usual [261]. On the other hand, the mechanism of P-407 in HL is related to the direct inhibition of LPL and hepatic lipase and indirect increases in the activity of CETP and LCAT [259].

In addition to the traditionally used animal models in the study of HL, genetically modified animal models of HL have drawn increasing attention in recent years. The obese Zucker rat model is the most prevalent model of HL and was introduced in 1961 as a result of cross-breeding of Sherman and Merck Stock M rats. Obesity is transmitted by mutation of a single gene called *fa* or fat allele [218, 262, 263]. The milky appearance of blood serum is the most striking sign of HL in these animals. Total fatty acids are about 4-fold higher than in lean animals [263]. The measurement of CHOL and TG of Obese and Lean Zucker rat models demonstrated extensively and significantly higher levels for Obese Zucker rats (4.28±0.41 vs. 1.78±0.06 mmol/L for CHOL and 1.18±0.17 vs. 0.54±0.09 mmol/L for TG levels). In addition higher concentrations of HDL and LDL were measured in the Obese Zucker rat model in comparison with the lean animals (2.83±0.39 vs. 1.12±0.06 mmol/L for HDL and 0.93±0.17 vs. 0.41±0.08 mmol/l for LDL) [262].

Other genetically engineered murine models of HL have also been established during the past few years. Stroke-prone spontaneously hypertensive rats or Stroke-prone spontaneously hypertensive *fa/fa* rats are comparable with Zucker *fa/fa* fatties in terms of the concentrations of CHOL and TG [264]. The LA/N corpulent rat is another genetically engineered rat model with significant dyslipidaemic signs. Both male and female rats were severly hypertriglyceridemic (282–512 mg/100 ml) and moderately hypercholesterolemic (74–84 mg/100 ml)[265].

Several knock-out mice models of HL have also been established recently. For instance knock out Apo E mice with extremely elevated serum CHOL levels compared to the wild type were developed in three separate labs [266-268]. Apo E is a major apolipoprotein controlling plasma lipid levels. In addition, apo E is the major constituent of CM, VLDL and their remnants [251]. It is also one of the components that determines the binding of the corresponding particles to the related receptors.

Some other examples in this regard could be VLDL receptor knockout mice with high serum concentrations of TGs, LDL receptor knockout mice with high serum concentrations of CHOL and lecithin cholesterol acyl transferase-deficient mice with low levels of HDL in plasma and consequently high levels of CHOL.

Overall, all of these animal models have their own limitations. The most important pitfall of all of these models ignoring their origin is their distance from the reality of HL in humans. For instance in the P-407 rat model of hyperlipidemia, the serum concentrations of CHOL and TG are much higher than normal. On the other hand it produces a hyperlipidemic state rapidly without overt signs of toxicity. The toxicity of some of the other exogenous compounds such as triton-W1339 (hemolysis) limits the wide use of these systems for long term investigational purposes [259]. In the genetically engineered animal models, other signs of metabolic syndrome such as hyperglucosemia and hypertension concomitantly occur with hyperlipidemia, which limits the use of these models as pure models of HL. In practice, there is no perfect model for HL among the genetically engineered animals.

In this thesis project, P-407 was chosen to produce an animal model of HL. P-407 a thermoreversible, non immunogenic block copolymer consisting of ethylene oxide and propylene oxide blocks arranged in a triblock structure. It is commonly used in drug formulations as the vehicle for oral, rectal, topical, ophthalmic, nasal and injectable delivery of drugs [269]. Pharmacokinetic data of P-407 in rat species indicated extensive tissue distribution (kidney and liver) and a long half-life for this drug (~ 21h) [270]. A change in lipid metabolism in hepatic tissue is the most prevalent toxic side effect of this drug [269]. The reason for choosing this model despite the dramatic alteration in CHOL and TG fractions in plasma is wide acceptance and vast use among different investigators [219, 234, 271]. This model is not only easy to manipulate but also is less toxic to the animals than many of the other chemically-induced models; based on our experience the induction of HL by this model does not cause any physical or emotional damage to the rats.

1.5 *Amiodarone*

1.5.1 Chemical Structure

Fifty years a go, scientists at the Labaz laboratory in Belgium modified the chemical structure of khelin (4, 9-dimethoxy-7-methyl-5H-furo[3,2-g][1]benzopyran-5-one), a natural product derived from *Ammi visnaga* [272] with known coronary dilator properties, in order to have potent coronary dilators [273]. Their research further led to discovery of a potent antianginal drug called "amiodarone". The antiarrhythmic properties of amiodarone (AM) (2-butyl-3-benzofuranyl-4-[2-(diethylamino)-ethoxy]-3,5-diiodophenyl-ketone (Figure 18) were discovered later due to its ability to produce a clinically important increase in action potential [274]. At the moment, AM is classified as the most important antiarrhythmic drug and can reduce the risk of mortality in patients with severe congestive heart failure or after acute myocardial infarction [275].

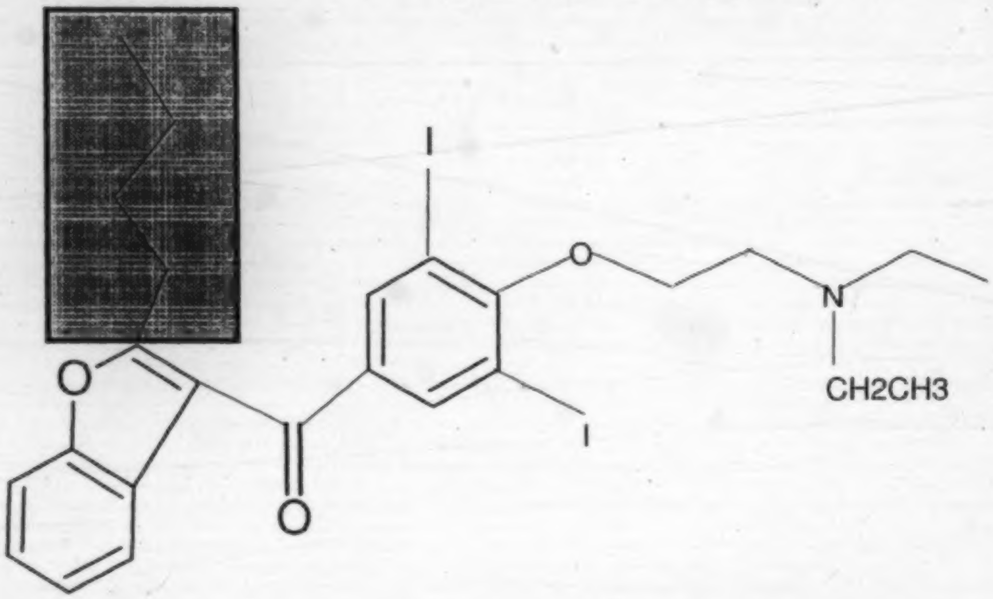

Figure 18: Chemical structure of amiodarone. Shaded area (butyl side chain) is one of the main parts of the molecule responsible for the unique pharmacokinetic properties of AM.

1.5.2 Pharmacology and Pharmacodynamics

Amiodarone is a potent broad spectrum class III antiarrhythmic drug (Vaughn-Williams classification) and is useful in treating a wide variety of cardiac arrhythmias, including atrial and ventricular arrhythmias. AM is the most complicated antiarrhythmic drug ever discovered. It has a number of electrophysiological effects that probably contribute to its antiarrhythmic efficacy. It also has a complex pharmacologic profile that limits its applicability in certain clinical situations but enhances it in others [276]. Despite its marked effect on prolonging repolarization, which is reflected as increased QTc interval, AM has a relatively weak torsadogenic side effect (the ability to induce Torsades de pointes) [277]. AM exerts its actions through multiple mechanisms, including potassium channel blockade, calcium and sodium channel suppression and noncompetitive α- and ß-adrenoreceptor antagonism [276, 278]. The drug also dilates coronary arteries and reduces resistance in coronary vessels. AM may also exert an antiarrhythmic effect by increasing coronary blood flow; especially in patients with severe ischemic heart disease [276]. The intravenous formulation of AM has been observed to produce vasodilation and consequent hypertension.

The noncompetitive α- and ß-adrenoreceptor antagonist effects of the drug accounts for its potent effect on sinus and atroventricular nodal function as well as its tendency to cause heart block and sinus bradycardia in patients with antecedent conduction disease [276].

In contrast to pure Class III potassium channel blocking drugs, AM decreases the dispersion of repolarization between ventricular subepicardial, subendocardial, midmyocardial cells and Purkinje fibers [277]. Amiodarone was first recognized to lengthen cardiac action potential duration (APD) after chronic treatment, but today AM is not only used as a therapeutic agent but also a prophylactic drug used in a wide range of cardiac rhythm disturbances [279].

1.5.3 Pharmacokinetics

Amiodarone is one the most unusual drugs used in humans. It is available as oral tablets and an iv injectable solution. There are many published data about the pharmacokinetics of AM. Absorption of AM is incomplete and it has relatively poor bioavailability (0.3-0.7) [280]. In human plasma, AM possesses a very large volume of distribution (66 L/kg) [281] and a correspondent long terminal half-life in single oral dose administration (12-80 h) [282]. The half-life of the drug after chronic administration is even longer (25-55 days) [281, 283]. Amiodarone has erratic, unpredictable absorption characteristics resulting in low and variable bioavailability after oral administration [281, 284]. The drug is also known to bind to circulating lipoproteins, which reportedly comprises 33.5% of its overall total protein binding (95.6%) in normolipidemic plasma [284, 285]. The pka of AM is reported to be 8.7±0.2. Furthermore the value of *Log P* for AM is reported to be 9 [286]. The drug has a low hepatic extraction ratio in humans but a moderate extraction ratio in rat [281, 287]. Amiodarone is completely eliminated by metabolism with no parent drug being detected in urine [280]. The therapeutic range of AM is narrow (0.5-2 mg/L), and therefore the chance of toxicity with this drug is high.

It seems that the butyl side chain (shaded area in Figure 18) of amiodarone is responsible for some of the unique pharmacokinetic properties of AM. The replacement of this side chain with methyl and ethyl acetate groups decreased the half-life of drug to only 12 and 6 min. respectively; however, the electrophysiological activity of AM had been retained [278].

1.5.4 Metabolism

Amiodarone is extensively metabolized, predominantly in the liver, although there is evidence for extrahepatic metabolism in some preclinical species [288, 289]. Among the five pathways involved in the metabolism of AM (N-deethylation, hydroxylation, O-dealkylation, deiodination, and glucuronidation), N-dealkylation is the most important [290, 291]. The immediate product of this metabolic pathway is desethylamiodarone (DEA), which is the main circulating metabolite of AM in human and rat [290].

One of the reasons for the poor bioavailability of AM could be its first-pass metabolism in intestine. Several enzymes have been identified as metabolizing AM to DEA in both liver and intestine. In humans, CYP3A4 and CYP2C8 are the main enzymes involved in the metabolism of AM to DEA [291, 292]. From a clinical point of view, AM inhibits CYP1A1, CYP1A2, CYP2B6, CYP2C9 and CYP2D6. In vitro studies demonstrated that DEA is more potent than the parent drug at inhibiting CYP3A4 [280].

Amiodarone is a potent inhibitor of P-gp, therefore it is expected to have drug interactions with P-gp substrates such as digoxin [280].

1.6 *Rationale and hypotheses*

1.6.1 Rationale

In humans given AM, the measurement of both DEA and AM in plasma is possible using conventional high-performance liquid chromatographic (HPLC) methods [293, 294] or by tandem liquid chromatographic mass spectrometry techniques [295, 296]. In contrast, after administration of AM to a commonly used preclinical species, the rat, it was observed that DEA concentrations were very low. Owing to this, the need to develop a more sensitive method for the measurement of DEA in rat plasma was desirable. Furthermore, the possibility of the measurement of AM and DEA in rat tissues by the current HPLC method was considered. Although the concentrations of AM and DEA in most tissues exceeded those in plasma, and their measurement in some tissues is feasible by the HPLC-UV detection [297], it was observed that use of the HPLC/UV method for assay of the drug in some other tissues (e.g. liver) was associated with co-elution of endogenous components, which could prove to be problematic.

The pharmacokinetics of AM may be dependent upon clinical status. For example, it has been demonstrated that the elimination half-life of AM is lower in normal volunteers than in cardiovascular patients [298]. Hyperlipoproteinemia is clearly identified as a major contributor towards an increased risk of atherosclerosis and coronary heart disease [299]. In addition to intrinsic hyperlipidemia, lipoproteins in plasma can be transiently increased following ingestion of a high fat meal. Lalloz and coworkers indicated that AM binds to circulating lipoproteins, which appears to comprise about 33.5% [285]of its overall total protein binding (95.6%) [284, 285] in plasma. It is known that a fatty meal can increase the bioavailability of some lipophilic molecules such as AM [142], which displays incomplete or slow oral absorption [284, 300]. The increased solubilization of lipophilic molecules in the digested fat content of food may facilitate an increase in drug absorption across the intestinal lumen. In addition to this increase in absorption, a postprandial decrease in systemic clearance as a result of a transient increase in binding of drug to lipoproteins may also contribute to an increase in AUC after ingestion of a high fat meal [132, 204].

Most current knowledge regarding the metabolism of AM has been obtained from human studies, although some data are available regarding the in vitro metabolism of the drug in rabbit and rat [301]. Nevertheless, few data are available regarding the drug-metabolizing enzyme(s) involved in AM biotransformation in the rat, which has been used as an animal model for AM pharmacokinetics [301]. In human liver the contribution of CYP3A4 and CYP2C8 enzymes in metabolism of AM to DEA has been demonstrated [291, 292]. Furthermore, in human intestine CYP3A4 is known to be a predominant CYP450 enzyme and to play an important role in the first pass metabolism of 50-70% of marketed drugs [302]. In addition, P-gp is also present at high levels in the villus tip enterocytes of the small intestine [303]. The presence of CYP3A4 and P-gp in the intestine and their interaction can affect the disposition of drugs that are dual substrates for these proteins [292]. It is known that AM is a co-substrate for both P-gp and CYP3A4 [297, 304]. Therefore, oral bioavailability of AM would likely be influenced by presystemic activities of these proteins. Furthermore, inhibition of either of these processes with KTZ would be predicted to yield higher systemic concentrations of AM and, perhaps, lower levels of circulating metabolite. To assess the relevance of the in vitro inhibitory finding of KTZ on AM metabolism, we undertook an in vivo experiment to determine the effect of KTZ inhibition on AM pharmacokinetics.

The effect of hyperlipidemia on the metabolism of AM, which happens mostly in hepatic tissue, is completely unknown. It has been observed that CYP450 enzymes are affected by some physiological and pathophysiological conditions. For instance the stimulation of immune system can inhibit drug metabolism. Changes of the immune system in inflammatory diseases are known to downregulate CYP450 enzymes in an enzyme-selective manner [305]. On the other hand the effect of diabetes on the some CYP450 enzyme is upregulation of some of these enzymes [306, 307]. Down regulation or upregulation of hepatic enzymes responsible for the hepatic metabolism of AM in hyperlipidemia could affect the plasma concentration of its prevalent metabolite DEA.

Due to the significant participation of DEA in the pharmacological and toxicological properties of AM, changes in plasma level of DEA could affect the pharmacology and toxicology of AM.

In addition to the hepatic metabolism of drugs, the extrahepatic biotransformation of drugs has also drawn the attention of many pharmaceutical and clinical researchers [308-311]. Among the extrahepatic tissues, the gastrointestinal tract (GIT) is well recognized as being an important presystemic metabolizing organ for orally administered drugs [48, 167]. The GIT is abundant in several phase I [312] and phase II [313] drug metabolizing enzymes. Specifically, it possesses CYP1A1, CYP2B1, CYP2C6, CYP2C11, CYP3A, CYP2D6 and CYP2J4 activities [314, 315]. Among these, CYP3A is the most prevalent metabolizing Phase I isoenzyme in mammalian species, including humans and rats [316]. Metabolism in the GIT can contribute to a low oral bioavailability [302, 317-319]. In general, the contribution of intestinal metabolism to the overall first pass metabolism of drugs is negligible in comparison with hepatic metabolism. This is due to the entry of the gastrointestinal blood flow into the portal vein, and the much greater number and breadth of metabolizing enzymes in the liver [320].

High fat meals can affect the oral bioavailability of many drugs. For some drugs a change in solubility can ensue. Oral lipids may also facilitate a bypass of first pass hepatic metabolism of lipoprotein-bound drugs via the intestinal lymphatic pathway [161]. Lipids may also influence drug transport protein activity [5, 118, 119, 121], and possibly metabolizing efficiency [250].

Hyperlipidemia, as the most prevalent predisposing factor for cardiac and brain strokes in developing countries [321], might increase or decrease the toxic properties of both AM and DEA. Our understanding about the tissue distribution of AM and its active metabolite DEA is limited. Tissue distribution of both AM and DEA after a single iv dose of AM in the hyperlipidemic simulated rat model can be used as a surrogate to predict the effect of hyperlipidemia on toxic effects of this drug in tachyarrhythmia patients

1.6.2 Hypothesis

1.6.2.1 Pharmacokinetics of AM in hyperlipidemia and high fat meal simulated rat model

An increase in plasma lipoproteins caused by ingestion of oral lipids or due to hyperlipidemia is postulated to increase the lipoprotein binding of AM in plasma.

It has been observed that only unbound fractions of drugs can be distributed into different tissues or cleared by the eliminating organ [322]. Based on this theory and due to the decrease in the unbound fraction of AM in plasma, a decrease in volume of distribution and clearance in both hyperlipidemic and oil treated rats is expected. Therefore, the total plasma concentration of AM is expected to show an increase; however the unbound fraction is expected to decrease. A change in the half-life of the drug is not expected due to the change in both clearance and volume of distribution. It is clear that the effect of oral lipid will not be as drastic as that expected with the hyperlipidemic model.

1.6.2.2 Determination of the enzyme (s) involved in the metabolism of AM to DEA in rat

There is a resemblance between human and rat in the enzymes involved in the metabolism of AM to DEA.

Based on visual inspection of the Michaelis- Menten graph and the fitting of the data, the choice of the enzyme model suitable for these studies will be possible. Based on these results, we can decide how many enzymes are involved in this metabolic procedure. It is hypothesized that the analogue enzymes of CYP3A4 in human are involved in the metabolism of AM to DEA in rat. These enzymes are CYP3A1 and CYP3A2. The expressions of these enzymes are different in liver and intestine of the rat.

1.6.2.3 Effect of hyperlipidemia on tissue distribution of AM and DEA in rat

i. *It is expected to see a decrease in the unbound fraction of AM and DEA in P-407 treated rats, hence altered concentration of drugs in some tissues, although due to the existence of LP receptors in some other tissues, it is expected to see higher concentrations of drugs in these tissues.*

ii. *Overall, alteration in lipoprotein binding of AM and DEA leads to a change in LP directed uptake of tissues by LP receptors, therefore, changes will be observed in tissue:plasma ratios in the hyperlipidemic rats.*

1.6.2.4 Effect of hyperlipidemia on hepatic metabolism of AM to DEA in rat

Due to a decrease in the expression of some metabolic enzymes involved in the metabolism of AM to DEA in the genetically obese Zucker rat model, an animal model resembling our model for hyperlipidemia [218], metabolism of AM to DEA in the liver is hypothesized to decrease in hyperlipidemia.

A decrease in the metabolism of AM to DEA might be the most important factor in the determination of the total body clearance, which in turn is hypothesized to be decreased due to the lipoprotein binding of AM. The underlying mechanism should be sought in downregulation of the enzymes responsible for this metabolic procedure; however it is not the only factor.

1.6.2.5 Effect of oral lipid on intestinal metabolism of AM to DEA in rat

Oral fat ingestion affects the intestinal metabolism of AM to DEA in rat.

Based on the results obtained from the effect of high fat meal on pharmacokinetics of HF in dog, it was observed that in postprandial conditions, AUC of HF increased 12-fold but the increase in the AUC of desbutyl halofantrine the active metabolite of HF was only 2-fold [204]. For another drug, amiodarone (AM), in humans, it was shown that the administration of a high fat content meal caused a somewhat greater increase in the concentrations of the parent drug (2.4-fold) than its primary circulating metabolite, desethylamiodarone (1.6-fold).

These interesting observations warranted further attention. One possible explanation for the discrepancy in metabolite to drug ratio in the high lipid meal state is a decrease in presystemic formation of the metabolite. Both halofantrine and amiodarone share a number of similarities from a pharmacokinetic perspective. Both are highly lipophilic, highly metabolized, and highly lipoprotein bound drugs. In order to better examine this issue, some studies, reported here, were performed involving amiodarone in which the ability of the GIT to metabolize AM to DEA was examined in the presence and absence of components (bile and lipid) present in the gut after a high fat meal. It was hypothesized that the metabolite to drug ratio would be decreased in the presence of these lipid components, in vitro and in vivo.

1.7 *Objectives*

Based on the rational of thesis as indicated, the following items were listed as the objective of the study

Development of an LC/MS method for AM and DEA measurement in rat specimens

Pharmacokinetics of AM in hyperlipidemia and high fat meal simulated rat model

Determination of the enzyme(s) involved in the metabolism of AM to DEA in rat

Effect of hyperlipidemia on tissue distribution of AM and DEA in rat

Effect of hyperlipidemia on hepatic metabolism of AM to DEA in rat

Effect of oral lipid on intestinal metabolism of AM to DEA in rat

2 EXPERIMENTAL

2.1 *Materials*

Amiodarone HCl (AM), ethopropazine HCl, ketoconazole (KTZ), and β-nicotinamide adenine dinucleotide phosphate tetrasodium (NADPH), sodium chloride, sodium bromide and sodium hydroxide were purchased from Sigma-Aldrich (St. Louis, MO). Desethylamiodarone (DEA) was obtained as a gift from Wyeth Research (Monmouth Junction, NJ). Methanol, acetonitrile, and hexane [all high performance liquid chromatography (HPLC) grade], triethylamine and sulfuric acid (both analytical grade) were purchased from EM Scientific (Gibbstown, NJ). Potassium dihydrogen orthophosphate, dipotassium hydrogen orthophosphate, potassium chloride, magnesium chloride hexahydrate, sucrose, and calcium chloride dihydrate (all analytical grades) were obtained from BDH (Toronto, ON, Canada). Cholesterol, peanut oil, Poloxamer 407 (P-407), sodium potassium tartarate, cupric sulfate anhydrous, bovine serum albumin (BSA), and Folin –Phenol reagent were obtained from Sigma (St.Louis, Mo, USA), Halothane BP was purchased from MTC Pharmaceuticals (Cambridge, ON, Canada). Isoflurane USP was purchased from Halocarbon Products Corporation (River Edge, NJ, USA). Heparin sodium injection, 1000 U/ml, was obtained from Leo Pharma Inc. (Thornhill, ON, Canada). Amiodarone HCl (150 mg/3 ml) as a sterile injectable solution was prepared by either Sandoz Canada (Sandoz Canada Inc. Quebec, Canada) or Sabex (50mg/ml) (Boucherville, Quebec, Canada). Ketoconazole oral tablets (Nizoral, Apotex, Canada) were purchased from the hospital pharmacy department at the University of Alberta Hospitals.

Enzymatic assay kits for determination of total cholesterol (CHOL) and triglyceride (TG) in human and rat plasma samples were purchased from Diagnostic Chemicals Limited (Charlottetown, Prince Edward Island, Canada).

Anti-rat polyclonal CYP3A2, anti-rat polyclonal CYP2B1/2 raised in rabbit, and anti-rat polyclonal CYP1A2 raised in mouse were purchased from Daiichi Pure Chemicals Co., Ltd. (Tokyo, Japan). Supersomes expressing either rat CYP1A1 or CYP3A1 with supplementation of cytochrome b5 and P450 reductase were purchased from BD Gentest (Woburn, MA).

Recombinant CYP1A2, CYP2B1/2, CYP2C6, CYP3A1, actin anti-rat antibodies, goat anti-rabbit IgG HPR, goat anti-mouse IgG HPR and low range markers were purchased from Santa Cruz Biotechnology Inc. (Santa Cruz, CA). Recombinant CYP2C11 and CYP3A2 were purchased from Cedarlane® Laboratories Limited (Hornby, Ontario, Canada). LDH kit (Lactate dehydrogenase) used for the assessment of intestinal tissue viability was purchased from Sigma-Aldrich, Canada (Oakville, ON, Canada)

2.2 *Methods*

2.2.1 Assays

2.2.1.1 Instrumentation

a) HPLC

For analysis of AM and DEA in some parts of the study an HPLC system was used. The HPLC system consisted of Waters 600- multisolvent delivery system pump, a Waters ™ 717 plus autosampler, Waters ™ 486 tunable absorbance detector. A CR501 Chromatopack Schimadzu integrator or EZ-Chrom software (Alltech, Pleasanthon, CA, USA) were used for data collection.

The chromatographic separations of AM, DEA and internal standard were accomplished using a 100mm×8mm I.D. Nova-Pak C8 analytical column cartridge placed in a radial compression module (Waters, Milford MA, USA). A guard-Pak pre-column Module (Waters, Milford MA, USA) containing an ODS cartridge insert was placed serially just before the analytical column.

b) LC/MS

For analysis of AM and DEA in some other parts of the study the LC/MS system with electrospray ionization source was used. The mass spectrometer was operating in positive ion mode with selective ion recorder (SIR) acquisition mode. The nebulizing gas was obtained from an in house high purity nitrogen source. The temperature of the source was set at 150°C and the voltage of the capillary and cone was 3.2 KV. The cone voltage were set at 25, 40 and 50 V for IS, DEA and AM, respectively. The gas flow of desolvation and cone were set at 550 and 80 L/h, respectively.

Chromatographic separation was achieved using a C18, 3.5 µm (2.1×50 mm) column as the stationary phase (XTerra® MS, Ireland).

The mixture of standard compounds and internal standard were analyzed on the mass spectrometer (MS) using flow injection in scan mode to determine optimal fragmentation for each compound and establishment of the *m/z* values of the molecular ions.

2.2.1.2 Preparation of standard and stock solutions for drug analysis

The stock solution of AM for pharmacokinetic studies was prepared by dissolving 10.77 mg of AM HCl in 100 mg of methanol (equivalent to 100 µg/ml of AM base). For metabolism studies 107.7 mg of AM HCl was dissolved in 100 ml of methanol (equivalent to 1000 µg/ml). These solutions were stored in amber bottles in -30 °C and remained stable for more than 6 months. The working standard solutions prepared daily by sequential dilution of stock solution in methanol.

The stock solution of DEA for both pharmacokinetics and metabolism studies was prepared by dissolving 10 mg of DEA standard powder in 100 ml of methanol (100 µg/ml). The stock solution was kept in amber bottle at -30 ° C and remained stable for more than 6 months. The working standard solutions prepared daily by sequential dilution of stock solution in methanol.

The stock solution of ethopropazine HCl as internal standard (IS) prepared by dissolving 5.6 mg of ET HCl standard powder in 100 ml of methanol (equivalent to 50 μg/ml of ET base).

2.2.2 Extraction techniques

2.2.2.1 HPLC

The collected plasma samples were thawed on the day of analysis. Each sample was added 30 μl of a solution containing 50 μl/ml of ET as internal standard and 300 μl of acetonitrile for precipitation of proteins. The plasma or serum samples were then centrifuged at 3000 rpm for 3 min and the supernatants transferred to disposable glass tubes (13×100 mm) containing 300 μl of phosphate buffer solution (pH=5.9) and extracted with 3 ml hexane solution. The tubes were vortex-mixed for about 45 seconds and centrifuged at 3000 rpm for 3 min .The supernatant were transferred to new borosilicate glass tubes (12×75 mm) and dried for about 30 min under vacuum by a thermosavant (Savant Speedvac, Colin Drive, Holbrook, NY, USA). The dried samples were recnstituted in 120 μl of mobile phase and appropriate volumes (50-100 μl) were injected to HPLC.

2.2.2.2 LC/MS

To each 0.1 ml plasma sample was added 0.03 ml of IS. To extract the analytes from rat plasma, 0.3 ml of acetonitrile was added to a 2 ml polypropylene microcentrifuge tube. The tube was briefly vortex mixed (5 s) to precipitate plasma proteins. The tubes were subsequently centrifuged for 2 min and the supernatants were carefully transferred to new glass tubes using Pasteur pipets. To each tube, 0.3 ml of HPLC water and 3 ml of hexane were added. The tubes were then vortex mixed for 30 s and centrifuged at 3000 g for 3 min. The organic layer was transferred to new glass tubes and evaporated to dryness in vacuo. The residues were reconstituted using 1 ml of methanol and aliquots of 5-10 μL were injected into the LC/MS system.

For extraction from tissues, approximately 300 mg of each blotted, thawed tissue was homogenized in distilled water (1:3 w/w). An aliquot of 400 µg of homogenate of each tissue (equivalent to 100 mg of wet tissue) was transferred to a clean glass tube and 0.03 ml of IS (2.5 µg/ml) and 1 ml of acetonitrile were added to each tube. The tubes were subsequently vortex mixed (10 s) and centrifuged for 3 min in order to precipitate the protein content. The supernatant layers were transferred to new tubes and 6 ml of hexane were added. The tubes were then vortex mixed for 30 s and centrifuged at 3000 g for 3 min. The organic layer was transferred to new glass tubes and evaporated to dryness in vacuo. The residues were reconstituted using 1 ml of methanol and aliquots of 5-10 µL were injected into the LC/MS system.

2.2.3 Analytical techniques

2.2.3.1 HPLC

The mobile phase consisted of methanol: acetonitrile: [25 mM KH_2PO_4: 3 mM sulfuric acid: 3.6 mM triethylamine] in a combination of 63:12:25 V/V. Before use, the mobile phase was degassed by passing it through a 0.45 µm filter. The mobile phase was pumped at an isocratic flow rate of 1.5 ml/min at room temperature. Immediately after injection of the samples, the UV detection wave length was set at 254 nm. At 7 min post- injection, it was switched to 242 nm. The wave length of 254 nm represented the UV maximum of ET in methanol and 242 nm represented the UV maximum of AM and DEA in methanol [323].

2.2.3.2 LC/MS

The mobile phase was pumped as a linear gradient from methanol:formic acid 0.2%, 40:60 v/v to 90:10 v/v over 12 min, then back to the original 40:60 v/v composition over 3 min. Total analytical run time was 15 min. A constant flow rate of 0.2 ml/min was used throughout.

2.2.4 Standard curves

2.2.4.1 Pharmacokinetics and studies of distribution of AM and DEA in lipoprotein fraction in plasma

Standard curves in pharmacokinetic studies for both AM and DEA over the range of 35-100000 ng/ml were constructed by spiking not more than 50 μL of each working standard solutions of AM and DEA to 100 μL of blank plasma. A fixed volume of 30 μL of internal standard was added to each tube and extraction was accomplished by the same method described above.

2.2.4.2 Microsomal studies

In microsomal studies the volume of standard solution in each tube was 500 μl, which consisted of a mixture of phosphate buffer solution (pH=7.4) containing 5mM of magnesium chloride hexahydrate and microsomal protein from gut or liver (1 mg/ml). Adding the working standard solutions of AM and DEA over the range of 2.5-100000 ng/ml was based on the desired concentrations of the solution. Either HPLC or LC-MS method were used appropriately for the analysis of the samples.

2.2.4.3 Tissue distribution and everted gut studies

Standard curves over the range of 2.5-100000 ng/ml in tissue distribution and everted gut studies for both AM and DEA were constructed by spiking the desired amount of each working standard solutions of AM and DEA to 400 μL of blank tissue homogenate. A fixed volume of 30 μL of internal standard (2.5 mg/L) was added to each tube and extraction was accomplished by the same method described above.

2.2.5 Quantification of AM and DEA

Quantification was based on standard curves constructed using either peak height or peak area ratios of parent drug or metabolite to internal standard versus nominal parent drug or metabolite concentration.

2.2.5.1 Validation of modified HPLC method for DEA assay

Validation of the DEA assay method was accomplished by testing different concentrations of DEA intraday (33, 70, 125, 250, 500, 700, 1000 ng/ml) which were extracted from rat blank plasma.

2.2.5.2 Validation of LC/MS method

Complete validation assessment was made for plasma samples. For tissues, validation was determined using the results from quality control samples run along with standard curves [132].

For plasma, calibration samples of 0.1 ml containing AM, DEA and ET were constructed over the concentration range of 2.5-1000 ng/ml for both AM and DEA. The ratios of AM or DEA to ET peak height were calculated and plotted vs. nominal AM or DEA concentrations, respectively. Due to the wide range of concentrations, data for calibration curves were weighted by a factor of 1/concentration for DEA and 1/concentration^2 for AM.

Intraday accuracy and precision of the assay were determined using five different concentrations of DEA and AM, respectively in rat plasma. For both AM and DEA, the concentrations were chosen at 2.5, 10, 50, 250, 1000 ng/ml. Each concentration had a replicate of 5 samples. To permit the assessment of interday accuracy and precision, the assay was repeated on three separate days. For each daily run, a set of calibration samples separate from the validation samples was prepared to permit quantification of the peak height ratios of both AM and DEA to internal standard.

Precision was assessed by percentage coefficient of variation (CV %), which was calculated as:

$$\mathrm{CV\%}_{\mathrm{intraday}} = \frac{100 \times \mathrm{SD}}{\text{Mean measured concentration}}$$

and

$$\mathrm{CV\%}_{\mathrm{interday}} = \frac{\mathrm{CV\%}_{\mathrm{run\,1}} + \mathrm{CV\%}_{\mathrm{run\,2}} + \mathrm{CV\%}_{\mathrm{run\,3}}}{3}$$

Bias was assessed by determining percent error, which was calculated as:

$$\text{Mean \% error}_{\mathrm{intraday}} = 100 \times \frac{\text{measured concentration - expected concentration}}{\text{expected concentration}}$$

and

$$\text{Mean \% error}_{\mathrm{interday}} = \frac{\text{error \%}_{\mathrm{run\,1}} + \text{error \%}_{\mathrm{run\,2}} + \text{error \%}_{\mathrm{run\,3}}}{3}$$

2.2.6 In vivo and in vitro studies

All studies were approved by the University of Alberta Health Sciences Animal Policy and Welfare Committee. Male Sprague–Dawley rats (Charles River rats CRC, Quebec, Canada) were used in all of the pharmacokinetic, tissue distribution and everted gut metabolism studies of AM and DEA. Body weight was between 250-400 g and all of the rats were housed in the biological sciences animal house at temperature controlled rooms with a 12 h light per day. The animals were fed by a standard rodent's chow containing of 4.5% fat (Lab diet ® 5001, PMI nutrition LLC, Brentwood, USA). They had free access to food and water prior to experimentation.

2.2.6.1 Rat pharmacokinetics and tissue distribution studies

a) Surgical procedures

The day before the experiment, the jugular veins of the rats were catheterized with a cannula under halothane anesthetization (Surgivet, Waukesha, WI, USA). Each cannula was made by inserting 2-3 cm of silastic tubing (Laboratory tubing, 508-003, Dow corning, Midland, Michigan, USA) over the tip of approximately 5 cm length of polyethylene tubing (Intramedic®,Clay Adams, Sparks, MD, USA) with about 0.5 cm of overlap. The silastic tubing end was inserted to the right jugular vein and the polyethylene end was pulled out through the dorsal side of the neck. The exposed areas were closed using a surgical suture. The cannula was flushed with 100 u/ml heparin in 0.9% saline and the end of the cannula was capped with a 23 G stainless steel needle, which was crimped using pliers. After recovery, each rat was allowed to have free access to water but not food. The morning after, each rat was transferred to a metabolic cage and after adaptation for approximately 30 minutes with free allowance to water, they were dosed intravenously or orally (feeding gavage) with AM based on the protocol of the study. After obtaining the four hour sample they were given food.

b) Dosing and sample collection

I. Preparation of dosing solutions

All of the dosage solutions were prepared fresh on the morning of pharmacokinetic studies. The intravenous dosages of AM were prepared by dilution of AM injectable solution (AM hydrochloride vial 150 mg/3 ml) in normal saline to a final concentration of 12.5 mg/ml.

The oral dosages of AM were prepared by dilution of AM injectable solution in normal saline to a final concentration of 25 mg/ml. Oral KTZ suspension (10.95 mg/ml) was prepared in methylcellulose 1 % by crushing KTZ tablets 200 mg (Nizoral®). Peanut oil+ cholesterol solution was prepared by dissolving cholesterol powder (1% W/V) in peanut oil. The mixture was kept in room temperature for ~ 1h to complete the solubility.

Poloxamer 407 (P-407) solution was prepared by dissolving 2.05 g of pluronic F-127 in 13.7 ml of normal saline. The mixture was kept in a fridge overnight to complete the solubility.

II. Sample collection in the pharmacokinetic studies

For iv studies, blood samples (100-200 μl) were collected at approximately 0.083, 0.33, 0.67, 1, 2, 3, 4, 6, 8, 10, 24, 32, 48, 144 hrs after the dosing in polypropylene tubes. After collection, each blood sample was centrifuged for about 3 min and plasma was transferred to a new polypropylene tube and stored at -30° C until analyzed by HPLC or LC/MS.

For oral studies, blood samples (100-200 μl) were collected at approximately 0.25, 0.5, 1, 2, 3, 4, 6, 8, 10, 24, 48, 144 hrs after the dosing in polypropylene tubes. After collection, each blood sample was centrifuged for about 3 min and plasma or serum was transferred to a new polypropylene tube and stored at -30° C until analyzed by either HPLC or LC/MS.

In drug interaction studies the last plasma samples were collected at 48 hrs.

III. Sample collection in tissue distribution studies

Normolipoproteinemic (NL) and hyperlipidemic (HL) plasma was obtained by exsanguination of rats by cardiac puncture under anesthesia with halothane. Blood was collected in heparinized tubes, centrifuged for 10 min at 3000 g and plasma separated.
In addition to plasma, heart, liver, kidney, lung, brain, fat and spleen were also collected at different time points based on the protocol of the study. The excised tissues were kept in separate tubes at -30°C and then analyzed for both AM and DEA by LC/MS.

2.2.6.2 Everted gut metabolism

In order to study the effect of a high fat meal on the intestinal metabolism of AM to DEA in different intestinal segments of the rat, 4 groups of animals (n=4-6) were employed. Rats in each group had free access to food and water prior to experimentation. All rats received rodent chow up to the time of experimentation, although in one subgroup the animals (n=4) were pretreated with two doses of peanut oil enriched with cholesterol 1% w/v (2 ml/kg) given 2.5 h and 30 min before the harvesting of the intestinal segments.

At the time of the experiment, rats were anesthetized under isoflurane/oxygen delivered by anesthetic machine and a single incision was made in their abdomen. The bile duct of each rat was closed using a single thread knot. Below the pyloric sphincter, the intestinal tissue was cut into 5 segments of approximately 10 cm. Each segment was rinsed with ice cold Krebs-Heinseleit bicarbonate buffer (KH) containing 118 mM sodium chloride, 4.75 mM KCl, 2.50 mM calcium chloride, 1.19 mM KH_2PO_4, 1.19 mM $MgSO_4$, 25 mM sodium hydrogen carbonate, and 11 mM dextrose [Aronson, 1977 #523; Aronson, 1977 #520]. The pH was adjusted to 7.4-7.6 using either HCl or sodium Hydroxide. Each segment was everted using a glass rod. One end of the everted sac was ligated with a silk thread and tied. The other end was left open for filling with KH (37°C) and then tied with silk thread. Each segment was then placed into a jacketed tissue bath containing 10 μg/ml (14.7 μM) of AM HCl for injection (8 μL per chamber). The total volume of buffer solution in each chamber was 40 ml.

The segments were incubated with AM in the presence of a number of different compositions of buffer solutions. These were pH 7.4 KH (n=5 rats), KH+5% simulated bile solution (SBS) (n=4 rats), and KH+25% SBS (n=4 rats). The intestinal segments from the rats pretreated with peanut oil were incubated with KH+25% SBS. In one of the groups (n=4 rats), gut segments were exposed to KH-25% SBS plus 5% soybean oil emulsion (INLP).

Each chamber was continuously aerated with a mixture of oxygen and carbon dioxide (95: 5) at 37°C for 2 h. After the end of the incubation time, a needle attached to a syringe was inserted into the sac and an aliquot of the solution was collected for analysis of AM and DEA. Each segment was then fully removed from the incubation chamber, blotted dry with tissue paper and weighed, then subjected to homogenization and assay for AM and DEA.

2.2.7 Animal allocations

2.2.7.1 Pharmacokinetic studies

Based on the design of the study, rats were divided into different groups based on the route of administration and the prior treatment.

Group A (n=7); 25 mg/kg of AM solution was administered as intravenous injection (NL rats).

Group B (n=7); 25mg/kg of AM solution was administered intravenously with the pretreatment of 2 ml/kg of peanut oil+ cholesterol orally (≅ 0.5-0.7ml) 0.5 hr before and 2 hrs after the dosing.

Group C (n=7); 25 mg/kg of AM solution was administered intravenously with the pretreatment of P-407 solution (1g/kg) approximately 36 h before the study as an ip injection (HL rats).

Group D (n=6); 50 mg/kg of AM solution was administered orally by a feeding gavage (≅ 0.5-0.7 ml).

Group E (n=6); 50 mg/kg of AM was administered orally by a feeding gavage with the pretreatment of 2 ml/kg of peanut oil enriched with 1% W/V cholesterol orally (≅ 0.5-0.7ml) 0.5 hr before and 2 hrs after the dosing.

Group F (n=5); 25 mg/kg of AM solution with the pretreatment of oral administration of KTZ oral suspension (17.1 mg/kg), 30 min before the surgery, 30 minutes before AM administration and 6 hrs after AM administration.

Group G (n=5); 50 mg/kg of AM solution administered orally with the pretreatment of oral administration of KTZ oral suspension (17.1 mg/kg) in not more than 0.6 ml, 30 min before the surgery, 30 minutes before AM administration and 6 hrs after AM administration.

2.2.7.2 Tissue distribution

In order to assess the effect of HL on the disposition of AM, rats were allocated into two groups of normolipidemia (NL) and HL. About thirty-six hours before the tissue distribution experiment, one group of rats was rendered HL by a single intraperitoneal (i.p) injection of 1 g/kg P-407 (0.13 g/ml solution in cold normal saline). To ensure the proper injection of the dose, the animals were lightly anesthetized with halothane, injected with P-407 and allowed to recover. The same amount of normal saline was injected intraperitonealy to NL animals under halothane.

In two separate groups of NL and HL rats (n=4 in each group), following the administration of 25 mg/kg of drug and scarifying of the rat, thyroid glands were excised at 24 h post dose and kept at -30 °C freezer to be assayed for both AM and DEA by LC/MS.

2.2.7.3 Everted gut metabolism

The composition of each chamber in which everted gut segments were incubated with AM were different in each group and defined as follows:

Group A (n=5), Kerbs-Henesleit bicarbonate buffer (pH=7.4) (KH)

Group B (n=4), KH+5% simulated bile solution (5% SBS)

Group C and D, E (n=4 / group) KH+25% SBS.

Rats in group D were pretreated with 2 doses of peanut oil+1% of cholesterol (2 ml/kg) administered 4 hrs and 1 hr before the onset of study.

Segments in group E were treated with 5% soybean oil emulsion (Intralipid) (INLP)

Simulated rat bile solution (SBS) was prepared as a mixture of 10 mmol/L bile extract (4.9 g/L), 12.5 mg/L lipase, 0.1 mmol/L cholesterol (0.6 g/L) and 0.8 g/L lecithin in Krebs-Henseleit bicarbonate buffer (qs to 1L). In order to activate lipase and complete the solubility, the solution was kept in sonicator bath for 4-6 h [324-326] at 37°C. Lipase was added to represent the digestive enzyme present in the GI tract, and in the INLP group to permit partial hydrolysis of the triglycerides from the soybean oil constituents.

2.2.8 In vitro studies

2.2.8.1 Distribution of AM and DEA in human and rat plasma lipid fractions (in vitro)

a) Treatment of plasma samples

Pooled human and rat plasma samples were added to Beckman Ultraclear ultracentrifuge tubes in 3 ml aliquots. The mixture of AM and DEA was added such that the final concentration in the plasma was 1,000 ng/ml AM and 500 ng/ml DEA. Both AM and DEA were dissolved in methanol and the final volume of methanol added to each plasma sample was not more than 0.01%. At this volume, the composition of plasma lipoproteins is not affected by methanol. The plasma samples were incubated at 37°C for 60 min. The incubation was stopped by the addition of 1.020 g of sodium bromide to adjust the density of the plasma and then the samples were rapidly cooled on ice to 4° C for a minimum of 2 h [327].

b) Separation of lipoprotein components

Sodium bromide density solutions (1.006d, 1.063d and 1.21d) were prepared by dissolving appropriate amounts of sodium chloride, sodium bromide and sodium hydroxide in water. The solutions were cooled to 4° C prior to preparation of the gradient. Three ml of the cooled, treated plasma samples, adjusted to a density of approximately 1.25d with sodium bromide, was added to an ultracentrifuge tube (Beckman Coulter: Fullerton, CA). Density solutions were carefully layered on top of the plasma in the order

1.21d, 1.063d then 1.006d. The tubes were balanced and placed into individual titanium buckets and capped. The buckets were loaded on a SW 41 Ti swinging bucket rotor (Beckman Coulter) and centrifuged at 40,000 rpm at 15° C for 18 h in a Beckman L8-80M Ultracentrifuge (Beckman Coulter) or a Beckman LE-80 Ultracentrifuge (Beckman Coulter). Upon completion, the tubes were removed and four distinct regions were observed and labeled. The layers correspond to the triglyceride-rich lipoproteins (TRL) comprised of very low density lipoproteins and any chylomicrons present, low density lipoproteins (LDL), high density lipoproteins (HDL) and the lipoprotein deficient plasma fraction (LPDP). These layers were removed using a Pasteur pipette and added to disposable glass test tubes and the volumes measured and recorded [327].

c) Lipid measurement

Total cholesterol and TG concentrations were determined using peroxidase enzymatic cholesterol and triglyceride assay kits. Two ml of CHOL or TG reagents was added to 10 ml of human or rat NL or HL plasma samples or 10-100 μl of each NL or HL fractions. Normolipidemic plasma was defined as having CHOL and TG concentrations of <200 mg/dl. Tubes were incubated at 37°C for 5 or 10 min and scanned at 505 or 515 nm, respectively, using an colorimetric spectrophotometer [327].

2.2.8.2 Microsomal studies

Microsomal studies were accomplished for various purposes. Some studies were directed toward the identification of the enzymes involved in the hepatic and extra-hepatic metabolism of AM to DEA. A total number of 8 male Sprague–Dawley rats were used in in vitro microsomal studies. At the second group the effect of hyperlipidemia on the hepatic metabolism of AM to DEA was studied. At the third group, the effect of a high fat meal on extra-hepatic metabolism of AM to DEA was investigated. For the extra-hepatic metabolism of AM to DEA, the most focus was concentrated on intestinal metabolism of AM to DEA. In part two, 8 male Sprague–Dawley rats were employed to study the effect of hyperlipidemia on the hepatic metabolism of AM to DEA. For this purpose, 4 rats were rendered HL by ip administration of P-407 36 h before the onset of the study. In NL rats, the same amount of normal saline was administered intraperitonealy. In part three, a total number of 8 male Sprague–Dawley rats were employed to study the effect of oral fat on intestinal metabolism of AM to DEA. Peanut oil at the dosage of 2 ml/kg was administered by to one group of rats (n=4) 4 and one h before the onset of the study.

a) Microsomal preparation

All of the animals were sacrificed under mild halothane or isoflurane anesthesia and either their liver or intestine or both (upper 20 cm of small intestine in part one and the whole small intestine in the part two and three) were removed and washed thoroughly in cold KCl solution (1.15% W/V in distilled water). Both tissues cut into pieces and homogenized separately in cold sucrose solution (0.25 M in distilled water) by using a homogenizer (5 g of tissues in 25 ml of sucrose). After homogenization, each tissue was centrifuged at 10,000 rpm for 8 minutes in Optiseal propylene tubes using refrigerated ultracentrifuge (Beckman L-80 ultracentrifuge, Beckman instruments, Inc. Palo alto, Ca. USA). Then supernatants were transferred to new Optiseal propylene tubes and centrifuged again at 14,000 rpm for 10 minutes. Centrifugation continued again by transferring supernatants to new Optiseal propylene tubes and adding calcium cloride dihydrate 1M (10 µl/1ml of supernatant) at 21,500 rpm for 15 more minutes. Then the pellets were resuspended in KCl 1.15% solution and centrifuged at 21,500 rpm for 15 minutes. The pellets were collected in sucrose 0.25 M solution and stored at -80 ° C freezer [328].

b) Lowry assay method for protein concentration in microsomal preparations

The Lowry assay method is based on comparing the concentration of an unknown protein preparation with serial standard solutions of bovine serum albumin (BSA). In order to assay the concentration of protein in microsomal preparations of liver and gut tissues, the following solutions were required:

Reagent A contained; 1ml of Cupric Sulfate 1% in distilled water, 1ml of Na.K.tartarate (sodium and potassium tartarate) 2% in distilled water, 20 ml of Na_2CO_3 anhydrous 10% in 0.5 M sodium Hydroxide.

Reagent B contained; 1/10 diluted solution of Folin-Phenol reagent in distilled water.

Working standard solutions of BSA were prepared at the concentrations of 500, 400, 300, 200, 100, 0 µg/ml of BSA in distilled water from the stock solution of 500 µg/ml (50 mg/100 H2O).

To a number of clean test tubes containing 10 µl of microsomal preparation and 240 ml of distilled water (unknown concentration of protein) or 250 µL of each standard solution, 250 µL of reagent A were added and incubated them in room temperature for 10 minutes. In the next step and under continuous vortex mixing, 750 µL of reagent B was added to each of the test tubes and samples incubated at 50 °C for 10 more minutes. At the last step 200µl of each mix were transferred to a well in the ELISA plate and analyzed using an ELISA reader at 600 nm [329].

c) *Total CYP450 measurement*

Hepatic microsomal CYP content was measured by a difference spectrum for their carbon mono oxide-reduced form by the method of Omura and Sato [330]. Briefly, microsomal preparations were adjusted to 1 mg/ml protein with water, which was placed in both sample and reference cells. After recording the baseline, carbon mono oxide was bubled into the samples for 30-60 s to form the carbon oxide–CYP complex. Then, a few milligrams of solid sodium thiocianate were added to reduce the carbon mono oxide–CYP complex. Solid sodium thiocianate was also added to the reference cell. The difference in absorbance between sample and reference cell was scanned from 400 to 500 nm.

CYP content was calculated by the following equation:

$$\text{CYP content (nmoL/mg protein)} = \frac{OD_{450} - OD_{490}}{91} \times 1000$$

d) *Microsomal incubation studies*

Each 0.5-ml incubate contained 1 mg/ml protein from each of the microsomal preparations from each individual rat or from pooled microsomes, 0.1 to 200 μ M AM HCl, 1 mM NADPH, and 5 mM magnesium chloride hexahydrate dissolved in 0.5 M potassium phosphate buffer (pH = 7.4). The substrate was added to the liver or intestinal microsomal suspension and the oxidative reactions were started with the addition of NADPH after a 5-min preequilibration period. All incubations were performed in quadruplicate in a 37°C water bath shaker for 30 min. Incubation conditions were optimized so that the rate of metabolism was linear with respect to incubation time and microsomal protein concentration. The incubation terminated by adding 1.5 ml of acetonitrile and cooling down the tubes in ice.

e) *Chemical inhibition and immunoinhibition studies in rat liver and intestinal microsomes*

All of the inhibition studies were accomplished in 16 - 125 mm flint glass disposable culture tubes. For chemical inhibition studies, KTZ (1.30– 47.0 μM) was added to microsomal incubations from the individual rats in the presence of different concentrations of AM (16– 94 μM). The inhibitor (KTZ) was dissolved in methanol. An aliquot of inhibitor was added and tubes were incubated with different concentrations of AM.

In immunoinhibition studies, 20 μl/ml concentrations of the CYP3A2, CYP2B1/2, and CYP1A2 antibodies were added separately to the microsomal mixture incubate containing 0.4 mg/ml pooled microsomal protein and a definite AM concentration (64 and 94 μM for liver and intestine, respectively). The percentage of inhibition was determined by comparing the metabolite formation in the presence of antibody to that of matching controls containing preimmune rabbit serum in place of the antibody.

f) *Metabolism by heterogeneously expressed CYP enzymes*

To further characterize which P450 in rat mediates the formation of DEA, AM was incubated with a panel of supersomes, which were expressed from rat CYP complementary DNA using a baculovirus expression system. Incubations were performed with rat recombinant CYP1A1 and CYP3A1. Reactions were carried out at concentrations of 37.6 μM and 18.8 μM for AM and KTZ, respectively. Because this experiment showed linearity in the concentrations between 2-20 pmol/ml of supersomes, a concentration of 10 pmol/ml of each supersome protein was chosen for this experiment.

g) *Western blot analysis*

Western blot analysis was performed using a previously described method with minor modification to quantify the effect of HL on some important CYP450 contents including CYP1A2, CYP2B1/2, CYP2C6, CYP2C11, CYP2D1, CYP3A1 and CYP3A2 [331]. Briefly, 100 μg of each individual microsomal protein was denatured by diluting with loading buffer and boiling for 5 min at 100°C. Then each sample was loaded onto a 10% SDS-polyacrylamide gel and electrophoresed at 120 V for 2 h. The separated proteins were transferred to Trans-Blot nitrocellulose membrane (0.45 μm) in a buffer containing 25 mM Tri–HCl, 192 mM glycine, and 20% (v/v) methanol. Protein blots were blocked overnight at 4 °C in a solution containing 5% skim milk powder, 2% bovine serum albumin and 0.5% Tween-20 in Tris-buffered saline buffer. There after, the blocking solution was removed and the blots were rinsed three times in a wash buffer (0.1% Tween-20 in TBS). Membranes were incubated with primary antibodies (1/500 or 1/1000 dilution) of either monoclonal goat anti-rat or monoclonal mouse anti rat CYP1A2, CYP2B1/2, CYP2C6, CYP2C11, CYP2D1, CYP3A1 and CYP3A2 antibodies for 2 h at 4 °C in TBS containing 0.01% sodium azide and 0.05% Tween-20. The primary antibody solution was removed and blots were rinsed three times with a wash buffer, followed by incubation with horseradish peroxidase conjugated with rabbit or mouse anti-goat IgG secondary antibody (1/5000 dilution) for 1 h at room temperature and washed as previously described. Immunoactive proteins were detected using the enhanced chemiluminescence method (Amersham, Arlington Heights, IL) and the intensity of different CYP protein bands were quantified and compared with the unspecific protein band in each blot, using ImageJ® [331].

2.2.9 Data analysis

2.2.9.1 Pharmacokinetic analysis

Noncompartmental methods were used to calculate the pharmacokinetic parameters. The elimination rate constant (λ_z) was estimated by subjecting the plasma concentrations in the terminal phase to linear regression analysis. The terminal elimination phase half-life ($t_{1/2}$) was calculated by dividing 0.693 by λ_z. The concentration at time 0 h after i.v. dosing was estimated by back extrapolation to time zero using the first two measured concentrations (5 min and 20 min) after dosing. The AUC $_{0-\infty}$ after dosing was calculated using the combined log-linear trapezoidal rule from time 0 h postdose to the time of the last measured concentration plus the quotient of the last measured concentration divided by λ_z.

Clearance (CL) was calculated as $CL = \frac{Dose}{AUC_{0-\infty}}$, and steady-state volume of distribution (Vd_{ss}) was calculated as $Vd_{ss} = \frac{CL}{AUMC}$, where AUMC is the area under the first moment plasma concentration vs. time curve. AUMC was determined by the following equation [332]

$$AUMC = \int_0^\infty tcp(t)dt \quad \text{.........} \quad Eq=1$$

The absolute oral bioavailability (F) of AM, assuming linear kinetics, was calculated by dividing the AUC_{oral} by $AUC_{i.v.}$ correcting for dose, as follows

$$F = \frac{(\text{mean oral } AUC \times Dose_{iv})}{(\text{mean iv } AUC \times Dose_{oral})} \quad \text{.........} \quad Eq=2$$

The calculation was repeated using partial AUC_{0_24h} and for $AUC_{0-\infty}$. In making these calculations, care was taken to ensure that for fasted F, the oral and i.v. AUC of fasted animals were used, and that for oral lipid-fed animals, the oral and i.v. AUC of oral lipid-fed animals was used.

2.2.9.2 Tissue distribution

In the tissue distribution studies, because of the destructive study design, AUC could not be determined for individual rats in each group. For this purpose the Bailer method was used [333].

2.2.9.3 Lipoprotein fraction distribution studies

The partitioning of analyte was calculated using the measured concentrations in the fraction aliquots multiplied by the volumes obtained at the time of separation. The percentage recovered was determined by comparing the total mass recovered from all fractions to the total mass added to the plasma at the onset of the ultracentrifugation.

2.2.9.4 Microsomal studies

The rate of DEA formation in both liver and intestinal microsomes was obtained by plotting the formed DEA at various substrate concentrations. Both single and multiple enzyme models for metabolism of AM to DEA were fitted to the formation rate versus time data using nonlinear curve-fitting routines using an in-house written program based on Microsoft Excel (Microsoft, Redmond, WA) and the Solver routine. The Michaelis-Menten model for a single enzyme was used as follows:

$$\mathit{Rate}\text{ of DEA formation} = \frac{V_{max} \times [AM]^n}{K_m + [AM]^n} \quad \dots\dots\dots\dots\dots\dots\dots\dots\dots\dots\dots\dots \mathit{Eq=3}$$

where Vmax is the maximal rate of formation (capacity), km is the affinity constant, [AM] is the concentration of AM, and n is the shape factor required to fit sigmoidal shapes. When n = 1, the model reduced to the simple Michaelis-Menten equation.

One of the two-enzyme models was used, consisting of a single saturable and a second linear component, as follows:

$$\textit{Rate}\text{ of DEA formation} = \frac{V_{max} \times [AM]}{K_m + [AM]} + E_2 \times [AM] \quad \ldots\ldots\ldots\ldots \quad \textit{Eq=4}$$

where K_{m1} and V_{max1} were the kinetic constants for a high-affinity enzyme, and E_2 represented the Vmax/km ratio for the low-affinity enzyme. The optimal choice of enzyme model was judged by the residual sum of squares and the Akaike Information Criterion.

Intrinsic clearance (Clint) was calculated with calculating the ratio of Vmax to Km. In sigmoidal conditions, CLmax, which was obtained graphically from the clearance plot (rate/[s] versus [s] plot), was used instead of CLint.

The simple competitive inhibition model was considered for the effects of KTZ as defined in the equation below, with ki as the dissociation constant of the inhibitor-enzyme complex) and [I] the inhibitor concentration.

$$K_{m(I)} = K_{m(1)} \times (1 + \frac{I}{K_i}) \quad \ldots\ldots\ldots\ldots \quad \textit{Eq=5}$$

2.2.10 Statistical analysis

2.2.10.1 Pharmacokinetic studies

Statistical analysis was performed using the student's paired or unpaired t-test, (*p* value of less than 0.05 was considered statistically significant) or ANOVA as appropriate. Data analysis was performed using Microsoft Excel 2000. All data expressed as a mean±standard deviation, unless otherwise stated.

2.2.10.2 Tissue distribution

In the tissue distribution studies, because of the destructive study design, AUC could not be determined for individual rats in each group. For this purpose the Bailer method was used.

Compiled data were expressed as mean ± SD unless otherwise indicated. In this study, $AUC_{0\text{-}72}$ for AM and DEA were determined in each specimen and Bailer method was used to estimate SD from partial AUC to assess significance of differences. In this test, α was 0.05, the critical value of Z for the 2 –sided tests after Bonferroni adjustment was 2.24, and the observed value for Z was calculated as previously described. The tissue to plasma (Kp) concentration ratios were also determined for AUC or for postdistributive phase samples [333].

2.2.10.3 Everted gut metabolism

Compiled data are expressed as mean±SD unless otherwise indicated. One way ANOVA, Duncan's Multiple Range post hoc test and Student paired or unpaired t-tests were used as appropriate to assess the significance of differences between groups. Microsoft Excel (Microsoft, Redmond WA) or SPSS version 12 (SPSS Inc., Chicago, IL) were used in statistical analysis of data. The level of significance was set at $p<0.05$.

2.2.10.4 Lipoprotein fraction distribution studies

Compiled data were expressed as mean±SD unless otherwise indicated. Statistical analysis was performed using SigmaStat version 3.5 (Systat Software). Each data set was analyzed for normality and homogeneity of variances in order to determine the choice of statistical method. For ranking analyte association in the various fractions, Kruskal-Wallis One Way Analysis of Variance on Ranks with Dunn's Method or Student-Newman-Keuls method of post-hoc tests were used. Student unpaired t tests were also used for the interpretation of differences between species and between NL and HL plasma and fractions in TG and CHOL content. The alpha value was set a priori at 0.05.

2.2.10.5 Microsomal studies

Compiled data are expressed as mean±SD unless otherwise indicated. One way ANOVA, Duncan's Multiple Range post hoc test and Student paired or unpaired t-tests were used as appropriate to assess the significance of differences between groups. Microsoft Excel (Microsoft, Redmond WA) or SPSS version 12 (SPSS Inc., Chicago, IL) were used in statistical analysis of data. The level of significance was set at $p<0.05$.

2.2.10.6 Western blot

Student's paired or unpaired t tests were used as appropriate to assess the significance of differences between groups. Microsoft Excel was used in statistical analysis of data. The level of significance was set at $p < 0.05$.

2.3 *Results*

2.3.1 Assays

2.3.1.1 HPLC

a) Chromatography

A previously reported HPLC method for AM was tested for its ability to quantify DEA [323]. In the validated modified chromatographic method, peaks corresponding to the internal standard (IS), DEA and AM eluted free of interfering substances in rat plasma, at approximately 3.4, 10.5 and 12 minutes respectively using a Nova-Pak C8 analytical column cartridge (Figure 19).

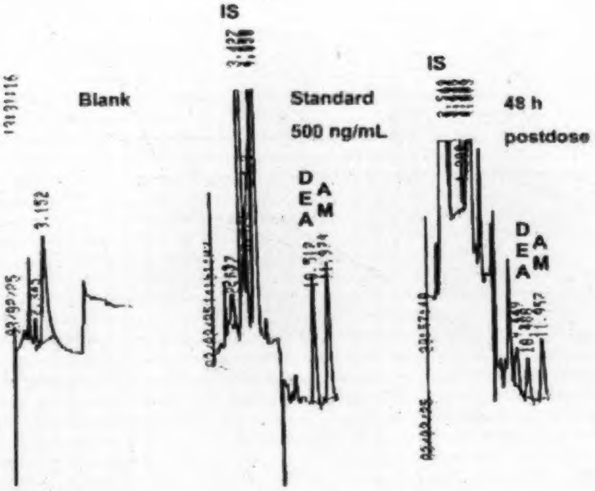

Figure 19: HPLC chromatograms of drug free rat plasma, extracted rat plasma spiked with 500 ng/ml of AM and DEA and extracted plasma from traeated rats with 25 mg/kg of AM as single iv injection, 48 postdose. Both samples were spiked with 1500 ng/ml of ET before extraction procedure

There was highly linear relationship (r ^{2}=0.999) between peak height ratios (metabolite: internal standard) and the corresponding plasma concentrations over a range of 35 to 1000 ng/ml for DEA (Figure 20).

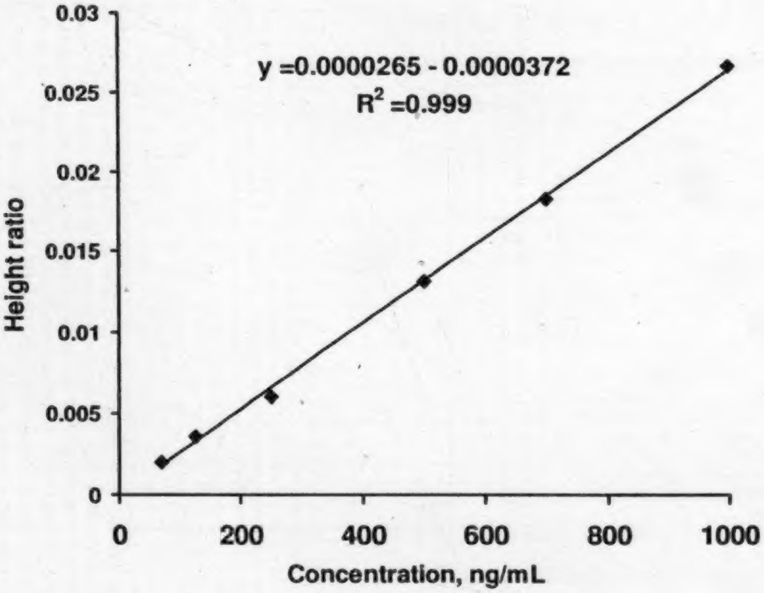

Figure 20: A representative standard curve of DEA in rat plasma (From 35 to 1000 ng/ml). Data weighted by a factor of 1/concentration

b) Assay validation

The interday validation of HPLC method was assessed for DEA. The method was already validated and published in 2001 for AM [323]. The coefficient of variation was less than 12.6% over a range of 35-1000 ng/ml of DEA concentrations (Table 1). Mean error was less than 10.3%.

Table 1: Validation data for DEA measured by the HPLC method from 35 to 1000ng/ml (intraday) (n=5)

Nominal concentration, ng/ml	Mean±SD	CV%	Error%
35	37.7±4.88	12.9	7.83
70	73.4±9.22	12.6	4.80
125	121±11.6	9.55	-2.90
250	232±18	7.76	-7.10
500	466±5.99	1.28	-6.81
700	676±28.5	4.21	-3.47
1000	1103±62.6	5.68	10.3

2.3.1.2 LC/MS

c) Chromatography

The molecular ions of IS, DEA and AM were represented by peaks with m/z values of 313.10, 617.73 and 645.83, respectively (Figure 20). The response of the DEA molecular ion was not as strong as AM, using the instrument conditions. However, under these conditions, the mass spectrum of DEA displayed a notable daughter fragment with m/z of 546.9 (Figure 20). Because both this fragment and molecular ion m/z were unique to DEA, both of these ions were monitored for peak area detection to maximize the DEA assay selectivity and sensitivity (Figure 21). The retention times of eluted IS, DEA and AM were approximately 4, 9.8 and 10 min, respectively (Figure 22).

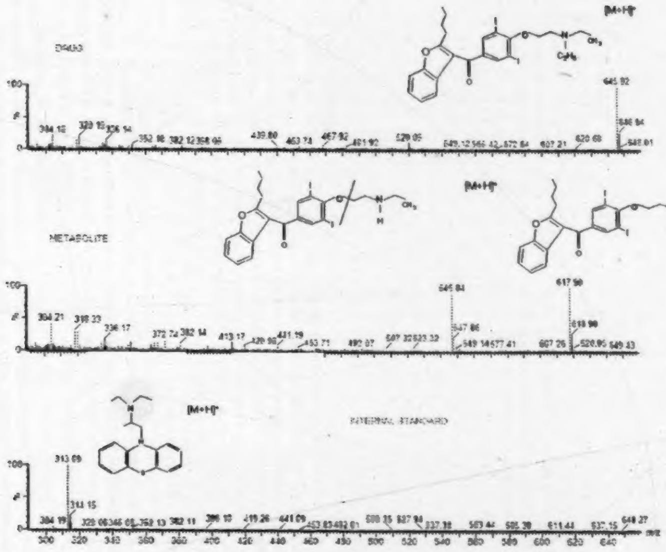

Figure 21: Mass spectra of drug (AM) (*m/z*=645.92), metabolite (DEA) (*m/z*=617.90 and 546.84) and ethopropazine (internal standard) (*m/z*=313.09)

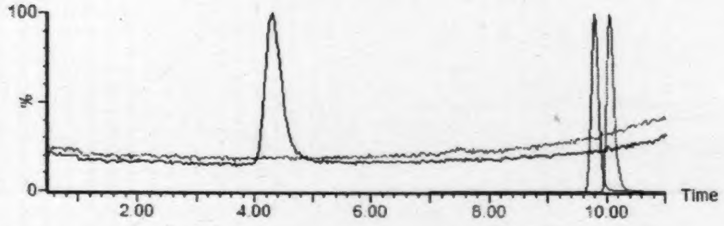

Figure 22: Overlay SIR chromatograms of blank plasma, I.S. (4.32 min), DEA (9.74 min) and AM (10.0 min) after extraction from rat plasma

Each peak was symmetrical, and there was no evidence of interference from endogenous compounds in plasma or tissues. The average extraction recoveries in plasma were 93.2 and 77.7% for 25 and 500 ng/ml of AM, respectively. The average extraction recoveries in plasma were 81 and 76% for 25 and 500 ng/ml of DEA, respectively. Highly linear relationships were noted between the peak area or height ratios and rat plasma concentrations of both AM and DEA. A representative standard curve in plasma using peak area ratios yielded slopes of 0.00252 and 0.0021, respectively, for AM and DEA. Corresponding intercepts were 0.001 and -0.0083, respectively. The mean r^2 for the three standard curves were 0.9999 for AM and 0.9998 for DEA, respectively, whether analyte: IS peak height or peak area ratios were used for quantification (Figure 23). Linearity of the assay method in tissues was observed in standards ranging from 5-1000 ng/g of tissues. A representative standard curve in liver using peak area ratios yielded slopes of 0.00316 and 0.00358, respectively, for AM and DEA. Corresponding intercepts were 0.00388 and -0.016, respectively, for AM and DEA (Figure 24)

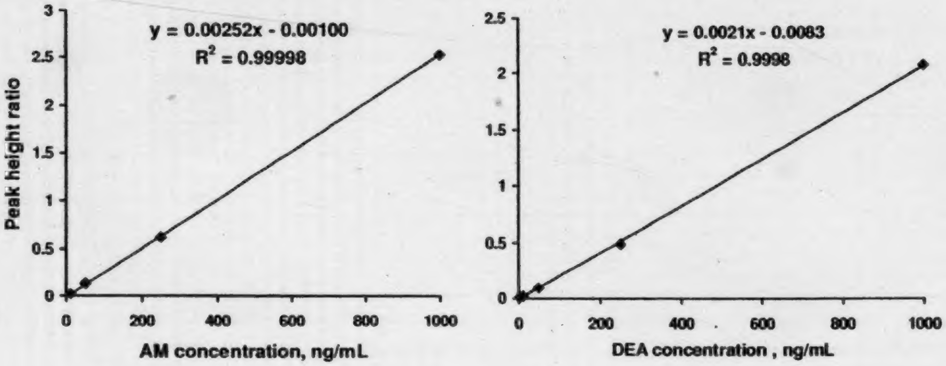

Figure 23: Linearity of the LC-MS assay in rat plasma from 2.5 to 1000 ng/ml for both AM and DEA

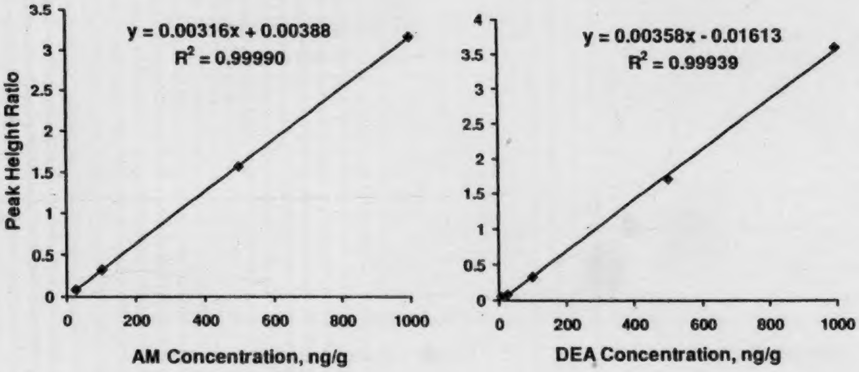

Figure 24: Linearity of the assay in rat liver from 5-1000 ng/ml for both AM and DEA

d) Assay validation

For AM and DEA, the assay CVs for both the intraday and interday assessments were equal to or less than 18% (Table 2). Mean interday error in rat plasma was less than 12% for both drug and metabolite. Based on the interday coefficient of variation and mean error, both of which yielded values of less than 20%, it can be claimed that the LLQ of the assay was 2.5 ng/ml based on 0.1 ml of rat plasma. The sample preparation time for 20 plasma samples was ~90 min.

Table 2: Validation data for the assay of AM and DEA in rat plasma by LC/MS

Expected concentration (ng/ml)		Intraday mean ±SD (Intraday CV% in parenthesis), ng/ml			Interday mean±SD, ng/ml	Interday CV%	Interday mean error %
2.5	AM	2.53±0.269 (10.6)	2.56±0.371 (14.5)	2.77±0.493 (17.9)	2.62±0.130	15.8	11.9
	DEA	2.79±0.136 (4.87)	2.93±0.507 (17.3)	2.60±0.431 (16.8)	2.77±0.166	15.0	-0.514
10	AM	9.82±0.996 (10.2)	9.60±0.586 (6.10)	10.5±0.536 (5.11)	9.97±0.468	7.12	4.99
	DEA	10.8±0.869 (8.04)	11.7±0.992 (8.47)	9.62±1.26 (13.2)	10.7±1.05	9.90	7.09
50	AM	53.5±4.90 (9.16)	47.0±1.91 (4.06)	48.6±3.59 (7.39)	49.7±3.38	6.87	-1.35
	DEA	50.5±5.11 (10.1)	45.0±6.37 (14.2)	45.4±5.75 (12.1)	46.9±3.07	12.1	-6.10
250	AM	292±39.0 (13.4)	244±6.58 (2.69)	254±33.2 (13.1)	263±25.4	9.71	3.37
	DEA	242±23.3 (9.64)	233±11.9 (5.09)	259±31.1 (12.1)	245±12.9	8.92	-5.19
1000	AM	1052±46.7 (4.43)	1150±109 (10.2)	1187±86.4 (7.28)	1130±69.3	7.31	10.4
	DEA	1034±113 (10.9)	1122±93.5 (8.33)	1060±62.6 (5.91)	1072±45.3	8.39	6.48

2.3.2 Pharmacokinetics

2.3.2.1 The effect of hyperlipidemia and high fat meal on the pharmacokinetics of AM

In the hyperlipidemic rats pretreated with P-407, plasma concentrations of AM were substantially and significantly higher than those in control rats (Figures 25, 27, 28). Oral lipid also appeared to increase the plasma concentrations of AM after iv dosing, particularly in the first 24 h post-dose, significantly (Figures 25, 26, 28, 31). The increase in plasma concentrations of AM was most marked in the hyperlipidemic rats. Plasma concentrations declined in a shallow manner in the terminal phase of all rats administered AM.

After iv doses of AM, the plasma AUC was increased significantly in the presence of hyperlipidemia. The AUC in hyperlipidemic animals were significantly higher than both groups of normolipidemic animals. Compared to the fasted animals, the mean AUC_{0-24} and $AUC_{0-\infty}$ were 16- and 12- fold higher in the hyperlipidemic rats, respectively (Tables 3, 5, 8). In a direct statistical comparison (Student's t-test) between fasted animals and those fed with oral lipid, a significant increase in AUC_{0-24} and $AUC_{0-\infty}$, was detected. However, when the post hoc Duncan's test was used in combination with all three groups of animals given iv AM, the AUC_{0-24} but not $AUC_{0-\infty}$ of postprandial animals was found to be different from the fasted animals (Tables 3, 4, 5, 8).

The CL and Vdss of hyperlipidemic animals were significantly lower than that of both normolipidemic and peanut oil treated groups of animals given iv drug. The calculations of CL and Vdss revealed that hyperlipidemia was associated with significant reductions of 12- and 23-fold, respectively, compared to fasted normolipidemic animals. Although the CL of AM was significantly higher (1.5-fold) in the normolipidemic fasted than in the lipid-fed animals, there was no difference in Vdss. Half-life was not observed to be different between any of the groups given iv drug (Tables 3, 4, 5, 8).

After oral lipid, significant increases were detected in systemic exposure of AM when given orally (Figures 29, 30, 31). Compared to fasted animals, there were increases of 2.1, 1.8 and 2.7-fold in the AUC_{0-24}, $AUC_{0-\infty}$ and Cmax, respectively, of lipid fed animals (Tables 6, 7, 8). There was, however, no change observed in tmax or terminal phase t½ of oral AM after the administration of oral lipid. There was variability observed in the plasma concentration vs. time profiles, particularly during the absorption phase, leading to secondary Cmax values in some of the rats. Using $AUC_{0-\infty}$, the oral F of AM was estimated to be 35% and 46% in control and peanut oil treated animals, respectively. The partial AUC from 0-24 h was also used to calculate F. In this case, the estimates of F in fasted and oral lipid-fed animals were 28% and 44%, respectively (Tables 6, 7, 8).

The mean Cmax of DEA was considerably lower than that of AM in each of the groups. Although the detection limit of DEA in plasma was more than its quantifiable concentration (35 ng/ml), a complete plasma concentration vs. time profile of DEA concentration was not obtained in most of the rats, and hence, AUC could not be reported (Table 8).

Table 3: The individual relevant pharmacokinetic data in seven normolipidemic (NL) rats after the intravenous administration of 25 mg/kg of AM

Rat	AUC_{0-24} mg·h/L	$AUC_{0-\infty}$ mg·h/L	CL ml/h/kg	$t_{1/2}$ h	Vd_{ss} L/kg
1	11.5	15.6	1600	37.7	38.8
2	8.40	11.8	2121	37.8	55.7
3	11.8	15.0	1668	30.8	32.1
4	15.5	35.8	698	54.5	48.4
5	14.5	20.1	1243	26	28.2
6	11.8	19.3	1298	46.3	55.9
7	14.4	24.5	1021	74.8	70.0

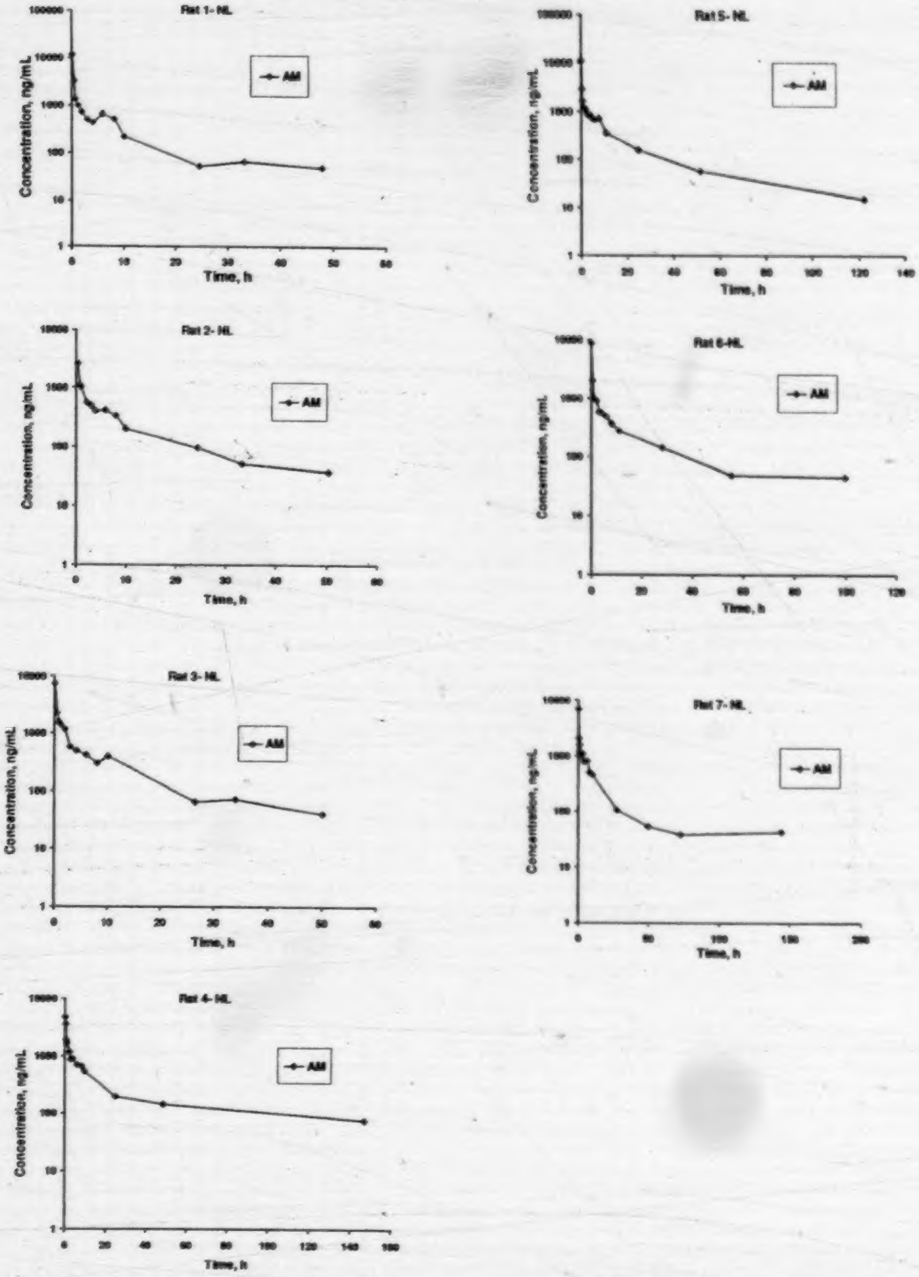

Figure 25: Individual plasma concentration versus time curves of AM in seven normolipidemic (NL) control rats after iv injection of 25 mg/kg of drug

Table 4: The individual relevant pharmacokinetic data in seven peanut oil+1% cholesterol treated rats after the intravenous administration of 25 mg/kg of AM

Rat	AUC_{0-24} mg.h/L	$AUC_{0-\infty}$ mg.h/L	CL ml/h/kg	$t_{1/2}$ h	Vd_{ss} L/kg
1	12.4	22.5	1112	47.0	38.8
2	20.9	33.1	755	43.0	36.0
3	15.8	28.2	886	58.0	51.9
4	19.1	32.1	778	64.7	38.1
5	20.1	27.2	920	29.2	19.7
6	15.9	30.5	820	29.31	37.5
7	13.1	23.2	1077	55.3	68.3

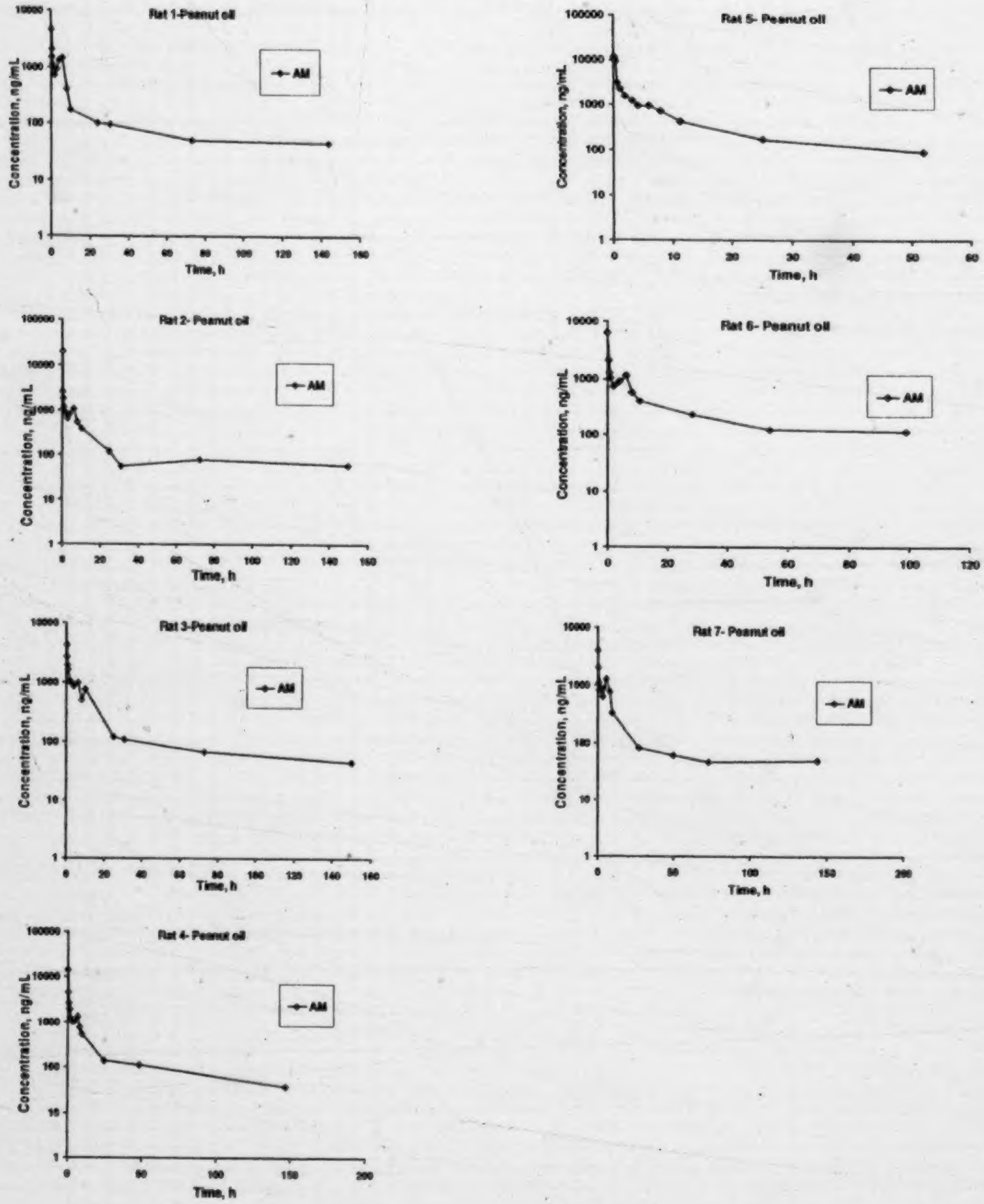

Figure 26: Individual plasma concentration versus time curves of AM in seven rats treated with 1% cholesterol in peanut oil after iv injection of 25 mg/kg of drug

Table 5: The individual relevant pharmacokinetic data in seven P-407 treated rats after the intravenous administration of 25 mg/kg of AM

Rat	AUC_{0-24} mg.h/L	$AUC_{0-\infty}$ mg.h/L	CL ml/h/kg	$t_{1/2}$ h	Vd_{ss} L/kg
1	134	143	175	54.1	0.349
2	233	276	91	29.8	1.23
3	99.0	134	186	19.7	8.09
4	197	231	108	61.9	2.26
5	255	295	84.6	93.7	0.613
6	225	254	98.6	56.3	1.32
7	238	286	87.3	40.1	0.418

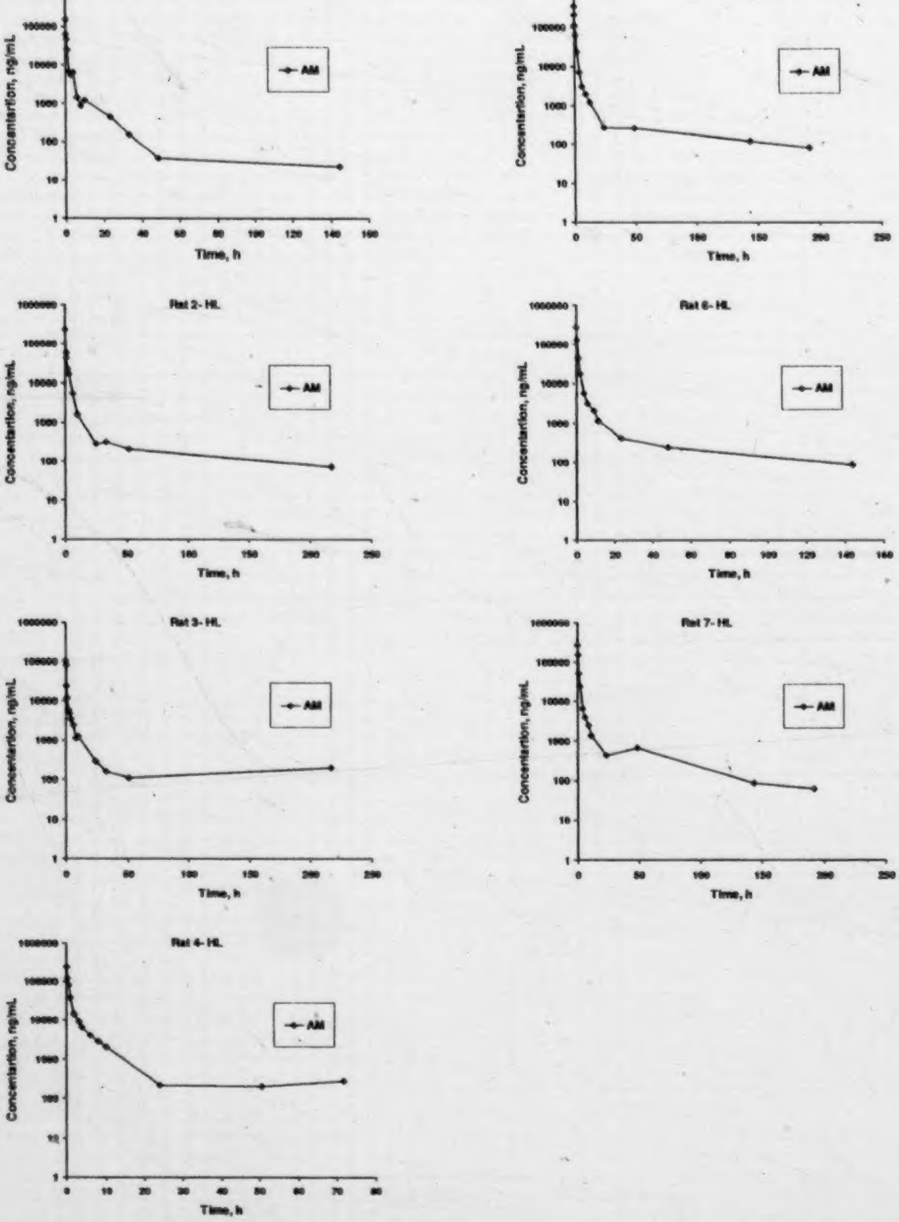

Figure 27: Individual plasma concentration versus time curves of AM in seven P-407 treated rats after iv injection of 25 mg/kg of drug

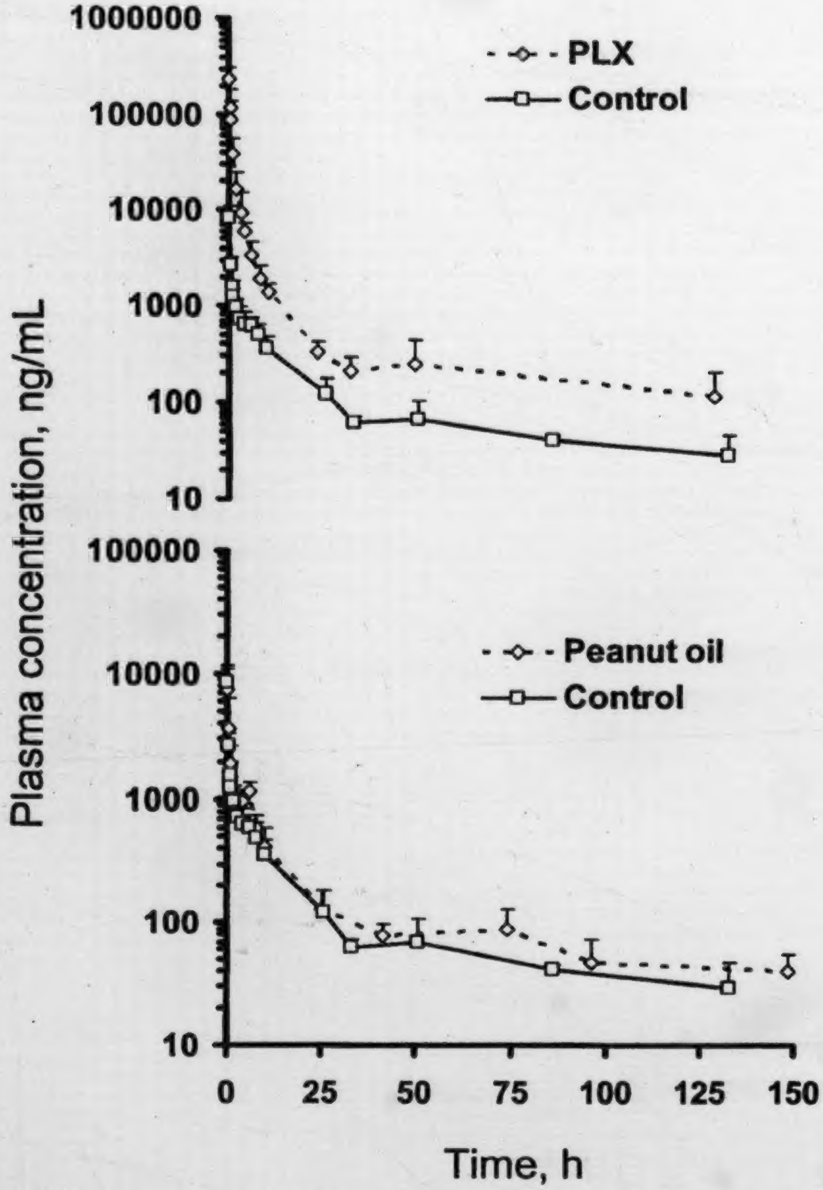

Figure 28: Mean ± SD plasma concentration versus time profile of amiodarone after 25 mg/kg intravenous doses of amiodarone HCl given to normolipidemic (n=7), hyperlipidemic (PLX treated or HL rats n=7) peanut oil fed (n=7) rats

Table 6: The individual relevant pharmacokinetic data in six NL rats after the oral administration of 50 mg/kg of AM

Rat	$AUC_{0\text{-}24}$ (mg.h/L)	$AUC_{0\text{-}\infty}$ (mg.h/L)	$t_{1/2}$ (h)	t_{max} (h)	C_{max} (ng/ml)
1	5.63	22.0	68.1	23.9	366
2	5.36	11.9	35.9	8.18	317
3	6.34	10.7	45.2	10.1	963
4	9.17	15.1	29.2	2.18	823
5	6.10	8.11	20.7	2.07	509
6	9.11	17.7	95.5	2.1	991

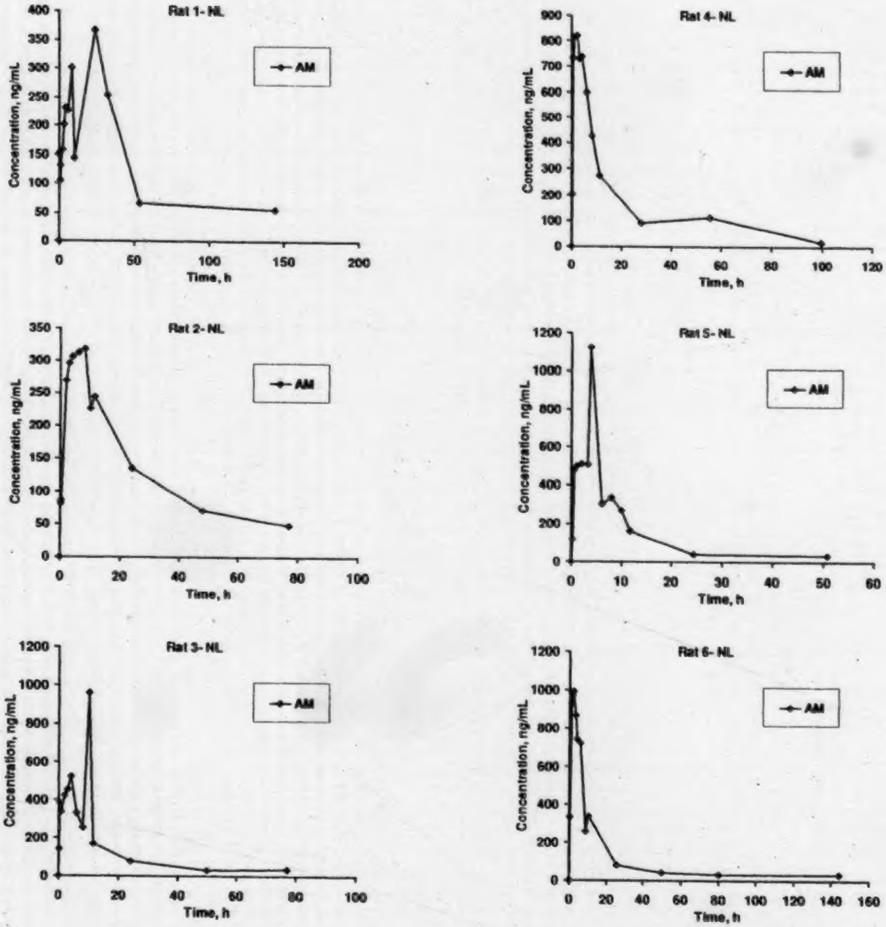

Figure 29: Individual plasma concentration versus time curves of AM in six control rats after oral administration of 50 mg/kg of drug

Table 7: The individual relevant pharmacokinetic data in six peanut oil +1% cholesterol treated rats after the oral administration of 50 mg/kg of AM

Rat	AUC_{0-24} (mg.h/L)	$AUC_{0-\infty}$ (mg.h/L)	$t_{1/2}$ (h)	t_{max} (h)	C_{max} (mg/L)
1	12.7	32.6	130	3.17	1181
2	18.8	20.9	17.5	6.02	2904
3	16.7	33.9	254	2.93	1875
4	14.5	28.1	64.5	5.98	2318
5	16.4	24.1	103	6.27	1553
6	10.2	17.1	50.3	10	828

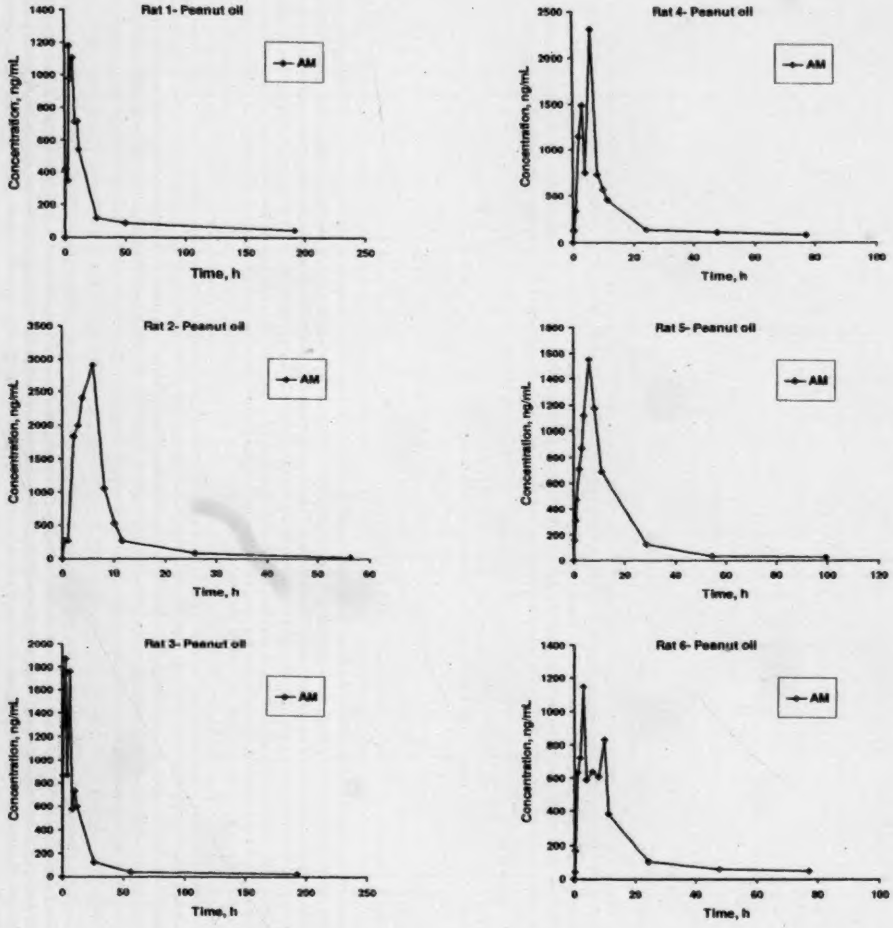

Figure 30: Individual plasma concentration versus time curves of AM in six peanut oil-treated rats (PO) after oral administration of 50 mg/kg of drug

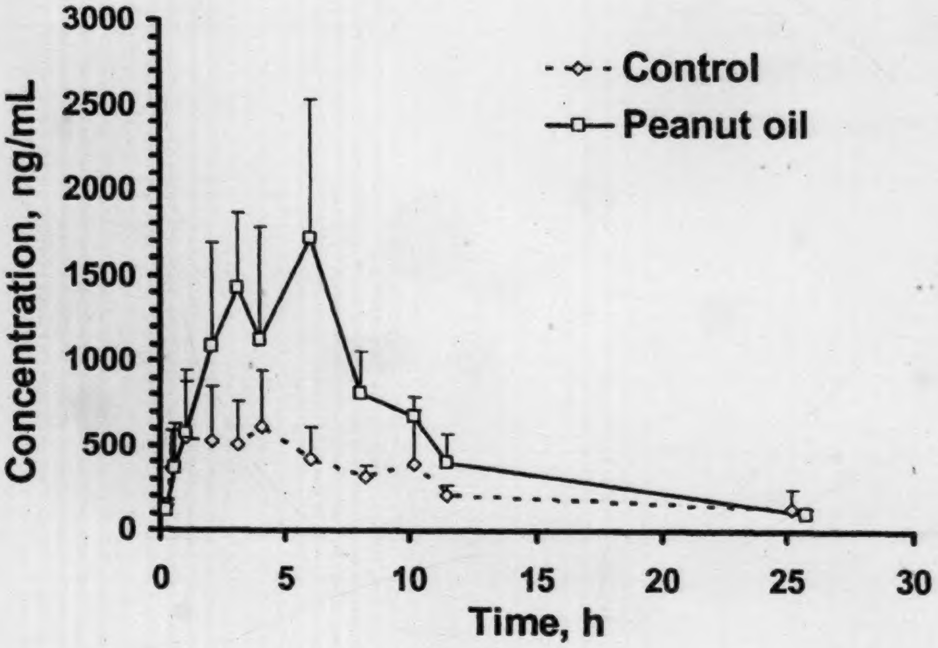

Figure 31: Mean ± SD plasma concentration versus time profile of amiodarone for the first 24 h after 50 mg/kg oral doses of amiodarone HCl given to normolipidemic (n=6) and peanut oil fed (n=6) rats

Table 8: Pharmacokinetics of amiodarone after administration to rats in control (fasted normolipidemic) rats and in animals pretreated with peanut oil or poloxamer 407

Group A **Control** **(*n*=7)**	**Group B** **Peanut oil** **(*n*=7)**	**Group C** **Poloxamer** **(*n*=7)**	**Group D** **Control (*n*=6)**	**Group E** **Peanut oil (*n*=6)**
Intravenous (25 mg/kg AM HCl)			**Oral (50 mg/kg AM HCl)**	
Amiodarone pharmacokinetic parameters				
AUC$_{0-24}$ (mg·h/L)				
12.6±2.42 (8.40-15.5)	16.8±3.37[a] (12.4-20.9)	197±58.8[a,b] (99.0-255)	6.95±1.73 (5.36-9.17)	14.9±3.11[a] (10.2-18.8)
AUC$_{0-\infty}$ (mg·h/L)				
20.3±7.98 (11.8-35.8)	28.1±4.15 (22.5-33.1)	231±66.9a,b (134-295)	14.3±5.06 (8.11-22.0)	26.1±6.61[a] (17.1-33.9)
t$_{1/2}$ (h)				
44.0±16.5 (26.0-74.8)	46.6±13.8 (29.2-64.7)	50.8±24.2 (19.7-93.7)	49.1±28.0 (20.7-95.5)	103±83.7 (17.5-254)
CL (ml/h/kg)				
1378±465 (698-2121)	907±141[a] (755-1111)	119±43.1[a,b] (84.6-186)	-	-
Vdss (L/kg)				
47.0±14.9 (28.2-69.9)	41.5±15.1 (19.7-68.3)	2.04±2.75[a,b] (3.48-8.09)	-	-
C$_{max}$ (ng/ml)				
-	-	-	662±301 (317-991)	1776.4±759[a] (828-2903)
t$_{max}$ (h)				
-	-	-	8.09±8.51 (2.07-23.9)	5.73±2.57 (2.93-10)
Desethylamiodarone pharmacokinetic parameters				
C$_{max}$ (ng/ml)				
135±158	150±126	405±286	52.0±36.6	32.7±34.8
t$_{max}$ (h)				
0.801±1.30	2.94±4.00	12.9±25.3	9.13±8.00	7.09±2.44

[a] Significantly different from control rats

[b] Significantly different from control and peanut oil treated rats

2.3.2.2 Drug interaction

KTZ pretreatment gave rise to a significant increase in plasma concentrations of i.v. administered AM in comparison with control rats (Figures 32, 33, 36). In rats given AM orally, significant increases were also detected in systemic disposition of AM upon administration of KTZ (Figures 34, 35, 36). After i.v. doses of AM, the mean plasma AUC_{0-48} and $AUC_{0-\infty}$ were increased 1.67 and 1.60–fold respectively in KTZ treated rats compared to the control animals (Tables 9, 10, 13). The CL and Vdss of AM in KTZ-treated rats were significantly lower than that of control rats. No significant difference was observed in the t½ of i.v. AM in the presence and absence of KTZ (Tables 9, 10, 13).

Compared to control animals, KTZ caused 3.07 and 2.06 fold increases in AUC_{0-48} and $AUC_{0-\infty}$ respectively, in the rats given AM orally. Administration of KTZ led to a substantial increase (137%) in Cmax of AM after its oral administration (Tables 11, 12, 13 Figures 34, 35, 36). No significant differences were observed in t½ and tmax of AM with or without treatment of KTZ (Tables 11, 12, 13). Using $AUC_{0-\infty}$, the oral bioavailabilities of AM (F) were estimated to be 37% and 47% in control and KTZ-treated rats respectively. Similar estimates of F were obtained if partial AUC was used from 0-48 h (28% and 52% in control and KTZ-treated rats, respectively).

The mean Cmax of DEA was considerably lower than that of AM in each of the groups (Table 13). However, there were no differences between KTZ-treated and control animals given either iv or oral AM (Table 13). Although the amounts of DEA detected in some plasma samples were greater than the lower limit of quantification of the assay (35 ng/ml), many of the samples were not quantifiable for DEA. Hence, a complete plasma concentration vs. time profile of DEA concentration was not obtained in most of the rats, and the AUC could not be reported.

Table 9: The individual relevant pharmacokinetic data in drug interaction study after iv administration of 25 mg/kg of AM to six control rats

Rat number	AUC_{0-48} (mg.h/L)	$AUC_{0-\infty}$ (mg.h/L)	CL (ml/h/kg)	$t_{1/2}$ (h)	Vd_{ss} (L/kg)
1	12.9	18.5	1345	78.8	73.8
2	13.2	16.5	1512	57.8	51.5
3	19.5	23.0	1086	17.2	24.2
4	17.2	20.2	1236	35.9	30.4
5	17.4	19.3	1293	27.9	43.5
6	12.6	13.4	1860	19.0	22.1

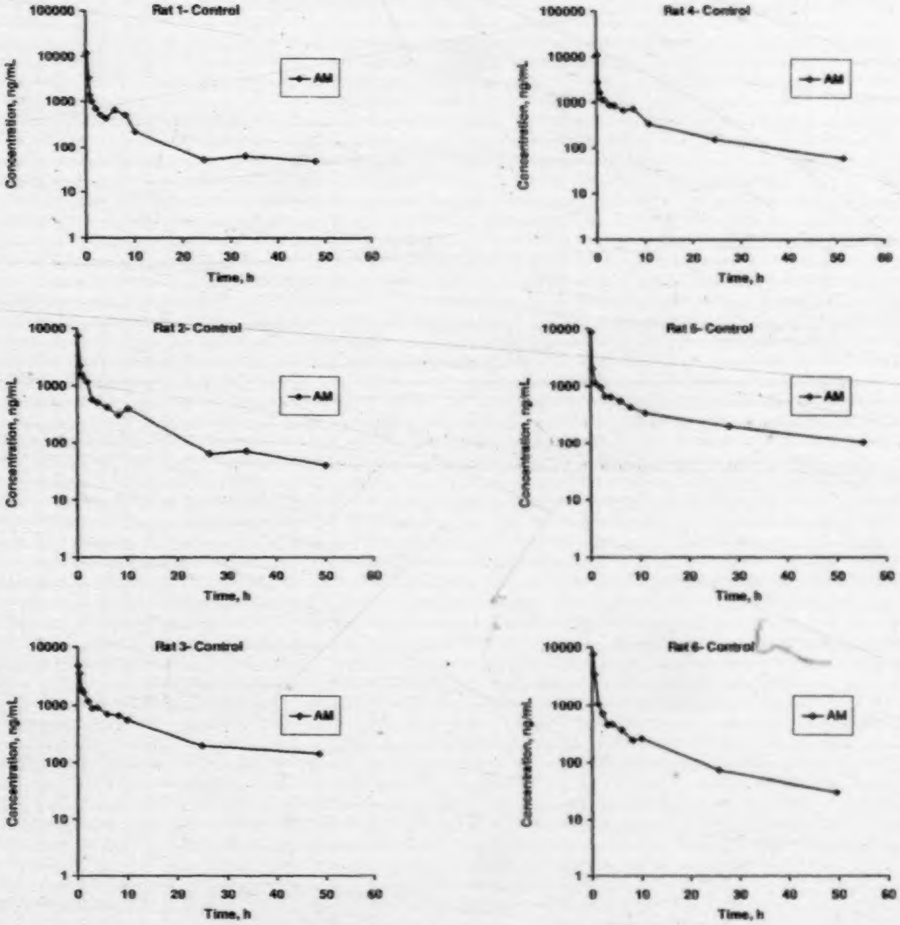

Figure 32: Individual plasma concentration versus time curves of AM in six control rats after iv administration of 25 mg/kg of AM

Table 10: The individual relevant pharmacokinetic data in drug interaction study after iv administration of 25 mg/kg of AM to six KTZ treated rats

Rat number	AUC_{0-48} (mg.h/L)	$AUC_{0-\infty}$ (mg.h/L)	CL (ml/h/kg)	$t_{1/2}$ (h)	Vd_{ss} (L/kg)
1	34.1	34.9	717	10.1	9.01
2	21.3	28.5	879	59.5	37.0
3	21.0	22.2	1126	18.8	16.4
4	20.7	22.4	1114	14.8	20.0
5	32.0	41.5	602	55	23.2
6	24.7	27.9	895	22.5	15.8

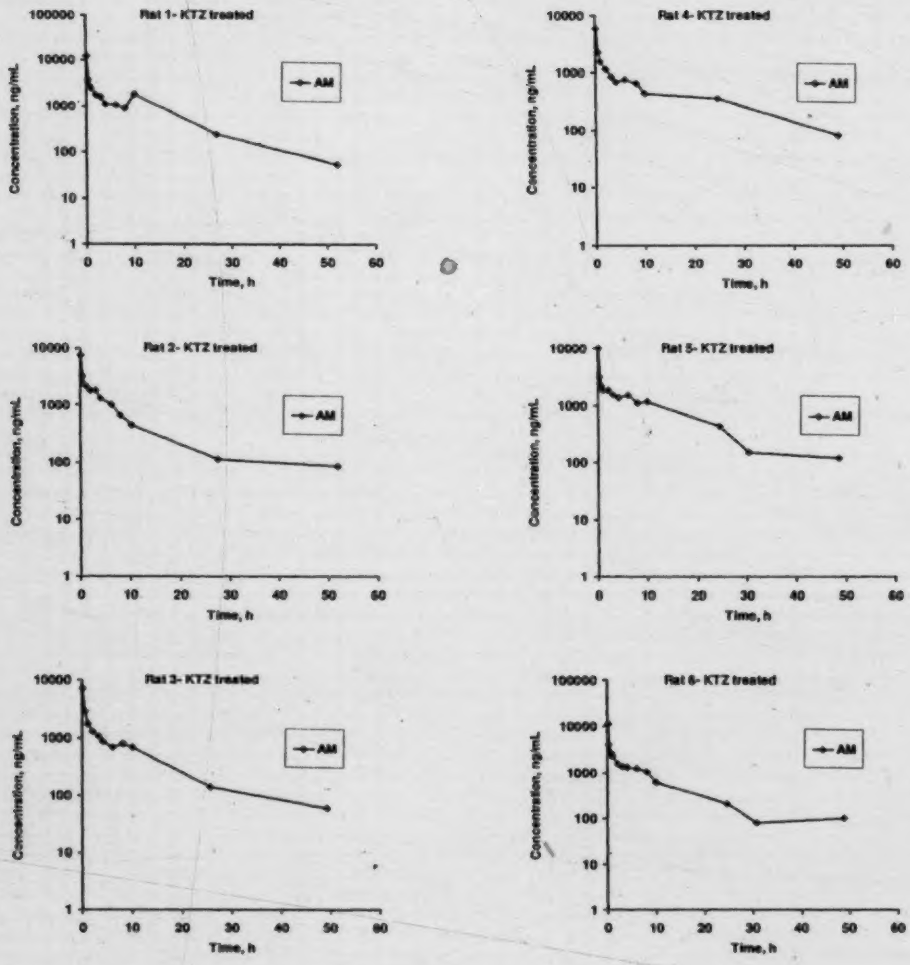

Figure 33: Individual plasma concentration versus time curves of AM in six KTZ treated rats after iv administration of 25 mg/kg of AM

Table 11: The individual relevant pharmacokinetic data in five control rats after oral administration of 50mg/kg of AM (drug interaction study)

Rat	$AUC_{(0\text{-}48)}$ (mg.h/L)	$AUC_{0\text{-}\infty}$ (mg.h/L)	$t_{1/2}$ (h)	t_{max} (h)	C_{max} (ng/ml)
1	9.25	24.1	69.8	5.93	387
2	7.71	9.82	20.8	8.18	317
3	7.76	8.47	16.9	10.1	963
4	12.0	17.3	32.7	2.18	823
5	7.06	8.11	20.7	3.87	1123

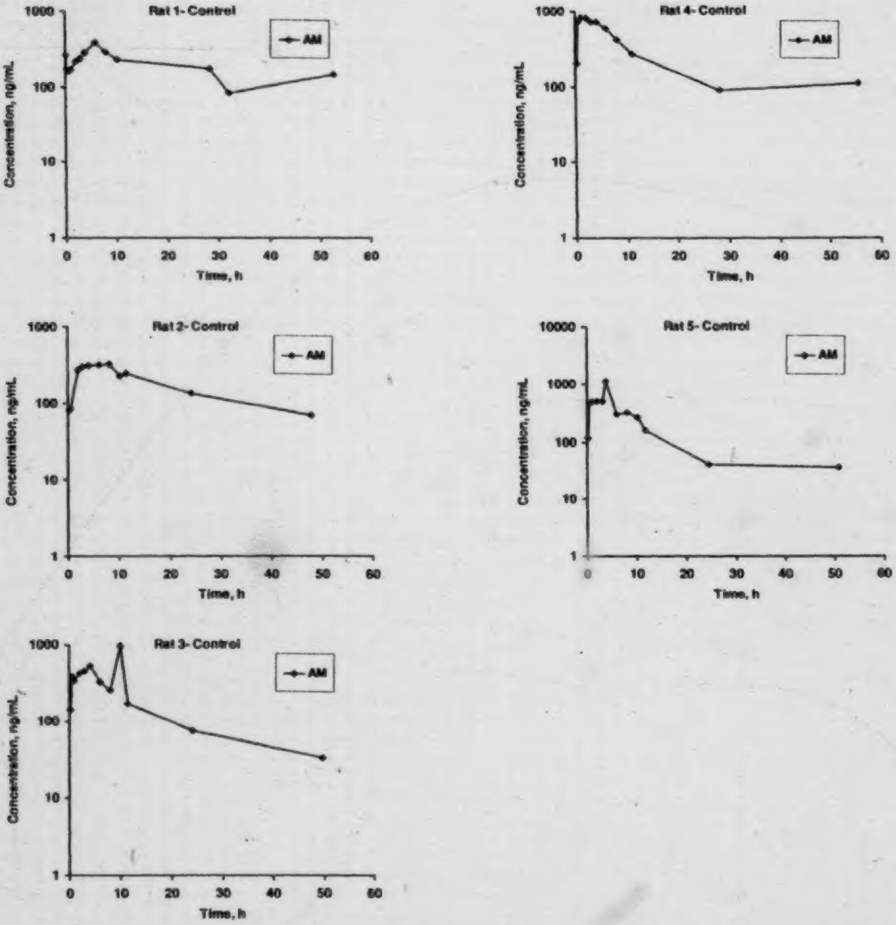

Figure 34: Individual plasma concentration versus time curves of AM in five control rats after oral administration of 50 mg/kg of AM (drug interaction study)

Table 12: The individual relevant pharmacokinetic data in drug interaction study after oral administration of 50 mg/kg of AM to five KTZ-treated rats

Rat	AUC_{0-48} (mg.h/L)	$AUC_{0-\infty}$ (mg.h/L)	$t_{1/2}$ (h)	t_{max} (h)	C_{max} (ng/ml)
1	36.8	39.3	11.3	8.0	2296
2	35.9	36.6	8.20	8.0	2218
3	17.7	18.3	9.73	7.72	1329
4	19.6	20.7	11.1	2.08	1347
5	24.1	25.0	9.24	10.3	1390

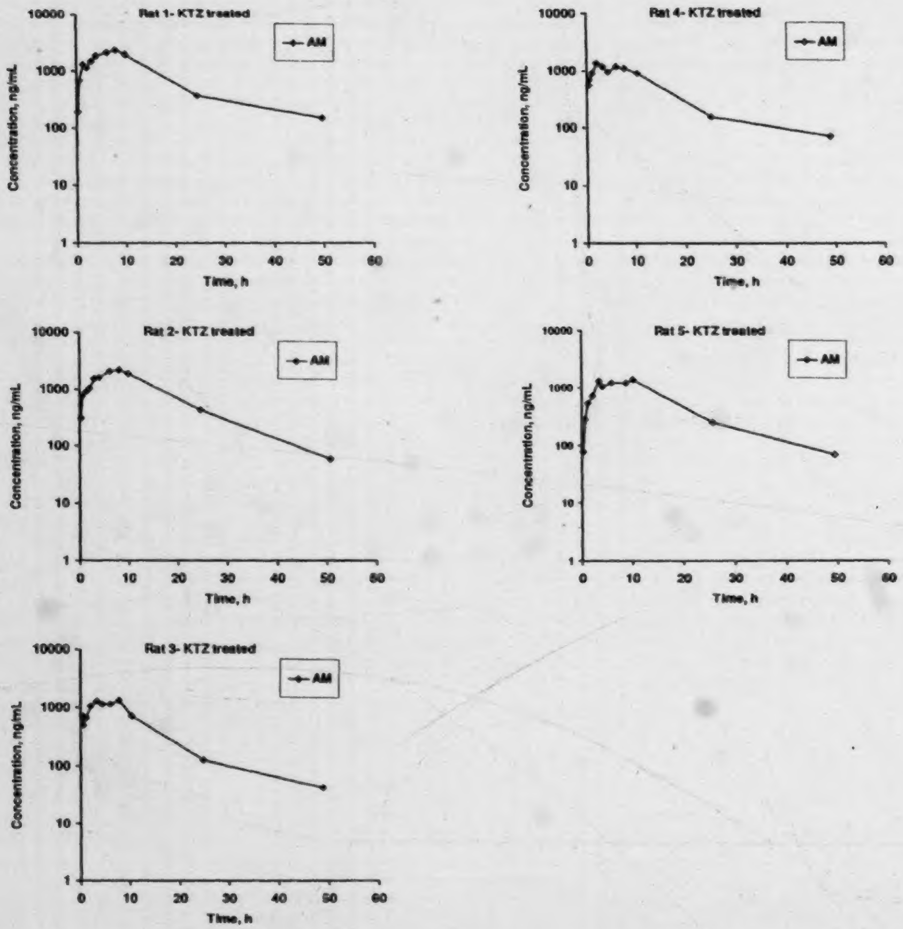

Figure 35: Individual plasma concentration versus time curves of AM in five KTZ-treated rats after oral administration of 50 mg/kg of AM

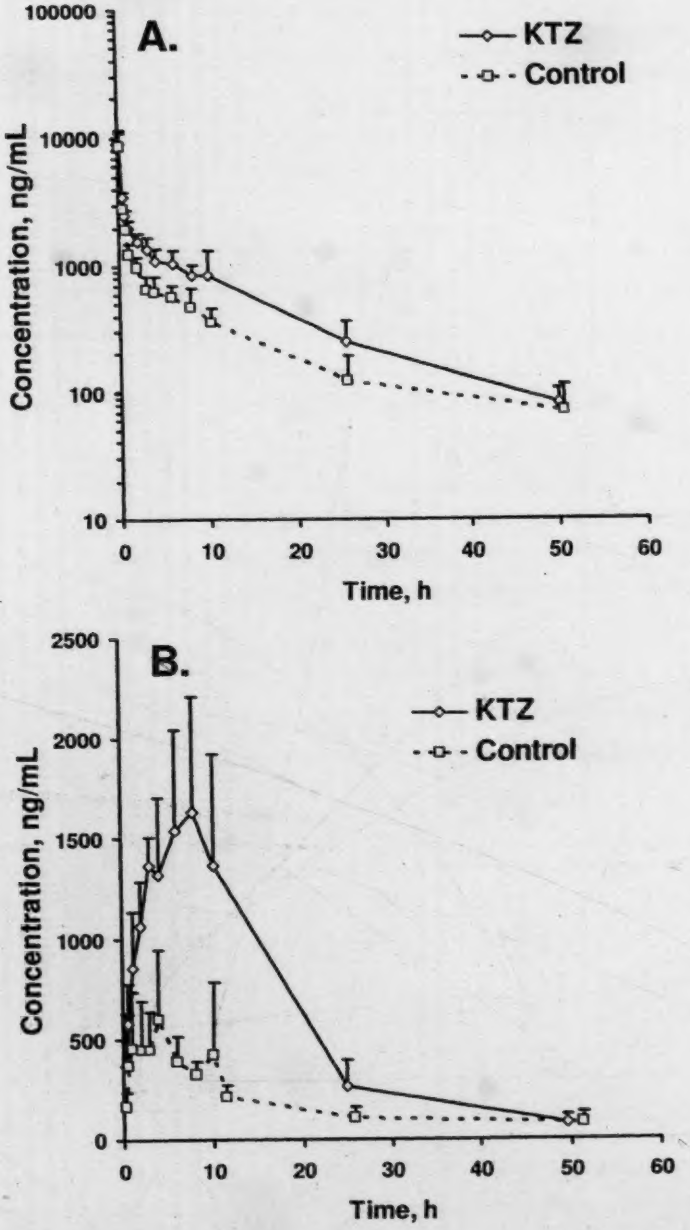

Figure 36: Mean ± SD plasma concentration versus time profile of amiodarone with and without ketoconazole after single 25 mg/kg intravenous (A) or 50 mg/kg oral (B) doses of amiodarone HCl

Table 13: Pharmacokinetic parameters (mean±SD, range in parenthesis) of amiodarone and desethylamiodarone after i.v. and oral administration in rats in the absence (controls) and presence of oral ketoconazole (17.1 mg/kg × 3 doses over 1 day)

Intravenous (25 mg/kg AM HCl)		Oral (50 mg/kg AM HCl)	
Control (n=6)	KTZ (n=6)	Control(n=5)	KTZ(n=5)
AUC0-48h, mg×h/L			
15.4±2.90 (12.6-19.5)	25.6±6.02* (20.6-34.1)	8.73±1.98 (7.06-12.0)	26.8±9.03* (17.7-36.8)
AUC0-∞ (mg×h/L)			
18.5±3.27 (13.4-23.0)	29.6±7.49* (22.2-41.5)	13.6±6.97 (8.11-24.1)	28.0±9.4^{6*} (18.3-39.3)
CL (ml/h/kg)			
1390±269 (1086-1860)	889±209* (602-1126)	-	-
Vdss (L/kg)			
40.9±19.7 (22.1-51.5)	20.2±9.47* (9.01-37.0)	-	-
T1/2 (h)			
39.4±24.2 (17.2-78.8)	30.1±21.5 (10.1-59.5)	32.2 ± 21.9 (16.9-69.8)	9.93 ±1.31 (8.21-11.3)
Cmax (ng/ml)			
-	-	723±355 (317-1123)	1716±495* (1329-2296)
Median tmax(h)			
-	-	5.93 (2.18-10.1)	8.00 (2.08-10.3)
Desethylamiodarone pharmacokinetics parameters			
Cmax (ng/ml)			
66.2±50.0	86.1±55.1	49.1±29.5	138±93.3
Median tmax (h)			
0.369 (0.083-3.7)	24.4 (0.116-49.3)	5.93 (3.21-10.2)	10.0 (6.06-10.5)

* Denotes significantly difference from similarly dosed control rats

2.3.3 Tissue distribution

In the plasma of NL rats, the total triglyceride and cholesterol concentrations were 0.549±0.219 and 1.03±0.356 mM, respectively. In contrast, in the plasma of HL rats, the total triglyceride (46.7±18.6 mM) and cholesterol (29.3±6.97 mM) concentrations were substantially and significantly higher.

Due to the high sensitivity of the assay method, AM and DEA were detected in all of the tissues. After single-dose i.v. administration of AM to all rats, the plasma concentrations immediately rapidly declined. By 12 h after dosing the terminal phase appeared to be log-linear, indicating that postdistributive conditions had been reached (Figure 37). In all of the NL tissues except for fat, there was no evidence of delayed tissue uptake as the first concentration at 5 min postdose was the highest. In contrast, delayed tissue concentrations of AM were noted in the lung, kidney, spleen, and fat of HL animals. In the HL rats for most time points the concentrations were higher in HL than NL rats, and the concentrations in the terminal phase declined more rapidly (Figure 37). For specific tissues concentrations vs. time profile shapes generally were similar for the HL and NL groups, although in some tissues concentrations were higher in HL animals, and in others the reverse was the case.

For DEA similar to AM, the DEA concentrations in the terminal phase declined more rapidly in the HL animals. However, at all time points concentrations were higher for the HL rats (Figure 38). In NL animals there was evidence of delayed appearance of DEA in kidney, spleen, fat, brain and heart. In HL delayed appearance of DEA was evident in all of the tissues, including the plasma. The delay was in general much more noticeable in the HL rats.

The mean± SD of the compiled results were noted for the AUC $_{0\text{-}72h}$ (μg·h/g) in Table 14. The order of mean AUC of AM from the highest to lowest in NL tissues were lung> spleen> kidney> liver> fat> brain> heart> plasma. In contrast, the order of mean AUC of AM from the highest to lowest in HL tissues were spleen> liver >lung >heart >kidney >fat >plasma> brain. For DEA, the order of mean AUC from the highest to lowest in NL tissues was lung> kidney >spleen >liver >heart >fat >brain >plasma. The order of mean AUC of DEA from the highest to lowest in HL tissues was lung> liver> kidney> heart> plasma> brain> fat> spleen (Table 14, Figures 37, 38).

Compared to NL (Table 14), HL was associated with significant increases in both the AM and DEA plasma AUC (8 and 23-fold-respectively). The AUC of AM was also significantly increased in heart (2-fold), liver (2.5-fold) and spleen (5.6-fold). In contrast, in HL brain, kidney and lung the measured AM AUC were significantly decreased by 16-, 2.0- and 1.9-fold, respectively (Figure 37, Table 14). For DEA, there were no significant increases in AUC noted in any HL tissue. However, in HL kidney, lung and spleen there were significant decreases of 3.0, 1.9 and 33.7-fold, respectively in the AUC of DEA (Figure 38, Table 14). In thyroid, no significant differences were observed between the concentrations of AM and DEA in NL and HL rats 24 h postdose (Figure 39).

The calculated Kp for the AM or DEA AUC in HL animals were consistently lower than what was observed in NL animals (Table 14). Although the mean value is reported, statistical analysis could not be performed on the differences in Kp based on AUC data because of the study design (one timed sample per animal) (Table 14). To permit a statistical comparison, during the postdistributive phase of the concentration vs. time curves (24 h or longer) for both AM and DEA (Figures 37 and 38), a constant ratio is expected between concentrations of drug or metabolite in tissue and plasma. Therefore, for AM, when the mean postdistributive Kp for each tissue sample was compared (Figure 40), no significant differences in Kp could be discerned between NL and HL tissues except in spleen and brain, where the lower and higher Kp were observed in NL, respectively. For DEA however, the postdistributive Kp in NL were significantly higher than HL in lung, kidney and spleen.

The calculated AUC ratios of DEA:AM in several of the NL tissues (heart, kidney, liver and spleen) were higher than in HL specimens (Table 14). In lung the mean DEA:AM ratios in both NL and HL animals were equal. In brain however, the ratio of DEA:AM in HL was 39-fold higher than that of NL rats. Fat had a somewhat higher mean DEA:AM

AUC ratio in the HL animals as well (Table 14). During the postdistributive phase of the concentration vs. time curves, which occurs at ~24 h for both AM and DEA, the calculated ratios of DEA:AM in kidney and spleen of the NL animals were all significantly higher than those of HL rats (Figure 40). In lung also this ratio in NL animals was higher but due to the high variability, the difference was not significant (Figure 41).

Table 14: The mean± SD of the AUC0-72 (µg.h/g) of AM and DEA in different tissues of Sprague –Dawley rats after IV injection of 25 mg/kg of AM

Tissues	Plasma	Brain	Heart	Kidney	Liver	Lung	Fat	Spleen
NL								
AM	16.7±2.38	182±12.5	146±17.4	577±55.7	313±22.3	924±73.6	222±41.5	607±38.2
K_p	—	10.9	8.74	34.6	18.7	55.3	13.3	36.3
DEA	0.728±0.112	4.72±0.636	32.6±23.6	75.3±8.36	33.0±4.05	159±20.8	5.28±1.06	51.9±6.69
K_p	—	6.48	44.8	103.4	45.3	218	7.25	71.3
DEA:AM	0.0436	0.0259	0.223	0.131	0.105	0.172	0.0238	0.0855
HL								
AM	134±25.8*	11.4±1.17*	279±49.2*	289±25.0*	786±146*	478±61.8*	253±45.1	3373±382*
K_p	—	0.0851	2.08	2.16	5.87	3.57	1.89	25.2
DEA	17.0±5.37*	11.5±8.01	17.3±3.20	24.8±2.44*	62.3±14.1	82.5±12.8*	8.09±2.21	1.54±0.191*
K_p	—	0.676	1.02	1.46	3.66	4.85	0.476	0.0906
DEA:AM	0.126	1.01	0.0620	0.0858	0.0793	0.173	0.0320	0.00609
Mean HL:NL ratio (AM)	8.02	0.0626	1.91	0.501	2.51	0.518	1.14	5.56
Mean HL:NL ratio (DEA)	23.4	2.44	0.531	0.329	1.89	0.519	1.53	0.0297

Asterisks represents significant differences between the NL and HL (Bailer's test, p<0.05).

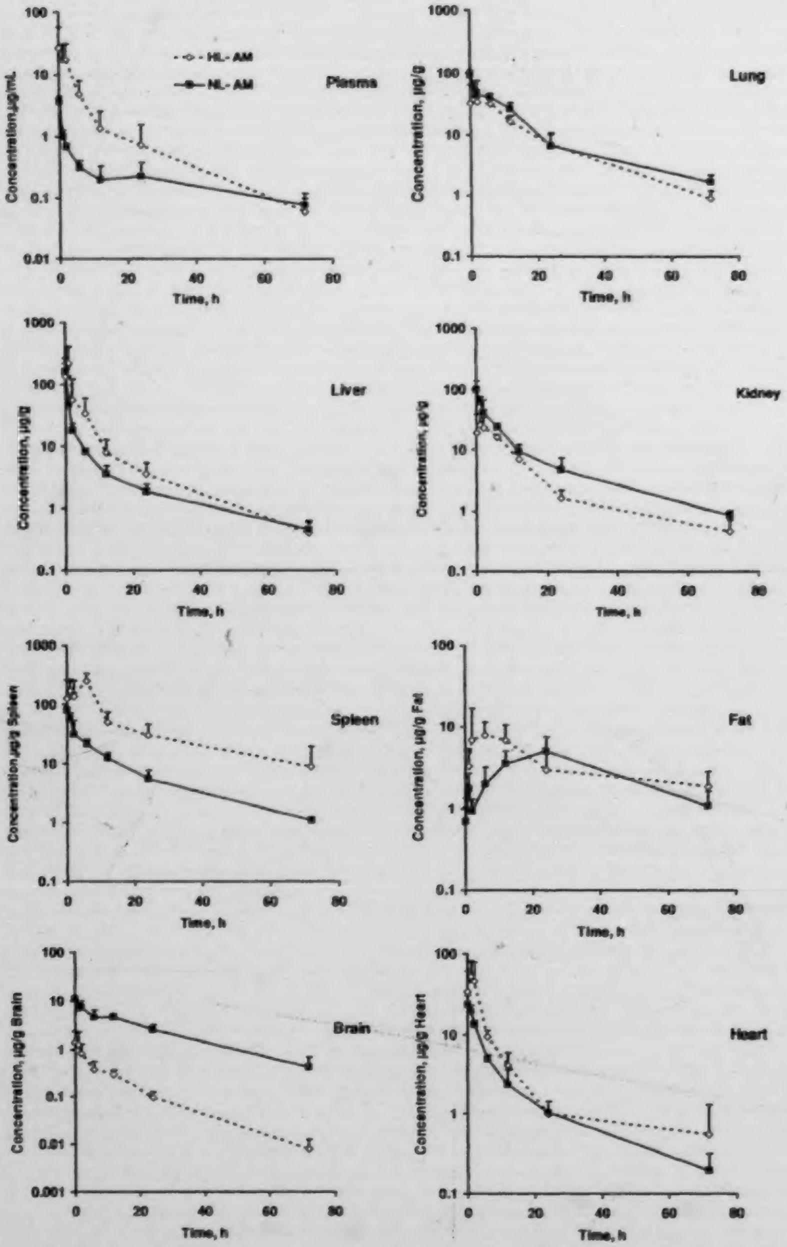

Figure 37: Amiodarone concentration-time profile in plasma, lung, liver, kidney, spleen, fat, brain and heart following single intravenous administration of 25 mg/kg in of amiodarone in control (NL) and P-407-treated (HL) rats

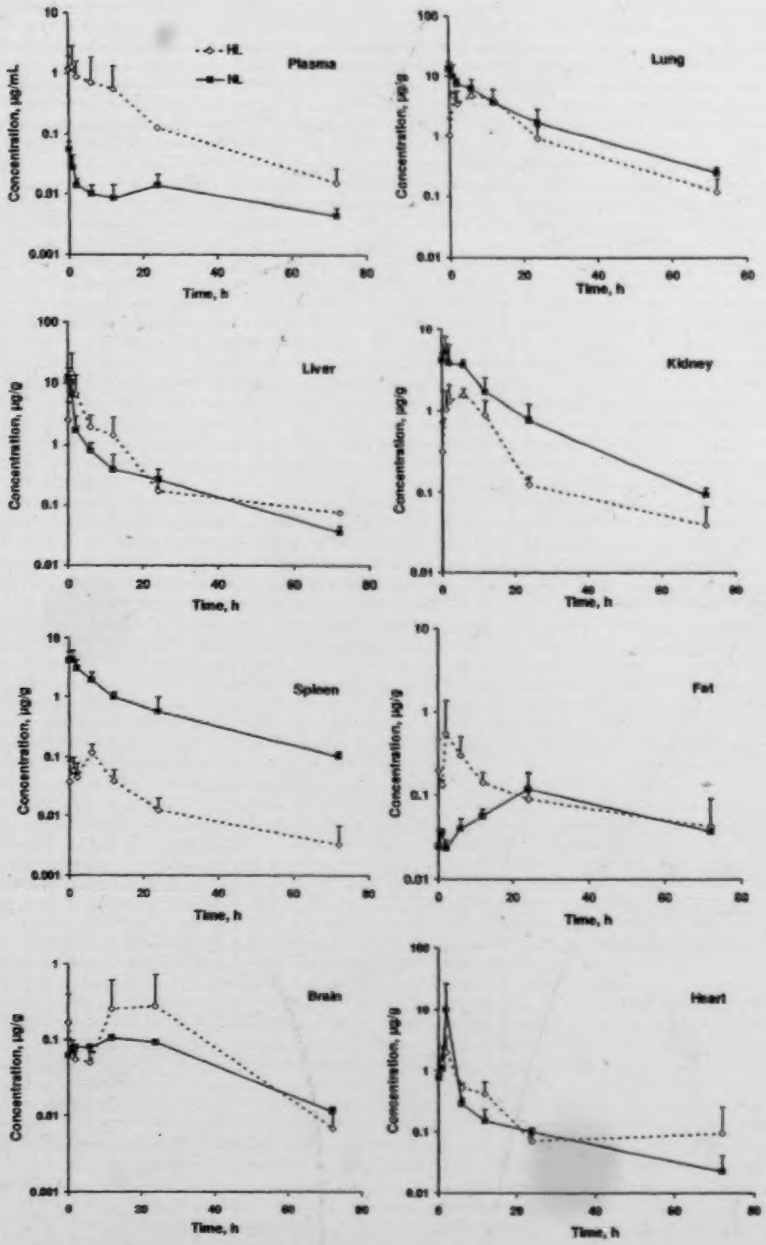

Figure 38: Desethylamiodarone concentration–time profile in plasma, lung, liver, kidney, spleen, fat, brain and heart following single iv. administration of 25 mg/kg of amiodarone in control (NL) and P-407-treated (HL) rats

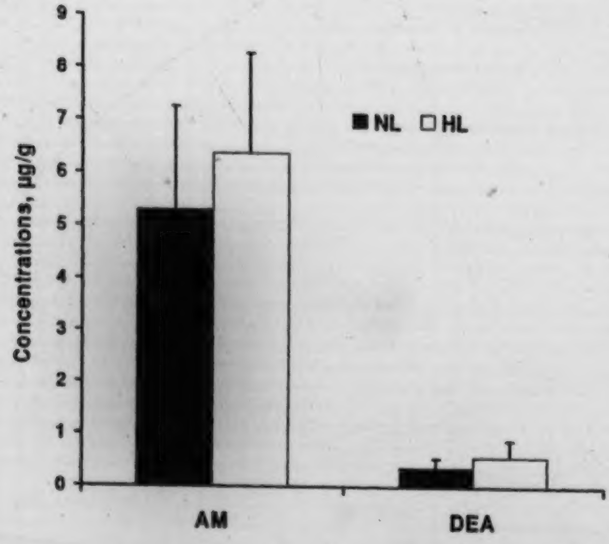

Figure 39: The examination of the effect of hyperlipidemia on distribution of amiodarone and desethylamiodarone in thyroid glands 24 h postdose

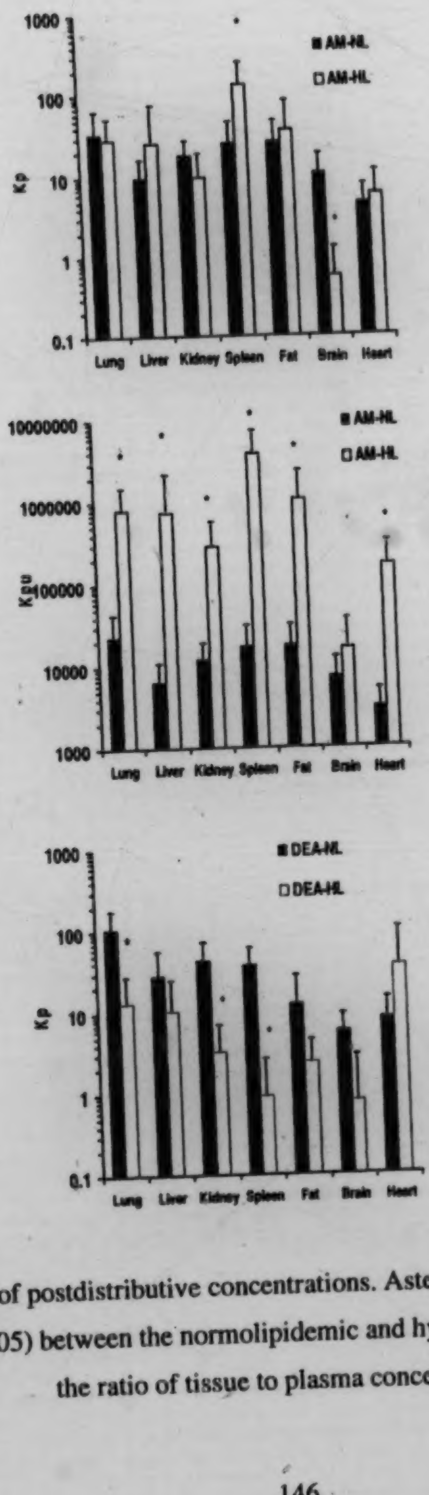

Figure 40: Kp of postdistributive concentrations. Asterisks indicate the significant differences (P<0.05) between the normolipidemic and hyperlipidemic rats. Kp indicates the ratio of tissue to plasma concentrations

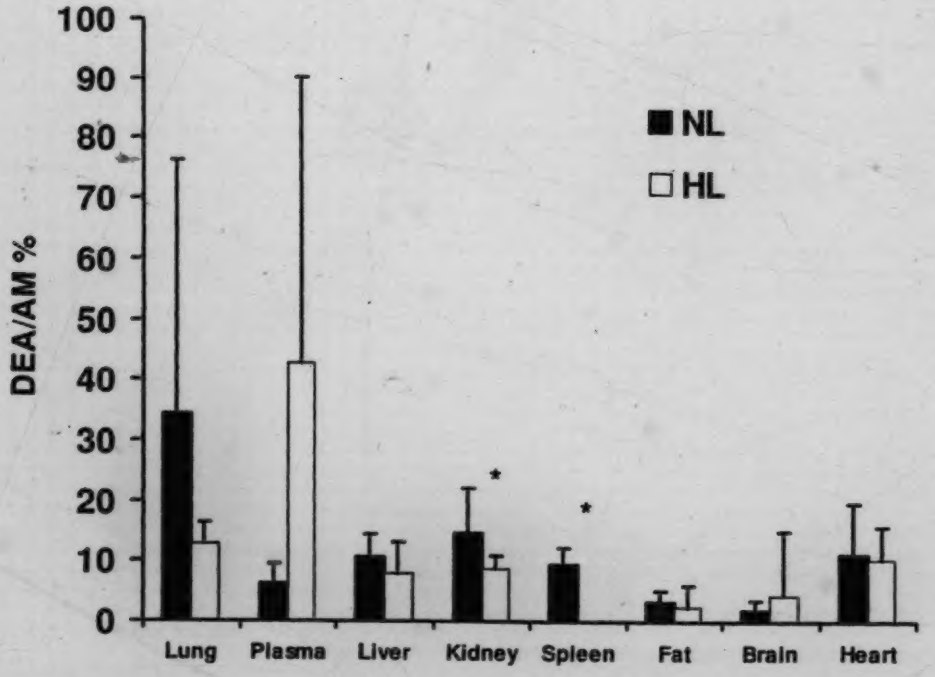

Figure 41: The ratio of postdistributive concentrations of DEA to AM. Asterisks indicate the significant differences (P<0.05) between the normolipidemic and hyperlipidemic rats

2.3.4 In vitro everted gut metabolism

No AM or DEA was detected in the serosal solutions within the everted intestinal segments. On the other hand, both AM and DEA were present within the GIT tissue segments (Figure 42), thus indicating the ability of the intestine to absorb and metabolize the drug. For each segment, there was little evidence of significant difference in the uptake of AM between treatments (Figure 42 upper panels). Only in the first duodenal segment (G1), there was a difference detected, in which the KH+5% SBS was significantly different from KH alone. In general this was the case for DEA as well in which in the first segment the peanut oil (PO) pretreated group had a significantly lower DEA concentration than the KH control treatment. With respect to the treatment groups themselves, each segment in general seemed to take up AM to an equivalent degree (Figure 42 bottom left hand panel). Within treatments, there was also little significant difference in the DEA concentration between segments (Figure 42 bottom right hand panel). The lone exception was in the peanut oil-pretreated group, in which segment G3 had more DEA within it than some of the other segments.

More differences were discernable when the ratio of metabolite to drug within the segments was evaluated (Figure 43 left panel). When viewed by segment, the rank order of mean ratios of the treatment groups was generally peanut oil pretreated < KH+25% SBS < KH < KH+5% SBS. In segments G1 and G3 no significant differences were noted. In each of these groups the peanut oil pretreatment had the lowest ratio. In segment G4 and G5, the KH+5% SBS had the highest ratio ($p<0.05$). When viewed by treatment group, there was little difference in this ratio between segments (Figure 43 right panel).

Because of the similarities in the uptake and generation of drug and metabolite, respectively, between the segments (Figure 42 upper panels), we performed a comparative analysis of the data by compiling the mean of all of the segments for each treatment together. For AM the KH control group had the highest uptake of drug and presence of metabolite. For DEA the lowest concentrations were present in the peanut oil pretreated group. Similarly, the lowest ratio of metabolite to drug was present in the peanut oil pretreated group.

In total there were three groups of everted gut incubations exposed to 25% SBS. These included KH+25% SBS, KH+25% SBS+ 5% INLP, and the peanut-oil pretreated groups (Figure 44). In the KH+25% SBS+5% INLP group there was a significant decrease in the uptake of AM in the GIT tissues. With respect to DEA concentration, the highest amount was measured in the KH+25% SBS exposed segments. The DEA formation, expressed as a percent of AM, was lowest in the peanut oil-pretreated animals. In this parameter, there was no difference between the 25% SBS and 25% SBS+5% INLP segments.

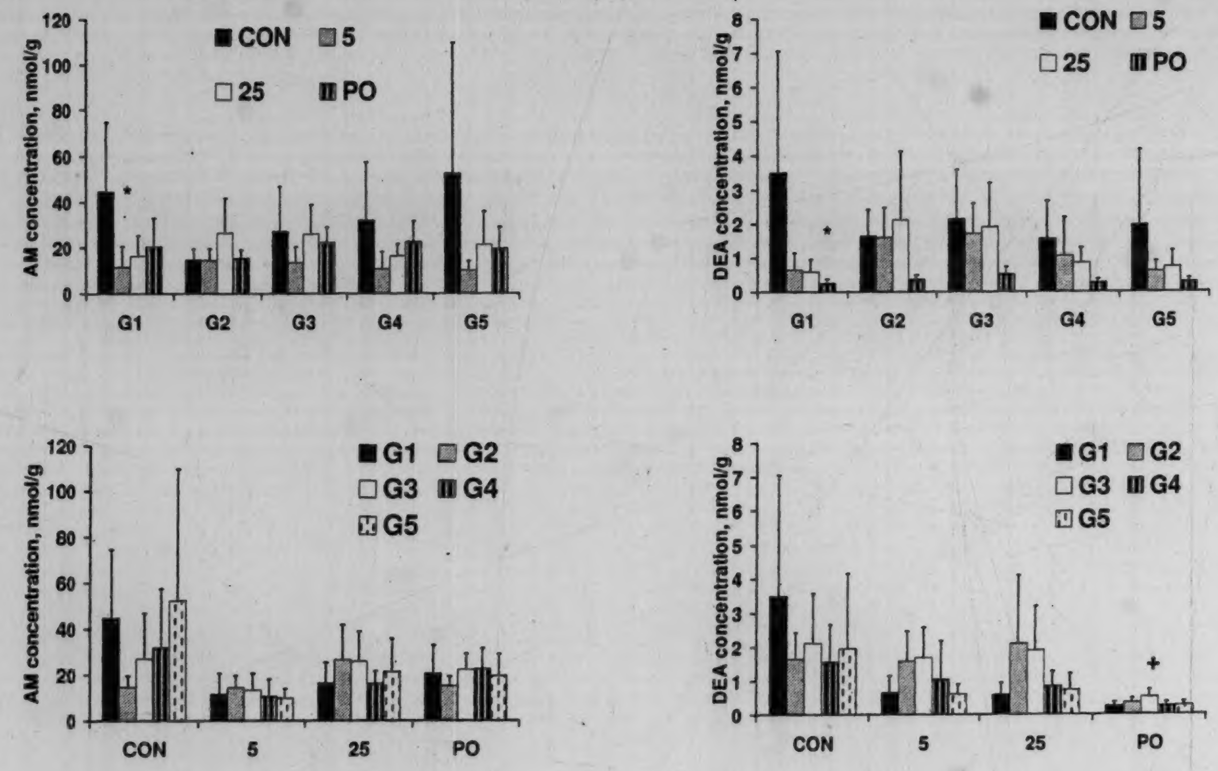

Figure 42: Concentrations of AM and DEA in gut segments (G1-G5) after incubation of everted gut for 2 hours. Treatments Were: rats given normal diet, with guts incubated with control (Krebs-Heinseleit, CON), 5% SBS in Krebs-Heinseleit (5), 25% SBS in Krebs-Heinseleit (25), and peanut oil treated rats (PO), with guts incubated with 25% SBS in Krebs-Heinseleit

* significantly different between the noted treatments from control incubation. + significantly different from G1, G4 and G5

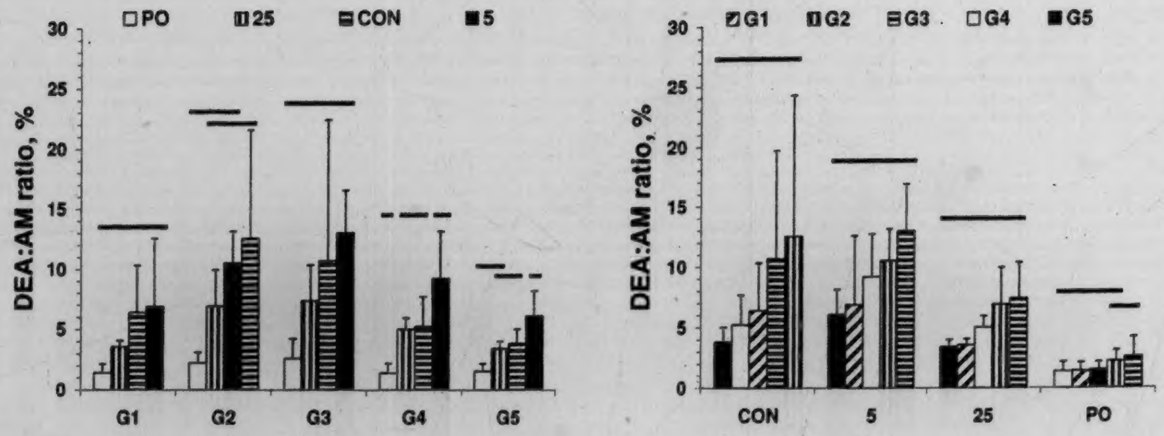

Figure 43: The ratio of DEA to AM in each segment expressed as a percent of the total amount of AM present in each segment (G1-G5). Treatments were rats given normal diet, with guts incubated with control (Krebs-Heinseleit, CON), 5% SBS in Krebs-Heinseleit (5), 25% SBS in Krebs-Heinseleit (25), and peanut oil treated rats (PO), with guts incubated with 25% SBS in Krebs-Heinseleit

Continuous lines over each bar indicate no significant difference between the encompassed groups. Broken lines between groups indicate significant differences

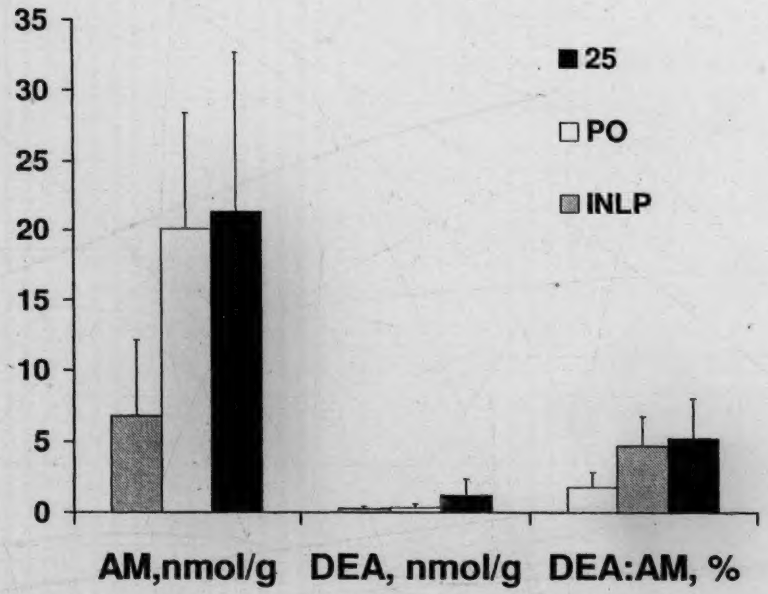

Figure 44: Concentrations of AM, DEA and metabolite: drug ratio, when all segments (G1-G5) from incubations involving 25% SBS were combined. Broken lines between groups indicate significant differences. 25% SBS in Krebs-Heinseleit (25), peanut oil treated rats (PO), with guts incubated with 25% SBS in Krebs-Heinseleit, 25% SBS in Krebs-Heinseleit with 5% Intralipid (INLP)

2.3.5 In vitro distribution of AM and DEA in NL and HL lipoprotein plasma fractions of human and rat

2.3.5.1 Triglyceride (TG) and cholesterol (CHOL) measurement

Hyperlipidemia caused 4.21 and 2.24-fold increases in the TG and total CHOL levels in human plasma, respectively (Table 15). In HL rats, however, the increases in TG and CHOL levels were more drastic than in HL humans. P-407 caused 32.9 and 42.3-fold increases in TG and CHOL in rat plasma, respectively (Table 15). In HL human plasma, the concentrations of TG were higher in all of the isolated fractions compared to NL plasma (Table 16).

Table 15: The mean ±SD cholesterol and triglyceride present in human and rat plasma samples before the separation of lipoprotein fractions

Species	Triglyceride	Cholesterol
NL-Human	92±5.87	144±15.3
HL-Human	388±48.9*	322±167
NL-Rat	109±22.4	57.1±0.860
HL-Rat	3569±430*	2418±517*

Asterisks represent significant differences between normolipidemic (NL) and hyperlipidemic (HL) of the same species (Student's unpaired t test, $p<0.05$)

The largest increase was observed in the TRL fraction. Although the HDL fraction was less than the lower limit of quantitation of the assay, in each of the other fractions tested the HL rat plasma had, similar to human, increases in the TG levels compared to NL plasma (Table 16). For CHOL, a somewhat different pattern emerged. For example, compared to NL plasma, in HL human plasma a large increase in CHOL was observed only in the TRL fraction (Table 16). In contrast, in the HL rat plasma the CHOL concentrations were greatly increased in the TRL and the LDL fractions, compared to NL plasma (Table 16).

Table 16: The mean ±SD triglyceride and cholesterol concentrations (mg/dL) in plasma lipoprotein fractions from normolipidemic (NL) and hyperlipidemic (HL) plasma specimens of human and rat

Species	TRL	LDL	HDL	LPDP
	Triglyceride			
NL-Human	17.1±3.30	12.9±5.40	9.90±0.296	6.64±0.207
HL- Human	278±67.2*	94.6±5.47*	52.4±3.58*	48.2±2.96*
NL-Rat	15.4±1.70	7.29±2.08	5.99±0.932	4.38±1.03
HL-Rat	1861±150*	93.3±8.13*	ND	33.3±8.61*
	Cholesterol			
NL-Human	10.0±3.05	51.8±29.7	19.4±0.682	5.41±1.14
HL- Human	134±25.3*	60.7±1.74	9.93±4.55	ND
NL-Rat	8.14±1.91	10.6±0.227	19.8±4.79	1.89±0.479
HL-Rat	2698±186*	237±41.7*	18.8±6.01	2.23±1.05

Asterisks represent significant differences between NL and HL of the same species (Student's unpaired t test, $p<0.05$)

2.3.5.2 Recovery

The recovery of AM from the spiked human plasma samples ranged from 61 to over 86% (Table 17). The presence of HL caused a significant decrease in the recovery of AM. In rat however, the recovery of AM was higher and the effect of HL was more pronounced (Table 17). Recovery of AM in NL rat plasma was over 100%, which decreased around 50% in HL (Table 17). For DEA the overall recovery was less variable than AM (Table 17). The presence of HL caused no significant change in the recovery of DEA in both human and rat plasma samples (Table 17).

Table 17: Association of AM and DEA in each fraction of normolipidemic (NL) and hyperlipidemic (HL) human and rat plasma samples

Sample	Recovery in each fraction (ng)				Total Recovery (% incubated)
	TRL	LDL	HDL	LPDP	
Amiodarone					
NL-Human	432±52.2	292±172	592±99.7	1213±130	84.3±2.07
HL-Human	911±171*	408±149	247±38.4*	350±26.2*	63.8±6.50*
NL- Rat	261±54.6	533±351	821±312	1784±248	103±8.02
HL- Rat	1365±229*	167±82.4*	15.2±6.70*	32.0±40.8*	59.0±7.34*
Desethylamiodarone					
NL-Human	93.6±16.7	119±48.9	285±51.0	438±59.6	62.4±3.86
HL-Human	345±122*	209±65.9*	190±27.6*	297±26.5*	69.6±13.1
NL- Rat	30.6±7.28	72.3±51.3	204±74.6	875±106	78.8±13.5
HL- Rat	705±131*	196±52.7*	40.4±11.8*	79.3±29.2*	69.6±8.31

Asterisks represent significant differences between NL and HL of the same species (Student's unpaired t test, $p<0.05$)

2.3.5.3 Comparison of normolipidemic and hyperlipidemic plasma

Upon normalizing the fractional recoveries to overall recovery from plasma, it was observed that in all of the NL plasma from both species, AM and DEA were most associated with LPDP ($p<0.05$). The LPDP fraction represents the most polar of the fractions (Figure 45, Table 18). The next most polar lipoprotein fraction, HDL, was second in abundance for both drug and metabolite in all species. The lowest degree of association of both drug and metabolite occurred in the most apolar lipoprotein fractions represented by LDL and TRL, respectively (Figure 45, Table 18).

In HL plasma, the patterns of association of both drug and metabolite were markedly changed (Figure 45, Table 18). For both species, there was a shift of both AM and DEA in HL plasma from the more polar LP fractions to the less polar fractions. In both species, the highest association of AM and DEA in HL plasma was in the TRL fraction. The lowest association of both analytes was in the HDL fraction. With the exception of DEA in human HL plasma, in the other incubations involving AM and DEA the LDL fraction possessed the second highest association of analyte, next to TRL.

Table 18: Percentage of association of AM and DEA in each fraction of normolipidemic (NL) and hyperlipidemic (HL) human and rat plasma samples

Sample	Recovery % in each fraction			
	TRL	LDL	HDL	LPDP
		Amiodarone		
NL-Human	17.1±2.07	11.6±6.68	23.5±4.29	47.9±4.33
HL-Human	47.6±8.33	21.2±7.02	12.9±1.61	18.3±0.969
NL-Rat	7.91±2.14	14.7±5.30	23.8±4.36	53.6±7.07
HL- Rat	86.6±6.53	11.0±6.21	0.510±0.632	1.89±2.19
		Desethylamiodarone		
NL-Human	10.1±2.30	12. 7±4.74	30.5±5.75	46.7±4.95
HL-Human	32.6±4.87	19.8±3.43	18.7±4.02	28.9±3.55
NL-Rat	2.59±0.471	5.72±2.93	17.1±4.59	74.6±6.19
HL- Rat	68.8±7.25	19.7±6.52	3.92±0.768	7.68±2.51

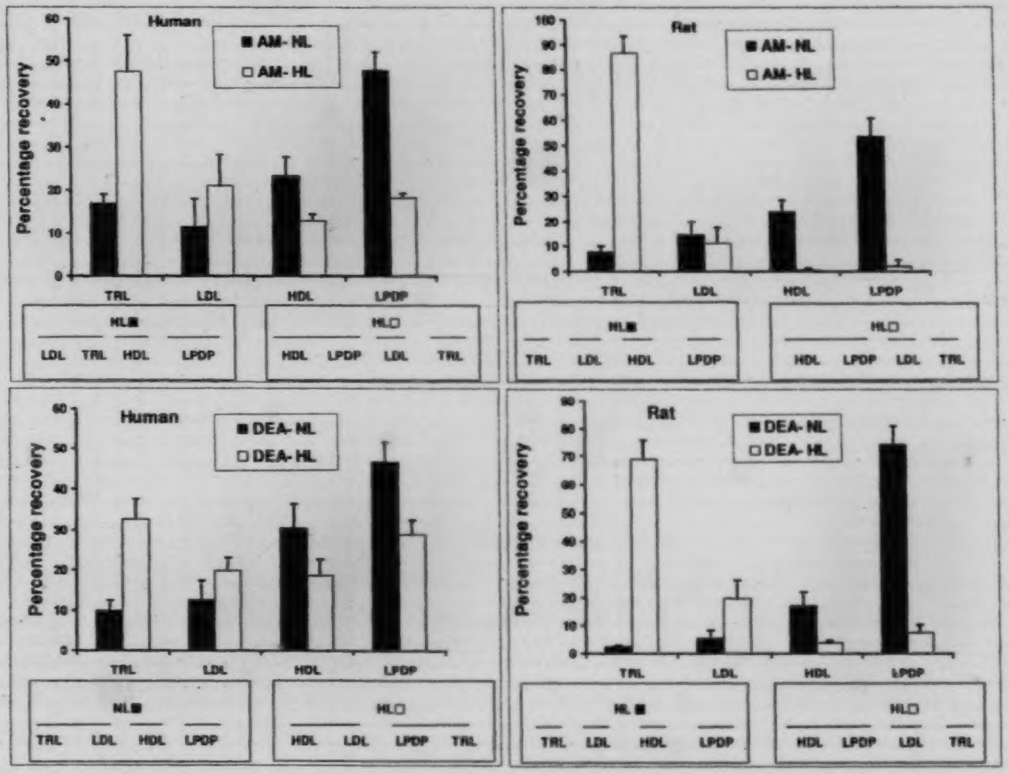

Figure 45: Association of amiodarone (AM) and desethylamiodarone (DEA) with lipoprotein fractions isolated from hyperlipidemic (HL) or normolipidemic (NL) plasma, expressed as percent of total recovery of drug and metabolite. Continuous lines over fractions indicates lack of significance between fractions encompassed by the lines; fractions not encompassed within lines are significantly different from those fractions encompassed by the lines (Kruskal-Wallis One Way Analysis of Variance on Ranks, p<0.05)

2.3.5.4 Interspecies differences

With respect to interspecies comparisons, the patterns of recovery of both AM and DEA in the fractions were quite similar in both species (Figures 45 and 46). However, there were some significant interspecies differences noted in the percent association within fractions. The shift of drug into the TRL fraction of HL plasma was more dramatic for rat than human plasma for drug and metabolite, with significantly higher levels (~2-fold) of association of AM and DEA in rat TRL fractions at the expense of the LPDP and HDL fraction uptake (Figure 46, Table 18). To illustrate this observation, the associations of AM with rat LPDP and HDL fractions were 10 and 26-fold higher than in the corresponding human fractions, respectively (Figure 46, Table 18).

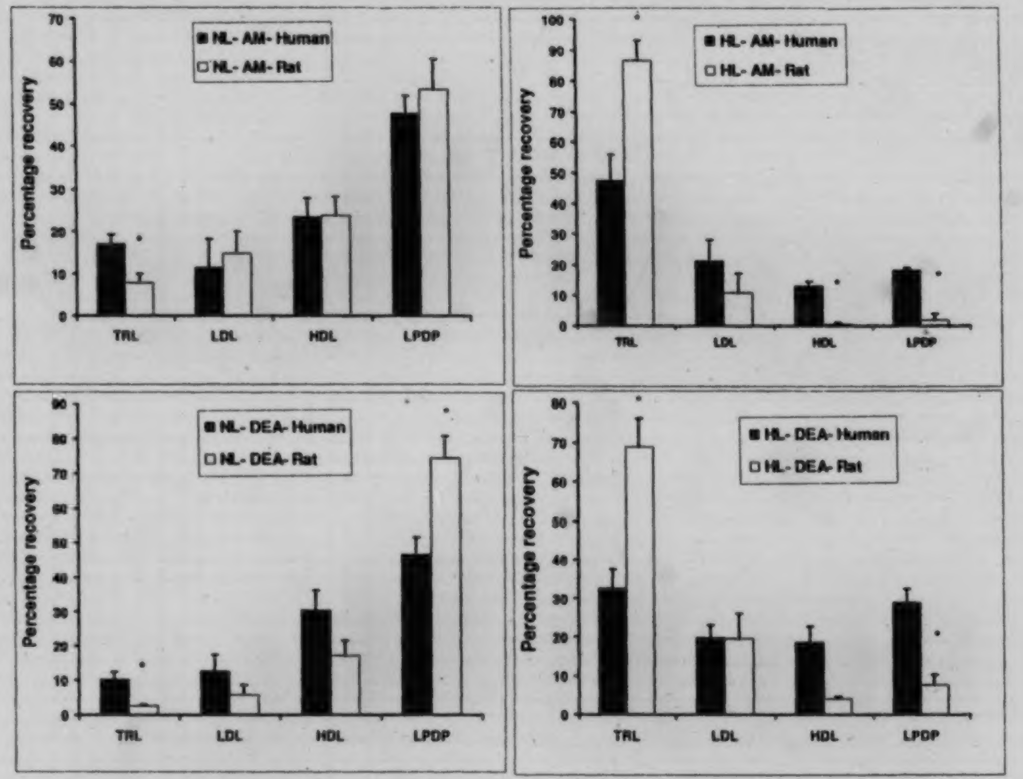

Figure 46: Mean±SD differences between human and rat for disposition of AM and DEA within different lipoprotein fractions from NL and HL plasma. * represent significant differences. (Student's unpaired t-test, $p<0.05$)

2.3.5.5 Comparison of the ratio of DEA to AM in different fractions

The ratio of DEA to AM in human plasma lipoprotein fractions did not seem to be affected very much by HL (Table 19). The ratios stayed fairly constant with the exception of LPDP, where the DEA:AM ratio significantly increased by approximately 1.6-fold. In contrast, HL caused the metabolite to drug ratios to be markedly changed in each of the LP fractions in rat. The ratio of DEA to AM in TRL, LDL, HDL and LPDP fractions of rat HL plasma were 2.34, 4.97, 7.0 and 4.7-fold higher ($p<0.05$), respectively, than in the corresponding fractions in rat NL plasma (Table 19).

Table 19: Ratio (mean±SD) of DEA: AM within each fraction derived from normolipidemic (NL) and hyperlipidemic (HL) plasma

Plasma	TRL	LDL	HDL	LPDP
NL-Human	0.587±0.0683	1.19±0.287	1.31±0.144	0.975±0.0282*
HL-Human	0.703±0.171	0.993±0.222	1.47±0.385	1.58±0.176
NL-Rat	0.338±0.0685*	0.390±0.148*	0.712±0.0849*	1.40±0.112*
HL-Rat	0.793±0.0350	1.94±0.362	5.02±2.76	6.62±3.83

Asterisks represent significant differences between NL and HL of the same species (Student's unpaired t test, $p<0.05$)

2.3.6 In vitro metabolism of AM to DEA in hepatic and intestine of rat (Microsomal studies)

2.3.6.1 Part 1- Microsomal incubation studies for the identification of enzymes involved in the metabolism of AM to DEA

a) Metabolism of AM in liver

In liver, as AM concentrations increased there was an increase in the formation rate of DEA. It was found that in liver microsomes, the kinetic profile of DEA formation vs. concentration conformed well to the Michaelis-Menten model with one enzyme in all of the individual livers (Figures 47, 49 Tables 20 and 21). However there did appear to be some deviation from the model with the highest mean concentration. The estimated km, Vmax and intrinsic clearance (CLint) were determined in liver (Table 22). The variability assessed by coefficient of variation was substantially higher for km (74%) than Vmax (21%).

Table 20: Rate of In vitro metabolism of AM to DEA in four individual rat livers (Real data)

Liver 1		Liver 2		Liver 3		Liver 4		Mean±SD	
AM+DEA (μM)	DEA (pmol/min/ mg protein)	AM+DEA (μM)	DEA (pmol/min/ mg protein)	AM+DEA (μM)	DEA (pmol/min/ mg protein)	AM+DEA (μM)	DEA (pmol/min/ mg protein)	AM+DEA (μM)	DEA(pmol/min/ mg protein)
148	406	151	401	186	261	124	213	152	320±98.3
98.8	278	77.6	263	87.9	186	72.7	153	84.3	220±60.0
37.6	236	31.3	180	44.3	163	35.5	123	37.2	175±46.7
14.5	128	13.3	110	18.0	99.8	16.9	76.1	15.7	104±21.8
5.54	58.3	7.03	57.2	6.84	48.6	10.8	48.9	7.56	53.2±5.20
0.986	15.4	2.30	25.7	2.26	21.6	6.21	23.2	2.94	21.5±4.34
		0.763	8.94	0.375	9.63	4.84	11.46	1.99	9.99±1.28

Table 21: Rate of In vitro metabolism of AM to DEA in four individual rat livers (Fitted data)

Liver 1		Liver 2		Liver 3		Liver 4		Mean±SD	
AM+DEA (µM)	DEA (pmol/min/ mg protein)	AM+DEA (µM)	DEA (pmol/min/ mg protein)	AM+DEA (µM)	DEA (pmol/min/ mg protein)	AM+DEA (µM)	DEA (pmol/min/ mg protein)	AM+DEA (µM)	DEA(pmol/min/ mg protein)
148	354	151	356	186	221	124	212	152	286±79.8
98.8	324	77.6	292	87.9	196	72.7	169	84.3	245±74.3
37.6	229	31.3	188	44.3	161	35.5	112	37.2	173±49.2
14.5	130	13.3	104	18.0	107	16.9	64.4	15.7	101±27.3
5.54	61.2	7.03	61.6	6.84	55.0	10.8	44.4	7.56	55.6±8.03
0.986	12.3	2.30	22.1	2.26	21.3	6.21	27.0	2.94	20.7±6.12
		0.763	7.60	0.375	3.80	4.84	21.5	1.99	11±9.30

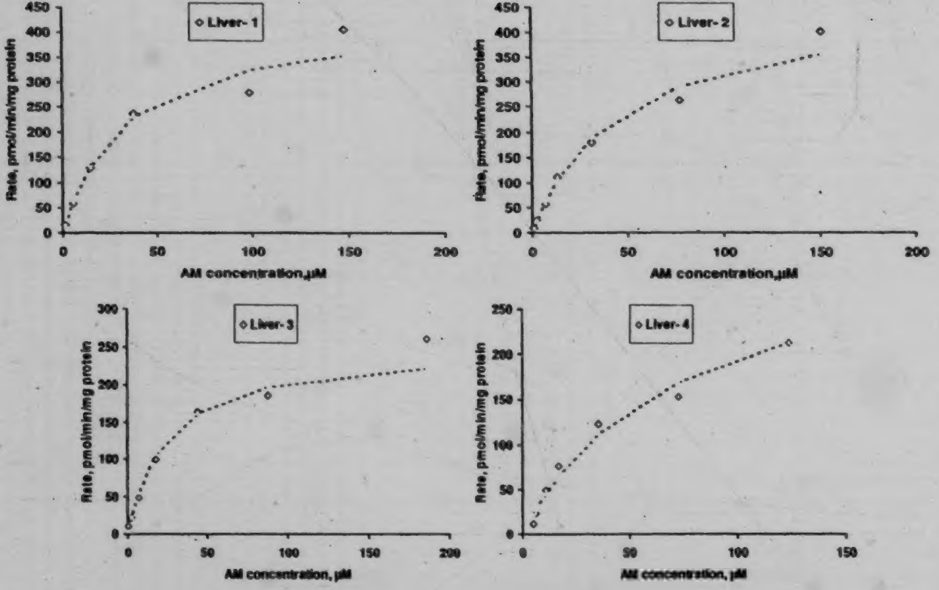

Figure 47: Rate of DEA formation in liver microsomes of Sprague-Dawley rat after 30 min incubation with increasing concentration of AM (Fitted data)

Table 22: Enzyme kinetic parameters for DEA formation by individual rat liver microsomes, based on results of fitted data

	Km (μM)	Vmax (pmol/min/mg protein)	Clint (μL/min/mg protein)
Liver -1	33.8	435	12.9
Liver -2	45.8	464	10.1
Liver -3	24.3	250	10.3
Liver -4	70.2	333	4.74
Mean±SD	43.5±32.1	370±78.4	9.51±3.42

b) *Metabolism of AM in Jejunum*

In intestinal microsomes, as AM concentrations increased there was an increase in the formation rate of DEA (Figures 48, 49 Table 23). In contrast to liver microsomes, over the range of concentrations studied, a linear model best fit the DEA formation vs. AM concentration relationship (r^2>0.99) in intestinal microsomes (Figure 48). As a result, determination of km, Vmax and CLint was not possible.

Table 23: Rate of In vitro microsomal metabolism of AM to DEA in four individual intestines (Real data)

Gut 1		Gut 2		Gut 3		Gut 4		Mean±SD	
AM+DEA (µM)	DEA (pmol/min/ mg protein)	AM+DEA (µM)	DEA (pmol/min/ mg protein)	AM+DEA (µM)	DEA (pmol/min/ mg protein)	AM+DEA (µM)	DEA (pmol/min/ mg protein)	AM+DEA (µM)	DEA(pmol/min/ mg protein)
143	42.7	173	123	188	57.4	128	88.3	158	77.9±35.6
51.3	23.8	78.5	38.2	107	25.3	82.1	44.8	80.0	33.0±10.1
26.1	10.5	33.7	19.1	49.9	18.5	32.8	30.7	35.6	19.7±8.29
13.2	3.66	12.9	4.52	21.8	9.99	17.8	16.5	16.4	8.67±5.93
8.14	1.78	8.10	2.36	10.7	6.64	11.0	9.20	9.47	4.99±3.54
				4.10	5.19	6.62	5.89	5.36	5.54±0.488
				1.34	5.02	5.07	4.83	3.21	4.92±0.131

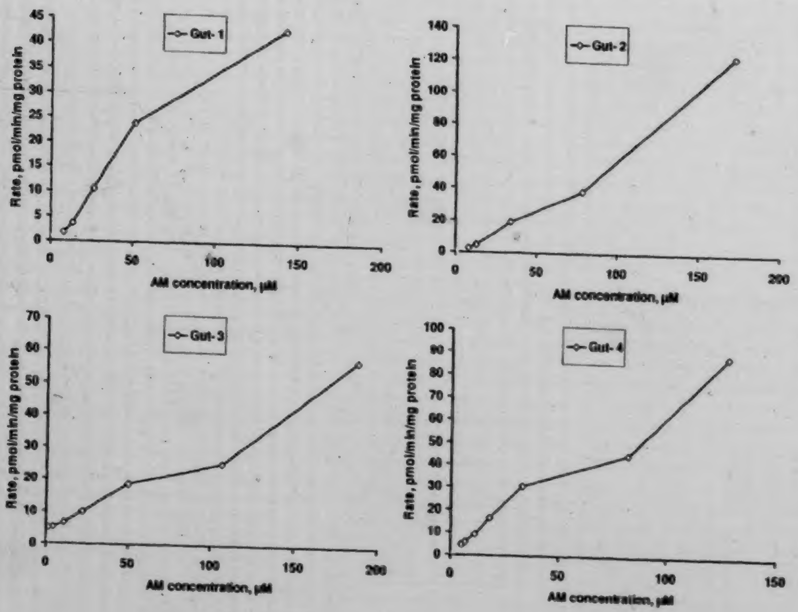

Figure 48: Rate of DEA formation in intestinal microsomes of Sprague-Dawley rat after 30 min incubation with increasing concentration of AM

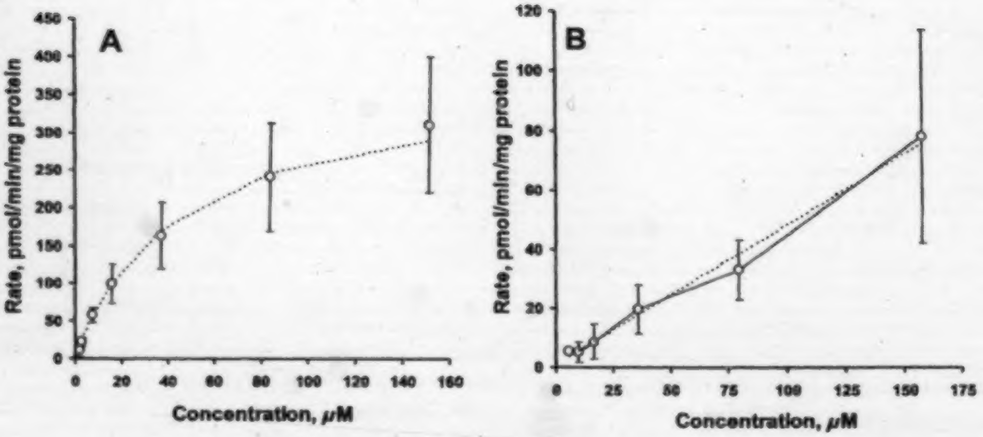

Figure 49: Rate (mean ± SD) of DEA formation in liver (A) and intestinal (B) microsomes of Sprague-Dawley rat after 30 min incubation with increasing concentration of AM (x-axis)

c) *Chemical Inhibition in liver*

As the concentration of KTZ was increased in the chemical inhibition study, a progressive decrease was noted in the formation rate of DEA in rat liver microsomes (Figures 50, 52 Table 24). In comparison to control incubations, all of the incubations in which KTZ was added yielded significantly lower DEA formation rates, for each of the three AM concentrations studied (Figures 50 and 52, Table 24). In general, as KTZ concentrations were increased, there were significant decreases in formation rates of DEA in the samples.

Table 24: Effect of increasing concentrations of ketoconazole on DEA formation in the presence of three concentrations of AM in liver microsomes

	KTZ=0				
AM, µM	Liver1(pmol/min/mg protein)	Liver2(pmol/min/mg protein)	Liver3(pmol/min/mg protein)	Liver4(pmol/min/mg protein)	Mean±SD(pmol/min/mg protein)
64	256	243	174	159	208±48.5
32	203	176	136	106	155±42.8
16	135	113	92.2	63.5	101±30.3
	KTZ=1.3 µM				
64	157	162	171	120	152±22.2
32	97.2	80.3	113	83.0	93.3±14.9
16	65.2	49.9	59.3	66.9	60.4±7.67
	KTZ=3.2 µM				
64	169	123	120	98.8	128±29.8
32	70.2	55.1	78.6	53.4	64.3±12.2
16	42.5	34.7	43.1	33.1	38.4±5.20
	KTZ=6.4 µM				
64	159	90.6	111	68.1	107±38.7
32	65.5	45.5	65.5	43.3	54.9±12.2
16	35.1	30.6	40.3	32.6	34.7±4.20
	KTZ=32 µM				
64	80.9	61.6	56.5	50.9	62.5±13.1
32	38.2	16.5	34.0	27.0	28.9±9.47
16	17.3	8.93	14.9	15.6	14.2±3.63

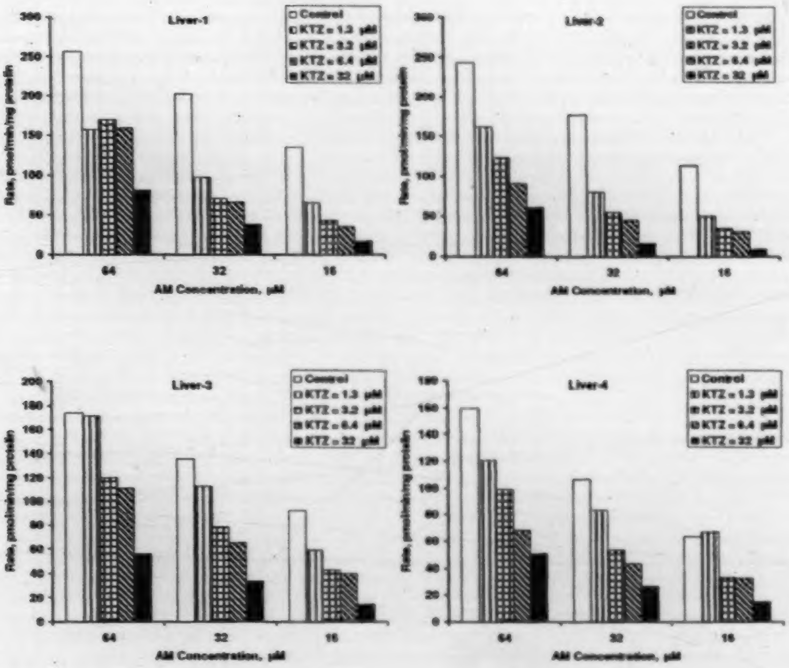

Figure 50: Effect of increasing concentrations of ketoconazole on DEA formation in individual liver microsomes of four individual rats

d) Chemical inhibition in intestine

KTZ did not seem to have the same effects on DEA formation. At the highest concentration of AM exposed to intestinal microsomes, no significant difference was observed in the formation of metabolite with increasing concentrations of inhibitor (Figure 51, 52 Table 25). Similar to liver, at lower concentrations of AM (23.5 and 47 μM), the formation of DEA in intestine was significantly lower than in control incubations when KTZ was present. There was, however, a difference in the pattern of effect of KTZ in intestine as compared with liver, because in intestine, KTZ did not result in a markedly progressive decrease in DEA formation at KTZ concentrations above 1.88 μM (Figures 51 and 52, Table 25).

Table 25: Effect of increasing concentrations of ketoconazole on DEA formation in the presence of three concentrations of AM in rat intestinal microsomes

	KTZ=0				
AM, µM	Gut 1(pmol/min/mg protein)	Gut 2(pmol/min/mg protein)	Gut 3(pmol/min/mg protein)	Gut 4(pmol/min/mg protein)	Mean±SD(pmol/min/mg protein)
94	38.4	43.4	25.4	48.3	38.9±9.87
47	23.2	28.4	18.5	38.5	27.2±8.59
23.5	9.80	12.8	12.0	24.2	14.7±6.48
	KTZ= 1.88 µM				
94	52.0	58.6	23.6	34.9	42.3±16.0
47	17.1	18.4	9.19	20.8	16.4±5.03
23.5	9.28	13.1	5.36	9.61	9.33±3.15
	KTZ=4.75 µM				
94	37.04	46.8	20.7	31.3	34.0±10.9
47	14.9	14.6	9.50	15.1	13.5±2.69
23.5	6.59	10.9	4.54	7.46	7.36±2.63
	KTZ=9.4 µM				
94	40.1	52.5	21.0	24.9	34.6±14.5
47	14.9	16.9	10.2	14.8	14.2±2.82
23.5	6.90	9.39	3.75	6.89	6.73±2.31
	KTZ= 47 µM				
94	53.8	68.5	29.0	36.5	46.9±17.7
47	20.3	17.5	10.0	13.3	15.3±4.53
23.5	7.57	7.74	5.01	5.00	6.33±1.53

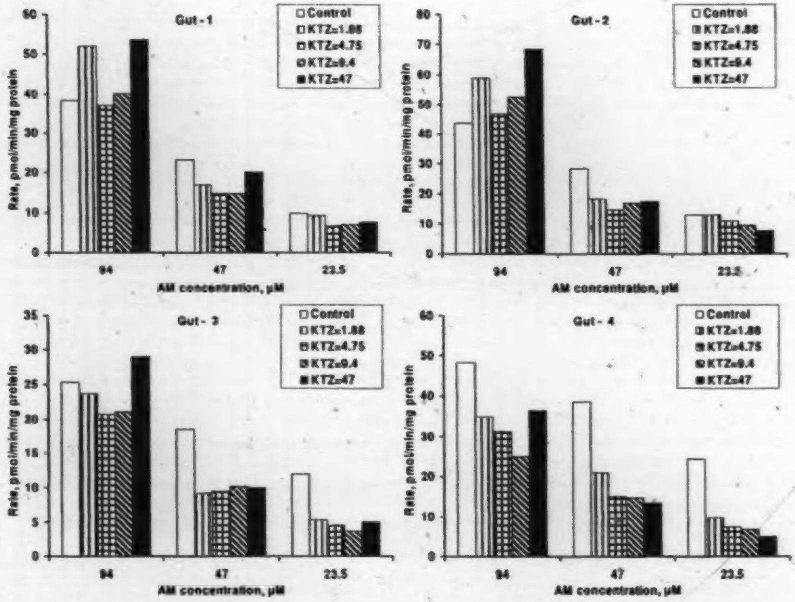

Figure 51: Effect of increasing concentrations of KTZ on DEA formation in individual intestinal microsomes of four individual rats

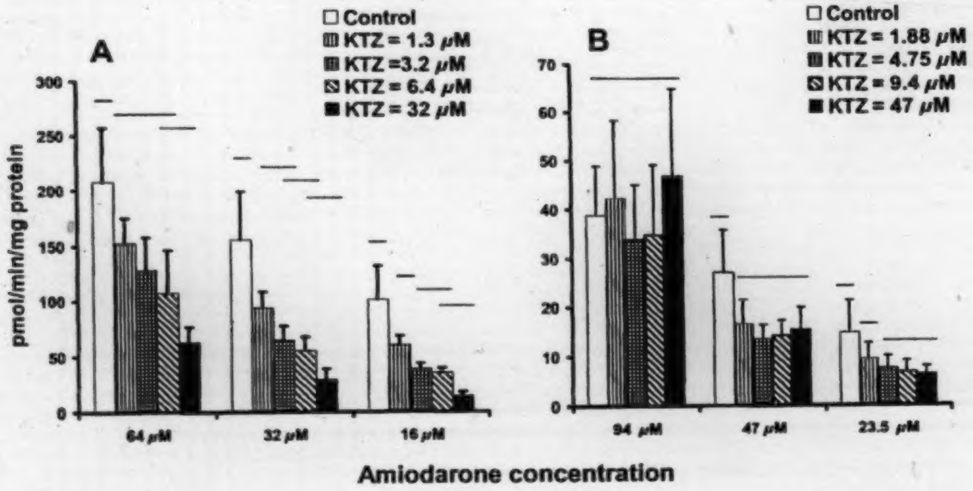

Figure 52: Effect of increasing concentrations of ketoconazole on DEA formation (y-axis) in the presence of three concentrations of AM. A. Liver microsomes, B. Intestinal microsomes. Breaks between horizontal lines above data bars denote significant differences from other data at the same concentration of AM (Duncan's multiple range post-hoc test)

e) Inhibition constant

The inhibition constant, ki, was determined by the use of Dixon plot analysis in the liver microsomes (Figure 53). The one-enzyme model did not fit well to the inhibition data; thus, a two-enzyme model was used, with involvement of a high-affinity and a low-affinity enzyme (*Eq*=3). This model provided an optimal fit to the data and was used to estimate the ki for the inhibition of DEA by KTZ (Figure 53). Based on this two-enzyme kinetic model, ki was determined to be 2.74 ± 3.50 μM KTZ (range, 0.391–7.94 μM) (Table 26). This analysis was not possible in intestinal microsomes due to the poor quality of the fit of the model to the data.

Table 26: Determination of kinetic parameters in rat liver microsomes based on fitting data on a two enzyme model

Parameter	Liver 1	Liver 2	Liver 3	Liver 4	Mean±SD
Vmax1 (pmol/min/mg protein)	308	231	144	332	254±85.1
Km1 (μM)	23.3	22.3	12.0	70.2	31.9±26.0
E2 (μL/min/mg protein)	13.3	10.4	12.0	4.74	10.1±3.75
Ki (μM)	1.22	0.391	1.39	7.94	2.74±3.50

E2 denotes the intrinsic clearance of low affinity enzyme.

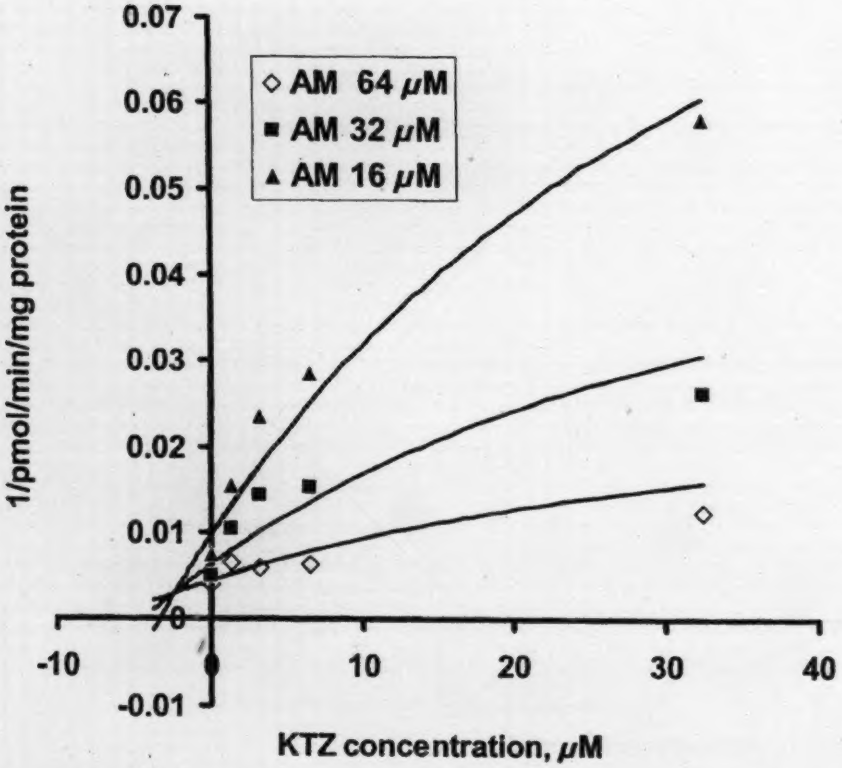

Figure 53: Determination of ki in rat liver microsomes by Dixon plot. Data were fitted to a two enzyme model with results of model fits being represented by the solid lines

f) Immunoinhibition studies

Anti-CYP1A2, CYP3A2, CYP2B1/2 antibodies were employed to better identify the CYP enzymes involved in the metabolism of AM in liver and intestine microsomes. No significant differences were observed in the formation of DEA with CYP1A2 and CYP2B1/2 antibodies in both liver and intestine microsomes (Figure 54). However, the formation of DEA was significantly decreased in using anti-CYP3A2 in liver, but not intestinal microsomes.

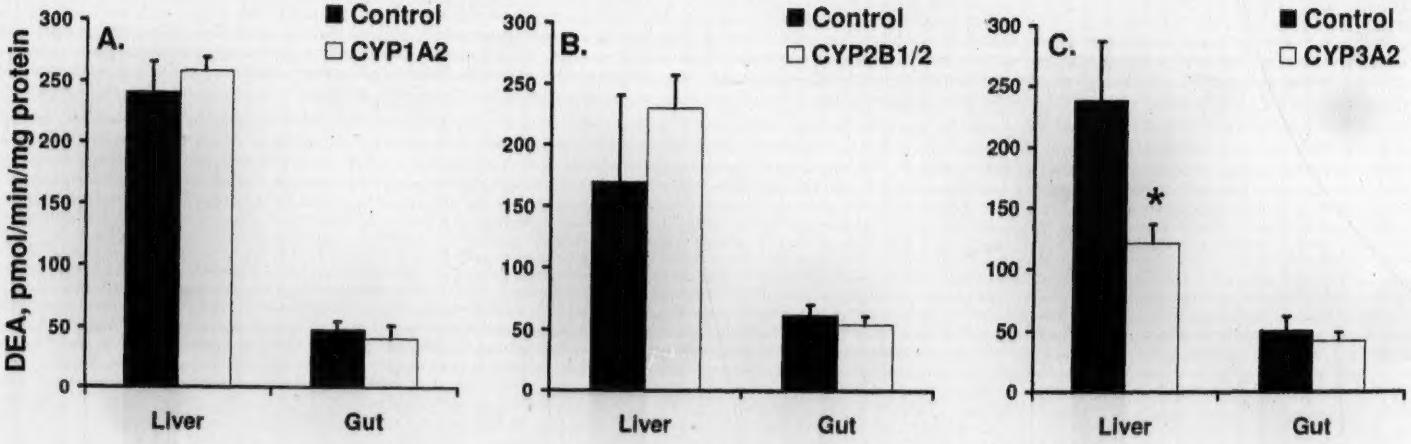

Figure 54: Immunoinhibition studies in liver and intestinal (gut) microsomal protein (0.4 mg/ml) coincubated with amiodarone (64 and 94 μM for liver and intestine respectively) and antibodies to either A.) CYP1A2; B.) CYP2B1/2 or C.) CYP3A2. Matching control incubations without antibody are shown

*Denotes significant difference from corresponding control incubation

When AM was incubated in the presence of rat CYP1A1 and CYP3A1 supersomes, DEA was observed to be formed in both cases (Figure 55). In addition, when KTZ (18.8 μM) was added, significant decreases were observed in the formation rate of DEA.

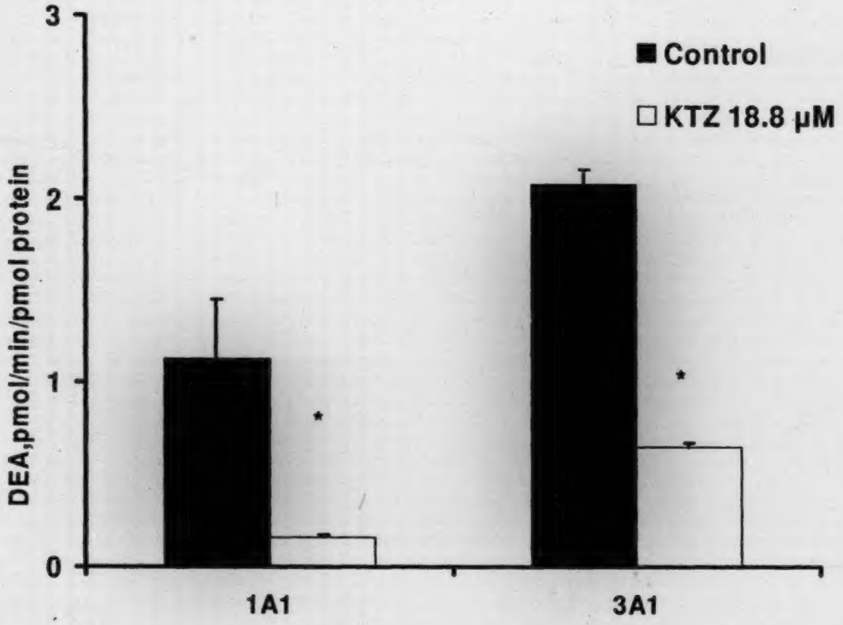

Figure 55: Formation of DEA from 37.6 μM AM in the presence of CYP1A1 or CYP3A1 Supersomes, in the absence (control) and presence of 18.8 μM KTZ. Asterisks denote significant difference from corresponding control incubation

2.3.6.2 Part 2- Effect of hyperlipidemia on the hepatic metabolism of AM to DEA

The total CYP was significantly lower in microsomal protein from HL (0.407±0.0883) than NL (0.788± 0.183 nmol/mg protein) livers (Figure 56). In liver microsomes of both NL and HL rats, as AM concentrations increased, there were increases in the formation rates of DEA. The kinetic profile of DEA formation vs. concentration conformed well to the sigmoidal Michaelis-Menten model with one enzyme (Tables 27-30, Figures 57, 60A). Eadie-Hofstee plots of both NL and HL data displayed convexity suggesting sigmoidal kinetics (Figure 58, 60B). The fit of the sigmoidal model to the data was improved over the simple non-sigmoidal model, and the two enzyme Hill equation. The CLmax was therefore estimated by plotting the data in clearance plot as depicted in Figure 59, 59C.

The estimated km, Vmax, and clearance maximum (CLmax) were determined in each of the liver microsomal specimens (Table 31). There are apparent higher rates of DEA formation in NL than in HL (Figure 57, 59A). There were no significant differences discernable between the km and the Vmax of NL and HL rat hepatic microsomes (Table 31). There was a higher degree of variability in the estimated Vmax and in particular km in HL compared to NL. In contrast, for CLmax the variability was the same for both NL and HL, and the difference was significant between them, with NL being greater than HL (1.46-fold).

When P-407 was added directly (5 mg/ml) to the microsomal incubates, there was no significant impact on the formation of DEA from AM. The formation rates were 91.3±9.82 and 89.4±10.4 pmol/min/mg protein in the absence and presence of P-407, respectively.

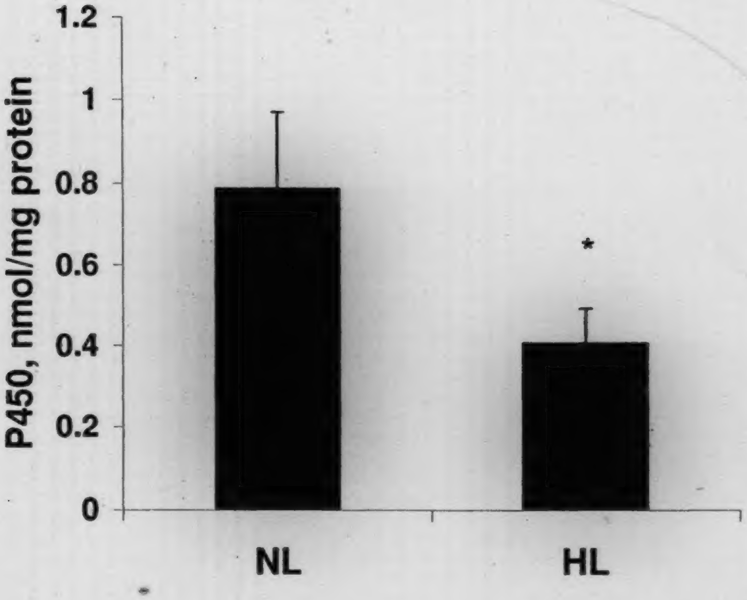

Figure 56: Comparison the levels of total P450 in normolipidemic and hyperlipidemic rat liver microsomes. Asterisks denotes the significant difference between two groups ($P<0.05$)

Table 27: Rate of In vitro metabolism of AM to DEA in four individual rat normolipidemic (NL) livers (Real data)

Liver 1		Liver 2		Liver 3		Liver 4		Mean±SD	
AM+DEA (µM)	DEA (pmol/min/ mg protein)	AM+DEA (µM)	DEA (pmol/min/ mg protein)	AM+DEA (µM)	DEA (pmol/min/ mg protein)	AM+DEA (µM)	DEA (pmol/min/ mg protein)	AM+DEA (µM)	DEA(pmol/min/ mg protein)
220	216	244	278	256	377	296	350	254	305±72.6
204	211	187	221	181	293	197	244	192	242±36.4
115	178	116	219	113	308	115	235	115	235±54.0
103	163	105	238	101	263	101	211	102	218±43.0
79.6	116	97.2	183	85.4	174	72.8	160	83.8	158±29.7
67.5	101	63.1	129	69.3	159	56.3	91.0	64.1	120±30.5
36.7	57.5	36.1	72.6	37.1	87.6	36.3	73.2	36.6	72.7±12.3
14.7	24.1	17.5	37.3	17.1	35.2	20.5	40.6	17.5	34.3±7.16
3.20	3.99	3.34	5.56	3.65	4.78	3.55	5.66	3.43	5.00±0.781
0.674	0.625	0.891	1.01	0.697	0.925	1.09	1.15	0.838	0.928±0.223
0.142	0.125	0.209	0.258	0.307	0.325	0.212	0.339	0.218	0.261±0.098

Table 28: Rate of In vitro metabolism of AM to DEA in four individual normolipidemic (NL) rat livers (Fitted data)

Liver 1		Liver 2		Liver 3		Liver 4		Mean±SD	
AM+DEA (μM)	DEA (pmol/min/ mg protein)	AM+DEA (μM)	DEA (pmol/min/ mg protein)	AM+DEA (μM)	DEA (pmol/min/ mg protein)	AM+DEA (μM)	DEA (pmol/min/ mg protein)	AM+DEA (μM)	DEA(pmol/min/ mg protein)
220	225	244	276	256	376	296	331	254	302±65.8
204	218	187	254	181	331	197	288	192	273±48.2
115	161	116	210	113	256	115	214	115	210±38.7
103	150	105	198	101	236	101	195	102	195±35.1
79.6	124	97.2	190	85.4	207	72.8	150	83.8	168±37.7
67.5	108	63.1	139	69.3	173	56.3	117	64.1	134±28.6
36.7	61.0	36.1	81.6	37.1	88.4	36.3	73.5	36.6	76.2±11.8
14.7	22.1	17.5	34.7	17.1	32.7	20.5	36.8	17.5	31.6±6.52
3.20	3.42	3.34	3.62	3.65	3.63	3.55	3.49	3.43	3.54±0.102
0.674	0.484	0.891	0.559	0.697	0.363	1.09	0.679	0.838	0.541±0.149
0.142	0.068	0.209	0.0709	0.307	0105	0.212	0.070	0.218	0.078±0.018

Table 29: Rate of In vitro metabolism of AM to DEA in four individual hyperlipidemic (HL) rat livers (Real data)

Liver 1		Liver 2		Liver 3		Liver 4		Mean±SD	
AM+DEA (µM)	DEA (pmol/min/ mg protein)	AM+DEA (µM)	DEA (pmol/min/ mg protein)	AM+DEA (µM)	DEA (pmol/min/ mg protein)	AM+DEA (µM)	DEA (pmol/min/ mg protein)	AM+DEA (µM)	DEA(pmol/min/ mg protein)
235	181	229	174	271	195	227	215	240	191±18.0
189	183	200	1781	216	184	174	176	194	180±4.0
98.5	96.7	147	169	118	124	107	172	118	140±36.6
96.9	116	103	171	100	134	95.6	128	98.9	137±24.0
94.5	100	98.7	127	97.4	146	92.6	127	95.8	125±18.7
73.7	72.3	83.9	99.7	79.4	104	72.9	103	77.5	94.5±14.9
33.8	37.3	40	54.1	64.7	92.8	40.0	63.6	44.6	61.9±23.3
17.3	20.3	16.9	24.5	19.7	26.9	22.9	40.2	19.2	28.0±8.60
3.91	4.15	5.76	7.70	5.63	7.06	4.14	6.32	4.86	6.31±1.54
0.911	0.716	1.48	1.46	3.41	3.37	1.32	1.89	1.78	1.86±1.12
0.273	0.223	0.331	0.353	0.272	0.278	0.311	0.432	0.297	0.321±0.091

Table 30: Rate of In vitro metabolism of AM to DEA in four individual hyperlipidemic (HL) rat livers (Fitted data)

Liver 1		Liver 2		Liver 3		Liver 4		Mean±SD	
AM+DEA (µM)	DEA (pmol/min/ mg protein)	AM+DEA (µM)	DEA (pmol/min/ mg protein)	AM+DEA (µM)	DEA (pmol/min/ mg protein)	AM+DEA (µM)	DEA (pmol/min/ mg protein)	AM+DEA (µM)	DEA(pmol/min/ mg protein)
235	194	229	190	271	197	227	213	240	198±10.0
189	169	200	182	216	184	174	189	194	181±8.39
98.5	104	147	161	118	141	107	144	118	138±24.2
96.9	102	103	138	100	128	95.6	133	98.9	126±16.0
94.5	100	98.7	132	97.4	126	92.6	131	95.8	122±14.9
73.7	80.9	83.9	120	79.4	109	72.9	110	77.5	105±16.9
33.8	38.4	40	64.5	64.7	93.7	40.0	66.7	44.6	65.8±22.6
17.3	19.2	16.9	23.4	19.7	28.4	22.9	39.0	19.2	27.5±8.55
3.91	3.83	5.76	5.57	5.63	6.14	4.14	6.27	4.86	5.45±1.13
0.911	0.766	1.48	0.825	3.41	3.30	1.32	1.77	1.78	1.66±1.18
0.273	0.201	0.331	0.093	0.272	0.122	0.311	0.344	0.297	0.190±0.112

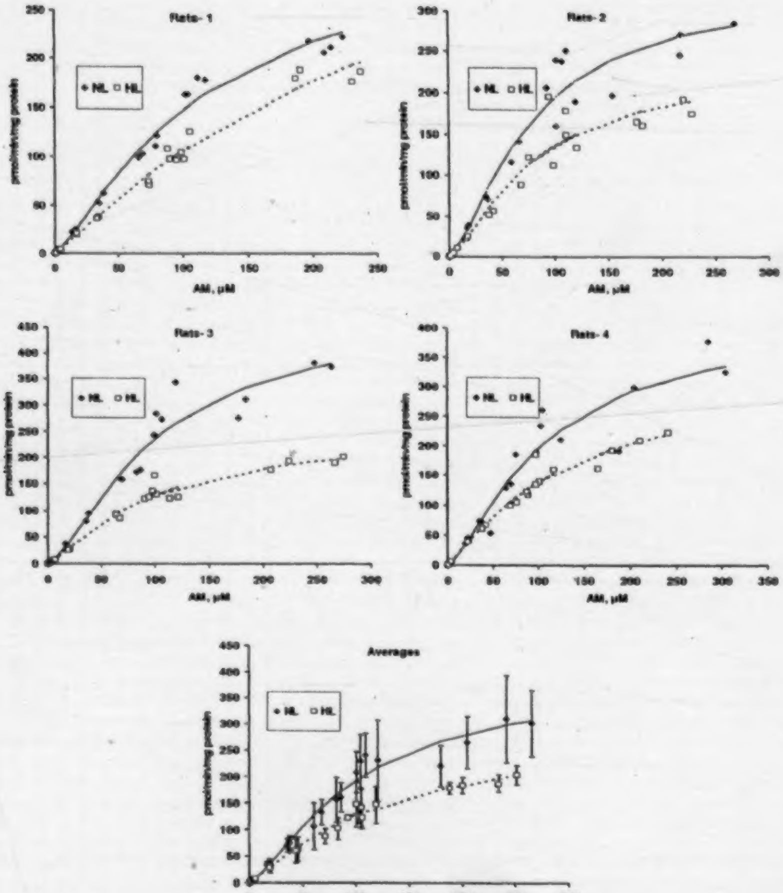

Figure 57: Michaelis-Menten plots (single liver microsomes) in the formation of desethylamiodarone from amiodarone (AM) in normolipidemic (NL) and hyperlipidemic (HL) liver microsomes of Sprague- Dawley rat (Fitted data)

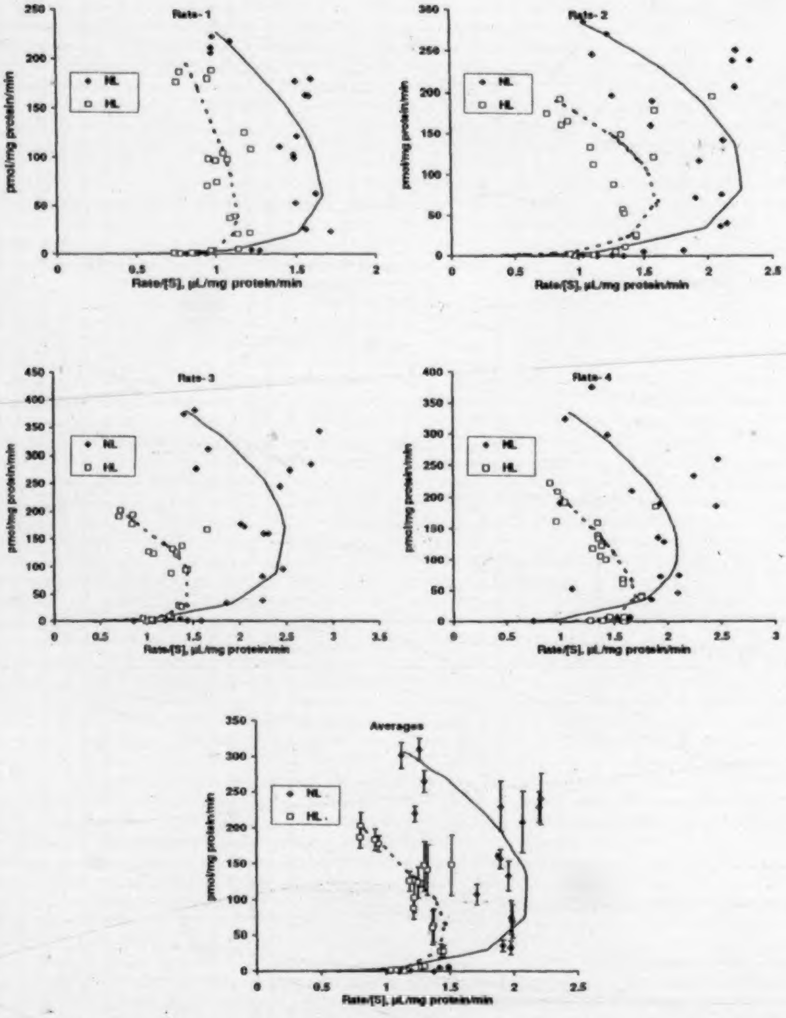

Figure 58: Eadie-Hofstee plots (single liver microsomes) in the formation of desethylamiodarone from amiodarone (AM) in normolipidemic (NL) and hyperlipidemic (HL) liver microsomes of Sprague- Dawley rat (Fitted data)

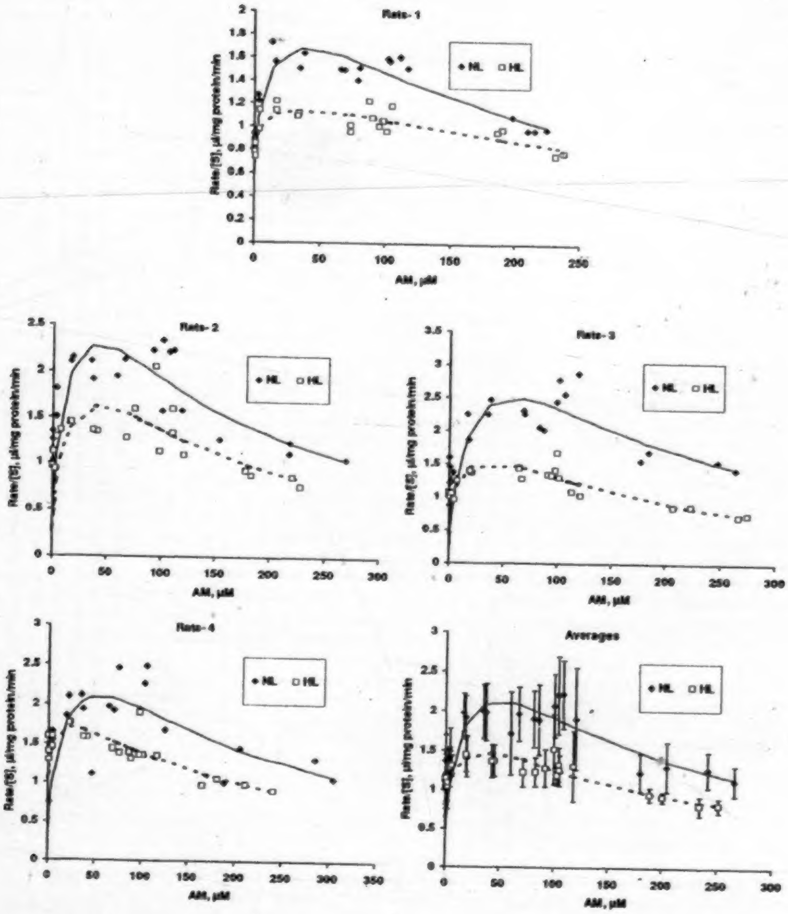

Figure 59: Clearance plots (single liver microsomes) in the formation of desethylamiodarone from amiodarone (AM) in normolipidemic (NL) and hyperlipidemic (HL) liver microsomes of Sprague- Dawley rat (Fitted data)

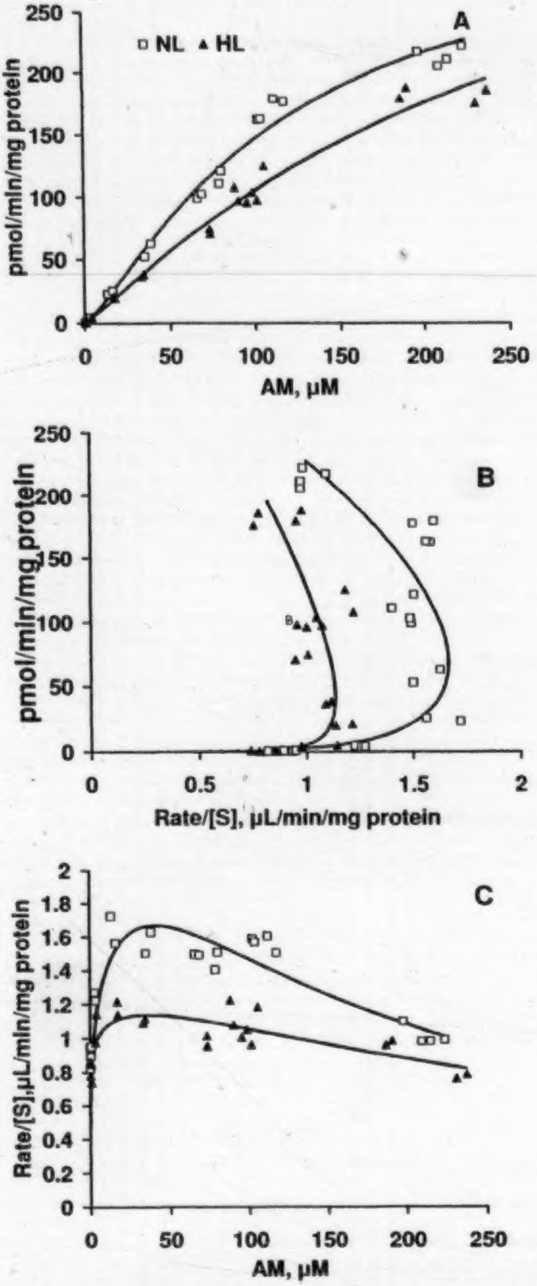

Figure 60: Representative Michaelis-Menthen (A), Eadie-Hofstee (B) and clearance (C) plots in formation of desethylamiodarone from amiodarone (AM) in normolipidemic (NL) and hyperlipidemic (HL) liver microsomes of Sprague- Dawley rat

Table 31: Enzyme kinetic parameters for desethylamiodarone formation by rat NL and HL liver microsomes from four individual rats, based on results of fitting of data

	Km (μM)	Vmax (pmol/min/mg protein)	CLmax (μl/min/mg protein)
NL			
Liver- 1	118	327	1.66
Liver- 2	79.7	333	2.59
Liver- 3	101	473	2.49
Liver- 4	109	415	2.08
Mean±SD	102±16.3	387±69.8	2.12±0.349
HL			
Liver- 1	266	417	1.14
Liver- 2	77.0	230	1.61
Liver- 3	94.3	247	1.45
Liver- 4	136	332	1.71
Mean±SD	143±85.3	306±86.1	1.48±0.251*

Asterisks represents significant differences between the NL and HL (Student's unpaired t-test, $p<0.05$)

2.3.7 Western blot analysis

Expression of CYP2C11, CYP3A1 and CYP3A2 were significantly decreased in the hepatic microsomes of HL rats (39.6, 51.9 and 38.4 % reductions, respectively) when compared with NL rats. On the other hand the expression of CYP1A2, CYP2B1/2 and CYP2C6 and CYP2D1 did not change (Figure 61).

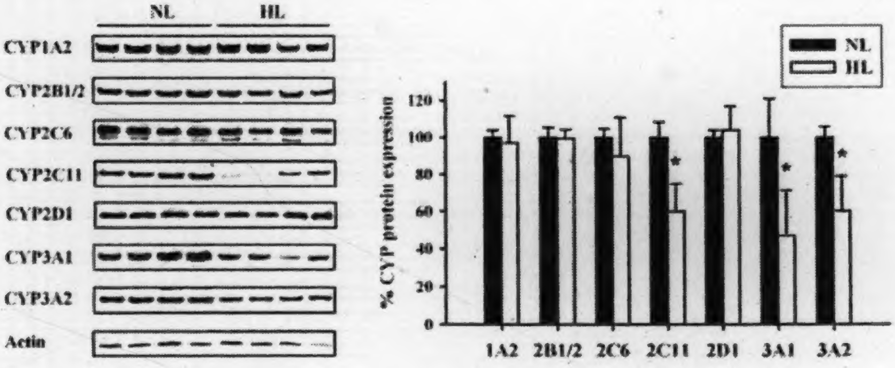

Figure 61: The effect of hyperlipidemia (HL) on expression of different P450 enzymes in Sprague- Dawley rat liver microsomes shown by Western blot.

* denotes significant difference compared to normolipidemic liver microsomes

3 DISCUSSION AND CONCLUSION

3.1 *Discussion*

3.1.1 A liquid chromatography-mass spectrometry assay method for simultaneous determination of amiodarone and desethylamiodarone in rat specimens

The method was capable of measuring concentrations of AM and DEA in rat plasma at much lower levels than previously possible using conventional HPLC-UV methods [323]. The method was specific and highly sensitive, and was validated to plasma concentrations of 2.5 ng/ml for both drug and metabolite, based on 100 μL of rat plasma. This represented a 14-fold increase in sensitivity compared to our own HPLC/UV assay method for assay of drug in rat plasma, in which the lower limit of quantitation was validated at 35 ng/ml based on 0.1 ml of plasma [323]. The sensitivity was sufficient to follow plasma concentrations of AM and DEA for 144 and 48 h, respectively, after i.v. administration of AM to a rat.

Although the developed method is clearly preferable to conventional HPLC-UV methods, there are other available methods utilizing mass spectrometric detection (Table 32). Each of the methods affords high sensitivity and specificity. However, it is of note that none of the LC/MS-MS assays reported using specimen (plasma) volumes of less than 1 ml. A volume of this size is inappropriate for assay of samples from small rodents involved in non-terminal pharmacokinetic studies with serial blood sampling. Furthermore, although LC/MS-MS should be more sensitive than LC/MS, because of the large volumes of specimen required (Table 32), in fact the current LC/MS method using 0.1 ml of plasma has at least a similar sensitivity based on the validated LLQ. The current method uses liquid-liquid extraction rather than solid-phase extraction which, depending on preference and time requirement, may or may not be an advantage to our method [334]. To our knowledge, the current method is the only one using LC/MS methodology, which is not as expensive to acquire as LC/MS-MS instrumentation.

Table 32: Available methods for determination of amiodarone (AM) and desethylamiodarone (DEA) in biological fluids, using mass detection

Species	Matrix	Volume	LLQ(AM)	LLQ(DEA)	Method	Reference
Human	Plasma	1.0 ml	3 ng/ml	3 ng/ml	LC/MS-MS	[296]
Human	Plasma	1.0 ml	1 ng/ml	0.5 ng/ml	LC/MS-MS	[295]
Horse	Plasma	1.0 ml	5 ng/ml	5 ng/ml	LC/MS-MS	[335]
Rat	Plasma	0.1 ml	2.5 ng/ml	2.5 ng/ml	LC/MS	Current method

As noted above, the circulating level of DEA in plasma of rats is reported to be lower than what is observed in human [294, 336, 337]. These discrepancies reflect the interspecies differences between the pharmacokinetics of AM and DEA in humans and rats. The low DEA:AM ratio of concentrations in rat plasma might be related to a higher volume of distribution, higher clearance or lower formation rate in rat compared to human. Nevertheless, the previously reported HPLC/UV method presented a major limitation in the characterization of DEA pharmacokinetics after administration of AM. Although several HPLC assays [338, 339] as well as capillary electrophoresis methods [340] are available for the measurement of both AM and DEA in plasma, the requirement for high volumes of plasma (0.5-1 ml) are limiting factors for their use in the rat. The current assay affords the ability to measure the drug and metabolite in rat plasma using small sample volumes.

After administration of AM to rats and assay of plasma samples, the eluted peaks representing AM, DEA and IS were all found to be free of interference. There did not appear to be a lag time for the appearance of the metabolite in the plasma, suggesting rapid uptake into the eliminating organs with metabolism. The obtained $AUC_{0\text{-}144h}$ for AM after the administration of a 25 mg/kg iv bolus dose in this study is comparable with that of the conventional HPLC method developed by Jun and Brocks [323].

The measurement of AM and DEA in rat tissues is another application of the current method. Although the concentrations of AM and DEA in most tissues exceeded those in plasma, and their measurement in some tissues are feasible by the HPLC-UV detection [297], it was observed that use of the HPLC/UV method for assay of drug in some tissues (e.g. liver) was associated with co-elution of endogenous components, which could prove to be problematic. The LC/MS method was able to measure tissue concentrations of 5 ng/g for both AM and DEA. However due to the high concentrations of both drug and metabolite in tissues in comparison with plasma, the necessity of exceeding a sensitivity limit of 2.5 ng/g was not critical.

3.1.2 Pharmacokinetics of Amiodarone in Hyperlipidemic and High Fat Meal Simulated Rat Models

Poloxamer 407, a hydrophilic non-ionic surface active agent, has been shown to cause significant elevation in plasma cholesterol and triglycerides in various rodent models, including rat [341]. It has been demonstrated that poloxamer 407 exerts its actions by inhibiting plasma lipoprotein lipase and probably cholesterol 7α-hydroxylase [341]. In the present study, the pharmacokinetics of AM in rats were markedly affected by the large increases in plasma lipoprotein levels induced by P-407 [259, 341-343]. Notable decreases in CL and Vdss, and increases in AUC were observed (Table 8). It is likely that this increase in plasma concentrations was attributable to a change in the unbound fraction of the drug, which was observed to decrease by 25-fold in P-407 plasma. Changes of this magnitude in the P-407 hyperlipidemic rat model have been observed for the enantiomers of halofantrine [132]. After administration of oral lipid to the rats, the changes were not as great as those observed in P-407-treated animals. Nevertheless, a significant change in CL was detected between the oral lipid-fed and fasted groups (Table 8). A significant increase was also observed in the AUC compared with fasted normolipidemic rats in a direct 2-way comparison. These were the expected results on CL and AUC if the oral lipid were to cause an increase in the fraction bound to chylomicrons and VLDL. Similar to these results, similar changes were previously observed in halofantrine pharmacokinetics in rats administered single oral doses of peanut oil [132].

Oral consumption of lipid caused significant increases in AUC_{0_24} (2.1-fold) and AUC_{0_∞} (1.8- fold) of orally administered AM compared with fasted rats (Table 8). The increase in Cmax was also significant (2.7-fold; Table 8). Quantitatively, these findings in rats were very similar to those seen in humans given AM in the presence and absence of a high fat meal [142]. In human studies, the AUC and Cmax of AM were observed to be 2.4- and 3.8-fold higher, respectively, in the fed compared with the fasted state [142]. These increases in exposure of the animals to AM are probably best explained by an increase in the delivery of the drug to the blood circulation, secondary to an increase in the solubility of the drug in the gastrointestinal tract. In humans, after food ingestion, bile output and luminal concentration of bile components peak within 30 min in the proximal small intestine, due to constriction of the gall bladder [142]. The net effect is an increase in micellization of lipophilic drugs in the duodenum, an increase in solubility and ultimately oral bioavailability. In rats there is no gall bladder, and the flow of bile into the duodenum from the common bile duct is continuous. This raises the question; why does rat behave so similarly to humans with respect to the effect of lipid on the bioavailability of amiodarone and halofantrine? Although the bile flow is continuous in rat, it is known that in fasted rats both bile flow and rate of excretion of bile acids into the intestinal tract is diminished [344]. Further, ingestion of food is known to stimulate the rate of bile flow into the duodenum [325]. In addition to an increase in bile flow, food components (glucose or triglyceride) infused intraduodenally cause an increase in biliary output of bile acid and PC in the rat [326], as is the case in humans upon contraction of the gall bladder. To our knowledge, however, there are no data available that have been focused on the output of bile and its composition following a bolus of lipid, as was performed in our study.

It has been demonstrated that in the postprandial state, failure to take into account the decreased CL of halofantrine can result in an overestimate of the impact of a high fat meal on the increase in bioavailability [132]. In a typical food effect study, the dose normalized oral AUC after food is compared with that in the fasted state. The AUC of i.v. administered drug in the fasted and fed states is not usually available from the same study subjects. The impact of not having the i.v. data can be simulated using our results. If the F were determined as in a typical study, the oral fed AUC would be divided by the fasted AUC. Using the AUC_{0_∞} data (Table 8), the relative bioavailability was calculated to be 1.83-fold higher in the fed rats. However, the actual increase in bioavailability in the fed state is calculated as absolute F_{fed} divided by absolute F_{fasted}, which from our results show only a 1.31- fold higher extent of AM absorption after lipid. Thus, the effect of food on oral bioavailability in the absence of the appropriate AUC data after i.v. doses would be overestimated by 40%.

The hepatic extraction ratio of AM was calculated using the average value of hepatic blood flow in 250 g rats [345] and the CL of drug in our rats calculated after i.v. doses (Table 8). Assuming complete metabolism by the liver, significant differences in extraction ratio were determined between the fasted (0.72±0.24), oral lipid-fed (0.47±0.14) and hyperlipidemic rats (0.062±0.023). The estimated extraction ratio in the fasted animals was higher than that directly found (0.49±0.013) in studies involving isolated perfused rat liver [287], which suggests the involvement of extrahepatic elimination in the rat after administration of AM. This study tried to characterize the complete profile of DEA but the concentrations were in many cases below the lower limit of quantitation of the assay. This may indicate a more rapid CL or perhaps a more extensive Vdss of the formed metabolite, compared with the parent drug. It is also possible that in the rat, DEA is formed to a lesser extent than in human. Wyss et al. had reported a similar finding to ours, in that concentrations of DEA (expressed as radioactive equivalents) measured after i.v. doses of 50 mg/ kg AM were much lower in plasma than parent drug [337]. Recently it was shown that not only DEA, but also a hydroxylated benzofuran metabolite, is formed in the rat after administration of AM [346].

3.1.3 Determination of the enzyme (s) involved in the metabolism of amiodarone in rat liver and intestine of rat: The contribution of Cytochrome P450 3A isoforms

The role of P450 in the biotransformation of AM to DEA and its first-pass elimination in different tissues such as liver, kidney, intestine, and lung has attracted attention [288, 297]. In the present study, the role of hepatic and intestinal microsomes in biotransformation of AM to DEA was attempted. The study findings demonstrated a considerable difference between rat liver and intestinal microsomes in their ability to metabolize AM to DEA. Over the range of concentrations studied, liver microsomal protein showed a consistently higher rate of metabolism than intestinal microsomes (Figure 49). Kinetic constants could be reasonably derived for the metabolism of AM in liver using the single enzyme Michaelis-Menten model, but this was not the case for intestinal microsomes. However, it was of note that in liver microsomes, there appeared to be some deviation from the model with the highest mean concentration, and in three of the four livers, Eadie-Hofstee plots [347] suggested the possibility of more than one enzyme being involved in liver formation of DEA. Given the linearity over the range of concentrations studied in intestinal microsomes (Figure 49), it appears that the enzymes involved in metabolism of AM to DEA in intestine have a markedly lower affinity for AM than those in liver. This implied that there were tissue-specific enzymes involved in the formation of DEA. To our knowledge, there are no available reports describing the metabolism by human intestinal microsomes for comparison with our rat data.

In microsomes isolated from human livers, it has been reported that the mean *V*max, *k*m, and CLint were 68.7 pmol/min/mg protein, 38.9 μM, and 1.76 μl/min/mg protein, respectively [291]. In comparison, in our study, the *V*max, *k*m and CLint in rat livers were observed to be 5.4-fold, 1.1-fold, and 5.4-fold higher than those values reported for human liver (Table 22). This is consistent with the higher total body CL noted in rats (23 ml/min/kg) (previously observed in our studies) versus humans (range of means: 1.9 to 8.2 ml/min/kg) [283, 348, 349].

Based on the differential findings in the kinetic profiles between liver and intestinal formation of DEA from AM, it appeared there was more than one enzyme involved in the biotransformation, which warranted further study. Guengerich and Shimada (1991) proposed five different in vitro approaches for elucidation of catalytic activities of P450 in human liver [350]. In our study, we selected three of these approaches to better identify the responsible enzymes. These included inhibition by a presumed chemical inhibitor of CYP3A in rat (KTZ), immunoinhibition, and Supersomes.

In liver, as the concentrations of KTZ were increased, there was a progressive decrease observed in the formation rate of DEA irrespective of the concentration of AM initially present (Figure 52A). In intestinal microsomes containing either 23.5 or 47 μM AM, this pattern differed in that there was a decline in rate with a low concentration of KTZ, but with additional amounts of KTZ, there was no perceptible enhancement in the inhibition of DEA formation (Figure 52B). Clearly, there was a difference in the involved P450 enzymes in this biotransformation between these two tissues, suggesting the involvement of different P450s in the formation of DEA from the parent drug, AM.

Although KTZ has been identified to be a selective inhibitor of CYP3A4 in human microsomes [351, 352], it has been reported that in rat, KTZ is not as selective an inhibitor of CYP3A [351]. Use of Dixon plots for determination of ki suggested that there are two P450 enzymes involved in the metabolism of AM in rat liver microsomes (Figure 53). The inhibition data fit well to a two-enzyme model, where one enzyme had high capacity and high affinity, and the second had low capacity and low affinity for AM. Incubation of microsomes with anti-P450 antibodies indicated that in liver, but not intestine, CYP3A2 was involved in the formation of DEA from parent drug. There were no decreases noted in the formation of DEA in the presence of antibodies to CYP1A2 and 2B1/2, respectively, suggesting that these enzymes are not involved in this biotransformation (Figure 54).

CYP1A1 is a metabolic enzyme responsible for chemical activation of xenobiotics to carcinogenic derivatives in some extrahepatic tissues such as lung [353, 354]. Use of

Supersomes established a role for CYP1A1 and CYP3A1 in the formation of DEA (Figure 55). In addition, both of these enzymes were significantly inhibited by the addition of KTZ. The inhibition by KTZ of CYP1A1 was more marked (96%) than that of CYP3A1 (78%). Due to high expression of CYP1A1 and CYP3A1 in rat intestine [312, 352, 355], we can conclude that the aforementioned enzymes are involved in the metabolic biotransformation of AM to DEA in intestine. It is of note that in addition to intestine, CYP1A1 is also an important enzyme found in lung [353, 356]. Furthermore, high expression of CYP1A1, CYP1A2, CYP2B1, CYP3A1, and CYP3A2 has been shown to occur constitutively within small hepatocytes of adult rats. The ability of KTZ to inhibit intestinal CYP1A1 activity in humans has previously been demonstrated [357].

Our previously calculated high extraction ratio of AM reported in rat incorporates both hepatic and extrahepatic elimination in other tissues such as intestine, lung, or kidney. Based on previous reports [337], circulating DEA levels in the rat are much lower than those observed in human [142]. This finding could be due to this pathway being of minor importance in the elimination of AM in the rat. Alternatively, the low concentrations of DEA observed in the rat may be due to a faster CL and perhaps larger *V*d of DEA in comparison to AM. To our knowledge, there are no reports of DEA, CL, or *V*dss in rats after i.v. dosing. To assess the relevance of the in vitro findings, we undertook an in vivo experiment to determine the effect of KTZ inhibition on AM pharmacokinetics.

As previously observed, the concentrations of DEA were near the lower limit of quantitation of the assay in all groups of rats after i.v. and oral administration of AM. Nevertheless, administration of oral KTZ caused significant increases (1.60- fold) in the $AUC_{0-\infty}$ and a decrease (1.56-fold) in CL of AM after i.v. administration of AM (Table 13; Figure 36A). Furthermore, there was an unexpected decrease (2-fold) in the *V*dss of KTZ-treated versus control rats (Table 37). A similar finding has been observed in other studies involving nifedipine, docetaxel, and almotriptan coadministered with KTZ. The concomitant administration of oral KTZ and i.v. 0.5 mg/kg nifedipine to dogs showed 1.83-fold increase in AUC, and 1.73- and 1.2-fold decreases in the CL and *V*dss, respectively [358]. Similarly, coadministration of 12.5 mg of almotriptan, a selective 5-

HT1B/1D agonist, and 400 mg of KTZ to healthy volunteers generated a 44% decrease in the *Vz/F* of almotriptan [359]. In subjects given KTZ (200 mg/day for 3 consecutive days orally) with docetaxel (10 mg/m2), an 18.7% decrease in docetaxel *V*dss was reported [360]. The underlying reasons for these observations have not been addressed. The possibility of a displacement interaction at the level of tissue binding, or an increase in the capacity and/or affinity of binding to plasma proteins, could explain the results.

After oral administration of AM, the effects of KTZ on exposure to AM were greater than those observed after its i.v. administration (Table 13; Figure 36B). Given the demonstrated ability of AM to be metabolized by rat intestine (Figure 49B; Table 22), this is perhaps not surprising. KTZ is recognized as a dual P-gp/CYP3A1 inhibitor [361], and AM is also identified as a substrate of P-gp [297]. In addition to inhibition of intestinal CYP3A1, the additional contribution of inhibition of intestinal CYP1A1 and reduced P-gp-mediated efflux are likely contributors to the increased oral bioavailability after coadministration of AM with KTZ.

3.1.4 The influence of hyperlipoproteinemia on in vitro distribution of amiodarone and desethylamiodarone in human and rat plasma lipoproteins

It is commonly believed that it is the unbound fraction of drug in blood that is pharmacologically relevant, based on the premise that only the unbound drug can transverse cell membranes and reach its intended target for pharmacological activity. The plasma proteins most commonly involved in binding of drugs are albumin and alpha-acid glycoprotein [362]. In comparison, only a small number of drugs are known to significantly incorporate into lipoproteins [363]. However, the association of drugs with lipoproteins may not involve a simple reversible binding phenomenon, as is the case with the other major classes of plasma proteins. This is due to the complex nature of lipoproteins, which are heterogeneous structures comprised of many different types of lipids and proteins [198]. Indeed, one of the unique aspects of lipoproteins is in their inclusion of specific apoproteins that are involved in tissue mediated uptake of drug, which potentially can increase measures of drug action or toxicity beyond that anticipated by the change in unbound fraction. Given that each of the various classes of lipoproteins differs in the nature of the apoproteins involved in cellular recognition of the lipoprotein particle, it is important to understand which lipoprotein fraction a drug associates with. Although prior to this study there was some information in the literature indicating that amiodarone could bind to lipoproteins in plasma [285], this is the first study to evaluate the intraplasma distribution of AM and DEA in lipoprotein fractions, in both NL and HL plasma.

The data indicated that in NL plasma both AM and its major metabolite are taken up by the lipoprotein rich fractions of both rat and human species (Table 17, Figures 45 and 46). For AM, approximately half of the association in NL plasma is with the lipoprotein rich fractions (Figure 45). Of these, HDL has the highest affinity for the drug. The pattern of distribution of DEA was qualitatively similar, with approximately 30 and 50% of metabolite residing, respectively, within the lipoprotein-rich fractions of rat and human. Similar to AM, the association of DEA in the lipoprotein-rich fractions was highest in the HDL fraction in NL plasma.

In the presence of HL plasma, there was a substantial shift of drug and metabolite, apparently mostly from the LPDP fraction to the most apolar of the lipoprotein fractions, TRL, which is particularly rich in chylomicron and very low density lipoproteins (Figure 45). The shift was more dramatic for the rat, but the pattern of change was similar for both species. The reason for the more dramatic change in the HL rat plasma compared to human is possibly due to the larger increases in plasma TG and CHOL in the rat P-407-treated plasma opposed to that seem in the HL human plasma.

This change in the LP association in HL is in line with the changes observed in the pharmacokinetics of the drug in the HL state. In P-407 treated rats, induction of HL caused a major change in the pharmacokinetics of the drug, with significant and substantial decreases being observed in the unbound fraction, clearance and volume of distribution. It was also found that there was a significance increase in AUC of the drug after oral dosing of AM to NL rats concomitantly administered oral lipid, and that part of the increase in AUC was due to a decrease in the clearance of the drug as an apparent consequence of increased lipoprotein binding. In the previous study in rats the chromatographic assay used was not able to characterize the pharmacokinetics of the metabolite in the NL vs. HL state. It was of note that in human, but not rat, that the metabolite to drug ratio stayed relatively constant.

Amiodarone is a drug for which a narrow therapeutic range has been established, and for which therapeutic drug monitoring is warranted [280]. Our findings in conjunction with the previous study in rats might explain part of the variability that might be associated with AM therapy, in that HL patients might also be expected to have higher plasma concentrations of the drug than NL patients given the same dose level. Another aspect of use with AM is the fact that it is associated with changes in lipoprotein levels with chronic use. In particular, it has been shown that HDL plasma concentrations are increased with long term administration of AM [364]. This may be a secondary effect of hypothyroidism, which is a known side effect of treatment with the drug, and which can precipitate changes in lipid metabolism and plasma lipoprotein profile. Interestingly, in NL plasma the lipoprotein fraction with the highest level of affinity for AM and DEA was HDL, which raises the possibility of a change in plasma concentrations of the drug with repeated doses.

3.1.5 The impact of hyperlipidemia on the tissue distribution and hepatic metabolism of amiodarone and its active metabolite desethylamiodarone in the rat

The intraperitoneal injection of a single dose of P-407 to rats (1 g/kg) causes a profound increase in circulating lipoprotein levels by modification of a number of biochemical pathways [365]. In rats treated with P-407, marked changes in the pharmacokinetic parameters of AM have been reported by our lab. Specifically, decreases in unbound fraction (25-fold), CL (12-fold) and Vd (23-fold) were seen, with substantial increases in drug total bound+ unbound plasma concentrations. This increase in plasma protein binding is likely due to an increase in uptake of drug by the triglyceride-rich fractions of plasma (LDL and VLDL).

The current study (Table 14) resulted in similar values of AM plasma AUC from those reported earlier. Based on the results of our previous study, mean unbound fractions of AM in plasma from NL and HL rats were estimated to be 0.147% and 0.00345%, respectively. Based on these estimates, assuming that there is linear binding over the course of the plasma concentration versus time profile, we can estimate that our mean unbound AUC of AM in NL and HL rats are approximately 25 and 4.3 ng·h/ml, respectively, thus representing an approximately 5.75-fold higher unbound AUC in NL versus HL rats. This is a reasonable comparison considering that previously in rats given three oral dose levels (25, 50 and 100 mg/kg/d for 13 days [366] there were increases noted in the mean serum concentrations across the range of doses, suggesting that nonlinear protein binding does not occur. Therefore, in HL, AM might be expected to be associated with across the board decreases in the distribution to the peripheral tissues, given that it possesses a moderate hepatic extraction ratio in rat. Indeed, the volume of distribution of AM was reduced 23-fold in the HL state in line with the change in unbound fraction previously described. Indeed, in brain, kidney, and lung significant decreases in AM uptake were observed in HL. This observation, however, was not uniform in all tissues. In some HL tissues, including the liver, spleen, and notably the target organ for effect of the drug, the heart, AUC were significantly higher. Only fat showed no changes in AUC in HL.

In general, the relative kp of total drug AUC in our study matched well with the values reported previously in NL Sprague-Dawley rats given radiolabeled AM 50 mg/kg iv [337]. In the HL rats, decreases were seen for each of the tissues studied (Table 14), although the kp between tissues differed widely. Such a decrease in kp was previously observed for cyclosporine A in the same P-407 rat model of HL. Although this was not possible for AUC, statistical comparison of kp was possible using the compiled post distributive concentrations, where there is an expectation of constant tissue to plasma concentration ratios. In those comparisons, except for spleen (HL>NL) and brain (NL>HL), there was no significant difference between HL and NL (Figure 40). Given that uptake of drug into tissues is normally dependent to some degree on the plasma unbound fraction, we also calculated the kpu (tissue AUC to unbound plasma concentration). In this case the relative picture changed. In all cases except for brain the kpu was higher for HL than corresponding NL tissues. Similar to the kp, however, the same relative trend in tissue to plasma partitioning was observed. The probablility is high that most of the changes in kp were due to lipoprotein binding, although there may be some component of changes in tissue binding that might have also been reflected in the changes in kp and kpu (Table 32)

Our previous findings indicated that the highest association of AM in HL rat plasma was with the TRL (triglyceride rich lipoproteins) fraction, which is particularly rich in chylomicron (CM) and very low density lipoproteins (VLDL). The association of AM in low density lipoprotein (LDL) was the second highest after the TRL fraction in HL rat plasma. These findings might help explain the high AM AUC in some tissues such as liver, heart and spleen of HL rats. It is known that VLDL receptors mRNA are highly expressed in various tissues. The VLDL receptor mRNA levels in heart are highest, followed by muscle, kidney, adipose tissue, brain and macrophages of adult mouse [367]. In contrast, the mRNA level of VLDL receptors was barely detectable in liver of adult mouse. In neonatal rat liver, however, the expression of VLDL receptor mRNA was about 3-fold higher [367]. In contrast, LDL receptors were found to be abundantly expressed in mammals' liver [368]. Given the increased association of AM with VLDL and LDL, the corollary with the tissue distribution of LDL and VLDL receptors is in line with the observation. The high capacity of bone marrow and spleen macrophages to clear CM particles from the rat blood circulation has been demonstrated [369]. Such a mechanism might have been responsible for increased uptake of AM by spleen in HL.

The effect of HL on the biodistribution of AM in this animal model yielded some interesting differences from another LP-bound drug, cyclosporine A. For AM here it was found that AUC were increased in heart and spleen, but decreased in kidney. These findings were opposite to those seen for cyclosporine A. Only in liver was HL associated with similar relative outcomes (increased AUC compared to NL). It would appear the HL affects pharmacokinetics of lipoprotein bound drugs in a drug-specific manner. It is not possible at this time, given the information available, to provide a definitive explanation for these differences. However, drug-specific alterations in binding to specific lipoprotein classes in HL might be a cause of the differences. For example, it is known what the plasma lipoprotein disposition of AM in P-407 HL plasma is associated with a major shift of drug into VLDL fractions. It is not clear as to what happens to cyclosporine A in this type of HL plasma. In another study the kidney levels of amphotericin B were observed to be substantially higher in obese Zucker rat model in comparison with the control lean rats [220].

Assuming that this model of HL is in line with the situation in HL patients, these finding are of potential significance from a therapeutic perspective. An increased delivery of drug to the heart has the potential to confer a given dose of the drug with greater potency. Also, because the liver is the major site of AM metabolism and effectively elimination of the drug, an increased hepatic delivery might afford AM with a higher CL. The increased hepatic concentrations of AM were in line with the observation that the unbound fraction, which decreased by 25-fold, was changed more than the CL of the drug (8 to 12-fold). It is conceivable that the decrease in the unbound fraction was compensated by an increased delivery of the lipoprotein-bound drug to the liver, where metabolism could proceed at a higher rate.

The possibility of HL-induced changes in the hepatic metabolism of AM to DEA was also assessed. Initially we noted that the formation of DEA from AM was decreased in microsomal protein of HL rats. This was accompanied by a significant decrease in the total CYP activity in microsomal protein. Based on these findings we proceeded with a complete metabolic characterization of the drug using rat hepatic microsomes. We had previously assessed the hepatic microsomal metabolism of amiodarone in rat. Although in the current study we saw a very similar profile to that observed previously, here we had extended the number of incubations and assessed the metabolism over a wider range of AM concentrations. By doing so through kinetic analysis we were able to detect some sigmoidicity in the product velocity vs. substrate concentration curves (Figure 60A) when the one enzyme Hill equation with shape factor was assessed. This was very noticeable in the Eadie-Hofstee plot (Figure 60B). By constructing a clearance plot we were more accurately able to calculate the kinetic parameters for DEA formation.

The kinetic analysis confirmed that there was a lower formation rate of DEA in HL livers. There was a non significant decrease in Vmax in the HL microsomes. However the clearance plot showed that the CLmax in the HL state was significantly lower. This was in line with the reduction in the total CYP measured in the HL microsomes. Recently it was reported that in the Zucker obese rat that there was a significant decrease in the expression of a number of drug metabolizing and transport enzymes [218]. To explore this possibility for the P-407 model of HL, we processed our microsomal protein to examine the expression of some selected hepatic CYP isoenzymes, some of which were known in rat to be involved in DEA formation. The results of the Western blot analysis indicated that HL either suppresses expression or increases the rate of enzyme turnovers of CYP2C11, CYP3A1 and CYP3A2. The involvement of CYP1A, CYP3A1, CYP3A2 in the metabolism of AM to DEA in hepatic microsomes of rat is known from our previous research. In our previous study it appeared that CYP1B1/2 was not involved in DEA formation. In rat it is not known as to the extent of involvement of CYP2C and

CYP2D isoenzymes in DEA formation, although it is known that in humans CYP2C isoenzymes are involved [370]. Further examination of CYP-mediated involvement in DEA formation in rat is warranted. Although there was some decrease in the effective intrinsic CL (CLmax) of AM to DEA, there was a 2.5-fold higher uptake of AM to the liver (Table 14) which was higher than the decrease observed in CLmax (32%). This may help explain the significant increase of DEA in the plasma, the higher mean DEA/AM ratio in plasma, and the high concentrations of DEA present in the liver (Table 14).

Despite the resemblance in the trend of lipoprotein association for AM and DEA in HL rats, there were some notable discrepancies between AM and DEA in their uptake in different tissues of HL rats. In plasma, similar to AM, the DEA AUC was significantly and substantially increased in the HL rats. However, there were significantly lower DEA AUC (Table 14) and postdistributive Kp (Table 14 and Figure 40), and DEA:AM ratio (Figure 41) in spleen, lung and kidney of HL rats compared with the NL animals. This trend was opposite of parent drug for spleen and lung, where increases were observed in HL. Except for the anticipated decrease in unbound fraction in HL, we cannot provide other possible explanations for the decreases of DEA in these tissues. In brain, liver, heart and fat there was no effect of HL on exposure to DEA.

Table 32: The tissue to plasma partition coefficients. The kp represents the partitioning based on total plasma concentrations. The AUC of unbound AM was calculated using unbound fractions of AM in NL and HL rats as previously reported. The kpu represents the tissue to unbound plasma AUC ratios. Parentheses depict the HL:NL ratios of partition coefficient.

	Plasma	Brain	Heart	Kidney	Liver	Lung	Fat	Spleen
	AUC, μg·h/ml	Kp						
NL								
AM total drug	16.7	10.9	8.74	34.6	18.7	55.3	13.3	36.3
AM unbound drug	0.0245	7429	5959	23551	12776	37714	9061	24776
DEA	0.728	6.48	44.8	103.4	45.3	218	7.25	71.3
HL								
AM total drug	134 (8.02)	0.0851 (0.00781)	2.08 (0.238)	2.16 (0.0624)	5.87 (0.314)	3.57 (0.0646)	1.89 (0.142)	25.2 (0.694)
AM unbound drug	0.00462 (0.189)	2466 (0.333)	60350 (10.1)	62514 (2.66)	170020 (13.3)	103396 (2.75)	54726 (6.05)	729613 (29.5)
DEA	17.0 (23)	0.676 (0.097))	1.02 (0.023)	1.46 (0.014)	3.66 (0.081)	4.85 (0.022)	0.476 (0.066))	0.0906 (0.0013)

3.1.6 The impact of lipids on the intestinal metabolism of amiodarone to desethylamiodarone in the rat

The in vitro everted rat gut sac model has been successfully used in the characterization of intestinal metabolism of many drugs including testosterone [371], bupropion [372], midazolam [373] and dextromethorphan [374]. The employment of such a method in conjunction with microsomal intestinal metabolism could help to elucidate the role of the intestine in the first pass metabolism of drugs.

Previously it was demonstrated that DEA could be formed from microsomal protein isolated from the intestinal tract of rat. The present results further demonstrated that in an intact tissue environment, AM could be directly metabolized to DEA. This left open the possibility that the intestinal tract plays a role in the first pass metabolism of AM to DEA. Given the observations for halofantrine and AM after ingestion of a high fat meal, we then carried out our experiments investigating the influence of bile components and lipids on this metabolism.

It was found that within intestinal segments, there was little difference in AM or DEA present between the treatment groups (Figure 42 upper panels). Similarly, within treatment group, there was little difference between the concentrations of AM and DEA in the five segments. Although mean values in some cases were much higher for some treatment groups than others, in most of these treatments the variability was high and there were no significant differences noted from other treatments (Figure 42, top panels). The most relevant comparator is the DEA data after normalization to the amount of AM present in the tissues (Figure 43). Some trends and differences became apparent. With respect to comparative DEA:AM ratios within each segment (Figure 43, left panel), in general the highest level of DEA-forming activity was apparent in the KH+5% SBS treatment group, and lowest in the peanut oil-pretreated animals for which gut segments were incubated in KH+25% SBS. This infers that the prior administration of peanut oil causes some inhibition in the ability of the gastrointestinal tract to metabolize AM to DEA. Further, it appears that lower concentrations of causes an increase in metabolizing efficiency compared to no SBS or high concentrations of SBS (Figure 43 left panel). In general, there was little significant difference noted in the intersegment metabolizing efficiency within each treatment group (Figure 43, right panel). This being said, it is of note that for most treatments the most distal segment (G5) seemed to have the lowest level of activity, whereas the mid section (G3) had the highest.

Because of the inter-segment similarities in the uptake of AM and DEA formation (Figure 42 lower panel), we also undertook and analysis of the sum of all five intestinal segments for each treatment (Figure 62). In this case, overall, the control KH incubations had the highest levels of AM and DEA. For the important comparator of DEA: AM, however, it was found that the lowest metabolizing efficiency for DEA formation was in the peanut oil-treated group incubated with KH+25% SBS. The highest level of activity was present in the KH+5% SBS. Both of these findings mirrored those of the segments evaluated separately (Figure 43, left panel).

It was of note that there was no drug or metabolite detected at quantifiable concentrations in the serosal fluids within the everted gut sacs. This is consistent with the large volume of distribution of AM in the rat, which is in excess of 40 L/kg after intravenous doses of 25 mg/kg, indicated by our previous work. The absence of a sink-effect including the influence of extensive plasma protein binding in the closed system represented by the everted gut system was clearly evident. In a previous study it was similarly shown that in Ussing chambers and gastrointestinal tract in which AM was spiked on one side of the membrane the majority of the drug and metabolite were present in the tissue.

There were three KH-25% SBS gut treatments utilized in the experiments. These included pretreatment of the rats with normal diet or simulated high fat meals consisting of 1% cholesterol in peanut oil. The everted guts from rats with normal diet were exposed to KH+25% SBS alone or KH+25% SBS+5% Intralipid (INLP). The peanut oil pretreated everted rat guts were exposed to KH+25% SBS solution. It was found that guts pretreated with 1% cholesterol in peanut oil had the lowest level of measurable DEA forming ability (Figure 44). The lower uptake of AM in the everted guts exposed to KH+25% SBS+5% Intralipid (INLP) can perhaps be attributed to sequestration into mixed micelles, which akin to plasma protein binding, limited the ability of the gut tissue to readily take up the drug. Despite the lower uptake, the DEA:AM ratio was similar to that of KH+25%SBS alone, suggesting that low concentrations of lipid did not alter the metabolizing efficiency of the tissues.

This raises the question as to why peanut oil-pretreatment causes a decrease in metabolizing efficiency within the intestinal tract. It has been observed that high concentrations of plasma lipoproteins can cause a down-regulation of some hepatic CYP isoenzymes. Whether this is true of the intestines remains to be determined. It is known, however, that several fatty acids can inhibit CYP enzymes in different species including human and rat. For instance Hirunpanich et al. [375] examined the inhibitory effect of some saturated fatty acids , monounsaturated fatty acids (MUFA) and polyunsaturated fatty acids (PUFAs) on the formation of 6-β-hydroxytestosterone from testosterone in rat liver microsomes. The results indicated that SFAs had a very weak inhibitory effect on the CYP3A mediated metabolism of testosterone. However, PUFAs (linoleic acid (LA), linolenic acid (LNA), arachidonic acid (AA), eicosapentaenoic acid and docosahexaenoic acid (DHA)) exhibited strong inhibitory effects (SFAs<MUFAs<PUFAs). The presence of strong inhibitory effect of MUFAs and PUFAs on testosterone 6β-hydroxylation suggested that the existence of double bonds of fatty acids is mandatory for CYP3A inhibition [375]. Furthermore it was noted that the inhibitory effect of MUFAs was related to the length of the carbon chain. In this case, the inhibitory effect of linoleic acid (C18) on CYP3A-mediated metabolism of testosterone was more than undecanoic acid (C11) but less than eurucic acid (C22) [375].

In a similar fashion, SFAs had no inhibitory effects on the activities of a number of human CYP isoenzymes (CYP1A2, 2C9, 2C19, 2D6, 2E1 and 3A4) at SFA concentrations up to 200 μM. However all of the PUFAs completely inhibited CYP2C9 (diclofenac 4-hydroxylation) and CYP2C19 (mephenytoin 4-hydroxylation) metabolic reactions. Additionally, these PUFAs competitively inhibited the metabolic reactions catalyzed by CYP1A2 (phenacetin O-deethylation), CYP2E1 (chloroxazone 6-hydroxylation) and CYP3A4 (midazolam 1- hydroxylation) to a lower extent [376]. The main product of the linoleic acid metabolism, AA [377], was also observed to have significant inhibitory effects on the CYP1A1 and 1A2 dependent 7-ethoxycoumarin O-deethylations, CYP2C8 taxol 6α- hydroxylation and CYP2C19 dependent R-warfarin 7-hydroxylation in human liver microsomes at the concentration of 50 μM [378]. Inhibition of CYP through the inhibitory effects of fatty acids was offered as an explanation for the increase in the bioavailabilities of saquinavir and cyclosporine after ingestion of DHA by rats in either liver or gut. Moreover, DHA had no significant effect on the basolateral to apical transport of [^{3}H] CYA in the Caco-2 cell monolayer [379]. Based on the obtained results, the authors in this study concluded that the increase in the bioavailability of CYA after oral administration of drug in the presence of DHA might be due to the inhibition of intestinal metabolism of CYA in the intestinal tract but not due to the increase in the absorption of drug [379].

In our study animals were pretreated with 1% cholesterol in peanut oil. Peanut oil is a strong source of monounsaturated fatty acids (MUFAs) (81%), mostly oleic acid [380]. Furthermore some other SFAs (palmitic acid (16:0), stearic acid (18:0), behenic acid (22:0) and lignoceric acid (24:0)), MSFAs (eicosanoic acid (arachidic acid)(20:1)) and PUFAs (linoleic acid (18:2) and arachidonic acid (20:4)) are also present in varying amounts in different varieties of peanut oil [381]. In rat AM is known to be metabolized by some of the CYP isoforms present in the intestinal tract. Given the known influence of oils on CYP activity and the study results, it would appear that the decrease in metabolism of AM to DEA is caused by inhibition of intestinal CYP.

On the other hand, no significant difference was observed between the intestinal metabolism of AM to DEA in microsomes of control untreated rats and the rats treated with peanut oil. This suggests that peanut oil does not affect the expression of the CYP isoenzymes in the intestinal tract known to be involved in the metabolism of AM (CYP1A1, CYP2B1/2, CYP3A1 and CYP3A2). Had there been a change it should have been reflected in the in vitro microsomal metabolism. When microsomes are prepared, most of the other cellular constituents are removed, including any free fatty acids that might be present in the cells. This perhaps explains the discrepancy between the everted gut preparations and microsomal preparations in their DEA forming ability.

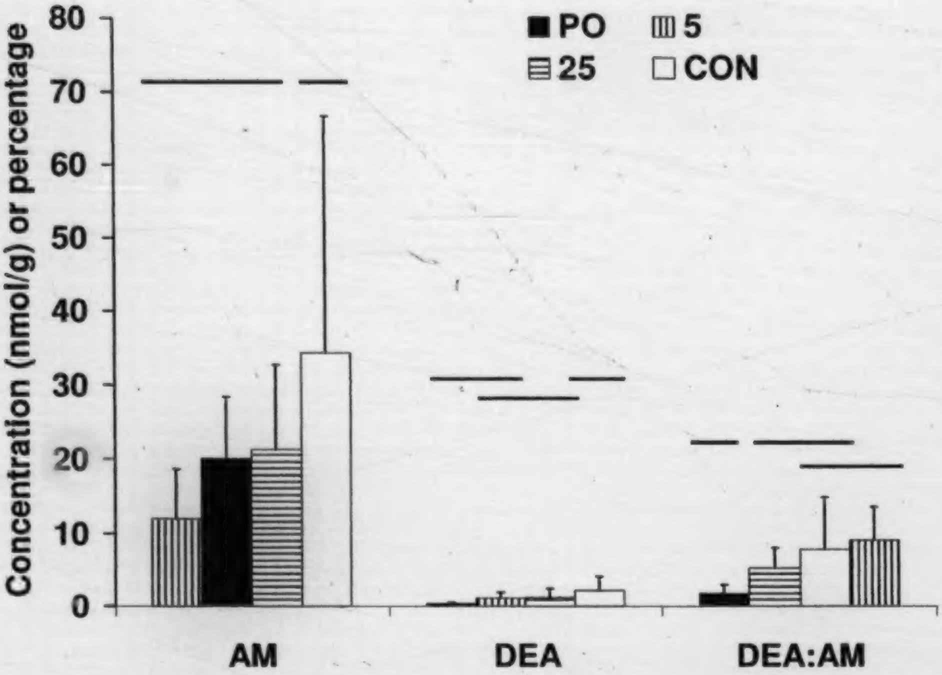

Figure 62: Concentrations of AM, DEA and metabolite:drug ratio when all segments (G1-G5) were combined. Broken lines between groups indicate significant differences. Krebs-Henseleit (CON), 5% SBS in Krebs-Heinseleit (5), 25% SBS in Krebs-Heinseleit (25), 25% SBS in Krebs-Heinseleit in peanut oil rats (PO)

Conclusion

Protein binding is known to alter plasma concentrations of drugs and consequently affect their pharmacokinetic behaviors. Amongst the different protein fractions in plasma, lipoproteins have drawn great attention during the past few years. It has been demonstrated that lipoprotein binding of drugs comprises only a small fraction of the bound drug in plasma, but the pharmacological effects of such binding may be classically important [363, 382].

Lipophilic nature is the first prerequisite criterion for lipoprotein binding of drugs and lipophilic drugs have the natural tendency to bind to lipoproteins (LPs) in plasma [363]. Alteration in LP fractions in plasma following HL, regardless of the reason is known to modify the plasma concentrations and consequently pharmacokinetics of lipophilic drugs [383]. The examination of such effects has been observed in the pharmacokinetics of halofantrine (HF) in the beagle dog model after postprandial state [144]. An increase in the level of LPs in plasma might happen transiently following the ingestion of high fat meal [384] or might be due to the existence of familial hyperlipidemia [385]. The latter is found to be the most predisposing factor in pathogenesis of hyperlipidemia [385].

Hyperlipidemia by itself is also the main reason for altering tissue distribution of lipophilic drugs [386]. Based on the natural tendency of drugs to incorporate into different lipoprotein fractions (VLDL, LDL or HDL) in plasma and the existence of the related receptors (VLDL and LDL receptors) in tissues, the delivery of drugs to different tissues could be determined in hyperlipidemia. Based on this theory, delivery of cyclosporine A in liver tissue was postulated by Aweeka et al. [387].

Oral lipids on the other hand, have been observed to influence the level of CYP450 enzymes [388]. This influence is completely dependent on the kind of oil and the duration of nourishment. The secondary effect of such influence was observed on the alteration in the uptake and metabolism of some drugs in hepatocytes including cyclosporine A [389]. Unfortunately, our knowledge about the mechanistic procedure in this regard in in vivo models is not profound.

The studies in this dissertation were particularly directed toward the measurement of the effects of HL on the pharmacokinetics, tissue distribution, hepatic and intestinal metabolism of AM and partly DEA, in the most prevalent preclinical species, rat.

In these studies, two previously developed rodent models for hyperlipidemia (HL) were used. In the first model, lipoprotein fractions were transiently increased by the ingestion of cholesterol enriched (1%) peanut oil to rats. As the second model, poloxamer 407 (P-407) at the dose of 1 g/kg was intraperitonealy administered to rats. Although the implication of the second model (P-407) seems to be far from the real hyperlipidemic model due its drastic effects on the lipoprotein fractions, the trend of the in vitro association of AM and DEA in both human and rat NL and HL plasma fractions showed close similarity in this regard. Tthe evaluation of the in vitro distribution of AM and DEA in human and rat in different fractions of HL and NL human and rat plasma indicated that in the NL condition most of the parent drug and its primary metabolite were distributed in the LPDP fraction of plasma. A similar trend of drug and metabolite localization in NL plasma was noted for rat and human. The presence of hyperlipidemia caused a major change of AM and DEA from the more polar lipoprotein fractions to the less polar fractions represented by LDL and TRL.

These models were also successfully used for the determination of AM pharmacokinetics in HL. The results indicated that increased levels of lipoproteins due to HL or high fat meal could alter the pharmacokinetics of AM. Based on the in vitro distribution of AM in NL and HL models, the results obtained in in vivo part were quite anticipated.

In terms of tissue distribution, it was noted that tissue distribution of AM was modified in the presence of systemic HL. Surprisingly, it was observed that the increase in plasma concentration of AM in HL did not lead to decreases in all of the tissues. Indeed, the influence of HL on AM tissue distribution was not uniform, but rather tissue-specific.

The changes in DEA tissue AUC as a result of HL were not always in line with those observed for the parent drug. The obtained results show that for lipoprotein-bound drugs such as AM, changes in distribution to tissues in response to HL can be complex.

HL also caused a decrease in the metabolism of AM to DEA in rat liver. The decrease in CLmax was in line with the reduction in selective expression of some of the CYP isoforms known to be involved in the metabolism of AM in the rat. Some of these enzymes were identified by designing a traditional liver and intestinal microsomal study. The obtained results demonstrated that CYP3A1, CYP3A2 and CYP1A1 were quantitatively involved in metabolism of AM to DEA in both liver and intestine of rat species.

It was also found out that some part of the increase in the bioavailability of AM in the presence of oral lipid was attributable to the inhibitory effects of oral lipid on the presystemic metabolism of AM to DEA in intestinal tract, although the significance of this finding is not clear. The results of this study seem to indicate that the fatty acids content of peanut oil competitively interfere with the metabolism of AM in intestinal tissues.

Unfortunately, the time limitation did not provide enough opportunity to identify the other possibilities in the effect of oral fat on the presystemic metabolism of AM to DEA in GIT. One of the possibilities could be a bypass of the first pass metabolism of AM in liver. Due to the special structural features of LPs and their unique metabolic procedure, incorporation of lipophilic drugs with LPs follows the same physiological fates as LPs [159]. For instance, in concomitant use of oral lipophilic drugs with lipids, lipophilic drugs can incorporate into chylomicrons as the first product of lipid metabolism in body. The net result of such a physiological process would be the bypass of drug from first pass metabolism [159].

Future Directions

In order to maximize drug efficacy it is imperative that the effects of various disease states on their pharmacokinetic be understood. Hyperlipidemia (HL) is a prevalent clinical condition and occurs with or causes other cardiovascular diseases. In spite of this, the effect of HL has not been well studied with respect to its effects on the pharmacokinetics, metabolism and efficacy of lipoprotein-bound drugs such as AM. There are some directions that the work undertaken and described here can progress to better understand the effects of HL on drug disposition and effect.

In our studies we found increased uptake of AM in the heart. Hence it would be reasonable to see if there were associated increases in the AM-indiced effects on the electrocardiogram in the same rat model used here. This assessment would be necessary to evaluate either the efficacy or toxicity of AM in heart tissue.

The mechanistic cause of the increased uptake of AM in some tissues including heart in HL should be studied in more detail. The focus would be the roles of the receptors involved in this tissue uptake. Based on our findings, VLDL and LDL receptors might have a significant role in this uptake. The use of knock out rodent VLDL or LDL receptors models might be of use for this purpose.

Based on the contribution of CYP3A4, CYP2C8, CYP1A2, CYP2C19 and CYP2D6 in the dealkylation procedure of AM in human liver [370], the involvement of some other CYP isoenzymes might be evaluated in the metabolism of AM to DEA in rat. For this study, either chemical or immunological inhibition might be used. As it is indicated earlier, KTZ is a potent chemical inhibitor of both CYP1A1 and CYP3A1/2 isosyme in rat hepatic and intestinal microsomes. Hence, it might be interesting to assess the inhibitory effects of KTZ on other CYPs. Clearly, the employment of specific antibodies and supersomes would also be helpful in the assessment of the role of the other CYP isoenzymes in this metabolic procedure.

An examination of the interplay between the effect of HL on the pharmacokinetics, pharmacodynamics and metabolism of some other lipophilic molecules such as halofantrine, CYA and KTZ with high tendency toward LP binding is also warranted. The ability of these results to be extrapolated to a broader scope of LP-bound drugs based can only be determined through such evaluations.

REFERENCES

1. Chanmugam, P., et al., *Did fat intake in the United States really decline between 1989-1991 and 1994-1996?* J Am Diet Assoc, 2003. **103**(7): p. 867-72.
2. Kennedy, E.T., S.A. Bowman, and R. Powell, *Dietary-fat intake in the US population.* J Am Coll Nutr, 1999. **18**(3): p. 207-12.
3. Dayanikli, F., et al., *Early detection of abnormal coronary flow reserve in asymptomatic men at high risk for coronary artery disease using positron emission tomography.* Circulation, 1994. **90**(2): p. 808-17.
4. Mulligan, J.D., et al., *ABCA1 is essential for efficient basolateral cholesterol efflux during the absorption of dietary cholesterol in chickens.* J Biol Chem, 2003. **278**(15): p. 13356-66.
5. Sullivan, D.R., *The clinical and nutritional implications of lipid-lowering drugs that act in the gastrointestinal tract.* Curr Opin Lipidol, 2005. **16**(1): p. 39-45.
6. Nordskog, B.K., et al., *An examination of the factors affecting intestinal lymphatic transport of dietary lipids.* Adv Drug Deliv Rev, 2001. **50**(1-2): p. 21-44.
7. Hamosh, M. and R.O. Scow, *Lingual lipase and its role in the digestion of dietary lipid.* J Clin Invest, 1973. **52**(1): p. 88-95.
8. Moreau, H., et al., *Human preduodenal lipase is entirely of gastric fundic origin.* Gastroenterology, 1988. **95**(5): p. 1221-6.
9. Subbaiah, P.V., P.S. Sastry, and J. Ganguly, *Acylation of lysolecithin in the intestinal mucosa of rats.* Biochem J, 1970. **118**(2): p. 241-6.
10. Mu, H. and C.E. Hoy, *The digestion of dietary triacylglycerols.* Prog Lipid Res, 2004. **43**(2): p. 105-33.
11. Germann, W. and C. Stanfield, *The Gastrointestinal System*, in *Principles of Human Physiology*, W. Germann and S. CL, Editors. 2005, Pearson, Benjamin Cummings: Sanfransisco. p. 646-684.
12. Shiau, Y.F., *Mechanisms of intestinal fat absorption.* Am J Physiol, 1981. **240**(1): p. G1-9.
13. Hamosh, M., *A review. Fat digestion in the newborn: role of lingual lipase and preduodenal digestion.* Pediatr Res, 1979. **13**(5 Pt 1): p. 615-22.
14. Mattson, F.H. and L.W. Beck, *The specificity of pancreatic lipase for the primary hydroxyl groups of glycerides.* J Biol Chem, 1956. **219**(2): p. 735-40.
15. Morgan, R.G. and N.E. Hoffman, *The interaction of lipase, lipase cofactor and bile salts in triglyceride hydrolysis.* Biochim Biophys Acta, 1971. **248**(1): p. 143-8.
16. Borgstrom, B., *On the interactions between pancreatic lipase and colipase and the substrate, and the importance of bile salts.* J Lipid Res, 1975. **16**(6): p. 411-7.
17. Borgstrom, B. and C. Erlanson, *Pancreatic lipase and co-lipase. Interactions and effects of bile salts and other detergents.* Eur J Biochem, 1973. **37**(1): p. 60-8.
18. Borgstrom, B. and J. Donner, *Binding of bile salts to pancreatic colipase and lipase.* J Lipid Res, 1975. **16**(4): p. 287-92.
19. Thomson, A.B., et al., *Intestinal aspects of lipid absorption: in review.* Can J Physiol Pharmacol, 1989. **67**(3): p. 179-91.

20. Borgstrom, B., G. Lundh, and A. Hofmann, *The site of absorption of conjugated bile salts in man.* Gastroenterology, 1968. **54**(4): p. Suppl:781-3.
21. Lombardo, D., O. Guy, and C. Figarella, *Purification and characterization of a carboxyl ester hydrolase from human pancreatic juice.* Biochim Biophys Acta, 1978. **527**(1): p. 142-9.
22. Yao, L., et al., *Separation of micelles and vesicles within lumenal aspirates from healthy humans: solubilization of cholesterol after a meal.* J Lipid Res, 2002. **43**(4): p. 654-60.
23. Young, S.C. and D.Y. Hui, *Pancreatic lipase/colipase-mediated triacylglycerol hydrolysis is required for cholesterol transport from lipid emulsions to intestinal cells.* Biochem J, 1999. **339 (Pt 3)**: p. 615-20.
24. Bengtsson-Ellmark, S.H., et al., *Association between a polymorphism in the carboxyl ester lipase gene and serum cholesterol profile.* Eur J Hum Genet, 2004. **12**(8): p. 627-32.
25. Jansen, H., B. Breedveld, and K. Schoonderwoerd, *Role of lipoprotein lipases in postprandial lipid metabolism.* Atherosclerosis, 1998. **141 Suppl 1**: p. S31-4.
26. Lombardo, D., J. Fauvel, and O. Guy, *Studies on the substrate specificity of a carboxyl ester hydrolase from human pancreatic juice. I. Action on carboxyl esters, glycerides and phospholipids.* Biochim Biophys Acta, 1980. **611**(1): p. 136-46.
27. Stremmel, W., *Uptake of fatty acids by jejunal mucosal cells is mediated by a fatty acid binding membrane protein.* J Clin Invest, 1988. **82**(6): p. 2001-10.
28. Huggins, K.W., et al., *Pancreatic triglyceride lipase deficiency minimally affects dietary fat absorption but dramatically decreases dietary cholesterol absorption in mice.* J Biol Chem, 2003. **278**(44): p. 42899-905.
29. Lowe, M.E., et al., *Decreased neonatal dietary fat absorption and T cell cytotoxicity in pancreatic lipase-related protein 2-deficient mice.* J Biol Chem, 1998. **273**(47): p. 31215-21.
30. Hui, D.Y., *Molecular biology of enzymes involved with cholesterol ester hydrolysis in mammalian tissues.* Biochim Biophys Acta, 1996. **1303**(1): p. 1-14.
31. Strauss, E.W., *Electron microscopic study of intestinal fat absorption in vitro from mixed micelles containing linolenic acid, monoolein, and bile salt.* J Lipid Res, 1966. **7**(2): p. 307-23.
32. van den Bosch, H., et al., *On the positional specificity of phospholipase A from pancreas.* Biochim Biophys Acta, 1965. **98**(3): p. 657-9.
33. Stremmel, W., et al., *Identification, isolation, and partial characterization of a fatty acid binding protein from rat jejunal microvillous membranes.* J Clin Invest, 1985. **75**(3): p. 1068-76.
34. Wilson, F.A., V.L. Sallee, and J.M. Dietschy, *Unstirred water layers in intestine: rate determinant of fatty acid absorption from micellar solutions.* Science, 1971. **174**(13): p. 1031-3.
35. Hui, D.Y. and P.N. Howles, *Molecular mechanisms of cholesterol absorption and transport in the intestine.* Semin Cell Dev Biol, 2005. **16**(2): p. 183-92.
36. Westergaard, H. and J.M. Dietschy, *The mechanism whereby bile acid micelles increase the rate of fatty acid and cholesterol uptake into the intestinal mucosal cell.* J Clin Invest, 1976. **58**(1): p. 97-108.

37. Chow, S.L. and D. Hollander, *A dual, concentration-dependent absorption mechanism of linoleic acid by rat jejunum in vitro.* J Lipid Res, 1979. **20**(3): p. 349-56.

38. Ockner, R.K. and J.A. Manning, *Fatty acid-binding protein in small intestine. Identification, isolation, and evidence for its role in cellular fatty acid transport.* J Clin Invest, 1974. **54**(2): p. 326-38.

39. Chijiiwa, K. and W.G. Linscheer, *Distribution and monomer activity of cholesterol in micellar bile salt: effect of cholesterol level.* Am J Physiol, 1987. **252**(3 Pt 1): p. G309-14.

40. Brousseau, M.E., *ATP-binding cassette transporter A1, fatty acids, and cholesterol absorption.* Curr Opin Lipidol, 2003. **14**(1): p. 35-40.

41. Iqbal, J. and M.M. Hussain, *Evidence for multiple complementary pathways for efficient cholesterol absorption in mice.* J Lipid Res, 2005. **46**(7): p. 1491-501.

42. Turley, S.D. and J.M. Dietschy, *Sterol absorption by the small intestine.* Curr Opin Lipidol, 2003. **14**(3): p. 233-40.

43. Thurnhofer, H. and H. Hauser, *Uptake of cholesterol by small intestinal brush border membrane is protein-mediated.* Biochemistry, 1990. **29**(8): p. 2142-8.

44. Hernandez, M., et al., *Intestinal absorption of cholesterol is mediated by a saturable, inhibitable transporter.* Biochim Biophys Acta, 2000. **1486**(2-3): p. 232-42.

45. Detmers, P.A., et al., *A target for cholesterol absorption inhibitors in the enterocyte brush border membrane.* Biochim Biophys Acta, 2000. **1486**(2-3): p. 243-52.

46. Altmann, S.W., et al., *The identification of intestinal scavenger receptor class B, type I (SR-BI) by expression cloning and its role in cholesterol absorption.* Biochim Biophys Acta, 2002. **1580**(1): p. 77-93.

47. Ezzet, F., et al., *The plasma concentration and LDL-C relationship in patients receiving ezetimibe.* J Clin Pharmacol, 2001. **41**(9): p. 943-9.

48. Knopp, R.H., et al., *Effects of ezetimibe, a new cholesterol absorption inhibitor, on plasma lipids in patients with primary hypercholesterolemia.* Eur Heart J, 2003. **24**(8): p. 729-41.

49. Hauser, H., et al., *Identification of a receptor mediating absorption of dietary cholesterol in the intestine.* Biochemistry, 1998. **37**(51): p. 17843-50.

50. Gordon, D.A. and H. Jamil, *Progress towards understanding the role of microsomal triglyceride transfer protein in apolipoprotein-B lipoprotein assembly.* Biochim Biophys Acta, 2000. **1486**(1): p. 72-83.

51. Vahouny, G.V., et al., *Sterol carrier protein2 (SCP2)-mediated transfer of cholesterol to mitochondrial inner membranes.* Biochem Biophys Res Commun, 1984. **122**(2): p. 509-15.

52. Scallen, T.J., et al., *Sterol carrier protein 2 and fatty acid-binding protein. Separate and distinct physiological functions.* J Biol Chem, 1985. **260**(8): p. 4733-9.

53. Lehner, R. and A. Kuksis, *Triacylglycerol synthesis by purified triacylglycerol synthetase of rat intestinal mucosa. Role of acyl-CoA acyltransferase.* J Biol Chem, 1995. **270**(23): p. 13630-6.

54. Field, R.B. and R.O. Scow, *Purification and characterization of rat lingual lipase.* J Biol Chem, 1983. **258**(23): p. 14563-9.
55. Naito, H., *Disordrs of lipid metabolism*, in *Clinnical Chemistry, theory, analysis, and correlation*, L. Kaplan, Pesce, JA, Editor. 1984, C.V. Mosby zCompany: St. Louis. p. 550- 593.
56. Iqbal, J., K. Anwar, and M.M. Hussain, *Multiple, independently regulated pathways of cholesterol transport across the intestinal epithelial cells.* J Biol Chem, 2003. **278**(34): p. 31610-20.
57. Tso, P. and S.R. Gollamudi, *Pluronic L-81: a potent inhibitor of the transport of intestinal chylomicrons.* Am J Physiol, 1984. **247**(1 Pt 1): p. G32-6.
58. Wetterau, J.R., M.C. Lin, and H. Jamil, *Microsomal triglyceride transfer protein.* Biochim Biophys Acta, 1997. **1345**(2): p. 136-50.
59. Ockner, R.K., F.B. Hughes, and K.J. Isselbacher, *Very low density lipoproteins in intestinal lymph: role in triglyceride and cholesterol transport during fat absorption.* J Clin Invest, 1969. **48**(12): p. 2367-73.
60. Ockner, R.K., F.B. Hughes, and K.J. Isselbacher, *Very low density lipoproteins in intestinal lymph: origin, composition, and role in lipid transport in the fasting state.* J Clin Invest, 1969. **48**(11): p. 2079-88.
61. Hayashi, H., et al., *Fat feeding increases size, but not number, of chylomicrons produced by small intestine.* Am J Physiol, 1990. **259**(5 Pt 1): p. G709-19.
62. Kumar, N.S. and C.M. Mansbach, 2nd, *Prechylomicron transport vesicle: isolation and partial characterization.* Am J Physiol, 1999. **276**(2 Pt 1): p. G378-86.
63. Matsuoka, K., et al., *COPII-coated vesicle formation reconstituted with purified coat proteins and chemically defined liposomes.* Cell, 1998. **93**(2): p. 263-75.
64. Siddiqi, S.A., et al., *COPII proteins are required for Golgi fusion but not for endoplasmic reticulum budding of the pre-chylomicron transport vesicle.* J Cell Sci, 2003. **116**(Pt 2): p. 415-27.
65. Tso, P. and J.A. Balint, *Formation and transport of chylomicrons by enterocytes to the lymphatics.* Am J Physiol, 1986. **250**(6 Pt 1): p. G715-26.
66. Hussain, M.M., *A proposed model for the assembly of chylomicrons.* Atherosclerosis, 2000. **148**(1): p. 1-15.
67. Pease, R.J., G.B. Harrison, and J. Scott, *Cotranslocational insertion of apolipoprotein B into the inner leaflet of the endoplasmic reticulum.* Nature, 1991. **353**(6343): p. 448-50.
68. Zilversmit, D.B., *The composition and structure of lymph chylomicrons in dog, rat, and man.* J Clin Invest, 1965. **44**(10): p. 1610-22.
69. Olofsson, S.O., et al., *Apolipoprotein B: structure, biosynthesis and role in the lipoprotein assembly process.* Atherosclerosis, 1987. **68**(1-2): p. 1-17.
70. Wu, X., et al., *Demonstration of a physical interaction between microsomal triglyceride transfer protein and apolipoprotein B during the assembly of ApoB-containing lipoproteins.* J Biol Chem, 1996. **271**(17): p. 10277-81.
71. Hamilton, R.L., et al., *Chylomicron-sized lipid particles are formed in the setting of apolipoprotein B deficiency.* J Lipid Res, 1998. **39**(8): p. 1543-57.

72. DiBona, D.R., L.C. Chen, and G.W. Sharp, *A study of intercellular spaces in the rabbit jejunum during acute volume expansion and after treatment with cholera toxin.* J Clin Invest, 1974. **53**(5): p. 1300-7.

73. Casley-Smith, J.R., *The identification of chylomicra and lipoproteins in tissue sections and their passage into jejunal lacteals.* J Cell Biol, 1962. **15**: p. 259-77.

74. Goldberg, I.J., Y. Kako, and E.P. Lutz, *Responses to eating: lipoproteins, lipolytic products and atherosclerosis.* Curr Opin Lipidol, 2000. **11**(3): p. 235-41.

75. Brown, M.S., P.T. Kovanen, and J.L. Goldstein, *Regulation of plasma cholesterol by lipoprotein receptors.* Science, 1981. **212**(4495): p. 628-35.

76. Xiang, S.Q., et al., *Differential binding of triglyceride-rich lipoproteins to lipoprotein lipase.* J Lipid Res, 1999. **40**(9): p. 1655-63.

77. Applebaum-Bowden, D., *Lipases and lecithin: cholesterol acyltransferase in the control of lipoprotein metabolism.* Curr Opin Lipidol, 199[illegible]. **6**(3): p. 130-5.

78. Goldberg, I.J., *Lipoprotein lipase and lipolysis: central roles in lipoprotein metabolism and atherogenesis.* J Lipid Res, 1996. **37**(4): p. 693-707.

79. Karpe, F. and M. Hultin, *Endogenous triglyceride-rich lipoproteins accumulate in rat plasma when competing with a chylomicron-like triglyceride emulsion for a common lipolytic pathway.* J Lipid Res, 1995. **36**(7): p. 1557-66.

80. Cooper, A.D., *Hepatic uptake of chylomicron remnants.* J Lipid Res, 1997. **38**(11): p. 2173-92.

81. Hussain, M.M., et al., *Chylomicron assembly and catabolism: role of apolipoproteins and receptors.* Biochim Biophys Acta, 1996. **1300**(3): p. 151-70.

82. Zechner, R., *The tissue-specific expression of lipoprotein lipase: implications for energy and lipoprotein metabolism.* Curr Opin Lipidol, 1997. **8**(2): p. 77-88.

83. Takahashi, S., et al., *The very low density lipoprotein (VLDL) receptor--a peripheral lipoprotein receptor for remnant lipoproteins into fatty acid active tissues.* Mol Cell Biochem, 2003. **248**(1-2): p. 121-7.

84. Felts, J.M., H. Itakura, and R.T. Crane, *The mechanism of assimilation of constituents of chylomicrons, very low density lipoproteins and remnants - a new theory.* Biochem Biophys Res Commun, 1975. **66**(4): p. 1467-75.

85. Hussain, M.M., et al., *Chylomicron metabolism in normal, cholesterol-fed, and Watanabe heritable hyperlipidemic rabbits. Saturation of the sequestration step of the remnant clearance pathway.* J Biol Chem, 1995. **270**(15): p. 8578-87.

86. Hussain, M.M., et al., *Clearance of chylomicron remnants by the low density lipoprotein receptor-related protein/alpha 2-macroglobulin receptor.* J Biol Chem, 1991. **266**(21): p. 13936-40.

87. Leblond, L. and Y.L. Marcel, *Uptake of high density lipoprotein cholesterol ester by HepG2 cells involves apolipoprotein E localized on the cell surface.* J Biol Chem, 1993. **268**(3): p. 1670-6.

88. Thuren, T., et al., *Hepatic lipase hydrolysis of lipid monolayers. Regulation by apolipoproteins.* J Biol Chem, 1991. **266**(8): p. 4853-61.

89. Ji, Z.S., et al., *Secretion-capture role for apolipoprotein E in remnant lipoprotein metabolism involving cell surface heparan sulfate proteoglycans.* J Biol Chem, 1994. **269**(4): p. 2764-72.

90. Choi, S.Y., et al., *Use of an anti-low density lipoprotein receptor antibody to quantify the role of the LDL receptor in the removal of chylomicron remnants in the mouse in vivo.* J Clin Invest, 1991. **88**(4): p. 1173-81.
91. Mokuno, H., et al., *Effect of the 39-kDa receptor-associated protein on the hepatic uptake and endocytosis of chylomicron remnants and low density lipoproteins in the rat.* J Biol Chem, 1994. **269**(18): p. 13238-43.
92. Fielding, C.J., *Lipoprotein receptors, plasma cholesterol metabolism, and the regulation of cellular free cholesterol concentration.* FASEB J, 1992. **6**(13): p. 3162-8.
93. Alexander, C.A., R.L. Hamilton, and R.J. Havel, *Subcellular localization of B apoprotein of plasma lipoproteins in rat liver.* J Cell Biol, 1976. **69**(2): p. 241-63.
94. Gibbons, G.F., et al., *Synthesis and function of hepatic very-low-density lipoprotein.* Biochem Soc Trans, 2004. **32**(Pt 1): p. 59-64.
95. Chang, T.Y., et al., *Roles of acyl-coenzyme A:cholesterol acyltransferase-1 and -2.* Curr Opin Lipidol, 2001. **12**(3): p. 289-96.
96. Tall, A., *Plasma lipid transfer proteins.* Annu Rev Biochem, 1995. **64**: p. 235-57.
97. Arbeeny, C.M. and V.A. Rifici, *The uptake of chylomicron remnants and very low density lipoprotein remnants by the perfused rat liver.* J Biol Chem, 1984. **259**(15): p. 9662-6.
98. Campos, H., D.M. Dreon, and R.M. Krauss, *Associations of hepatic and lipoprotein lipase activities with changes in dietary composition and low density lipoprotein subclasses.* J Lipid Res, 1995. **36**(3): p. 462-72.
99. Zambon, A., et al., *Relevance of hepatic lipase to the metabolism of triacylglycerol-rich lipoproteins.* Biochem Soc Trans, 2003. **31**(Pt 5): p. 1070-4.
100. Jansen, H., A.J. Verhoeven, and E.J. Sijbrands, *Hepatic lipase: a pro- or anti-atherogenic protein?* J Lipid Res, 2002. **43**(9): p. 1352-62.
101. Connelly, P.W., *The role of hepatic lipase in lipoprotein metabolism.* Clin Chim Acta, 1999. **286**(1-2): p. 243-55.
102. Cohen, J.C., G.L. Vega, and S.M. Grundy, *Hepatic lipase: new insights from genetic and metabolic studies.* Curr Opin Lipidol, 1999. **10**(3): p. 259-67.
103. Asami, T., T. Ciomartan, and M. Uchiyama, *Thyroxine inversely regulates serum intermediate density lipoprotein levels in children with congenital hypothyroidism.* Pediatr Int, 1999. **41**(3): p. 266-9.
104. van Berkel, T.J., et al., *Scavenger receptors: friend or foe in atherosclerosis?* Curr Opin Lipidol, 2005. **16**(5): p. 525-35.
105. Li, A.C. and C.K. Glass, *The macrophage foam cell as a target for therapeutic intervention.* Nat Med, 2002. **8**(11): p. 1235-42.
106. Acton, S., et al., *Identification of scavenger receptor SR-BI as a high density lipoprotein receptor.* Science, 1996. **271**(5248): p. 518-20.
107. Spronk, H.M., D. van der Voort, and H. Ten Cate, *Blood coagulation and the risk of atherothrombosis: a complex relationship.* Thromb J, 2004. **2**(1): p. 12.
108. Jonas, A., *Lecithin cholesterol acyltransferase.* Biochim Biophys Acta, 2000. **1529**(1-3): p. 245-56.
109. Fielding, C.J. and P.E. Fielding, *Molecular physiology of reverse cholesterol transport.* J Lipid Res, 1995. **36**(2): p. 211-28.

110. Hill, S.A. and M.J. McQueen, *Reverse cholesterol transport--a review of the process and its clinical implications.* Clin Biochem, 1997. **30**(7): p. 517-25.
111. Davidson, W.S., et al., *The role of apolipoprotein AI domains in lipid binding.* Proc Natl Acad Sci U S A, 1996. **93**(24): p. 13605-10.
112. Zannis, V.I., et al., *Intracellular and extracellular processing of human apolipoprotein A-I: secreted apolipoprotein A-I isoprotein 2 is a propeptide.* Proc Natl Acad Sci U S A, 1983. **80**(9): p. 2574-8.
113. Ha, Y.C. and P.J. Barter, *Differences in plasma cholesteryl ester transfer activity in sixteen vertebrate species.* Comp Biochem Physiol B, 1982. **71**(2): p. 265-9.
114. Li, H., et al., *Structural determination of lipid-bound ApoA-I using fluorescence resonance energy transfer.* J Biol Chem, 2000. **275**(47): p. 37048-54.
115. Bruce, C., et al., *Molecular determinants of plasma cholesteryl ester transfer protein binding to high density lipoproteins.* J Biol Chem, 1995. **270**(19): p. 11532-42.
116. Jiang, X.C., et al., *Dietary cholesterol increases transcription of the human cholesteryl ester transfer protein gene in transgenic mice. Dependence on natural flanking sequences.* J Clin Invest, 1992. **90**(4): p. 1290-5.
117. Fleisher, D., et al., *Drug, meal and formulation interactions influencing drug absorption after oral administration. Clinical implications.* Clin Pharmacokinet, 1999. **36**(3): p. 233-54.
118. Miles, C., et al., *CCK antagonist pre-treatment inhibits meal-enhanced drug absorption in dogs.* Regul Pept, 1997. **68**(1): p. 9-14.
119. Singh, B.N., *Effects of food on clinical pharmacokinetics.* Clin Pharmacokinet, 1999. **37**(3): p. 213-55.
120. Hunt, J.N. and M.T. Knox, *A relation between the chain length of fatty acids and the slowing of gastric emptying.* J Physiol, 1968. **194**(2): p. 327-36.
121. Sunesen, V.H., et al., *Effect of liquid volume and food intake on the absolute bioavailability of danazol, a poorly soluble drug.* Eur J Pharm Sci, 2005. **24**(4): p. 297-303.
122. Marathe, P.H., et al., *Evaluation of the effect of food on the pharmacokinetics of avitriptan.* Biopharm Drug Dispos, 1998. **19**(6): p. 381-94.
123. Bekersky, I., D. Dressler, and Q.A. Mekki, *Effect of low- and high-fat meals on tacrolimus absorption following 5 mg single oral doses to healthy human subjects.* J Clin Pharmacol, 2001. **41**(2): p. 176-82.
124. Teo, S.K., et al., *Effect of a high-fat meal on thalidomide pharmacokinetics and the relative bioavailability of oral formulations in healthy men and women.* Biopharm Drug Dispos, 2000. **21**(1): p. 33-40.
125. Brocks, D.R., S. Ala, and H.M. Aliabadi, *The effect of increased lipoprotein levels on the pharmacokinetics of cyclosporine A in the laboratory rat.* Biopharm Drug Dispos, 2006. **27**(1): p. 7-16.
126. Modi, N.B., et al., *Effect of food on the pharmacokinetics of osmotic controlled-release methylphenidate HCl in healthy subjects.* Biopharm Drug Dispos, 2000. **21**(1): p. 23-31.
127. Lennernas, H. and G. Fager, *Pharmacodynamics and pharmacokinetics of the HMG-CoA reductase inhibitors. Similarities and differences.* Clin Pharmacokinet, 1997. **32**(5): p. 403-25.

128. Naylor, L.J., V. Bakatselou, and J.B. Dressman, *Comparison of the mechanism of dissolution of hydrocortisone in simple and mixed micelle systems.* Pharm Res, 1993. **10**(6): p. 865-70.
129. Ogunbona, F.A., I.F. Smith, and O.S. Olawoye, *Fat contents of meals and bioavailability of griseofulvin in man.* J Pharm Pharmacol, 1985. **37**(4): p. 283-4.
130. Ginsburg, C.M., et al., *Effect of feeding on bioavailability of griseofulvin in children.* J Pediatr, 1983. **102**(2): p. 309-11.
131. Poelma, F.G., R. Breas, and J.J. Tukker, *Intestinal absorption of drugs. III. The influence of taurocholate on the disappearance kinetics of hydrophilic and lipophilic drugs from the small intestine of the rat.* Pharm Res, 1990. **7**(4): p. 392-7.
132. Brocks, D.R. and K.M. Wasan, *The influence of lipids on stereoselective pharmacokinetics of halofantrine: Important implications in food-effect studies involving drugs that bind to lipoproteins.* J Pharm Sci, 2002. **91**(8): p. 1817-26.
133. Milton, K.A., et al., *Pharmacokinetics of halofantrine in man: effects of food and dose size.* Br J Clin Pharmacol, 1989. **28**(1): p. 71-7.
134. Luner, P.E., S.R. Babu, and G.W. Radebaugh, *The effects of bile salts and lipids on the physicochemical behavior of gemfibrozil.* Pharm Res, 1994. **11**(12): p. 1755-60.
135. Dressman, J.B., et al., *Upper gastrointestinal (GI) pH in young, healthy men and women.* Pharm Res, 1990. **7**(7): p. 756-61.
136. Neubert, R., B. Fritsch, and G. Dongowski, *Interactions between food components and drugs. Part 3. Interactions between pectin and propranolol.* Pharmazie, 1995. **50**(6): p. 414-6.
137. Charman, W.N., et al., *Physiochemical and physiological mechanisms for the effects of food on drug absorption: the role of lipids and pH.* J Pharm Sci, 1997. **86**(3): p. 269-82.
138. Miyazaki, S., et al., *Interaction of drugs with bile components. II. Effect of bile on the absorption of indomethacin and phenylbutazine in rats.* Chem Pharm Bull (Tokyo), 1980. **28**(1): p. 323-6.
139. Bakatselou, V., R.C. Oppenheim, and J.B. Dressman, *Solubilization and wetting effects of bile salts on the dissolution of steroids.* Pharm Res, 1991. **8**(12): p. 1461-9.
140. TenHoor, C.N., V. Bakatselou, and J. Dressman, *Solubility of mefenamic acid under simulated fed- and fasted-state conditions.* Pharm Res, 1991. **8**(9): p. 1203-5.
141. Homer, L.M., C.R. Clarke, and A.J. Weingarten, *Effect of dietary fat on oral bioavailability of tepoxalin in dogs.* J Vet Pharmacol Ther, 2005. **28**(3): p. 287-91.
142. Meng, X., et al., *Bioavailability of amiodarone tablets administered with and without food in healthy subjects.* Am J Cardiol, 2001. **87**(4): p. 432-5.
143. McLure, J.A., J.O. Miners, and D.J. Birkett, *Nonspecific binding of drugs to human liver microsomes.* Br J Clin Pharmacol, 2000. **49**(5): p. 453-61.
144. Humberstone, A.J., C.J. Porter, and W.N. Charman, *A physicochemical basis for the effect of food on the absolute oral bioavailability of halofantrine.* J Pharm Sci, 1996. **85**(5): p. 525-9.

145. Crevoisier, C., et al., *Food increases the bioavailability of mefloquine.* Eur J Clin Pharmacol, 1997. **53**(2): p. 135-9.
146. Mottier, M.L., et al., *Transtegumental diffusion of benzimidazole anthelmintics into Moniezia benedeni: correlation with their octanol-water partition coefficients.* Exp Parasitol, 2003. **103**(1-2): p. 1-7.
147. Lange, H., R. Eggers, and J. Bircher, *Increased systemic availability of albendazole when taken with a fatty meal.* Eur J Clin Pharmacol, 1988. **34**(3): p. 315-7.
148. Yasui-Furukori, N., et al., *Effect of dietary fat content in meals on pharmacokinetics of quazepam.* J Clin Pharmacol, 2002. **42**(12): p. 1335-40.
149. Bramer, S.L. and W.P. Forbes, *Relative bioavailability and effects of a high fat meal on single dose cilostazol pharmacokinetics.* Clin Pharmacokinet, 1999. **37 Suppl 2**: p. 13-23.
150. Lane, M.E., M. O'Driscoll C, and O.I. Corrigan, *Quantitative estimation of the effects of bile salt surfactant systems on insulin stability and permeability in the rat intestine using a mass balance model.* J Pharm Pharmacol, 2005. **57**(2): p. 169-75.
151. Dongowski, G., et al., *The influence of bile salts and mixed micelles on the pharmacokinetics of quinine in rabbits.* Eur J Pharm Biopharm, 2005. **60**(1): p. 147-51.
152. Amidon, G.L., et al., *A theoretical basis for a biopharmaceutic drug classification: the correlation of in vitro drug product dissolution and in vivo bioavailability.* Pharm Res, 1995. **12**(3): p. 413-20.
153. Wu, C.Y. and L.Z. Benet, *Predicting drug disposition via application of BCS: transport/absorption/ elimination interplay and development of a biopharmaceutics drug disposition classification system.* Pharm Res, 2005. **22**(1): p. 11-23.
154. O'Driscoll, C.M., *Lipid-based formulations for intestinal lymphatic delivery.* Eur J Pharm Sci, 2002. **15**(5): p. 405-15.
155. Porter, C.J., N.L. Trevaskis, and W.N. Charman, *Lipids and lipid-based formulations: optimizing the oral delivery of lipophilic drugs.* Nat Rev Drug Discov, 2007. **6**(3): p. 231-48.
156. Seeballuck, F., et al., *Stimulation of triglyceride-rich lipoprotein secretion by polysorbate 80: in vitro and in vivo correlation using Caco-2 cells and a cannulated rat intestinal lymphatic model.* Pharm Res, 2004. **21**(12): p. 2320-6.
157. Khoo, S.M., et al., *A conscious dog model for assessing the absorption, enterocyte-based metabolism, and intestinal lymphatic transport of halofantrine.* J Pharm Sci, 2001. **90**(10): p. 1599-607.
158. Holm, R., et al., *Comparison of the lymphatic transport of halofantrine administered in disperse systems containing three different unsaturated fatty acids.* Pharm Res, 2001. **18**(9): p. 1299-304.
159. Porter, C.J. and W.N. Charman, *Intestinal lymphatic drug transport: an update.* Adv Drug Deliv Rev, 2001. **50**(1-2): p. 61-80.
160. Gershkovich, P. and A. Hoffman, *Uptake of lipophilic drugs by plasma derived isolated chylomicrons: linear correlation with intestinal lymphatic bioavailability.* Eur J Pharm Sci, 2005. **26**(5): p. 394-404.

161. Caliph, S.M., W.N. Charman, and C.J. Porter, *Effect of short-, medium-, and long-chain fatty acid-based vehicles on the absolute oral bioavailability and intestinal lymphatic transport of halofantrine and assessment of mass balance in lymph-cannulated and non-cannulated rats.* J Pharm Sci, 2000. **89**(8): p. 1073-84.
162. Palin, K.J., et al., *The effect of oils on the lymphatic absorption of DDT.* J Pharm Pharmacol, 1982. **34**(11): p. 707-10.
163. Constantinides, P.P., *Lipid microemulsions for improving drug dissolution and oral absorption: physical and biopharmaceutical aspects.* Pharm Res, 1995. **12**(11): p. 1561-72.
164. Nerurkar, M.M., et al., *Mechanistic roles of neutral surfactants on concurrent polarized and passive membrane transport of a model peptide in Caco-2 cells.* J Pharm Sci, 1997. **86**(7): p. 813-21.
165. Luchoomun, J. and M.M. Hussain, *Assembly and secretion of chylomicrons by differentiated Caco-2 cells. Nascent triglycerides and preformed phospholipids are preferentially used for lipoprotein assembly.* J Biol Chem, 1999. **274**(28): p. 19565-72.
166. Lupfert, C. and A. Reichel, *Development and application of physiologically based pharmacokinetic-modeling tools to support drug discovery.* Chem Biodivers, 2005. **2**(11): p. 1462-86.
167. Doherty, M.M. and W.N. Charman, *The mucosa of the small intestine: how clinically relevant as an organ of drug metabolism?* Clin Pharmacokinet, 2002. **41**(4): p. 235-53.
168. Bassissi, M.F., M. Alvinerie, and A. Lespine, *Macrocyclic lactones: distribution in plasma lipoproteins of several animal species including humans.* Comp Biochem Physiol C Toxicol Pharmacol, 2004. **138**(4): p. 437-44.
169. Keogh, J.B., et al., *Flow-mediated dilatation is impaired by a high-saturated fat diet but not by a high-carbohydrate diet.* Arterioscler Thromb Vasc Biol, 2005. **25**(6): p. 1274-9.
170. Williams, M.J., et al., *Impaired endothelial function following a meal rich in used cooking fat.* J Am Coll Cardiol, 1999. **33**(4): p. 1050-5.
171. Steer, P., et al., *The effect of a mixed meal on endothelium-dependent vasodilation is dependent on fat content in healthy humans.* Clin Sci (Lond), 2003. **105**(1): p. 81-7.
172. Plotnick, G.D., et al., *Effect of supplemental phytonutrients on impairment of the flow-mediated brachial artery vasoactivity after a single high-fat meal.* J Am Coll Cardiol, 2003. **41**(10): p. 1744-9.
173. Kuvin, J.T., et al., *A novel mechanism for the beneficial vascular effects of high-density lipoprotein cholesterol: enhanced vasorelaxation and increased endothelial nitric oxide synthase expression.* Am Heart J, 2002. **144**(1): p. 165-72.
174. Kruger, M.J., et al., *Dietary red palm oil reduces ischaemia-reperfusion injury in rats fed a hypercholesterolaemic diet.* Br J Nutr, 2007. **97**(4): p. 653-60.
175. Seifalian, A.M., et al., *The effect of graded steatosis on flow in the hepatic parenchymal microcirculation.* Transplantation, 1999. **68**(6): p. 780-4.
176. Ijaz, S., et al., *The role of nitric oxide in the modulation of hepatic microcirculation and tissue oxygenation in an experimental model of hepatic steatosis.* Microvasc Res, 2005. **70**(3): p. 129-36.

177. El-Badry, A.M., et al., *Prevention of reperfusion injury and microcirculatory failure in macrosteatotic mouse liver by omega-3 fatty acids.* Hepatology, 2007. **45**(4): p. 855-63.
178. Thomson, A.B., et al., *Dietary effects of omega 3-fatty acids on intestinal transport function.* Can J Physiol Pharmacol, 1988. **66**(8): p. 985-92.
179. Garg, M.L., et al., *Regional differences in lipid composition and incorporation of saturated and unsaturated fatty acids into microsomal membranes of rat small intestine.* Can J Physiol Pharmacol, 1988. **66**(6): p. 794-800.
180. Thomson, A.B., et al., *Dietary fat selectively alters transport properties of rat jejunum.* J Clin Invest, 1986. **77**(1): p. 279-88.
181. Keelan, M., et al., *Alterations in dietary fatty acid composition alter rat brush border membrane phospholipid fatty acid composition.* Diabetes Res, 1990. **14**(4): p. 165-70.
182. Rosella, O., A. Sinclair, and P.R. Gibson, *Polyunsaturated fatty acids reduce non-receptor-mediated transcellular permeation of protein across a model of intestinal epithelium in vitro.* J Gastroenterol Hepatol, 2000. **15**(6): p. 626-31.
183. Keelan, M., et al., *Improved intestinal form and function in diabetic rats fed long-term with a polyunsaturated fatty acid diet.* Diabetes Res, 1989. **10**(1): p. 43-7.
184. Thomson, A.B., M. Keelan, and M. Tavernini, *Early feeding of a high-cholesterol diet enhances intestinal permeability to lipids in rabbits.* Pediatr Res, 1987. **21**(4): p. 347-51.
185. Thomson, A.B., et al., *Influence of dietary fat composition on intestinal absorption in the rat.* Lipids, 1989. **24**(6): p. 494-501.
186. Vine, D.F., et al., *Effect of dietary fatty acids on the intestinal permeability of marker drug compounds in excised rat jejunum.* J Pharm Pharmacol, 2002. **54**(6): p. 809-19.
187. Ilback, N.G., et al., *Do surface-active lipids in food increase the intestinal permeability to toxic substances and allergenic agents?* Med Hypotheses, 2004. **63**(4): p. 724-30.
188. Onuki, Y., et al., *In vivo effects of highly purified docosahexaenoic acid on rectal insulin absorption.* Int J Pharm, 2000. **198**(2): p. 147-56.
189. Prabhu, S., M. Ortega, and C. Ma, *Novel lipid-based formulations enhancing the in vitro dissolution and permeability characteristics of a poorly water-soluble model drug, piroxicam.* Int J Pharm, 2005. **301**(1-2): p. 209-16.
190. Kono, H., et al., *Medium-chain triglycerides inhibit free radical formation and TNF-alpha production in rats given enteral ethanol.* Am J Physiol Gastrointest Liver Physiol, 2000. **278**(3): p. G467-76.
191. Kono, H., et al., *Protective effects of medium-chain triglycerides on the liver and gut in rats administered endotoxin.* Ann Surg, 2003. **237**(2): p. 246-55.
192. Yamagata, K., et al., *Polyunsaturated fatty acids induce tight junctions to form in brain capillary endothelial cells.* Neuroscience, 2003. **116**(3): p. 649-56.
193. Kim, H.J., et al., *A model for research on the blood-brain barrier disruption induced by unsaturated fatty acid emulsion.* Invest Radiol, 2005. **40**(5): p. 270-6.
194. Ecker, G.F. and C.R. Noe, *In silico prediction models for blood-brain barrier permeation.* Curr Med Chem, 2004. **11**(12): p. 1617-28.

195. Dehouck, B., et al., *A new function for the LDL receptor: transcytosis of LDL across the blood-brain barrier.* J Cell Biol, 1997. **138**(4): p. 877-89.
196. Kreuter, J., et al., *Apolipoprotein-mediated transport of nanoparticle-bound drugs across the blood-brain barrier.* J Drug Target, 2002. **10**(4): p. 317-25.
197. Luft, F.C., *After chylomicron remnants, what is left?* J Mol Med, 2004. **82**(7): p. 411-3.
198. Wasan, K.M. and S.M. Cassidy, *Role of plasma lipoproteins in modifying the biological activity of hydrophobic drugs.* J Pharm Sci, 1998. **87**(4): p. 411-24.
199. Tanaka, H. and K. Mizojiri, *Drug-protein binding and blood-brain barrier permeability.* J Pharmacol Exp Ther, 1999. **288**(3): p. 912-8.
200. Jolliet, P., et al., *Blood-to-brain transfer of various oxicams: effects of plasma binding on their brain delivery.* Pharm Res, 1997. **14**(5): p. 650-6.
201. Kwong, M. and K.M. Wasan, *Cholesteryl ester transfer protein facilitates the movement of water-insoluble drugs between lipoproteins: a novel biological function for a well-characterized lipid transfer protein.* Biochem Pharmacol, 2002. **64**(12): p. 1669-75.
202. Wasan, K.M., et al., *Pharmacokinetics, distribution in serum lipoproteins and tissues, and renal toxicities of amphotericin B and amphotericin B lipid complex in a hypercholesterolemic rabbit model: single-dose studies.* Antimicrob Agents Chemother, 1998. **42**(12): p. 3146-52.
203. Brocks, D.R., et al., *The stereoselective distribution of halofantrine enantiomers within human, dog, and rat plasma lipoproteins.* Pharm Res, 2000. **17**(4): p. 427-31.
204. Humberstone, A.J., et al., *Association of halofantrine with postprandially derived plasma lipoproteins decreases its clearance relative to administration in the fasted state.* J Pharm Sci, 1998. **87**(8): p. 936-42.
205. Ramaswamy, M., et al., *Species differences in the proportion of plasma lipoprotein lipid carried by high-density lipoproteins influence the distribution of free and liposomal nystatin in human, dog, and rat plasma.* Antimicrob Agents Chemother, 1999. **43**(6): p. 1424-8.
206. Sgoutas, D., et al., *Interaction of cyclosporin A with human lipoproteins.* J Pharm Pharmacol, 1986. **38**(8): p. 583-8.
207. Gurecki, J., V. Warty, and A. Sanghvi, *The transport of cyclosporine in association with plasma lipoproteins in heart and liver transplant patients.* Transplant Proc, 1985. **17**(4): p. 1997-2002.
208. Wasan, K.M., et al., *Cyclosporine transfer from low- and high-density lipoproteins is partially influenced by lipid transfer protein I triglyceride transfer activity.* Pharm Res, 1999. **16**(7): p. 1067-73.
209. Akhlaghi, F. and A.K. Trull, *Distribution of cyclosporin in organ transplant recipients.* Clin Pharmacokinet, 2002. **41**(9): p. 615-37.
210. Wasan, K.M., et al., *Differences in lipoprotein lipid concentration and composition modify the plasma distribution of cyclosporine.* Pharm Res, 1997. **14**(11): p. 1613-20.
211. Procyshyn, R.M., G. Tsai, and K.M. Wasan, *The influence of dyslipidemia on the plasma protein and lipoprotein distribution of haloperidol.* Eur Neuropsychopharmacol, 2003. **13**(1): p. 33-7.

212. Gaulin, B.D., et al., *Clozapine-associated elevation in serum triglycerides.* Am J Psychiatry, 1999. **156**(8): p. 1270-2.

213. Nakamura, T., et al., *Effect of serum triglyceride concentration on the fluctuation of whole blood concentration of cyclosporin A in patients.* Biol Pharm Bull, 2001. **24**(6): p. 683-7.

214. Wojcicki, J., et al., *Studies on the pharmacokinetics and pharmacodynamics of propranolol in hyperlipidemia.* J Clin Pharmacol, 1999. **39**(8): p. 826-33.

215. Bassissi, M.F., et al., *Influence of dyslipidemia on moxidectin distribution in plasma lipoproteins and on its pharmacokinetics.* Pharm Res, 2006. **23**(11): p. 2672-80.

216. Riou, L.M., et al., *Effects of increased lipid concentration and hyperemic blood flow on the intrinsic myocardial washout kinetics of (99m)TcN-NOET.* J Nucl Med, 2003. **44**(7): p. 1092-8.

217. Riou, L.M., et al., *The in vivo cardiac kinetics of Tc-99m N-NOET are accelerated in obese, hyperlipidemic Zucker rats.* J Nucl Cardiol, 2006. **13**(1): p. 75-82.

218. Kim, M.S., et al., *Differences in the pharmacokinetics of peroxisome proliferator-activated receptor agonists in genetically obese Zucker and sprague-dawley rats: implications of decreased glucuronidation in obese Zucker rats.* Drug Metab Dispos, 2004. **32**(9): p. 909-14.

219. Aliabadi, H.M., et al., *Insights into the effects of hyperlipoproteinemia on cyclosporine A biodistribution and relationship to renal function.* AAPS J, 2006. **8**(4): p. E672-81.

220. Vadiei, K., G. Lopez-Berestein, and D.R. Luke, *Disposition and toxicity of amphotericin-B in the hyperlipidemic Zucker rat model.* Int J Obes, 1990. **14**(6): p. 465-72.

221. Saeki, T., et al., *Specific drug binding by purified lipid-reconstituted P-glycoprotein: dependence on the lipid composition.* Biochim Biophys Acta, 1992. **1107**(1): p. 105-10.

222. Pallares-Trujillo, J., et al., *Role of cell cholesterol in modulating vincristine uptake and resistance.* Int J Cancer, 1993. **55**(4): p. 667-71.

223. Pallares-Trujillo, J., F.J. Lopez-Soriano, and J.M. Argiles, *Lipids: A key role in multidrug resistance? (Review).* Int J Oncol, 2000. **16**(4): p. 783-98.

224. Sinicrope, F.A., et al., *Modulation of P-glycoprotein-mediated drug transport by alterations in lipid fluidity of rat liver canalicular membrane vesicles.* J Biol Chem, 1992. **267**(35): p. 24995-5002.

225. Metherall, J.E., H. Li, and K. Waugh, *Role of multidrug resistance P-glycoproteins in cholesterol biosynthesis.* J Biol Chem, 1996. **271**(5): p. 2634-40.

226. Modok, S., C. Heyward, and R. Callaghan, *P-glycoprotein retains function when reconstituted into a sphingolipid- and cholesterol-rich environment.* J Lipid Res, 2004. **45**(10): p. 1910-8.

227. Debry, P., et al., *Role of multidrug resistance P-glycoproteins in cholesterol esterification.* J Biol Chem, 1997. **272**(2): p. 1026-31.

228. Nishimura, M., et al., *Role of soybean oil fat emulsion in the prevention of hepatic xenobiotic transporter mRNA up- and down-regulation induced by overdose of

fat-free total parenteral nutrition in infant rats. Drug Metab Pharmacokinet, 2005. **20**(1): p. 46-54.

229. Marsh, J.B., *Lipoprotein metabolism in the nephrotic syndrome.* Front Biosci, 2002. **7**: p. e326-38.
230. Fitos, I., et al., *Conformation selectivity in the binding of diazepam and analogues to alpha1-acid glycoprotein.* Bioorg Med Chem, 2007. **15**(14): p. 4857-62.
231. Ohnishi, T., et al., *Frontal analysis of drug-plasma lipoprotein binding using capillary electrophoresis.* J Pharm Biomed Anal, 2002. **27**(3-4): p. 607-14.
232. Vogeser, M. and J. Briegel, *Effect of temperature on protein binding of cortisol.* Clin Biochem, 2007. **40**(9-10): p. 724-7.
233. Rensen, P.C., et al., *Recombinant lipoproteins: lipoprotein-like lipid particles for drug targeting.* Adv Drug Deliv Rev, 2001. **47**(2-3): p. 251-76.
234. Eliot, L.A., R.T. Foster, and F. Jamali, *Effects of hyperlipidemia on the pharmacokinetics of nifedipine in the rat.* Pharm Res, 1999. **16**(2): p. 309-13.
235. Gupta, S.K. and L.Z. Benet, *High-fat meals increase the clearance of cyclosporine.* Pharm Res, 1990. **7**(1): p. 46-8.
236. Benedetti, M.S., R. Whomsley, and M. Canning, *Drug metabolism in the paediatric population and in the elderly.* Drug Discov Today, 2007. **12**(15-16): p. 599-610.
237. Oswald, S., et al., *Transporter-mediated uptake into cellular compartments.* Xenobiotica, 2007. **37**(10-11): p. 1171-95.
238. Roman, R.J., *P-450 metabolites of arachidonic acid in the control of cardiovascular function.* Physiol Rev, 2002. **82**(1): p. 131-85.
239. Castuma, C.E. and R.R. Brenner, *Effect of dietary cholesterol on microsomal membrane composition, dynamics and kinetic properties of UDPglucuronyl transferase.* Biochim Biophys Acta, 1986. **855**(2): p. 231-42.
240. Yoo, J.S., et al., *Modulation of the levels of cytochromes P450 in rat liver and lung by dietary lipid.* Biochem Pharmacol, 1992. **43**(12): p. 2535-42.
241. Dannenberg, A.J. and D. Zakim, *Dietary lipid regulates the amount and functional state of UDP-glucuronosyltransferase in rat liver.* J Nutr, 1992. **122**(8): p. 1607-13.
242. Lutz, M., et al., *Effect of dietary oils, cholesterol and antioxidant vitamin supplementation on liver microsomal fluidity and xenobiotic-metabolizing enzymes in rats.* Ann Nutr Metab, 1998. **42**(6): p. 350-9.
243. Saito, M. and M. Yamaguchi, *Liver microsomal mixed-function oxidases in response to polyunsaturated/saturated and n-6/n-3 fatty acid ratios of dietary lipids in rats.* Ann Nutr Metab, 1994. **38**(1): p. 28-39.
244. Kato, J., A. Ikemoto, and T. Mizutani, *The effect of dietary fatty acids on the expression levels and activities of hepatic drug metabolizing enzymes.* Journal of Health Science, 2003. **49**(2): p. 105-114.
245. Yang, E.K., et al., *Dietary lipids coinduce xenobiotic metabolizing enzymes in rat liver.* Biochim Biophys Acta, 1993. **1168**(1): p. 52-8.
246. Ko, Y.J., et al., *Comparison of the effect of fish oil and corn oil on chemical-induced hepatic enzyme-altered foci in rats.* J Agric Food Chem, 2000. **48**(9): p. 4144-50.

247. Chen, H.W., et al., *Dietary fat and garlic oil independently regulate hepatic cytochrome p(450) 2B1 and the placental form of glutathione S-transferase expression in rats.* J Nutr, 2001. **131**(5): p. 1438-43.

248. Dannenberg, A.J., E.K. Yang, and D. Aharon, *Dietary lipids induce phase 2 enzymes in rat small intestine.* Biochim Biophys Acta, 1993. **1210**(1): p. 8-12.

249. Reddy, B.S. and S. Sugie, *Effect of different levels of omega-3 and omega-6 fatty acids on azoxymethane-induced colon carcinogenesis in F344 rats.* Cancer Res, 1988. **48**(23): p. 6642-7.

250. Yoshinari, K., et al., *Hepatic CYP3A expression is attenuated in obese mice fed a high-fat diet.* Pharm Res, 2006. **23**(6): p. 1188-200.

251. Hofker, M.H., B.J. van Vlijmen, and L.M. Havekes, *Transgenic mouse models to study the role of APOE in hyperlipidemia and atherosclerosis.* Atherosclerosis, 1998. **137**(1): p. 1-11.

252. Getz, G.S. and C.A. Reardon, *Diet and murine atherosclerosis.* Arterioscler Thromb Vasc Biol, 2006. **26**(2): p. 242-9.

253. Frantz, I.D., Jr., H.S. Schneider, and B.T. Hinkelman, *Suppression of hepatic cholesterol synthesis in the rat by cholesterol feeding.* J Biol Chem, 1954. **206**(1): p. 465-9.

254. O'Brien, B.C. and R. Reiser, *Cholesterolemic responses of rats to human-type diet ingredients.* J Nutr, 1982. **112**(8): p. 1490-7.

255. Nagaoka, S., et al., *Effects of dietary polychlorinated biphenyls on cholesterol catabolism in rats.* Br J Nutr, 1990. **64**(1): p. 161-9.

256. Holt, P.R. and A.A. Dominguez, *Triton-induced hyperlipidemia: a model for studies of intestinal lipoprotein production.* Am J Physiol, 1980. **238**(5): p. G453-7.

257. Standeven, A.M., et al., *Retinoid-induced hypertriglyceridemia in rats is mediated by retinoic acid receptors.* Fundam Appl Toxicol, 1996. **33**(2): p. 264-71.

258. Cho, B.H., et al., *Effects of estrogen-induced hyperlipidemia on the erythrocyte membrane in chicks.* Lipids, 1988. **23**(9): p. 853-6.

259. Johnston, T.P., *The P-407-induced murine model of dose-controlled hyperlipidemia and atherosclerosis: a review of findings to date.* J Cardiovasc Pharmacol, 2004. **43**(4): p. 595-606.

260. Goldfarb, S., *Rapid increase in hepatic HMG CoA reductase activity and in vivo cholesterol synthesis after Triton WR 1339 injection.* J Lipid Res, 1978. **19**(4): p. 489-94.

261. Quazi, S., H. Yokogoshi, and A. Yoshida, *Effect of dietary fiber on hypercholesterolemia induced by dietary PCB or cholesterol in rats.* J Nutr, 1983. **113**(6): p. 1109-18.

262. Van Zwieten, P.A., et al., *Hypertensive diabetic rats in pharmacological studies.* Pharmacol Res, 1996. **33**(2): p. 95-105.

263. Zucker, L. and T. Zucker, *Fatty, A New mutation in the rat.* The Journal of Heredity, 1961. **52**(6): p. 275-278.

264. Hiraoka-Yamamoto, J., et al., *Establishment of a new animal model of metabolic syndrome: SHRSP fatty (fa/fa) rats.* Clin Exp Pharmacol Physiol, 2004. **31**(1-2): p. 107-9.

265. Dolphin, P.J., et al., *Serum lipids and lipoproteins in the atherosclerosis prone LA/N corpulent rat.* Biochim Biophys Acta, 1987. **919**(2): p. 140-8.

266. Piedrahita, J.A., et al., *Generation of mice carrying a mutant apolipoprotein E gene inactivated by gene targeting in embryonic stem cells.* Proc Natl Acad Sci U S A, 1992. **89**(10): p. 4471-5.

267. Plump, A.S., et al., *Severe hypercholesterolemia and atherosclerosis in apolipoprotein E-deficient mice created by homologous recombination in ES cells.* Cell, 1992. **71**(2): p. 343-53.

268. van Ree, J.H., et al., *Diet-induced hypercholesterolemia and atherosclerosis in heterozygous apolipoprotein E-deficient mice.* Atherosclerosis, 1994. **111**(1): p. 25-37.

269. Dumortier, G., et al., *A review of poloxamer 407 pharmaceutical and pharmacological characteristics.* Pharm Res, 2006. **23**(12): p. 2709-28.

270. Li, C., W.K. Palmer, and T.P. Johnston, *Disposition of poloxamer 407 in rats following a single intraperitoneal injection assessed using a simplified colorimetric assay.* J Pharm Biomed Anal, 1996. **14**(5): p. 659-65.

271. Cogger, V.C., et al., *Hyperlipidemia and surfactants: the liver sieve is a link.* Atherosclerosis, 2006. **189**(2): p. 273-81.

272. Duarte, J., et al., *Vasodilator effects of visnagin in isolated rat vascular smooth muscle.* Eur J Pharmacol, 1995. **286**(2): p. 115-22.

273. Bigler, L., et al., *Synthesis and cytotoxicity properties of amiodarone analogues.* Eur J Med Chem, 2007. **42**(6): p. 861-7.

274. Nattel, S. and M. Talajic, *Recent advances in understanding the pharmacology of amiodarone.* Drugs, 1988. **36**(2): p. 121-31.

275. Doval, H.C., et al., *Randomised trial of low-dose amiodarone in severe congestive heart failure. Grupo de Estudio de la Sobrevida en la Insuficiencia Cardiaca en Argentina (GESICA).* Lancet, 1994. **344**(8921): p. 493-8.

276. Kowey, P.R., et al., *Pharmacologic and pharmacokinetic profile of class III antiarrhythmic drugs.* Am J Cardiol, 1997. **80**(8A): p. 16G-23G.

277. Matyus, P., et al., *Novel antiarrhythmic compounds with combined class IB and class III mode of action.* Curr Med Chem, 2004. **11**(1): p. 61-9.

278. Morey, T.E., et al., *Structure-activity relationships and electrophysiological effects of short-acting amiodarone homologs in guinea pig isolated heart.* J Pharmacol Exp Ther, 2001. **297**(1): p. 260-6.

279. Newman, C.M., et al., *Amiodarone and the thyroid: a practical guide to the management of thyroid dysfunction induced by amiodarone therapy.* Heart, 1998. **79**(2): p. 121-7.

280. Bauman, J., H. Takahashi, and J. Fischer, *Clinical Pharmacokinetics of oral antiarrhythmic drugs*, in *Applied Pharmacokinetics and pharmacodynamics, Principles of therapeutic drug monitoring* M. Burton, et al., Editors. 2006, Lippincott Williams & Wilkins: Baltimore, Maryland. p. 440-462.

281. Thummell, K. and D. Shen, *Design and optimization of dosage regimens: Pharmacokinetic data*, in *Goodman and Gilman's The Pharmacological Basis of Therapeutics*, J. Hardman, L. Limbird, and A. Goodman Gilman, Editors. 2001, McGraw-Hill: New York. p. 1917–2023.

282. Kashima, A., et al., *Pharmacokinetic characteristics of amiodarone in long-term oral therapy in Japanese population.* Biol Pharm Bull, 2005. **28**(10): p. 1934-8.

283. Riva, E., et al., *Pharmacokinetics of amiodarone in man.* J Cardiovasc Pharmacol, 1982. **4**(2): p. 264-9.

284. Latini, R., G. Tognoni, and R.E. Kates, *Clinical pharmacokinetics of amiodarone.* Clin Pharmacokinet, 1984. **9**(2): p. 136-56.

285. Lalloz, M.R., et al., *Binding of amiodarone by serum proteins and the effects of drugs, hormones and other interacting ligands.* J Pharm Pharmacol, 1984. **36**(6): p. 366-72.

286. Kramer, S.D., J.C. Gautier, and P. Saudemon, *Considerations on the potentiometric log P determination.* Pharm Res, 1998. **15**(8): p. 1310-3.

287. Riva, E., et al., *Pharmacokinetics of amiodarone in rats.* J Cardiovasc Pharmacol, 1982. **4**(2): p. 270-5.

288. Rafeiro, E., et al., *In vitro hepatic, renal, and pulmonary N-dealkylation of amiodarone.* Biochem Pharmacol, 1990. **39**(10): p. 1627-9.

289. Daniels, J.M., et al., *Repeated amiodarone exposure in the rat: toxicity and effects on hepatic and extrahepatic monooxygenase activities.* Can J Physiol Pharmacol, 1990. **68**(9): p. 1261-8.

290. Soyama, A., et al., *Amiodarone N-deethylation by CYP2C8 and its variants, CYP2C8*3 and CYP2C8 P404A.* Pharmacol Toxicol, 2002. **91**(4): p. 174-8.

291. Trivier, J.M., et al., *Amiodarone N-deethylation in human liver microsomes: involvement of cytochrome P450 3A enzymes (first report).* Life Sci, 1993. **52**(10): p. PL91-6.

292. Fabre, G., et al., *Evidence for CYP3A-mediated N-deethylation of amiodarone in human liver microsomal fractions.* Drug Metab Dispos, 1993. **21**(6): p. 978-85.

293. Juenke, J.M., et al., *A rapid procedure for the monitoring of amiodarone and N-desethylamiodarone by HPLC-UV detection.* J Anal Toxicol, 2004. **28**(1): p. 63-6.

294. Teng, R., et al., *A pharmacokinetic study of the combined administration of amiodarone and ximelagatran, an oral direct thrombin inhibitor.* J Clin Pharmacol, 2004. **44**(9): p. 1063-71.

295. Kollroser, M. and C. Schober, *Determination of amiodarone and desethylamiodarone in human plasma by high-performance liquid chromatography-electrospray ionization tandem mass spectrometry with an ion trap detector.* J Chromatogr B Analyt Technol Biomed Life Sci, 2002. **766**(2): p. 219-26.

296. Ha, H.R., et al., *Identification and quantitation of novel metabolites of amiodarone in plasma of treated patients.* Eur J Pharm Sci, 2005. **24**(4): p. 271-9.

297. Kalitsky-Szirtes, J., et al., *Suppression of drug-metabolizing enzymes and efflux transporters in the intestine of endotoxin-treated rats.* Drug Metab Dispos, 2004. **32**(1): p. 20-7.

298. Mason, J.W., *Amiodarone.* N Engl J Med, 1987. **316**(8): p. 455-66.

299. Genest, J., et al., *Recommendations for the management of dyslipidemia and the prevention of cardiovascular disease: summary of the 2003 update.* CMAJ, 2003. **169**(9): p. 921-4.

300. Andreasen, F., et al., *Pharmacokinetics of amiodarone after intravenous and oral administration.* Eur J Clin Pharmacol, 1981. **19**(4): p. 293-9.

301. Young, R.A. and H.M. Mehendale, *In vitro metabolism of amiodarone by rabbit and rat liver and small intestine.* Drug Metab Dispos, 1986. **14**(4): p. 423-9.

302. Wacher, V.J., et al., *Role of P-glycoprotein and cytochrome P450 3A in limiting oral absorption of peptides and peptidomimetics.* J Pharm Sci, 1998. **87**(11): p. 1322-30.

303. Benet, L.Z., et al., *Intestinal MDR transport proteins and P-450 enzymes as barriers to oral drug delivery.* J Control Release, 1999. **62**(1-2): p. 25-31.

304. Katoh, M., et al., *Inhibitory effects of CYP3A4 substrates and their metabolites on P-glycoprotein-mediated transport.* Eur J Pharm Sci, 2001. **12**(4): p. 505-13.

305. Vuppugalla, R. and R. Mehvar, *Enzyme-selective effects of nitric oxide on affinity and maximum velocity of various rat cytochromes P450.* Drug Metab Dispos, 2005. **33**(6): p. 829-36.

306. Costa, C., et al., *Modifications in the metabolic pathways of benzene in streptozotocin-induced diabetic rat.* Arch Toxicol, 1999. **73**(6): p. 301-6.

307. Wang, T., et al., *Potentiation of thioacetamide liver injury in diabetic rats is due to induced CYP2E1.* J Pharmacol Exp Ther, 2000. **294**(2): p. 473-9.

308. Van Obbergh, L.J., et al., *Extrahepatic metabolism of sevoflurane in children undergoing orthotopic liver transplantation.* Anesthesiology, 2000. **92**(3): p. 683-6.

309. Thum, T., et al., *Expression of xenobiotic metabolizing enzymes in different lung compartments of smokers and nonsmokers.* Environ Health Perspect, 2006. **114**(11): p. 1655-61.

310. Zordoky, B.N. and A.O. El-Kadi, *H9c2 cell line is a valuable in vitro model to study the drug metabolizing enzymes in the heart.* J Pharmacol Toxicol Methods, 2007.

311. Nishimura, M. and S. Naito, *Tissue-specific mRNA expression profiles of human phase I metabolizing enzymes except for cytochrome P450 and phase II metabolizing enzymes.* Drug Metab Pharmacokinet, 2006. **21**(5): p. 357-74.

312. Kaminsky, L.S. and Q.Y. Zhang, *The small intestine as a xenobiotic-metabolizing organ.* Drug Metab Dispos, 2003. **31**(12): p. 1520-5.

313. Catania, V.A. and M.C. Carrillo, *Intestinal phase II detoxification systems: effect of low-protein diet in weanling rats.* Toxicol Lett, 1990. **54**(2-3): p. 263-70.

314. Zhang, Q.Y., et al., *Regulation of cytochrome P4501A1 expression in rat small intestine.* Drug Metab Dispos, 1997. **25**(1): p. 21-6.

315. Zhang, Q.Y., X. Ding, and L.S. Kaminsky, *CDNA cloning, heterologous expression, and characterization of rat intestinal CYP2J4.* Arch Biochem Biophys, 1997. **340**(2): p. 270-8.

316. Paine, M.F., et al., *Characterization of interintestinal and intraintestinal variations in human CYP3A-dependent metabolism.* J Pharmacol Exp Ther, 1997. **283**(3): p. 1552-62.

317. Paine, M.F., et al., *First-pass metabolism of midazolam by the human intestine.* Clin Pharmacol Ther, 1996. **60**(1): p. 14-24.

318. Back, D.J. and S.M. Rogers, *Review: first-pass metabolism by the gastrointestinal mucosa.* Aliment Pharmacol Ther, 1987. **1**(5): p. 339-57.

319. Shimomura, M., et al., *Roles of the jejunum and ileum in the first-pass effect as absorptive barriers for orally administered tacrolimus.* J Surg Res, 2002. **103**(2): p. 215-22.

320. Chhabra, R.S., *Intestinal absorption and metabolism of xenobiotics.* Environ Health Perspect, 1979. **33**: p. 61-9.

321. Nomura, E., et al., *Clinical characteristics of first-ever atherothrombotic infarction or lacunar infarction with hyperlipidemia (J-STARS-C): an analysis of data from the stroke data bank of Japan.* Intern Med, 2005. **44**(12): p. 1252-7.

322. Lin, J.H., *Tissue distribution and pharmacodynamics: a complicated relationship.* Curr Drug Metab, 2006. **7**(1): p. 39-65.

323. Jun, A.S. and D.R. Brocks, *High-performance liquid chromatography assay of amiodarone in rat plasma.* J Pharm Pharm Sci, 2001. **4**(3): p. 263-8.

324. Kido, Y., et al., *Epsilon-polylysine inhibits pancreatic lipase activity and suppresses postprandial hypertriacylglyceridemia in rats.* J Nutr, 2003. **133**(6): p. 1887-91.

325. Klaassen, C.D. and J.B. Watkins, 3rd, *Mechanisms of bile formation, hepatic uptake, and biliary excretion.* Pharmacol Rev, 1984. **36**(1): p. 1-67.

326. Knox, R., et al., *Effect of fat pre-feeding on bile flow and composition in the rat.* Biochim Biophys Acta, 1991. **1083**(1): p. 65-70.

327. Wasan, K.M. and J.S. Conklin, *Enhanced amphotericin B nephrotoxicity in intensive care patients with elevated levels of low-density lipoprotein cholesterol.* Clin Infect Dis, 1997. **24**(1): p. 78-80.

328. Barakat, M.M., A.O. El-Kadi, and P. du Souich, *L-NAME prevents in vivo the inactivation but not the down-regulation of hepatic cytochrome P450 caused by an acute inflammatory reaction.* Life Sci, 2001. **69**(13): p. 1559-71.

329. Lowry, O.H., et al., *Protein measurement with the Folin phenol reagent.* J Biol Chem, 1951. **193**(1): p. 265-75.

330. Omura, T. and R. Sato, *The Carbon Monoxide-Binding Pigment of Liver Microsomes. I. Evidence for Its Hemoprotein Nature.* J Biol Chem, 1964. **239**: p. 2370-8.

331. Korashy, H.M. and A.O. El-Kadi, *Differential effects of mercury, lead and copper on the constitutive and inducible expression of aryl hydrocarbon receptor (AHR)-regulated genes in cultured hepatoma Hepa 1c1c7 cells.* Toxicology, 2004. **201**(1-3): p. 153-72.

332. Berezhkovskiy, L.M., *Volume of distribution at steady state for a linear pharmacokinetic system with peripheral elimination.* J Pharm Sci, 2004. **93**(6): p. 1628-40.

333. Bailer, A.J., *Testing for the equality of area under the curves when using destructive measurement techniques.* J Pharmacokinet Biopharm, 1988. **16**(3): p. 303-9.

334. Pollak, P.T., T. Bouillon, and S.L. Shafer, *Population pharmacokinetics of long-term oral amiodarone therapy.* Clin Pharmacol Ther, 2000. **67**(6): p. 642-52.

335. Maes, A., et al., *Determination of amiodarone and desethylamiodarone in horse plasma and urine by high-performance liquid chromatography combined with UV detection and electrospray ionization mass spectrometry.* J Chromatogr B Analyt Technol Biomed Life Sci, 2006. **836**(1-2): p. 47-56.

336. Sarich, T.C., et al., *The pharmacokinetics and pharmacodynamics of ximelagatran, an oral direct thrombin inhibitor, are unaffected by a single dose of alcohol.* J Clin Pharmacol, 2004. **44**(4): p. 388-93.

337. Wyss, P.A., M.J. Moor, and M.H. Bickel, *Single-dose kinetics of tissue distribution, excretion and metabolism of amiodarone in rats.* J Pharmacol Exp Ther, 1990. **254**(2): p. 502-7.

338. Brien, J.F., S. Jimmo, and P.W. Armstrong, *Rapid high-performance liquid chromatographic analysis of amiodarone and N-desethyl-amiodarone in serum.* Can J Physiol Pharmacol, 1983. **61**(3): p. 245-8.

339. Moor, M.J., P.A. Wyss, and M.H. Bickel, *New procedure for the high-performance liquid chromatographic determination of amiodarone and desethylamiodarone with solid-phase extraction of rat plasma and tissue samples.* J Chromatogr, 1988. **431**(2): p. 455-60.

340. Zhang, C.X., Y. Aebi, and W. Thormann, *Microassay of amiodarone and desethylamiodarone in serum by capillary electrophoresis with head-column field-amplified sample stacking.* Clin Chem, 1996. **42**(11): p. 1805-11.

341. Johnston, T.P. and W.K. Palmer, *Mechanism of poloxamer 407-induced hypertriglyceridemia in the rat.* Biochem Pharmacol, 1993. **46**(6): p. 1037-42.

342. Wout, Z.G., et al., *Poloxamer 407-mediated changes in plasma cholesterol and triglycerides following intraperitoneal injection to rats.* J Parenter Sci Technol, 1992. **46**(6): p. 192-200.

343. Pec, E.A., Z.G. Wout, and T.P. Johnston, *Biological activity of urease formulated in poloxamer 407 after intraperitoneal injection in the rat.* J Pharm Sci, 1992. **81**(7): p. 626-30.

344. Dumaswala, R., D. Berkowitz, and J.E. Heubi, *Adaptive response of the enterohepatic circulation of bile acids to extrahepatic cholestasis.* Hepatology, 1996. **23**(3): p. 623-9.

345. Davies, B. and T. Morris, *Physiological parameters in laboratory animals and humans.* Pharm Res, 1993. **10**(7): p. 1093-5.

346. Myung, S.W., et al., *Characterization of amiodarone metabolites and impurities using liquid chromatography/atmospheric pressure chemical ionization mass spectrometry.* Rapid Commun Mass Spectrom, 2000. **14**(21): p. 2046-54.

347. Venkatakrishnan, K., et al., *Drug metabolism and drug interactions: application and clinical value of in vitro models.* Curr Drug Metab, 2003. **4**(5): p. 423-59.

348. Anastasiou-Nana, M., G.M. Levis, and S. Moulopoulos, *Pharmacokinetics of amiodarone after intravenous and oral administration.* Int J Clin Pharmacol Ther Toxicol, 1982. **20**(11): p. 524-9.

349. Vadiei, K., et al., *Population pharmacokinetics of intravenous amiodarone and comparison with two-stage pharmacokinetic analysis.* J Clin Pharmacol, 1997. **37**(7): p. 610-7.

350. Guengerich, F.P. and T. Shimada, *Oxidation of toxic and carcinogenic chemicals by human cytochrome P-450 enzymes.* Chem Res Toxicol, 1991. **4**(4): p. 391-407.

351. Eagling, V.A., J.F. Tjia, and D.J. Back, *Differential selectivity of cytochrome P450 inhibitors against probe substrates in human and rat liver microsomes.* Br J Clin Pharmacol, 1998. **45**(2): p. 107-14.

352. Turan, V.K., V.M. Mishin, and P.E. Thomas, *Clotrimazole is a selective and potent inhibitor of rat cytochrome P450 3A subfamily-related testosterone metabolism.* Drug Metab Dispos, 2001. **29**(6): p. 837-42.

353. Zhao, H.W., et al., *Effects of exposure to diesel exhaust particles (DEP) on pulmonary metabolic activation of mutagenic agents.* Mutat Res, 2004. **564**(2): p. 103-13.

354. Gharavi, N. and A.O. El-Kadi, *tert-Butylhydroquinone is a novel aryl hydrocarbon receptor ligand.* Drug Metab Dispos, 2005. **33**(3): p. 365-72.

355. Zhang, Q.Y., et al., *Characterization of rat small intestinal cytochrome P450 composition and inducibility.* Drug Metab Dispos, 1996. **24**(3): p. 322-8.

356. Seubert, J.M., C.J. Sinal, and J.R. Bend, *Acute sodium arsenite administration induces pulmonary CYP1A1 mRNA, protein and activity in the rat.* J Biochem Mol Toxicol, 2002. **16**(2): p. 84-95.

357. Paine, M.F., P. Schmiedlin-Ren, and P.B. Watkins, *Cytochrome P-450 1A1 expression in human small bowel: interindividual variation and inhibition by ketoconazole.* Drug Metab Dispos, 1999. **27**(3): p. 360-4.

358. Kuroha, M., et al., *Effect of oral ketoconazole on first-pass effect of nifedipine after oral administration in dogs.* J Pharm Sci, 2002. **91**(3): p. 868-73.

359. Fleishaker, J.C., et al., *Interaction between ketoconazole and almotriptan in healthy volunteers.* J Clin Pharmacol, 2003. **43**(4): p. 423-7.

360. Engels, F.K., et al., *Effect of cytochrome P450 3A4 inhibition on the pharmacokinetics of docetaxel.* Clin Pharmacol Ther, 2004. **75**(5): p. 448-54.

361. Ward, K.W., et al., *Development of an in vivo preclinical screen model to estimate absorption and first-pass hepatic extraction of xenobiotics. II. Use of ketoconazole to identify P-glycoprotein/CYP3A-limited bioavailability in the monkey.* Drug Metab Dispos, 2004. **32**(2): p. 172-7.

362. Koch-Weser, J. and E.M. Sellers, *Binding of drugs to serum albumin (first of two parts).* N Engl J Med, 1976. **294**(6): p. 311-6.

363. Procyshyn, R.M., T. Ho, and K.M. Wasan, *Competitive displacement of clozapine from plasma proteins in normolipidemic and hyperlipidemic plasma samples: clinical implications.* Drug Dev Ind Pharm, 2005. **31**(4-5): p. 331-7.

364. Pollak, P.T., *Clinical organ toxicity of antiarrhythmic compounds: ocular and pulmonary manifestations.* Am J Cardiol, 1999. **84**(9A): p. 37R-45R.

365. Wasan, K.M., et al., *Poloxamer 407-mediated alterations in the activities of enzymes regulating lipid metabolism in rats.* J Pharm Pharm Sci, 2003. **6**(2): p. 189-97.

366. Plomp, T.A., W.M. Wiersinga, and R.A. Maes, *Tissue distribution of amiodarone and desethylamiodarone in rats after repeated oral administration of various amiodarone dosages.* Arzneimittelforschung, 1985. **35**(12): p. 1805-10.

367. Tiebel, O., et al., *Mouse very low-density lipoprotein receptor (VLDLR): gene structure, tissue-specific expression and dietary and developmental regulation.* Atherosclerosis, 1999. **145**(2): p. 239-51.

368. Chung, N.S. and K.M. Wasan, *Potential role of the low-density lipoprotein receptor family as mediators of cellular drug uptake.* Adv Drug Deliv Rev, 2004. **56**(9): p. 1315-34.

369. Hussain, M.M., et al., *Chylomicron metabolism. Chylomicron uptake by bone marrow in different animal species.* J Biol Chem, 1989. **264**(30): p. 17931-8.

370. Ohyama, K., et al., *A significant role of human cytochrome P450 2C8 in amiodarone N-deethylation: an approach to predict the contribution with relative activity factor.* Drug Metab Dispos, 2000. **28**(11): p. 1303-10.

371. Arellano, C., et al., *Liquid chromatographic-mass spectrometric method to assess cytochrome P450-mediated metabolism of testosterone by rat everted gut sacs.* J Chromatogr B Analyt Technol Biomed Life Sci, 2004. **807**(2): p. 263-70.

372. Arellano, C., et al., *Validation of a liquid chromatography-mass spectrometry method to assess the metabolism of bupropion in rat everted gut sacs.* J Chromatogr B Analyt Technol Biomed Life Sci, 2005. **829**(1-2): p. 50-5.

373. Arellano, C., et al., *The metabolism of midazolam and comparison with other CYP enzyme substrates during intestinal absorption: in vitro studies with rat everted gut sacs.* J Pharm Pharm Sci, 2007. **10**(1): p. 26-36.

374. Arellano, C., et al., *Validation of a liquid chromatography-mass spectrometry method to assess the metabolism of dextromethorphan in rat everted gut sacs.* J Chromatogr B Analyt Technol Biomed Life Sci, 2005. **819**(1): p. 105-13.

375. Hirunpanich, V., B. Sethabouppha, and H. Sato, *Inhibitory effects of saturated and polyunsaturated fatty acids on the cytochrome P450 3A activity in rat liver microsomes.* Biol Pharm Bull, 2007. **30**(8): p. 1586-8.

376. Yao, H.T., et al., *The inhibitory effect of polyunsaturated fatty acids on human CYP enzymes.* Life Sci, 2006. **79**(26): p. 2432-40.

377. El-Badry, A.M., R. Graf, and P.A. Clavien, *Omega 3 - Omega 6: What is right for the liver?* J Hepatol, 2007. **47**(5): p. 718-25.

378. Yamazaki, H., M. Tanaka, and T. Shimada, *Highly sensitive high-performance liquid chromatographic assay for coumarin 7-hydroxylation and 7-ethoxycoumarin O-deethylation by human liver cytochrome P450 enzymes.* J Chromatogr B Biomed Sci Appl, 1999. **721**(1): p. 13-9.

379. Hirunpanich, V., et al., *Demonstration of docosahexaenoic acid as a bioavailability enhancer for CYP3A substrates: in vitro and in vivo evidence using cyclosporin in rats.* Drug Metab Dispos, 2006. **34**(2): p. 305-10.

380. Venkatachalam, M. and S.K. Sathe, *Chemical composition of selected edible nut seeds.* J Agric Food Chem, 2006. **54**(13): p. 4705-14.

381. Grosso, N.R., V. Nepote, and C.A. Guzman, *Chemical composition of some wild peanut species (Arachis L.) seeds.* J Agric Food Chem, 2000. **48**(3): p. 806-9.

382. Procyshyn, R.M., T. Ho, and K.M. Wasan, *The effects of competitive displacement on haloperidol's plasma distribution in normolipidemic and hyperlipidemic plasma.* Drug Dev Ind Pharm, 2005. **31**(9): p. 901-5.

383. Sugioka, N., et al., *Effect of plasma lipid on pharmacokinetics of ciclosporin and its relationship with plasma prednisolone level in renal transplant patients.* J Pharm Pharmacol, 2006. **58**(9): p. 1193-200.

384. Nicholls, S.J., et al., *Consumption of saturated fat impairs the anti-inflammatory properties of high-density lipoproteins and endothelial function.* J Am Coll Cardiol, 2006. **48**(4): p. 715-20.

385. Yuan, G., J. Wang, and R.A. Hegele, *Heterozygous familial hypercholesterolemia: an underrecognized cause of early cardiovascular disease.* Cmaj, 2006. **174**(8): p. 1124-9.

386. Ramaswamy, M., et al., *Amphotericin B lipid complex or amphotericin B multiple-dose administration to rabbits with elevated plasma cholesterol levels: pharmacokinetics in plasma and blood, plasma lipoprotein levels, distribution in tissues, and renal toxicities.* Antimicrob Agents Chemother, 2001. **45**(4): p. 1184-91.

387. Aweeka, F.T., et al., *Pharmacokinetics of orally and intravenously administered cyclosporine in pre-kidney transplant patients.* J Clin Pharmacol, 1994. **34**(1): p. 60-7.

388. Lii, C.K., C.W. Tsai, and C.C. Wu, *Garlic allyl sulfides display differential modulation of rat cytochrome P450 2B1 and the placental form glutathione S-transferase in various organs.* J Agric Food Chem, 2006. **54**(14): p. 5191-6.

389. Prueksaritanont, T., et al., *Transport and metabolism of cyclosporine in isolated rat hepatocytes. The effects of lipids.* Biochem Pharmacol, 1992. **43**(9): p. 1997-2006.